Fabrication of feather keratin bio-based materials: Thermoplastics and tissue engineered scaffolds

by

Yussef Esparza

A thesis submitted in partial fulfillment of the requirements for the degree of

Doctor of Philosophy

in

Bioresources and Food Engineering

Department of Agricultural, Food, and Nutritional Science
University of Alberta

Abstract

Chicken feathers are an abundant by-product from poultry industry. Feathers are composed of around 90% keratin, a valuable protein bioresource that have great potential for non-food applications. Keratin is characterized by a high content of cysteine residues forming disulfide bonds. This feature makes keratin an interesting biopolymer for the fabrication of mechanically resistant materials, including thermoplastics and tissue engineered scaffolds. Therefore, the overall objectives of the thesis are 1) to fabricate and improve mechanical properties of chicken feather thermoplastics; 2) to study and characterize the self-assembly of feather keratin hydrogels and their physical and biological properties; 3) to compare hydrogel properties of hair, wool and feather keratins; and 4) to evaluate the feasibility of electrospinning of feather keratin for the fabrication of nanofibrous scaffolds.

Chicken feathers were mixed with glycerol/propylene glycol plasticizers and thermally processed into plastic films. The tensile mechanical properties of films were evaluated. Incorporation of up to 2% graphite oxide nanoparticles resulted in enhanced tensile strength and Young modulus of plastic films, which were attributed to keratin intercalation into graphene oxide nanosheets and interaction between oxygen functionalities of graphite oxide with amino acid side groups of keratin, and plasticizers.

Chicken feather keratin was also studied for developing scaffolds for potential application in tissue engineering. Keratin from chicken feathers was solubilized in a solution containing urea, thiourea, and sodium metabisulfite. Keratin hydrogels were spontaneously formed during controlled dialysis of extracted keratin solution. Keratin gelation and stability of gels was mainly controlled by the extent of disulfide bond re-formation. Gelation at neutral pH proceeded slowly towards the formation of transparent gels, whereas rapid gelation occurred at pHs of 3 and 9 due

to isoelectric aggregation and increased rate of disulfide exchange reactions, respectively. Hydrogels had similar viscoelastic properties of adipose and dermal tissue. Increasing keratin concentration resulted in increased storage modulus of hydrogels; however, swelling capacity and porosity decreased with increased concentration. Hydrogel scaffolds supported the growth of human dermal fibroblasts (HDFa) over a period of 21 days. Cells infiltration was affected by the dense arrangement of keratin and lower porosity in hydrogels prepared at (10 and 12.5%), where the growth of cells was limited to the surface of scaffolds.

Keratin from different sources was compared for their hydrogel properties. Keratin from hair, wool and feathers were characterized by their molecular weight, amino acid composition, and thermal and conformational properties. Hydrogels from feather keratin demonstrated substantially higher storage modulus (~10 times higher) than others. However, higher swelling capacity (>3000%) was determined in hair and wool over feather keratin (1500%) hydrogels. The smaller molecular weight and β-sheet structure of feather keratin facilitated the self-assembly of rigid hydrogels. Whereas, higher molecular weight stretchable α-helix keratins in hair and wool resulted in weaker hydrogels. Fibroblasts showed the highest proliferation rate on feather keratin hydrogel scaffolds, which was attributed to their superior viscoelastic properties.

In the last part of the thesis, the potential of forming keratin nanofibers through electrospinning was evaluated. Electrospun keratin nanofiber were fabricated with non-toxic solvents and crosslinking reagents. Keratin was solubilized at room temperature in a 1 M NaOH solution. Poly(vinyl alcohol) (PVA)/citric acid aqueous solution was used as an aid for electrospinning. Solutions containing 10, 20, and 30% keratin/PVA mass ratio were successfully electrospun. The diameter of nanofibers decreased from 565 ± 154 nm in PVA to 274 ± 42nm in 20% keratin electrospun mats, which was attributed to a reduction in the viscosity of the solutions. Further

decrease in viscosity with 30% keratin resulted in beads-on-fiber. The resultant nanofibrous mats were thermally cross-linked by esterification of PVA hydroxyl groups with carbonyl groups in citric acid. The incorporation of keratin in PVA nanofiber was confirmed by FTIR and XPS results. Proliferation of fibroblasts after 14 days was higher in scaffolds containing 20% keratin, which was attributed to the superior biological properties of keratin and higher surface area to volume ratio compared to 30% keratin.

Feather keratin is a valuable bioresource for material applications. Feather plastics can be evaluated for applications including agricultural films. Keratin hydrogel and electrospun mat scaffolds support the proliferation of fibroblasts, making them potential materials for in vivo studies in skin tissue engineering.

PREFACE

Financial support for this work was granted by Alberta Livestock and Meat Agency Ltd. (ALMA), Natural Sciences and Engineering Research Council of Canada (NSERC), Becas Chile-CONICYT, Mitacs-accelerate program, and Graduate Student Association and Faculty of Graduate Studies and Research of the University of Alberta.

This thesis is an original work realized by Yussef Esparza. This thesis consist of eight chapters: Chapter 1 provides a general introduction and objectives of this thesis. Chapter 2 is a literature review. A version of Chapter 3 is published as "Preparation and characterization of graphite oxide nano-reinforced biocomposites from chicken feather keratin" in *Journal of Chemical Technology and Biotechnology*. A version of Chapter 4 entitled "Molecular mechanism and characterization of self-assembly of feather keratin gelation" was submitted to the *International Journal of Biological Macromolecules*. Versions of Chapter 5 "Characterization of hydrogel scaffolds from chicken feather keratin prepared by dialysis self-assembly", Chapter 6 "Hydrogels from feather keratin show stronger and higher cell proliferation than those from hair and wool keratins" and Chapter 7 "Preparation and characterization of thermally cross-linked poly(vinyl alcohol)/feather keratin nanofiber scaffolds" are expected for publication. Chapter 8 provides concluding remarks and future research directions and recommendations. I was responsible for literature reviews required for this thesis, experimental designs, performing of experiments, data collection and analysis, and writing of manuscripts. Dr. Jianping Wu, and Dr. Aman Ullah contributed to provide research guidance, design of experiments, data interpretation, manuscript preparation and edition. Mr. Nandika Bandara contributed with gelatin extraction and material preparation in Chapter 6. Dr. Yaman Boluk's contributed with experiment planning and laboratory equipment in Chapter 7.

ACKNOWLEDGEMENTS

I would like to take this opportunity to thank all people who helped me directly or indirectly with the realization of this thesis work and throughout my study program. First of all I would like to thank my supervisor Dr. Jianping Wu, for giving me the opportunity to join his research group. His guidance and encouragement helped with the consecution of this work. I would like to thank Dr. Aman Ullah for his academic support and guidance throughout my studies. My thanks to my supervisory committee member Dr. Thavaratnam Vasanthan and to my internal examiner Dr. Yaman Boluk for your time, willingness to cooperate, and technical guidance. I also thanks Dr. Brian Amsden for accepting the invitation to serve as external examiner and for allocating his time to the revision of this work.

I would also like to thank Graduate Program Administrator and lab managers of the Department of Agricultural, Food, and Nutritional Sciences, Mrs. Jody Forslund, Holly Horvath, Dr. Urmila Basu, Mrs. Nancy Turchinsky, Mrs. Heather Vandertol-Vanier, and Mrs. Robin Miles. I am deeply grateful from people who gave technical support throughout my studies, Mr. Lyle Boubier from, Dr. Jane Batcheller, Mr. Dimitre Karpuzov, Mr. Shihong Xu, Mr. Anqiang He, Mrs. Shiau-Yin Wu, Mrs. Arlene Oatway, Dr. Nathan Buzik, Dr. Mirko Betti, Dr. Lingyun Chen, and Ms. Mahsa Kalantari. I would like to thank my past and present laboratory and office mates for their support and friendship. Special thanks to my family and friends and to all my past mentors in the University of La Frontera and University of Alberta.

I am very thankful to the Agencies and Institutions that provided me financial support during my studies and thesis work; Alberta Livestock and Meat Agency Ltd. (ALMA), Natural Sciences and Engineering Research Council of Canada (NSERC), Becas Chile-CONICYT, and Graduate Student Association and Faculty of Graduate Studies and Research of the University of Alberta.

TABLE OF CONTENTS

LIST OF TABLES

LIST OF FIGURES

ABBREVIATIONS

2D: Two-dimension

3D: Three-dimension

ANOVA: Analysis of variance

ATR: Attenuated total reflection

BOAS: beads on a string

C/O: carbon/oxygen ratio

C1s: Carbon 1s

CF: Chicken feather

DAPI: 4',6-diamidino-2-phenylindole, dihydrochloride

DMEM: Dulbecco's Modified Eagle's Medium

DNA: Deoxyribonucleic acid

DNTB: 5,5'-Dithiobis(2-nitrobenzoic acid)

DSC: Differential scanning calorimetry

DTT: 1,4-dithiothreitol

ECM: Extracellular matrix

EDS: Glutamic acid-aspartic acid-serine

EDXS: Energy dispersive X-ray spectroscopy

FBK: Feather barb keratin

FBR: Foreign body reaction

FBS: Fetal bovine serum

Feather-g-PMA: Feather-grafted-poly(methyl acrylate)

FK: Feather keratin

FK: Feather keratin

FQK: Feather quill keratin

FSD: Fourier self-deconvolution

FTIR: Fourier transform infrared

FWHM: Full width at half maximum

GATR: Germanium attenuated total reflection

GO: Graphite oxide

H&E: Hematoxylin and eosin

HDFa: Adult human dermal fibroblasts

HEPES: 4-(2-hydroxyethyl)-1-piperazineethanesulfonic acid)

HFIP: Hexafluoropropanol

HK: hair keratin

H-NMR: Proton NMR

HPLC: High performance liquid chromatography

IAA: Iodoacetic acid

IUPAC: International Union of Pure and Applied Chemistry

KAPs: Keratin associated proteins

KES: Keratin extraction solution

KGD: Lysine-glycine-aspartic acid

LDV: Leucine-aspartic acid-valine

LRE: Leucine-arginine-glutamic acid

NEAA: Non-essential amino acid

NEM: N-ethylmaleimide

PBS: Phosphate saline buffer

PECAM-1: Platelet endothelial cell adhesion molecule

PEG: Poly(ethylene glycol)

PMA: Poly(methyl acrylate)

PVA: Poly(vinyl alcohol)

RE: Arginine-glutamic acid

RGD: Arginine-glycine-aspartic acid

RLD: Arginine-leucine-aspartic acid

SAOS: Small amplitude oscillatory shear

SDS: Sodium dodecyl sulfate

SDS-PAGE: Sodium dodecyl sulfate-Poly(acryl amide) gel electrophoresis

SEM: Scanning electron microscopy

SEM: Scanning electros microscopy

TEM: Transmission electron microscopy

TFA: Trifluoroacetic

TGA: Thermo-gravimetric analysis

TOF-SIMS: Time of flight-Secondary ion mass spectrometry

UV: Ultra violet

WK: Wool keratin

XPS: X-ray photoelectron spectroscopy

XRD: X-ray diffraction

CHAPTER 1. General introduction and thesis objectives

Proteins by-products are biodegradable, biocompatible, and abundant natural resources with great potential for applications as non-food materials (Reddy, 2015). One protein-rich by-product from the poultry industry is feather, accounting roughly for up to 10% of the live weight of chickens. It is estimated that approximately 100,000 tonnes of chicken feathers are generated yearly by the Canadian poultry industry (Agriculture and Agri-Food Canada, 2014). In the United States the amount of feathers generated is higher, accounting for 1.4-1.8 million tonnes yearly (Swisher, 2008). While worldwide feather generation reach approximately 8-9 million tonnes (Lasekan et al., 2013).

Feathers are mainly used in animal feeding. A high pressure and temperature treatment yield a product called feathermeal. Although rich in protein, feathermeal is deficient in methionine, histidine, and tryptophan amino acids. In addition, it has low digestibility and high protein composition variability (Papadopoulos et al., 1986; Grazziotin et al., 2007). Feathermeal is also used as soil fertilizer. Feathers are resistant to degradation by soil microorganisms; hence, the release of nitrogen is limited (Brebu and Spiridon, 2011). Thermal and biological hydrolysis of feather could improve feather degradation; however, the treatment raises the production costs, which is undesirable for commercialization purposes (Kornillowicz-Kowalska and Bohacz, 2011). Limited uses of feathers have led to increased waste destined to incineration and disposal in landfills, which raises environmental issues due to the generation of polluting and greenhouse gases and the persistence of feathers in the environment, respectively.

The use of feather for the fabrication of plastic films and reinforcement fibers represents an alternative source to petroleum-based plastics. Barbs of feathers have been used as reinforcement in plastic composites with improved mechanical and thermal properties (Barone et al., 2006;

Huda et al., 2012; Ghani et al., 2013; Grkovic et al., 2015). Feathers have also been used to produce biodegradable plastics films by thermo-molding with the aid of plasticizers (Barone et al., 2006; Barone and Arikan, 2007; Ullah et al., 2011). Thermal processing of feather plastics is desirable in term of costs and sustainability; however, feather plastics suffer from their poor mechanical properties, high hydrophilicity, and poor reproducibility (Poole and Church, 2015). The dispersion of nanoparticles in the polymer melt can result in effective stress transfer, leading to increased mechanical properties (Gong et al., 2010). Among nanoparticles, graphene and graphene oxide, have great potential due to their superior stiffness and high aspect ratio (Novoselov et al., 2004). The reinforcement of synthetic and natural polymers with graphene and graphene oxide has been investigated (Mahmoud, 2011; He et al., 2013; Rodriguez-Gonzalez et al., 2013). However, there are limited studies on thermal processing of protein-graphene composites. Feather-graphene composites through thermal processing could result in materials with improved properties.

Proteins are also a valuable resource for fabrication of cellular scaffolding biomaterials for tissue engineering. Scaffolds can be used by cells as a three-dimensional framework in which they can adhere, proliferate, and regenerate tissues. Several factors such as, the presence of cell adhesion sites, surface chemistry of protein and mechanical and microstructural properties of scaffolds are important for the modulation of cell behavior and tissue regeneration (Lee et al., 2008).

Feathers are composed of around 90-94% protein, 2-4% lipids, and residual amounts of moisture and ash. The main component of feathers is keratin. Keratins are a family of fibrous proteins also found in hair, skin, nails, wool, horns, bird's beaks, and reptile's scales. Keratins are water-insoluble, where semi-crystalline proteins are stabilized by abundant inter- and intra-molecular disulfide bonds. Keratins from birds and reptiles are homogenous proteins with a molecular

weight of 10 kDa and are mostly composed of a β-sheet structure. Keratins from mammals are heterogeneous proteins with a molecular weight of 10-75 kDa composed mainly of α-helix structure. Solubilization of keratin requires destabilization of hydrophobic/hydrogen bond interactions and disruption of disulfide bonds. Disruption of disulfide bonds yields cysteine thiols, which are very reactive and have the tendency to re-oxidize into disulfide bonds, resulting in insoluble keratin. Keratins are of particular interest in the fabrication of hydrogel and electrospun mat scaffolds due to their biocompatibility, accelerated wound healing property, and mechanical strength (Rouse and Van Dyke, 2010; Cavaco-Paulo et al., 2013).

Hydrogels are water-swollen polymeric cross-linked networks absorbing from 10-20% to thousands of their dry weight in water. They are excellent scaffold materials for treatment of chronic skin wounds (Madaghiele et al., 2014). Hydrogels fill the space of damaged tissue facilitating providing a temporary matrix for tissue regeneration. Keratin hydrogels from hair, wool and feathers have been successfully fabricated. During gelation the reformation of disulfide bonds is partially prevented by keratin pre-treatments such as, chemically blocking (Ikkai and Nato, 2002; Nakata et al., 2014; Han et al., 2015) and oxidation of thiols (De Guzman et al., 2011; Pace et al., 2014), partial hydrolysis (Hill et al., 2010; Wang et al., 2012; Wang et al., 2015), and formation of detergent-keratin complexes (Schrooyen et al., 2000; Tonin et al., 2007; Wang et al., 2017). The complete availability of free thiols during gelation of feather keratin could lead to the formation of strong hydrogels and scaffolds via disulfide crosslinking.

Electrospinning is a widely used technique to produce polymer nanofibres. Nanofibre scaffolds are promising wound dressing and skin scaffold materials as they mimic the nanofibrillar microstructure of connective tissue and provide large surface-area to volume ratio for cell-scaffold interaction (Sundaramurthi et al., 2014). Keratin from wool has been successfully

electrospun into non-woven mats (Aluigi et al., 2013). Feather barbs mixed with sodium dodecyl sulfate were electrospun, resulting in thick fibers of few micrometers (Xu et al., 2014). However, viscoelastic properties of keratin are usually poor which translate in difficulty to form uniform fibers through electrospinning. Therefore, electrospinning of keratin is usually performed by blending it with viscoelastic polymer solutions of poly(ethylene oxide), poly(caprolactone), poly(lactic acid), poly(vinyl alcohol), polyamide 6 and fibroin (Aluigi et al., 2007; Boakye et al., 2015; Park et al., 2015; Yen et al., 2016). Current limitations in the electrospinning of keratin are their low concentration in the blend, and use of costly and potentially harmful solvents and crosslinking chemicals. Electrospinning of feather keratin using harmless solvent and additives is desirable for biomedical applications.

Three hypotheses were proposed in this thesis research: 1) The tensile mechanical properties of feather thermo-plastics could be improved with nanoparticles. 2) Keratin from chicken feathers could be extracted and used to develop hydrogel scaffolds with appropriate physical and mechanical properties for skin tissue engineering. 3) Feather keratin would be adequate for the electrospinning of nanofiber scaffolds for skin tissue engineering.

The objectives of the research were:

1. To improve the mechanical properties of feather thermo-plastics by the incorporation of nanoparticles.

2. To study and characterize the molecular interactions responsible for the self-assembly of keratin hydrogels during dialysis.

3. To characterize the physical and biological properties of self-assembled feather keratin hydrogels for skin cell scaffolds.

4. To compare the chemical, physical, mechanical and biological properties of hydrogels scaffolds prepared from keratins from mammalian and avian sources.

5. To evaluate the feasibility of feather keratin electrospinning in the designing of nanofibre scaffolds for skin cells.

1.1. References

Agriculture and Agri-Food Canada. Retrieved online from http://www.agr.gc.ca/ on February 11th, 2015

Aluigi, A., Corbellini, A., Rombaldoni, F., & Mazzuchetti, G. (2013). Wool-derived keratin nanofiber membranes for dynamic adsorption of heavy-metal ions from aqueous solutions. *Textile Research Journal*, 83, 1574-1586.

Aluigi, A., Varesano, A., Montarsolo, A., Vineis, C., Ferrero, F., Mazzuchetti, G., & Tonin, C. (2007). Electrospinning of keratin/poly(ethylene oxide) blend nanofibers. , 104, 863-870.

Barone, J. R., & Arikan, O. (2007). Composting and biodegradation of thermally processed feather keratin polymer. *Polymer Degradation and Stability*, 92, 859-867.

Barone, J.R. & Schmidt, W. (2006). Compositions and films comprised of avian feather keratin. US Patent US7066995 B1.

Barone, J.R., Schmidt, W.F., & Gregoire, N.T. (2006). Extrusion of feather keratin. , 100, 1432-1442.

Boakye, M.A.D., Rijal, N.P., Adhikari, U., & Bhattarai, N. (2015). Fabrication and characterization of electrospun PCL-MgO-keratin-based composite nanofibers for biomedical applications. *Materials*, 8, 4080-4095.

Brebu, M., & Spiridon, I. (2011). Thermal degradation of keratin waste. *Journal of Analytical and Applied Pyrolysis*, 91, 288-295.

de Guzman, R.C., Merrill, M.R., Richter, J.R., Hamzi, R.I., Greengauz-Roberts, O.K., & Van Dyke, M.E. (2011). Mechanical and biological properties of keratose biomaterials. *Biomaterials*, 32, 8205-8217.

Ghani, S.A., Tan, S.J., & Yeng, T.S. (2013). Properties of chicken feather fiber-filled low-density polyethylene composites: The effect of polyethylene grafted maleic anhydride. *Polymer-Plastics Technology and Engineering*, 52, 495-500.

Gong, L., Kinloch, I.A., Young, R.J., Riaz, I., Jalil, R., & Novoselov, K.S. (2010). Interfacial stress transfer in graphene monolayer nanocomposite. *Advanced Materials*, 22, 2694-2697.

Grazziotin, A., Pimentel, F.A., Sangali, S., de Jong E.V., & Brandelli, A. (2007). Production of feather protein hydrolyzate by keratinolytic bacterium Vibrio sp. Kr2. *Bioresource Technology*, 98, 3172-3175.

Grkovic, M., Stojanovic, D.B., Kojovic, A., Strnad, S., Kreze, T., Aleksic, R., & Uskokovic, P.S. (2015). Keratin-polyethylene oxide bio-nanocomposites reinforced with ultrasonically functionalized graphene. *RSC Advances*, 5, 91280-91287.

Han, S., Ham, T.R., Haque, S., Sparks, J.L., Saul, J.M. (2015). Alkylation of human hair keratin for tunable hydrogel erosion and drug delivery in tissue engineering applications. *Acta Biomateralia*, 23, 201-213.

He, Y., Wang, X., Wu, D., Gong, Q., Qui, H., Liu, Y., Wu, T., Ma, J., & Gao, J. (2013). Biodegradable amylose films reinforced by graphene oxide and polyvinyl alcohol. *Materials Chemistry and Physics*, 142, 1-11.

Hill, P., Brantley, H., & Van Dyke, M. (2010). Some properties of keratin biomaterials: Kerateines. *Biomaterials*, 31, 585-593.

Huda, M.S., Schmidt, W.F., Misra, M., & Drzal, L.T. (2013). Effect of fiber surface treatment of poultry feather fibers on the properties of their polymer matrix composites. , 128, 1117-1124.

Ikkai, F., & Naito, S. (2002). Dynamic light scattering and circular dichroism studies on heat-induced gelation of hard-keratin protein aqueous solutions. *Biomacromolecules*, 3, 482-487.

Kornillowicz-Kowalska, T., & Bohacz, J. (2011). Biodegradation of keratin waste: Theory and practical aspects. *Waste Management*, 31, 1689-1701.

Lakesan, A., Bakar, F.A., & Hashim, D. (2013). Potential of chicken by-products as sources of useful biological resources. *Waste Management*, 33, 552-565.

Lee, J., Cuddihy, M.J., & Kotov, N.A. (2008). Three dimensional cell culture matrices: State of the art. *Tissue Engineering: Part B*, 14, 61-86.

Madaghiele, M., Demitri, C., Sannino, A., & Ambrosio, L. (2014). Polymeric hydrogels for burn wound care: Advanced skin wound dressings and regenerative templates. *Burns & Trauma*, 2, 153-161.

Mahmoud, W.E. (2011). Morphology and physical properties of poly(ethylene oxide) loaded graphene nanocomposites prepared by two different techniques. *European Polymer Journal*, 47, 1534-1540.

Nakata, R., Tachibana, A., & Tanabe, T. (2014). Preparation of keratin hydrogel/hydroxyapatite composite and its evaluation as controlled drug release carrier. *Materials Science and Engineering C*, 41, 59-64.

Novoselov, K.S., Geim, A.K., Morozov, S.V., Jiang, D., Zhang, Y., Dubonos, S.V., Grigorieva, I.V., & Firsov, A.A. (2004). Electric field effect in atomically thin carbon films. *Science*, 306, 666-669.

Pace, L.A., Plate, J.F., Mannava, S., Barnwell, J.C., Koman, L.A., Li, Z., Smith, T.L., & Van Dyke, M. (2014). A human hair keratin hydrogel scaffold enhances median nerve regeneration in nonhuman primates: An electrophysiological and histological study. *Tissue Engineering: Part A*, 20, 507-517.

Papadppoulos, M.C., El Boushy, A.R., Roodbeen, A.E., & Ketelaars, E.H. (1986). Effects of processing time and moisture content on amino acid composition and nitrogen characteristics of feather meal. *Animal Feed Science and Technology*, 14, 279-290.

Park, M., Shin, H-K., Panthi, G., Rabbani, M.M., Alam, A-M., Choi, J., Chung, H-J., Hong, S-T., & Kim H-Y. (2015). Novel preparation and characterization of human hair-based nanofibers using electrospinning process. *International Journal of Biological Macromolecules*, 76, 45-48.

Poole, A.J., & Church, J.S. (2015). The effects of physical and chemical treatments on Na_2S produced feather keratin films. *International Journal of Biological Macromolecules*, 73, 99-108.

Reddy, N. (2015). Non-food industrial applications of poultry feathers. *Waste Management*, 45, 91-107.

Rodriguez-Gonzalez, C., Kharissova, O.V., Martinez-Hernandez, A.L., Castano, V.M., & Velasco-Santos, C. (2013). Graphene oxide sheets covalently grafted with keratin obtained from chicken feathers. *Digest Journal of Nanomaterials and Biostructures*, 8, 127-138.

Rouse, J.G., & Van Dyke, M.E. (2010). A review of keratin-based biomaterials for biomedical applications. *Materials*, 3, 999-1014.

Schrooyen, P.M.M., Dijkstra, P.J., Oberthur, R.C., Bantjes, A., & Feijen, J. (2000). Partially carboxymethylated feather keratins. 1. Properties in aqueous systems. *Journal of Agricultural and Food Chemistry*, 48, 4326-4334.

Sundaramurthi, D., Krishnan, U.M., & Sethuraman, S. (2014). Electrospun nanofibers as scaffolds for skin tissue engineering. *Polymer Reviews*, 54, 348-376.

Tonin, C., Aluigi, A., Vineis, C., Varesano, A., Montarsolo, A., & Ferrero, F. (2007). Thermal and structural characterization of poly(ethylene-oxide)/keratin blend films. *Journal of Thermal Analysis and Calorimetry*, 89, 601-608.

Ullah, A., Vasanthan, T., Bressler, D., Elias, A.L., & Wu, J. (2011). Bioplastics from feather quill. *Biomacromolecules*, 12, 3826-3832.

Vasconcelos, A., & Cavaco-Paulo, A. (2013). The use of keratin in biomedical applications. *Current Drug Targets*, 14, 612-619.

Wang, J., Hao, S., Luo, T., Cheng, Z., Li, W., Gao, F., Guo, T., Gong, Y., & Wang, B. (2017). Feather keratin hydrogel for wound repair: Preparation, healing effect and biocompatibility evaluation. *Colloids and Surfaces B: Biointerfaces*, 149, 341-350.

Wang, S., Taraballi, F., Tan, L.P., Ng, K.W. (2012). Human keratin hydrogels support fibroblast attachment and proliferation in vitro. *Cell and Tissue Research*, 347, 795-802.

Wang, S., Wang, Z., Foo, S.E., Tan, N.S., Yuan, Y., Lin, W., & Ng, K.W. (2015). Culturing fibroblasts in 3D human hair keratin hydrogels. *ACS Applied Materials & Interfaces*, 7, 5187-5198.

Xu, H., Cai, S., Xu, L., & Yang, Y. (2014). Water-stable three-dimensional ultrafine fibrous scaffolds from keratin for cartilage tissue engineering. *Langmuir*, 30, 8461-8470.

Yen, K-C., Chen, C-Y., Huang, J-Y., Kuo, W-T., & Lin, F-H. (2016). Fabrication of keratin/fibroin membranes by electrospinning for vascular tissue engineering. *Journal of Materials Chemistry* B, 4, 237-244.

CHAPTER 2. Literature review: Valorization of keratin from chicken feathers for their utilization in the development of materials

2.1. Feathers

Feathers are complex appendages from the skin of birds. They provide a variety of functions such as thermal insulation, water resistance, camouflage and flight. Feathers are composed of a hierarchical branching structure in which a central structure called quill, which is divided into the rachis and calamus, is surrounded by branches called barbs or fibers. Each barb represents a central axis for branching projections called barbules (Figure 2.1). The mass proportion of quill to barbs varies depending on the location of feathers. Wing feathers for example are composed of equal parts of quill and barbs, whereas other parts contain less proportion of quill. The morphology of barbs is more consistent than the quills among feathers of different body locations (Schmidt, 2001).

Feathers account for up to 10% of the body weight of birds. They are composed of protein (90-92%), water (6-8%) and lipids (1-3%). Keratin is the main protein present in feathers. The chemical and conformational properties of keratin play an important role in the organization and structural properties of feathers (Bartels, 2003).

2.1.1 Keratins

Keratins are highly specialized fibrous proteins found in the protective outer layer (integument) in vertebrates (McKittrick et al., 2012). They are found abundantly in cornified epithelial tissues such as hair, wool, nails, skin, claws, hooves, horns, scales, feathers and beaks. After collagen, it is the most important biopolymer found in animals. Keratins are insoluble in water, organic

solvents, and weak acids and alkalis; in addition, they are resistant to common proteolytic enzymes such as pepsin and trypsin (Kornillowicz-Kowalska and Bohacz, 2011).

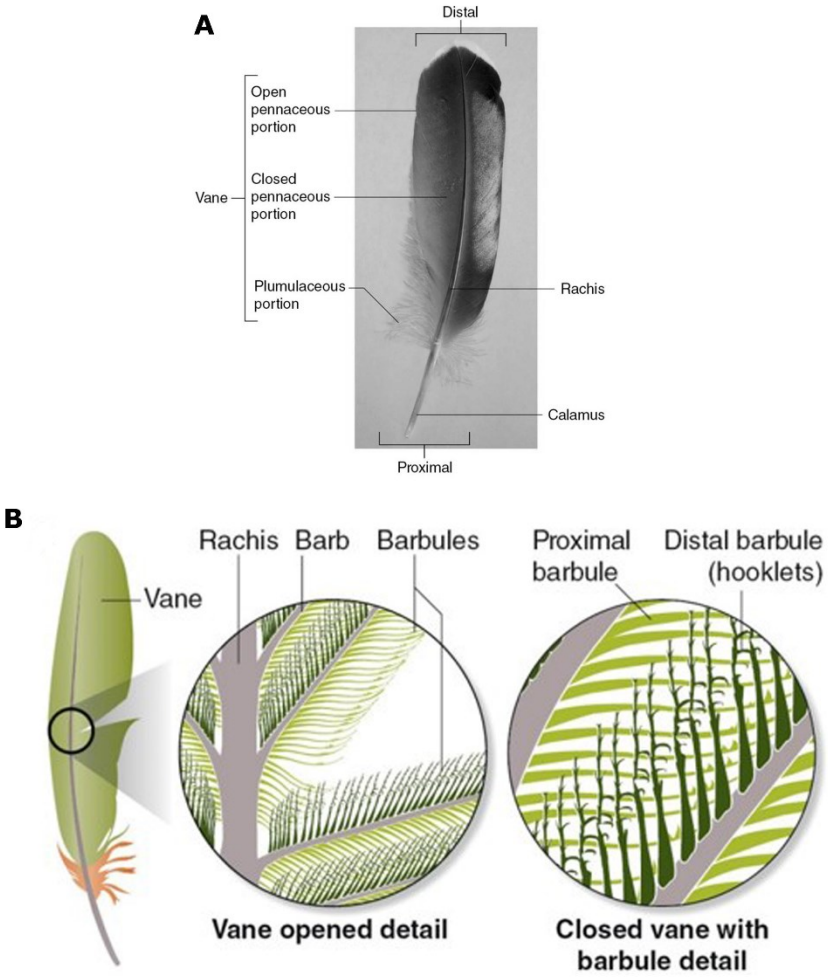

Figure 2.1. Morphology and structure of feathers (A) and organization of barbules and barbs (B) (Reprinted from Lovette and Fitzpatrick, 2016, with permission).

Keratin comprises about 90-92% of feathers. One of the main characteristics of keratin is the presence of high amount of cysteine amino acid residues. Other majority amino acids found in keratin are serine, proline, glutamic acid, valine and glycine (Table 2.1). The amino acid distribution of feather keratin is non-uniform; however acidic, basic, and cysteine residues are

more concentrated in the N- and C- terminal regions, whereas hydrophobic residues are more concentrated in the central part of keratins (Arai et al 1983; Feughelman, 1997). Amino acid composition of keratin is almost balanced in hydrophilic and hydrophobic amino acids (Table 2.1).

Table 2.1. Amino acid composition of chicken feathers (μmol/g)

Amino acid	μmol/g
Arginine	626 ± 34
Lysine	366 ± 34
Aspartic acid	543 ± 50
Glutamic acid	959 ± 68
Histidine	73 ± 5
Serine	1540 ± 66
Threonine	428 ± 39
Half-cystine	1140 ± 105
Tyrosine	177 ± 9
Glycine	2186 ± 129
Alanine	665 ± 47
Valine	761 ± 59
Leucine	1185 ± 75
Isoleucine	436 ± 33
Proline	343 ± 7
Phenylalanine	374 ± 29
Methionine	43 ± 3
Nitrogen %	16.2 ± 0.1
Polar/charged amino acids	49%
Non-polar amino acids	51%

The strength of keratins is mainly due to their protein structure stabilized by hydrogen bridges and covalent cysteine disulfide bonds. Based on the cysteine content, keratins can be classified into soft and hard keratin. Soft keratin, such as those in the outer layer of the epidermis and hair core, contain up to 2% of cysteine (Fraser et al., 1972). Hard keratins can contain up to 22%

cysteine in horns and nails, while flexible keratins can be found in hair, wool, feathers, and skin (10-14% cysteine, Filipello Marchisio, 2000).

Feather keratins are homogenous in terms of molecular weight. Feather barb and quill keratins are composed of 10 kDa units (Figure 2.2). Other keratins, as such from mammals (hair and wool keratins) are more heterogeneous proteins having a range of molecular weight from 10-75 kDa (Figure 2.2). Three main types of keratins can be identified from mammals tissues; keratin type I (acidic, 40-50k kDa), II (neutral/basic, 55-65 kDa), and keratin associated proteins (KAPs) which form extensive crosslinking with intermediate filaments through disulfide bonds, affecting strength and rigidity (Wu et al., 2008).

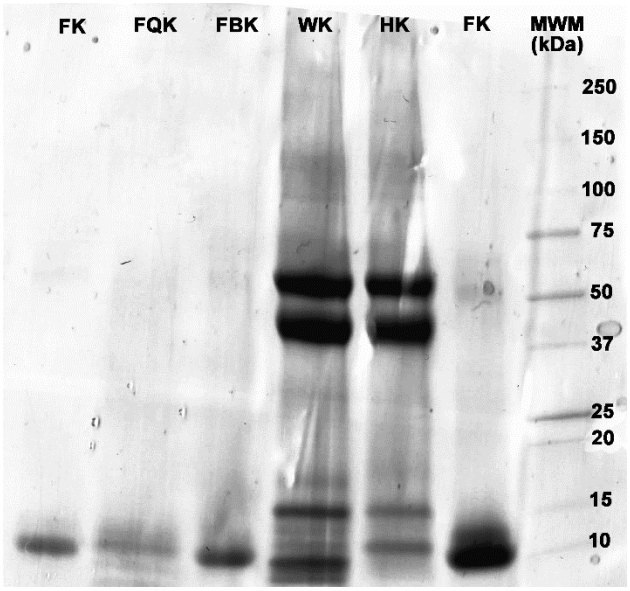

Figure 2.2. SDS-PAGE of keratin extracted from chicken feathers (FK), hair (HK), wool (WK), chicken feather barbs (FBK), and chicken feather quills (FQK).

In addition to the density of disulfide bonds, the organization of keratin's secondary structure also plays a major role in the mechanical resistance and flexibility of keratinous tissues. Early studies on x-ray diffraction identified important differences in secondary structure of keratins. α-

helical keratins (α-keratins) are more flexible proteins than β-sheet keratins (β-keratins). α-keratins undergo a α-helix→β-sheet transition when stretched; this transition is irreversible above 30% stretching (Astbury and Bell, 1941). Mammalian keratins are mostly formed by α-helices (Astbury and Woods, 1934). These helical domains are present in the central part of keratin filaments and assemble into heterodimers coiled coil structures by combination of basics and acidic subunits (Yu et al., 1993). In the case of feather keratins, they are mostly composed of β-sheet structures. β-keratins in feathers are twisted and held together by turns forming a helical filament (Fraser and Parry, 2008). Small portions of α-helix keratin can be found in feather barbs and barbules and down feathers, especially in the early development of feathers (Alibardi and Toni, 2008; Ng et al., 2012). It is estimated that the phase transition temperature of barbs is around 235°, whereas for quills is around 220°C (Schmidt, 2001). This is due to a more organized structure of keratin in barbs.

2.1.2. Extraction/solubilization of keratins

The abundance of disulfide and hydrogen bonds and semi-crystalline conformation of keratin in tissues, make their extraction a complex process (Goddard and Michaelis, 1934). Keratin is highly insoluble in water. Extraction of keratin in boiling water for 12 hours only yields 1.6% of keratin (Crewther et al., 1965). The most common approach is to solubilize keratins by disrupting disulfide and hydrophobic/hydrogen bonds interactions (Nakamura et al., 2002). Disruption of hydrophobic/hydrogen bond interactions is necessary to swell and expose amino acids from the crystalline structure of keratin. This is commonly achieved with high concentrations of urea (5 to 8 M), thioglycolic acid at alkaline pH (8 and higher), or guanidine hydrochloride (Crewther et al., 1965; Zoccola et al., 2009). Thiol chemicals such as mercaptans,

thioglycolic acid, and dithiothreitol disrupt disulfide bonds through disulfide exchange reactions (Figure 2.3). Sulfites action relies on sulfitolysis reaction (Figure 2.4). Sodium disulfide reduce disulfide bonds with the formation of perthiocysteine (Figure 2.5). Among disulfide reducing chemicals sulfites and sodium sulfide are considered safer and industrially viable (Poole et al, 2011; Nakamura et al., 2002). Disruption of disulfide bonds with thiols, sulfites, and sodium sulfite yields highly reactive cysteine thiols. It was noted that upon dilution or dialysis of disulfide reducing chemicals, keratin formed small aggregates (Woodin et al., 1953). In order to impart stability in water solutions several modifications during or post extraction including chemical blocking or oxidation of thiols, use of detergents, and partial or full hydrolysis have been considered (Schrooyen et al., 2000; Schrooyen et al., 2001; Ikkai and Nato, 2002).

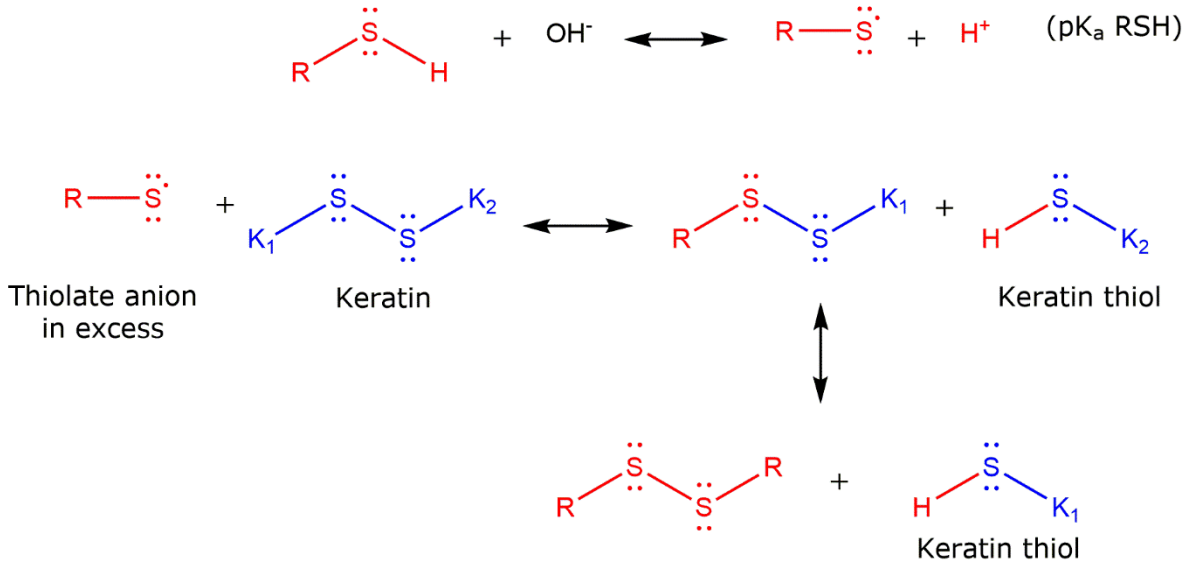

Figure 2.3. Scheme of thiol-disulfide interchange reactions. Thiol compound (RSH) is dissociated to give thiolate anion under basic pH. The pH for increased rate of dissociation depends on the pKa of the thiol compound. The thiolate anion formed is the reactive specie in the thiol-disulfide reaction. Thiolate is highly nucleophilic and attack sulfur atoms forming disulfide

bonds. The reaction proceeds favorable to the formation of keratin thiols if the thiolate anion is in excess (Singh and Whitesides, 1993).

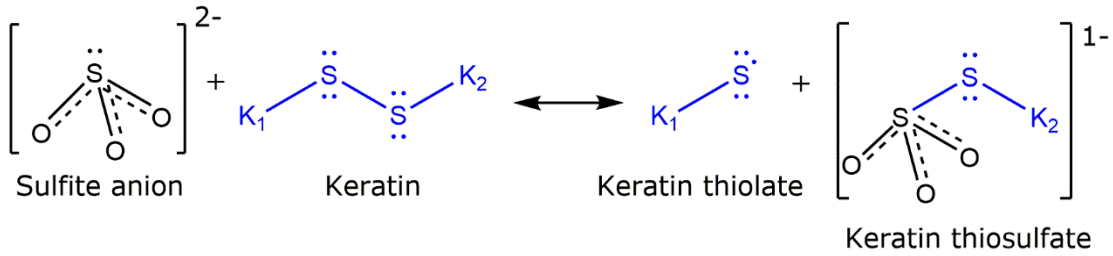

Figure 2.4. Schematic of sulfitolysis reaction. Sulfite anion (and also bisulfite HSO_3^-) are the main nucleophilic species attacking the sulfur atoms forming disulfide bonds in keratin. The reaction produces keratin thiolate (that can be protonated to form keratin thiol) and keratin thiosulfate (also named S-sulfo keratin, or S-sulfocysteine). The reaction proceeds faster at pHs between 3-7 (Wolfram and Underwood, 1966).

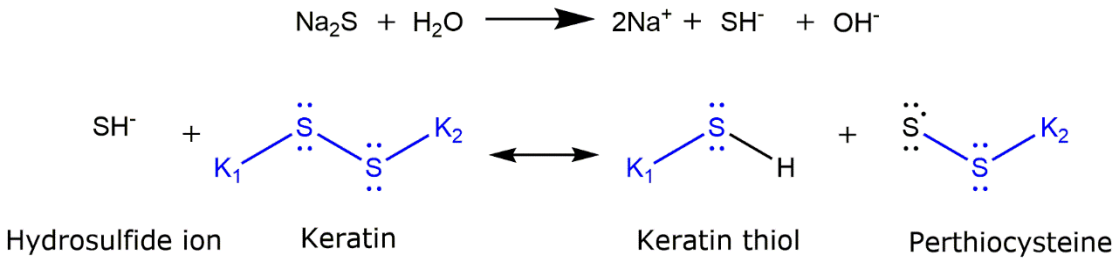

Figure 2.5. Sodium sulfide reacts in water to form the hydrosulfide and hydroxyl anions, which result in increased pH. The hydrosulfide anion attacks the disulfide bond giving keratin thiol and perthiocysteine. Perthiocysteine decomposes into sulfur and cysteine (Poole et al., 2011).

Cysteine thiol groups in keratins have strong nucleophilic tendency; they can react with iodoacetic acid, iodo acetamide, acrylates or anhydrides, to produce modified keratin (Schrooyen

et al., 2000; Ikkai and Nato, 2002; Hu et al., 2011; Reddy et al., 2013; Han et al., 2015). Upon modification, the thiol group remains permanently blocked and disulfide bonds cannot reform, which generally results in increased solubility (Schrooyen et al., 2000). Anionic detergents such as sodium dodecyl sulfate (SDS) added into extraction solutions, result in the formation of keratin-detergent complexes that help stabilize keratin in solution by electrostatic repulsion between SDS-keratin micelles (Schrooyen et al., 2001). Extraction with thioglycolic acid at pH 10-11 effectively solubilizes keratin but result in partial hydrolysis of keratin and reduction in the arginine content (Hill et al., 2010; Richter et al., 2012). Sodium sulfide extraction produces alkaline conditions (pH ~12) that hydrolyze keratin (Goddard and Michaelis, 1934; Nagai and Nishikawa, 1970; Poole et al., 2011; Wang et al., 2012). Chemical changes and crosslinking of amino acid, such as formation of dehydroalanine, lysinoalanine and lanthionine, also result from alkaline conditions (Asquith and Carthew, 1972; Friedman 1999; Poole et al., 2011). Depending on the time and temperature, alkaline conditions result in more severe damage of keratin (Coward-Kelly et al., 2006). Alkaline hydrolysis of keratin (pH > 10) in absence of disulfide reducing chemicals can split peptide bonds leaving the disulfide bonds intact (Crewther et al., 1965). Feather keratin treated with 0.1M NaOH at 90°C for 15 min resulted in half of the keratin being soluble and the other half removed by dialysis as free amino acids (Nagai and Nishikawa, 1970).

Blocking of cysteine thiol, and hydrolysis affect the chemical, conformational, and crosslinking ability of keratin. The use of harmful chemicals including persistent SDS-protein complexes that are difficult to remove can cause toxicity problems (Maclaren et al., 1968; Marshall and Williams 1986; Van de Sandt et al., 1995; Nakamura et al., 2002).

2.2. Bio-based plastics

The development of cost-effective plastics from renewable resources has emerged as an alternative for petroleum based materials. The great challenge is to develop materials from natural resources (bio-based) with comparable properties to those of conventional plastics. Bio-based plastics have also gained attention because of their potentially friendly environmental properties, such as, low carbon footprint, biodegradability and compostability (Gironi & Piemonte, 2011). Polymers from renewable resources including starch, cellulose, polysaccharides, lipids and proteins, have received special attention by researchers (Reddy et al., 2013).

Several protein raw materials can be found as wastes or low cost by-products from food industry activities. These include keratin, collagen, whey, gluten and pressed residue from oilseeds processing. Protein-based plastics can be considered for several types of applications like packaging, agriculture, biomedicine, coating and structural materials.

2.2.1. Protein-based plastics

Proteins are formed by combination of 20 amino acid monomers assembled in a polypeptide chain. The unique amino acid composition of a protein defines properties such as, secondary structure, hydrophobicity, thermal stability and solubility. Protein chains fold due to the formation of multiple inter- and intra-molecular interactions among amino acid functional groups. Hydrogen bonds, hydrophobic interactions, salt bridges and disulfide bonds lead to the formation of tertiary and quaternary protein structures.

The transformation of proteins into plastic materials relies on unfolding or denaturation of the protein by either thermal or chemical means. Once a protein is unfolded, the removal of

denaturing chemicals, cooling down or drying would allow the formation of new protein-protein interactions, leading to the alignment of protein chains into a different three dimensional network (Verbeek and van den Berg, 2010). A very common processing aid is plasticizer molecules. Plasticizers help improve the ductility of proteins that otherwise would yield a very brittle plastic. According to the International Union of Pure and Applied Chemistry (IUPAC) a plasticizer is "a substance or material incorporated in a material to increase its flexibility, workability or distensibility". Plasticizers lower the denaturation temperature of proteins by interfering with protein-protein interactions and increasing the inter polymer chain distance (Verbeek and van den Berg, 2010).

One of the great limitations of protein plastics is their poor mechanical performance, and high hydrophilicity. The great extent of hydrophilic pendant functional groups and incorporation of hydrophilic plasticizers result in the absorption of moisture, which soften and compromise the mechanical stability of protein plastics. Several attempts having basis on the chemical modification (i.e. acylation [Braüer et al., 2007; Hu et al., 2011], etherification [Reddy et al., 2011], grafting functional groups and monomer co-polymerization onto protein reactive side chains [Xi et al., 2005; Liu et al., 2008; Jin et al., 2011]), incorporation of hydrophobic plasticizers (Song and Zhen, 2008; Ullah et al., 2011), polymer blends (Graiver et al., 2004; Fang et al., 2009), and incorporation of cellulose fibers (Liu et al., 2005; Huang and Netravali, 2009) and nanoparticles (Luecha et al., 2010; Kumar et al., 2010) have been performed to overcome the limitations of bioplastics. In most cases, the simultaneous improvement of different bio-based plastic properties requires a combination of more than one of the approaches listed above.

2.2.2. Nanocomposites

Bio-based nanocomposites consist of a bio-based polymer matrix reinforced with strong and tough particles having at least one dimension in the nanometer range (1-100 nm) (Marquis et al., 2011). Nanocomposites have been investigated to overcome limitations of bio-based materials such as poor mechanical properties, as well as barrier properties. The dispersion of nanoparticles (1-100 nm) with high aspect ratio (ratio of length to thickness) and surface area, results into numerous interfacial contacts with polymers; therefore the mechanical load is transferred effectively to the nanoparticles. Due to the high aspect ratio and surface area of nanoparticles, the reinforcement of polymer matrix is usually achieved at low concentrations of less than 10% of the blend composition (Mittal, 2011).

Several types of nanoparticles, such as nanoclays, nanocarbons, metal oxide nanoparticles and cellulose nanofibers have been used as reinforcement, mostly in synthetic polymers, but also in some natural polymers mainly focused on dispersion nanoclays into starch (Cyras et al., 2008), chitosan (Darder et al., 2006), soy protein (Sasmal et al., 2009) and poly(lactic acid) (Bhatia et al., 2009). Among the different nanoparticles, nanocarbons such as graphene and graphene oxide represent the most promising material for use as reinforcement.

2.2.2.1. Graphene/graphene oxide

Graphite is an abundant carbon material that is formed by multiple graphene layers. Graphene is a material composed by a single layer of sp^2-hybridized carbon atoms packed in a hexagonal lattice that displays exceptional thermal, mechanical and electrical properties. The high interest in graphene raised in the last decade is due to the isolation and characterization of a single graphene nanosheets using scotch tape (Novoselov et al., 2004). Despite the great

properties of graphene its use is limited to the cost/efficient production of high purity single layer graphene (Potts et al., 2011).

The large scale production of graphene starts with the chemical oxidation of graphite, which result in graphite oxide (Figure 2.6). Graphite oxide is an early stage product in the production of single graphene-like sheets. It is composed of multiple layers of oxidized graphene (graphene oxide). The oxidation of graphite is traditionally performed using sulfuric acid, sodium nitrate, and potassium permanganate (Hummers and Offeman, 1958). The nitronium ion NO_2^+ from nitrate reacts with aromatic rings of graphene sheets in the presence of sulfuric acid (Figure 2.7). Further addition of potassium permanganate ($KMnO_4$) creates dimanganese heptoxide (Mn_2O_7) which is the main oxidizing specie in the reaction system (Figure 2.8). Mn_2O_7 is known to react violently with organic species and to selectively oxidize aliphatic double bound over aromatic double bonds (Tromel and Russ, 1987). The method is simple and produce high yield of graphite oxide. Graphene oxide sheets contain many functional groups including hydroxyl, epoxy, carbonyl and carboxyls that make it highly hydrophilic and water dispersible. This property allows further introduction of functional groups on its surface making it interesting for the development of nanocomposites (Stankovich et al., 2006). In addition, the abundance of oxygen functionalities make graphite oxide compatible with hydrophilic polymers, such as proteins.

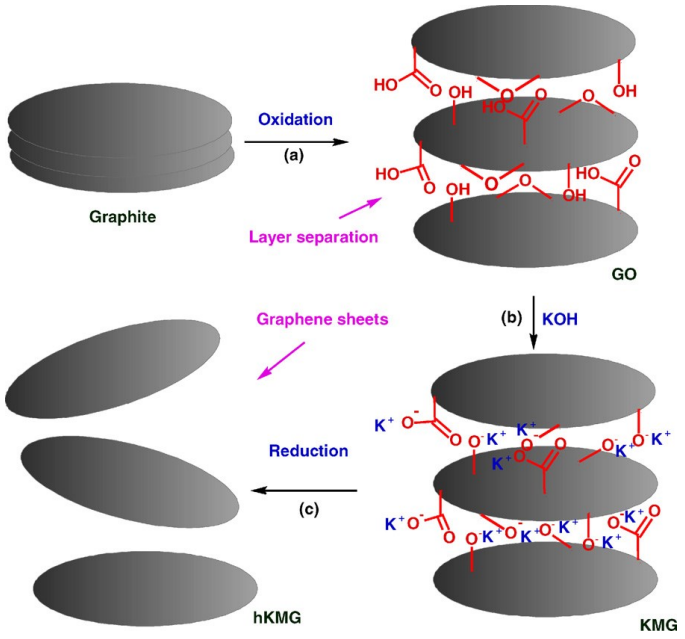

Figure 2.6. Schematic representation of main steps involved in preparation of graphene oxide. Graphite stack is oxidized to separate graphene platelets; graphene oxide is dispersed in water and treated with KOH (b), and finally reduced with hydrazine (c). (Reprinted from Kuilla et al., 2010, with permission).

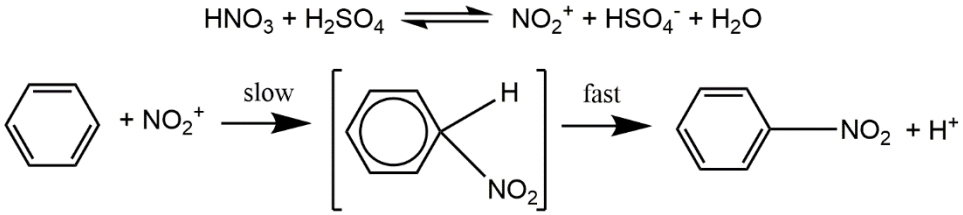

Figure 2.7. Schematic reaction of nitronium ion with aromatic rings in graphene.

Figure 2.8. Schematic reaction in the generation of the oxidizing specie MnO7.

There is limited information in the literature on the effect of graphene or graphene oxide on mechanical properties of bio-based plastic nanocomposites. Li et al. (2011) were able to increase the tensile strength of starch from 4.6 to 13.8 MPa by incorporation of 2.0% of graphene oxide. Ma et al., (2013) found a more pronounced effect of graphite oxide compared to reduced graphite oxide (graphene) on the tensile strength of thermoplastic starch. This was explained by the better compatibility between hydrophilic macromolecules (e.g. starch) and graphite oxide.

2.2.3. Processing

The development of composites and polymer blends has been mainly studied in solvent-based systems. This is not convenient for the production of large amounts of material and scale-up in the plastic industry. Solvent-based systems require large reactions tanks unable to operate in continuous mode; moreover, it implies the utilization of large amounts of hazardous solvents.

Melt processing such as extrusion can be performed in a single continuous process. In extrusion, the blend of polymer and additives are mixed at high temperature without the use of large amounts of solvents. This can be seen as an economical and environmental advantages. The use of extrusion as a reactive system has been reported in the chemical modification of functional groups of biopolymers, as well as in the production of fiber reinforced composites, carbon nanocomposites and highly exfoliated layered silicate bio-nanocomposites (Carlson et al., 1999; Dennis et al., 2001; Raquez et al., 2008; Villmow et al., 2008; Mulinari et al., 2009).

Extruder configuration features such as, type of screw (single or twin), screw sections or configurations (mixing, conveying and kneading zones), length, clearance between screw and barrel, feeding and heating zones and die geometry are important elements that influence the extent of chemical reactions (Janssen, 2004). Control of the reaction time in polymer processing

by extrusion is an important variable that can be manipulated by changing the screw speed, feed rate and extruder configuration. An extended time of reaction can be achieved by decreasing the screw speed and feed ratio; however, this may result in changes in reaction mixing efficiency and productivity, respectively.

In extrusion polymer-nanoparticle blends are subjected to high temperature and subjected to shear forces. The nanoparticles are exfoliated, and homogenously dispersed in the melted polymer (Mittal, 2011).

2.2.4. Keratin-based plastics

Feathers barbs have been used as reinforcement in synthetic polymer plastics. The resultant composites have shown improved mechanical and thermal properties (Barone et al., 2006; Uzun et al., 2011; Ahn et al., 2011; Barone et al., Huda and Yang, 2008; Ghani et al., 2013).

The highly cross-linked organization of keratin in feathers is an impediment for the development of thermoplastics. Thermoplastic formation of feathers is achieved by heat denaturation of keratin followed by re-crosslinking during cooling down. Reduction of disulfide bonds as well as the incorporation of plasticizers has been reported to improve the thermal processing of feather bioplastics (Barone et al., 2006; Ullah et al., 2011).

Several authors have reported the fabrication of films from chemically modified keratin films in order to reduce plasticizer content. Carboxymethylation of cysteine thiol groups of keratin using iodoacetamide, iodoacetic acid and bromosuccinic acid in the presence of 2-mercaptoethanol has been reported (Schrooyen et al., 2000). The carboxymethylation of cysteine thiol groups resulted in an increased keratin solubility; however, a high degree of modification of cysteine thiol groups which lead to decreased free thiol groups and thus reduced disulfide bonds

after re-oxidization, which resulted in poor mechanical properties of S-carboxymethylated feather bioplastics. Jin et al., (2011) reported the solution grafting of poly(methyl acrylate) (PMA) onto the surface of feathers in order to improve their thermoplastic properties. A grafting efficiency of 35% was obtained with a molar ratio of reductant/oxidant of 1.0, concentration of oxidant 0.010 mol/L, time 4 h, monomer concentration 40%, pH 5.5 and temperature of 60°C. The thermomolded feather-g-PMA films (feather grafted with poly(methyl acrylate), conditioned at 65% RH and 21°C x 24 h) had a tensile strength of 206.3 MPa, Young modulus 28.8 GPa and elongation at break 1.1%. The authors suggested that thiol groups are the preferred grafting sites in feather keratin. Martinez-Hernandez, (2003) have suggested that other groups such as N-H and O-H of keratin can act as reaction sites when grafting methyl methacrylate using a $KMnO_4$/malic acid redox system. Reddy et al., (2011) reported the etherification of whole feathers (fiber and quill) in solution with acrylonitrile to improve their thermoplasticity. Etherification of feathers hydroxyl groups resulted in lower tensile strength but higher elongation than the control in compression molded films prepared with 20% of glycerol. Hu et al., (2011) optimized the conditions for acetylation of chicken feathers in solution under acid conditions with acetic anhydride. Acetylated feathers were compression molded in the presence of 20% of glycerol, showing better transparency and thermoplasticity than unmodified feathers; however, mechanical properties of acetylated feather films were not reported.

2.3. Tissue engineering

It is well known now, that cells behave differently when cultured in flat surfaces than in three-dimensional substrates. Three-dimensional biomaterials (scaffolds) fill a gap in the injured tissue and provide a physical framework for cell colonization and regeneration. This can result in faster

healing and absence of scars in injured tissues (Groeber et al., 2011). The development of scaffolds requires an understanding of the cell behaviour and its surrounding environment in the tissue. These concepts will have an influence on the fabrication of biomaterials through the selection of macromolecules and polymers and different processing techniques. Therefore, the following sections will emphasize on the biology of cells and tissues and technology aspects for the development of cell scaffolds.

2.3.1. Animal cells and tissues

Cells are the essential building blocks of living organisms. It is estimated that there are more than 210 different types of differentiated cells in the mammalian body (Slack, 2007). Each cell type has a different subset of expressed genes and hence synthesizes different proteins and performs different functions. Different cells organize into three-dimensional structures forming different tissues, which subsequently organize into organs.

Most cells in the body can be classified into epithelial or mesenchymal cells. Epithelial cells adhere to each other forming a sheet of cells or epithelium. The epithelium usually covers the surface of tissues and lining of organs. For example the outer layer of skin (epidermis) is formed by a hierarchical structure of stacked epithelial cell (keratinocytes) layers. At difference from epithelial cells, mesenchymal cells are mostly scattered cells embedded in loose extracellular matrix. An example of mesenchymal cells are fibroblasts cells in the dermis. Fibroblasts are scattered in a soft extracellular matrix composed of proteins, and glycoproteins.

The formation of embryonic tissue involves cells dividing in an active manner through the cell cycle. In the first stage of the cycle the cell grows larger physically (G1 phase). In the second stage the cell synthesizes a full copy of the DNA in the nucleus. In the next stage the cell

will continue to grow and prepares for mitotic phase, in which the cell divides copying DNA and cytoplasm making two new cells (White and Dalton, 2005). At difference from embryonic development, most cells in mature organisms are in a reversible quiescent state (G0 phase, they have exited the cell cycle). For instance neurons and muscle are formed by active cell growth (division) and differentiation in the embryo but are quiescent in the adult organism. Similarly, fibroblasts in the connective tissue although remaining metabolically active they remain in a quiescent state in mature organisms (Lemons et al., 2010). However, quiescent cells can enter the cycle again and start dividing upon certain stimuli including damage of tissue. Stem cells are also recruited and differentiated to help healing (Cheung and Rando, 2013).

2.3.2. Cell culture

The fundamentals of in vitro cell culture were elucidated in the beginning of the 20th century. Pioneer work of the anatomist Ross Harrison in 1907 observing the growth of nerve fibers from explanted neural tubes from frog embryos triggered future developments. Cells were disaggregated by trypsinization from tissue explants and subsequently plated for the first time by Rous and Jones in 1916. Fibroblasts were subcultured by Carrel and Ebeling in 1923. However, advances in the 1950s with the establishment of continuous human cell lines (Gey et al., 1952) and defined culture media (Morgan et al., 1950; Dulbecco, 1952; Eagle 1955) defined more clearly the current protocols for tissue culture.

Cells are obtained from tissues by cellular outgrowth of explants of by enzymatic or mechanical disaggregation. The process is highly selective and facilitates the recovery of a pool of cells in a proliferative state. The primary culture obtained contains different cell types.

Subsequent isolation of particular cell types involves selective culture conditions and physical cell separation, which yields a cell line.

Cells are predominantly cultured on flat glass or plastic substrates. Cells require of particular conditions for culture such as a defined media with nutrients, pH, humidity, temperature and oxygen. The culture media contains a variety of cell nutrients, sugars, amino acids, and salts. Animal serum (from fetal bovine usually) is usually supplemented to the media to provide low levels of hormones and growth factors. The serum is obtained by centrifugation of coagulated blood from fetuses of up to three months. Due to its complexity and source variability, the exact composition and reproducibility of serum cannot be replicated (Gstraunthaler, 2003).

Cells cultured on flat surfaces adhere to the bottom through specific proteins synthesized during the first hours of incubation. Cells are capable of growing exponentially in vitro. Once they cover the available surface they need to be disaggregated (enzymatically or mechanically) and a small aliquot is re-seeded in a new flask. This process (sub-culturing) is necessary as over confluent cells tend to round up, detach from the surface and die (Freshney, 2006).

The culture of cells on flat surfaces such as petri dishes was adopted as a standard method in research. The conventional culture of cells in two-dimensional (2D) substrates has been of great importance in the understanding of cell biology, however it is not adequate to reproduce the complex and dynamic environment of body tissues (Baker and Chen, 2012). It has been demonstrated that cells (originally in a three-dimensional tissue environment) confined to a planar monolayer in vitro, exhibit unnatural behavior (Tibbitt et al., 2009). The dynamic three-dimensional (3D) environment of cells coordinates an intra-cellular signaling cascade that influences the cell phenotype and ultimately protein expression (Birger-dotter et al., 2005). As a

consequence, cells in 2D environment can exhibit reduced functionality and altered metabolism (Zhang 2004; Chukierman et al., 2001). For example, breast epithelial cells develop like tumor cells when cultured in 2D (Bissel et al., 2002). 3D substrates were developed with the aim to overcome the limitations of traditional 2D culture. 3D matrices offer a porous environment for cells. The main goal of 3D matrices is to mimic the extracellular matrix (ECM) environment of body tissues.

2.3.3. Cell-extra cellular matrix interactions

The extra cellular matrix (ECM) is the structural component that surround cells in multicellular organisms. It is composed of proteins, glycosaminoglycans and glycoproteins forming a water-swelled fibrous network in which cells are embedded. (Frantz et al., 2010). The ECM provides mechanic strength and structure of tissue. It also plays a key role in signaling and interactions between cells and cell-ECM. Cells adhere to ECM proteins including fibronectin, laminin, vitronectin, and collagen. Cell-ECM interactions are of significant importance in many cell processes including adhesion, migration, growth, differentiation, ECM remodeling and survival (Daley et al., 2008). Cellular adhesion to ECM is mediated by trans-membrane glycoproteins called integrins. Integrins are heterodimers composed of α and β subunits. 18 α subtypes and 8 β subtypes have been identified which results in 24 known integrin pairs (Barczyk et al., 2009). In the interior of the cell integrins are attached to a bundle of actin microfilaments, while at the outside they attach to ECM proteins (Figure 2.9). The actin-integrin adhesion is mediated by linker proteins while integrin-ECM interactions are mediated by particular amino acid sequences present in ECM proteins (Parsons et al., 2010). One of the most studied integrin ligands is the tripeptide motifs arginine-glycine-aspartic acid (RGD), which is present in proteins of the ECM

(e.g. fibronectin, vitronectin and collagen). Although many proteins contain this motif in their sequence only a limited number are likely to mediate cell attachment. This is mainly due to physical availability of the RGD motif at the surface or because certain neighbour amino acids, such as proline, affects its binding properties. Other integrin binding motifs include leucine-aspartic acid-valine (LDV), leucine-arginine-glutamic acid (LRE), arginine-glutamic acid (RE), lysine-glycine-aspartic acid (KGD) and arginine-leucine-aspartic acid (RLD) (Ruoslahti 1996). Cells sense mechanical stress through integrin-mediated signaling. Therefore, cell-ECM interactions are of significant importance on cell behavior.

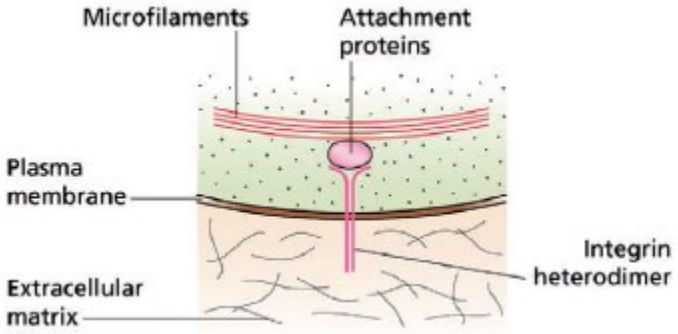

Figure 2.9. Schematic of cellular adhesion to the ECM (Reprinted from Slack, 2007, with permission).

The adhesion of cells cultured in vitro depends on the presence of ECM proteins in the serum supplemented media (fibronectin and vitronectin) as well as the synthesis of cell's own ECM proteins. In the past, glass and polystyrene were widely used; however, they resulted in limited cell adhesion. Nowadays traditional 2D culture substrates include modified polystyrene which has been treated to increase its hydrophilicity and therefore facilitate the adsorption of ECM proteins on the surface. Other methods include coating of surfaces with collagen. The attachment of cells depends mainly on the presence of integrin binding motifs but also on the

surface properties of the substrate. Several properties including surface wettability, topography, and protein conformation at the interface affect the selective adsorption of proteins to substrates (Thevenot et al., 2008). For instance hydrophilic/hydrophobic balance has been shown to affect the adsorption of serum proteins such as laminin, fibronectin and vitronectin that mediate cell attachment (Arima and Iwata, 2007). For instance these proteins are not readily absorbed to very hydrophilic surfaces, they rather absorb at surfaces with an intermediate wettability (Tamada and Ikada 1993; West and Hubbell 1997). Arima and Iwata (2007) concluded that increased protein absorption resulted in higher cell adhesion at contact angles between 40-70° and that it was also dependent on the surface functional groups.

2.3.4. Cellular Scaffolds

Tissue engineering relies on fabrication of three dimensional porous materials in which cells can attach, proliferate, differentiate and regenerate tissues. Cells use porous microarchitectures as a framework for the tissue regeneration. Hence, they have been commonly known as cellular scaffolds. Cell scaffolds offer promising applications in treatment of tissue injuries (e.g. skin, bone, cartilage and nerve) and organ dysfunction. Their successful application is particularly important considering the limitations of traditional treatments. For example, grafting and transplantation of tissues and organs are restricted to the availability of healthy tissues, and to the suitability of extra surgery procedures that it implies (autografts), or due to immunogenic responses, availability of donor's tissues and biocompatibility issues (allografts and xenografts) (Bose and Bandyopadhyay, 2013).

The main functions of cell scaffolds include the promotion of cell adhesion, extracellular matrix deposition, transport of gases and nutrients for cell survival, and cell proliferation and

differentiation. Scaffolds should biodegrade (by enzymatic cleavage or hydrolysis) at a rate paired to rate of tissue regeneration, and should provoke a minimal degree of inflammation or toxicity when implanted (Freed and Guilak, 2007).

Upon implantation proteins from blood adsorb rapidly onto biomaterial's surface, which triggers a series of reactions, known as the foreign body reactions (FBR). Aggregation and activation of platelet-fibrin layers is followed by the recruitment of inflammatory cells. Neutrophils from the blood stream arrive to wound site clearing out dead cells, bacteria and exogenous debris. The scaffold implanted is recognized as a foreign material but neutrophils are unable to phagocytose it. During this process cytokines released from neutrophils cause the differentiation of monocytes into macrophages. Macrophages attempt to remove the foreign body by phagocytosis, and secretion of enzymes and reactive species that aggravate the inflammatory response to chronic levels. If the material cannot be degraded, macrophages fuse into foreign body giant cells that surround the scaffold. Fibroblasts are recruited to the interface and secrete collagen layers around the foreign body forming a fibrous capsule in order to isolate it from the tissue.

The nature and conformational properties of adsorbed blood proteins may determine the response of macrophages; hence the integration of biomaterials within the body. Although it is not well understood, several factors including specific adsorption of blood proteins can affect the differentiation of macrophages from pro- to anti-inflamatory behavior (Sridharan et al., 2015). For instance small peptide sequences on fibrinogen are known to mediate a pro-inflammatory response on implanted surfaces (Thomsen and Gretzer, 2001). Modification of surface properties, including hydrophilic/hydrophobic balance, charge, and topography can affect the nature of the protein layer adsorbed and hence FBR outcome (Wilson et al., 2005). Several

attempts to modify the surface properties to control the adsorption of proteins have been developed, including PEGylation of surfaces or coating with other anti-fouling polymers and proteins (Chang et al., 2009). These approaches can minimize the effect of adsorbed proteins for biomaterials not intended to integrate with the body (e.g. sensors, drug delivery systems, hearth valves, catheters). However, this is a disadvantage for scaffolds intended for tissue regeneration. Without cell-adhesion proteins cells cannot infiltrate, adhere and remodel the scaffold for tissue regeneration). Although not completely understood, biomaterials containing ECM proteins have been used to modulate the response of immune cells to a pro-healing state and to promote host cells integration and tissue regeneration (Yu et al., 2015).

The mechanical properties of scaffolds have great influence on cell adhesion, growth, morphology and ultimately on tissue regeneration (Hoffman et al., 2011). For example the stiffness of scaffolds affect the adhesion and migration of fibroblasts. Yeung et al., (2005) found that actin microfibres were not developed when fibroblasts were cultured on soft substrates and that fibroblasts adhere and spread better on stiffer substrates. On the other hand, neurons develop more extended branches when cultured in soft substrates (Flanagan et al., 2002). It is believed that cells express a similar phenotype in scaffolds of similar stiffness of the original tissue (Bhana et al., 2010). It is not completely understood how cells can sense the stiffness of the ECM or scaffold when cultured in vitro. However, it is believed that upon stress, mechano-sensitive proteins, such as integrins, cadherins and platelet endothelial cell adhesion molecule-1 (PECAM-1), transmit mechanical signals to the cell that result in an increase of cell stiffness (Matthews et al., 2006).

2.3.4.1. Material selection

Scaffolds have been fabricated from different polymers and with different techniques into several morphologies including hydrogels, non-woven mats of nanofibers and films. Overall the selection of materials and techniques has great influence on the physical and biological properties of scaffolds.

Synthetic polymers such as poly(lactide), poly(glycolide), and poly(caprolactone) or their co-polymers, poly(ethylene glycol) (PEG) and poly(vinyl alcohol) (PVA) have been widely used for the development of tissue engineering scaffolds (Stratton et al., 2016). They possess suitable mechanical properties and good production reproducibility. The major limitation of synthetic polymers is lack of cell-specific integrins that affect adhesion, migration and cell-mediated biodegradation (Zhu and Marchant, 2011). In addition, it is recognized that the degradation products of some polymers (poly(lactide), poly(glycolide), and poly(caprolactone)) can lead to a drop in the local pH that can affect cells and tissues (Yoon and Fisher, 2009). Some strategies to overcome these limitations have been focused on modification of polymers by grafting or blending with hydrophilic natural and synthetic polymers.

The use of naturally derived polymers and especially proteins that are found in the extracellular matrix of tissues such as collagen, elastin, fibronectin and laminin has been widely explored to prepare scaffolds (Malafaya et al., 2007; Madaghiele et al., 2014). Due to the presence of integrin binding motifs sequences, proteins have shown to promote better cellular recognition and attachment. Main limitations in their use are their production variability, concerns about transmission of infectious agents and viruses, poor mechanical properties, fast biodegradation, and use of harmful cross-linking agents (Parenteau-Bareil et al., 2010; Dong and Lv, 2016). Strategies to solve some of these issues comprise the fabrication of scaffolds from

blends of synthetic polymers and proteins, use of harmless crosslinking methods, and use of different scaffold fabrication methods (Stratton et al., 2016; Ratheesh et al., 2016).

2.3.4.2. Hydrogels

Hydrogels are insoluble crosslinked polymeric materials that are able to retain substantial amount of water. They are very attractive materials to mimic the mechanical, microstructural features of the ECM. They have been widely explored for tissue engineering applications including wound dressings and drug and cell delivery for regeneration of skin, cartilage, smooth muscle, bone, nervous and adipose tissues (Drury and Mooney, 2003; Madaghiele et al., 2014).

Gel forming polymers can be of synthetic or natural origin. Water soluble synthetic polymers such as PEG and PVA form high viscosity solutions by entanglement of polymer long chains and interaction with water molecules. At a certain concentration the extent of hydrogen bonding between the polymer and water molecules and polymer entanglement difficult the free movement of water molecules. However, hydrogen bonds are not very strong in nature, they are weak and time-dependent. Therefore, water will tend to drain over the time. In order to promote stability crosslinking methods must be used. For example, covalent crosslinking between PEG chains can be achieved Ultra-violet (UV) exposure (Bryant and Anseth, 2001). PVA for instance can be physically crosslinked by repeated freeze-thawing cycles (Cascone et al., 1995), or chemically crosslinked with glutaraldehyde (Nuttelman et al., 2001), succinyl chloride, adipoyl chloride, sebacoyl chloride (Orienti et al., 2001) or citric acid at high temperatures (Shi and Yang, 2015).

At difference from synthetic polymers, proteins are formed by amino acids that carry different functional side groups including amino, carbonyl, thiol, and hydroxyl groups. The

formation of protein hydrogels can be seen as a two-step process, in which proteins are first denaturated or unfolded, which can be achieved by physical methods such as heating or high pressure or by the use of a denaturing chemical. The denaturation of protein causes the exposure of functional groups and hydrophobic portions that were inaccessible to solvent molecules initially. The second step involves the re-organization of denatured protein by formation of new protein-protein and protein-solvent molecular interactions. Upon exposure in aqueous media, hydrophobic groups have a strong tendency to aggregate in order to minimize the surface area in contact with water (Zayas, 1997). Depending on the properties of proteins such as molecular weight, amino acid composition, and protein concentration, the appearance and mechanical properties of gels can be affected. Generally high molecular weight and high protein concentrations are more favorable for the formation of hydrogels since both facilitate entanglement and encounter of protein chains. Highly hydrophobic proteins usually yield opaque hydrogels, whereas, more hydrophilic proteins might result in transparent and weaker hydrogels (Damodaran, 1997).

The main disadvantage of protein hydrogels is their poor mechanical properties and fast degradation. This is mainly due to the lack of covalent bonds between protein chains. Collagen and gelatin have been extensively used to produce hydrogel scaffolds. Collagen is an ECM protein with excellent cell adhesion properties, however, collagen and gelatin hydrogels tend to be weak and degrade fast under physiological conditions. Therefore, they are usually blended with synthetic polymers to fabricate composites, or cross-linked by physical or chemical methods (Annabi et al., 2009; Bhattarai et al., 2010; Van Vlierberghe et al., 2011; Kundu et al., 2012; Tirella et al., 2012; Wheeler et al., 2013; Ryan and O'Brien, 2015).

2.3.4.3. Electrospinning

Electrospinning is a promising technique for the fabrication of fibers within the range few nanometers to micrometers and very high surface area (tens to hundreds m^2/g). Electrospun fibres can be used in multiple applications, including cellular scaffolds, filters, coatings, sensors and membranes (Fang et al., 2008). In the electrospinning process a viscoelastic fluid, usually a polymer solution is fed to a capillary tip that is connected to a high voltage source. The high voltage, usually in the range of 0-30 kV or more causes a high electrostatic charge at the droplet surface. This results in droplet elongation into a conical shape known as the Taylor cone. Once the intensity of the electrical field increases to a certain value, the electrostatic forces overcome the surface tension of the solution and a liquid jet is released from the tip. The jet travels towards a collector with opposite charge or that is grounded while the solvent is evaporated (Figure 2.10).

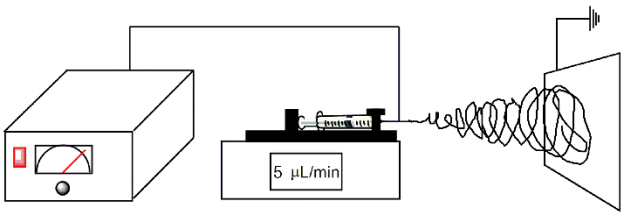

Figure 2.10. Schematic of the electrospinning setup.

The repulsion of charges at the surface causes stretching and thinning of the polymer solution, increasing the surface area of the jet. When enough charges are dissipated along the jet, surface tension of the solution tends to reduce the surface area by breaking up the jet into spherical droplets. The imbalance of electrostatic and surface tension forces results in bending instabilities during the path of the jet. Overall the bending instabilities cause further thinning of the jet before deposition (Thompson et al., 2007). In some cases the surface tension of the solution overcomes the viscoelastic forces of the jet during its path, resulting in droplets or formation of beads on a

string (BOAS) type of fibre morphologies, which are usually considered as defects (Aslanzadeh et al., 2016).

Polymer entanglements and increased electrostatic forces can overcome the effect of surface tension and prevents the jet from breaking up due to surface tension forces (Ramakrishna et al., 2005). Therefore in order to control fiber morphology one should consider the manipulation of these parameters. Polymer entanglements are closely related with the viscoelastic properties of the polymer solution, which in turn depend on the type of polymer, concentration, molecular weight, solvent and temperature. Electrostatic forces carried by the polymer and hence repulsion are closely related to the conductivity of solution, which in turn can be controlled by the type of polymer and solvent and addition of salts. In addition processing parameters such as the voltage applied can be modified to increase the charge density on the jet (Fong et al., 1999).

Fibers deposited on the collector might possess diameters from few nanometers to micrometers depending on electrospinning conditions. Usually higher solution viscosity will result in fibers with higher diameter. On the other hand, reduced fiber diameter is usually obtained by increasing the conductivity of polymer solutions. In addition other parameters including the feed rate and distance of the collector can affect fibre diameter. For instance decreasing the feed rate will allow a greater density of charges per unit of volume, which will lead to reduced fibre diameter. Similarly, increasing the distance of the collector will allow the jet travel to travel longer and stretch more, resulting in smaller fibres (Yuan et al., 2004). Nevertheless, one should be carefully when modifying such parameters in order to prevent the breakup of the jet into droplets.

Electrospun fibre mats have been considered for tissue engineering applications. Nanofibres mimic the morphology of ECM protein fibres. Mimicking the micro architecture of different connective tissues is considered a major advantage of electrospun mats for cell adhesion, proliferation and tissue regeneration. Therefore, electrospun scaffolds have been widely investigated for regeneration of tissues such as skin dermis and epidermis (Wang et al., 2013).

One of the major drawbacks of electrospinning mats is the lack of control over mechanical properties and vast packing of the fibers as they reach the collector. Due to the random orientation of fibers, electrospun mats usually tend to have poor mechanical properties (Yao et al., 2014). Crosslinking methods are often required to impart scaffold stability under physiological conditions and improve mechanical properties. In many cases crosslinking is achieved with potentially harmful chemicals and can lead to obstruction of scaffold pores (Sisson et al., 2009; Zhang et al., 2016). Overall pore obstruction can affect cell infiltration and mass transfer of gases and nutrients. Another potential disadvantage of electrospinning is the packing of fibres. Once fibres reach the collector, the opposite charge on it tends to flatten them. Subsequent deposition of fibres result in highly packed and very thin mats with fibers oriented almost exclusively in two dimensions. The limited thickness of nanofiber scaffolds and small pore size make the infiltration of cells difficult. This can be beneficial for mats used as wound dressing impeding the infiltration of bacteria to the wounded area (Lev et al., 2012). However they are a hindrance for cell infiltration in tissue regeneration. Several techniques can be used to produce fibres oriented in three dimensions including selective removal of a sacrificial polymer, collecting fibers in a water bath, and custom made collector for air collection of fibers (Wu and Hong, 2016).

2.3.4.4. Keratins scaffolds

Keratins are versatile proteins than can be used to fabricate materials with very different properties. Keratins have gained interest for the fabrication of scaffolds mainly due to their intrinsic biocompatibility, biodegradability, mechanical resistance and natural abundance (Rouse and Van Dyke, 2010). It has also been reported that keratin possesses peptide signaling sequences that promote cell adhesion. Keratins possess integrin binding domains such as leucine-aspartic acid-valine (LDV), glutamic acid-aspartic acid-serine (EDS) and arginine-glycine-aspartic acid (RGD) (Verma et al., 2008; Tachibana et al., 2002). Consequently they have shown to promote cell attachment and proliferation of different adherent cells (Yamauchi et al., 1998; Reichl, 2009; Balaji et al., 2012). Keratin hydrolyzates from chicken feathers were used to coat gelatin films in the treatment of full thickness wounds in dogs (Thilagar et al., 2007). Authors observed early formation of hair follicles and vascularization in keratin-gelatin scaffold than in basic fibroblast growth factor-coated gelatin films. Xu et al., (2013) reports that when hair keratin scaffolds were used to treat full thickness wound in rats, they showed good biocompatibility and biodegradation features; in addition earlier vascularization, less wound contraction and thicker epidermis when compared with non-treated wounds.

Reduced keratin (kerateine) scaffolds from hair have shown similar in vitro proliferation of fibroblasts than on fibronectin scaffolds (Hill et al., 2010). Degradation of subcutaneous implants of kerateine scaffolds showed slow degradation (60% of the original size after 6 months) characterized by absence of fibrous capsule formation. In addition they promoted early vascularization. On contrast, when scaffolds are prepared from keratose they tend to be more biodegradable and more suitable for short term applications (de Guzman et al., 2011).

Keratins that have been modified to block cysteine thiols (S-alkylated or keratose) tend to be more soluble in water but result in scaffolds with lower mechanical stability. On the other hand fully reduced keratins extracted in presence of thiol reducing agents (kerateines) tend to result in strong and more insoluble scaffolds. However, manipulation of fully reduced keratin solutions is challenging due to its tendency to form aggregates when thiol reducing agents are removed or diluted (Woodin 1953). Therefore, the majority of scaffolds from keratin have been fabricated from thiol-capped keratins and keratoses (de Guzman et al., 2011; Guo et al., 2015; Han et al., 20016), kerateine solutions stabilized by complexation with detergents that can remain in the scaffold (Xu et al., 2013; Xu et al., 2014; Ayutthaya et al., 2015; Fan et al., 2016; Aluigi et al., 2016), keratins extracted for long time at high temperatures that yield soluble hydrolyzates (Reichl et al., 2011) or under alkaline conditions (Hill et al., 2010).

Hydrogels and electrospun mats have been fabricated from keratin hair and wool mostly. Keratin hydrogels can be formed by removal or dilution of thiol chemicals although this method has not been widely used in the literature (Ozaki et al., 2014). Common methods usually involve air oxidation of cysteine thiols into disulfide bonds (Aboushwareb et al., 2008; Hill et al., 2010). Nakaji-Hirabayashi extracted keratins from hair and prepared hydrogels by mixing an aliquot of the solution (150 μl) with 5 mL of 30 mM MgCl and allowing the gel to sit at room temperature for 3 hours. Although the mechanism of gel formation is not discussed, the formation of hydrogel could be explained either by dilution, air oxidation or electrostatic aggregation. Keratin hydrogel have been fabricated by freeze-drying keratin solutions (Aboushwareb et al., 2008; Xu et al., 2013). Although mechanisms of gel formation have not been discussed is most likely that air oxidation during lyophilisation causes disulfide crosslinking. Thus understanding of gelation

mechanisms of keratin could lead to the fabrication of hydrogels with more controlled physical and biological properties.

Electrospinning of keratins have been investigated with the aim to produce nano- and microfibers that could have applications in tissue engineering and removal of contaminants. Other studies have merely dealt with the theory of electrospinning keratin solutions. Electrospinning of keratins is challenging due to the instability of reduced keratin solutions in absence of denaturant and disulfide reducing chemicals. Although electrospinning of keratin in the presence of these chemicals has not been studied, soluble keratins obtained by blockage of thiol groups, SDS-blends, or treated at high temperature and alkaline conditions (pH > 8) have been used for electrospinning. However, since their viscoelastic properties are not suitable for electrospinning, they need to be mixed with an aid polymer very often. Authors have reported the use of polyethylene oxide (Aluigi et al., 2008; Xing et al., 2011; Fan et al., 2016), polyamide 6 (Zoccola et al., 2007), poly(caprolactone) (Boakye et al., 2015; Jarvis et al., 2013), fibroin (Yen et al., 2016), polyvinyl alcohol (Li and Yang, 2014; Park et al., 2015), and poly(lactic acid) (Isarankura et al., 2015; Li et al., 2009) as polymer aid for the electrospinning of keratin. Few authors have reported the electrospinning of keratin without polymer aid. Keratin thiols were modified with iodoacetic acid (IAA). This modified keratin at 6% dissolved in 1,1,1,3,3,3-hexafluoro-2-isopropanol (HFIP) could be electrospun although it contained many beads. Aluigi et al., (2011) found that wool keratin extracted by sulfitolysis had low viscoelastic properties and was not suitable for electrospinning at 15% w/v in formic acid containing sulfite. However, later they report that by changing the electrospinning setup to a top-down configuration, dripping of low viscosity keratin could be avoided and fibres formed (Aluigi et al., 2013). Xu et al., (2014) were able to produce three-dimensionally oriented keratin fibres of 4.8 μm. To achieve this,

feather barb keratins were extracted for long time under mild alkaline and high temperature conditions. Solutions of extracted keratins at 25% were supplemented with SDS at 1:1 ratio of keratin. Authors reported that SDS is completely removed by dialysis and proved to support in vitro cellular growth. However, it is well known that keratin can form stable complexes with SDS (Schrooyen et al., 2001, Aluigi et al., 2007).

2.3.5. Skin tissue engineering

Skin is the largest organ of our bodies; its main function is acting as a physical barrier to the environment, protecting us against microbes, ultraviolet radiation, and toxic and exogenous compounds. Skin is composed of three main layers: epidermis, dermis and hypodermis. The epidermis is the upper layer having a thickness of 0.1-0.2 mm and consists mainly of stratified keratinocytes with different morphologies. The most upper part, the cornified stratum is formed by flattened cells that have lost their nuclei and organelles, and contain keratin filaments that have polymerized through the formation of disulfide bonds. The dermis is a vascularized tissue structurally conformed by collagen produced by fibroblasts that also produce elastin and proteoglycans. Other cells found in the dermis are mast cells and macrophages, as well as some nerve cells, sweat glands, hair roots and small quantities of striated muscle. The hypodermis or subcutaneous tissue is the thickest layer of skin, it is attached to the dermis by collagen and elastin fibers and it mainly contain adipocytes and acts as an energy reserve (Bottcher-Haberzeth et al., 2010).

After an injury, skin healing process is quite effective for small wounds in healthy patients. The wound healing process can be divided into four stages: homeostasis, inflammation, proliferation and maturation. The first step after a wound is formed has the aim to stop bleeding

at the site. Platelets aggregate to stop bleeding of injured vessels and a blood clot of fibrin is created. The inflammatory phase is characterized by the infiltration of neutrophils, macrophages and lymphocytes. Neutrophil's main function is to remove foreign microbes and cellular debris from the wound. Macrophages play a key role in the promotion and resolution of inflammation. Macrophages can undergo phenotypic transition from pro-inflammatory to anti-inflammatory (Sridharan et al., 2015). These latter trigger the transition to tissue repair. In the proliferative phases fibroblasts synthesize collagen and ECM components, while endothelial cells promote neovascularization and angiogenesis actively. In addition, re-epithelisation occurs by keratinocytes from the edges of the wound and from differentiated stem cells in hair follicles of sweet glands. The provisional tissue formed (granulation tissue) formed fills the wounded volume. In the remodeling phase vascular density is reduced and ECM is remodeled to that of normal tissue. This stage can last from weeks to years. Collagen type III produced in the proliferative phase is replaced with collagen type I. However, collagen I is deposited oriented in a single direction rather than randomly as in the original dermis, resulting in the formation of scars (Reinke and Sorg, 2012). Multiple factors can alter the healing process resulting in defective or no healing at all. Infection, vascular insufficiency, ageing, diabetes, medications, nutrition can directly or indirectly lead to impaired healing (Guo and DiPietro, 2010).

In many cases the healing process is effective without major intervention. However, the healing process of large wounds, wounds involving complete loss epidermis, or deeper involving partial the loss dermis and hypodermis require treatment. These include large and deep skin burns, diabetic and ulcer non-healing wounds, infected wounds with substantial loss of dermis, and wounds that cannot be closed without affecting motility of surrounding tissues (Groeber et al., 2011; MacNeil, 2008; Karp et al., 2003). Large wounds can result in extensive scar formation

resulting in impaired mobility and cosmetic defects. Without intervention, such wounds can result in prolonged infection, necrosis, amputation or even death of the patient. The gold standard for the treatment of such wounds is skin transplantation. Transplantation of skin and treatment for such kind of injuries; however, they are limited and expensive. Autografts are limited by the amount of available skin of the patient, and the need of an extra surgery. On the other hand allografts and xenografts may present compatibility problems and risk of transmission of diseases (Greaves et al., 2013).

Different tissue engineered materials for skin treatment are commercially available offering shorter healing periods but high initial costs (Nyame et al., 2014). Although these commercial scaffolds offer a great advance in the treatment of wounds, they have several limitations including allergy, poor integration with the host tissue, short shelf life, inadequate mechanical properties, ethical issues and high cost. Research continues with the aim to understand better the potential of natural and synthetic macromolecules scaffolds for skin tissue engineering applications.

2.4. References

Aboushwareb, T., Eberli, D., Ward, C., Broda, C., Holcomb, J., Atala, A., & Van Dyke, M. (2008). A keratin biomaterial gel hemostat derived from human hair: Evaluation in a rabbit model of lethal liver injury. *Journal of Biomedical Materials Research Part B: Applied Biomaterials,* 90, 45-54.

Ahn, H.K., Huda, M.S., Smith, M.C., Mulbry, W., Schmidt, W.F., & Ill J.B.R. (2011). Biodegradability of injection molded bioplastics pots containing polylactic acid and poultry feather fiber. *Bioresource Technology*, 102, 4930-4933.

Alibardi, L., & Toni, M. (2008). Cytochemical and molecular characteristics of the process of cornification during feather morphogenesis. *Progress in Histochemistry and Cytochemistry*, 43, 1-69.

Aluigi, A., Corbellini, A., Rombaldoni, F., & Mazzuchetti, G. (2013). Wool-derived keratin nanofiber membranes for dynamic adsorption of heavy-metal ions from aqueous solutions. *Textile Research Journal*, 83, 1574-1586.

Aluigi, A., Sotgiu, G., Ferroni, C., Duchi, S., Lucarelli, E., Martini, C., Posati, T., Guerrini, S., Ballestri, M., Corticelli, F., & Varchi, G. (2016). Chlorin e6 keratin nanoparticles for photodynamic anticancer therapy. *RSC Advances*, 6, 33910-33918.

Aluigi, A., Tonetti, C., Vineis, C., Tonin, C., & Mazzuchetti, G. (2011). Adsorption of copper(II) ions by keratin/PA6 blend nanofibers. *European Polymer Journal*, 47, 1756-1764.

Aluigi, A., Vineis, C., Varesano, A., Mazzuchetti, G., Ferrero, F., & Tonin, C. (2008). Structure and properties of keratin/PEO blend nanofibers. *European Polymer Journal*, 44, 2465-2475.

Annabi, N., Mithieux, S.M., Boughton, E.A., Ruys, A.J., Weiss, A.S., & Dehghani, F. (2009). Synthesis of highly porous cross-linked elastin hydrogels and their interaction with fibroblasts in vitro. *Biomaterials*, 30, 4550-4557.

Arai, K.M., Takahashi, R., Yokote, Y., & Akahane, K. (1983). Amino-acid sequence of feather keratin from fowl. *European Journal of Biochemistry*, 132, 501-507.

Arima, Y., & Iwata, H. (2007). Effect of wettability and surface functional groups on protein adsorption and cell adhesion using well-defined mixed self-assembled monolayers. *Biomaterials*, 28, 3074-3082.

Aslanzadeh, A., Zhu, Z., Luo, Q., Ahvazi, B., Boluk, Y., & Ayranci, C. (2016). Electrospinning of colloidal lignin in poly(ethylene oxide) N,N-dimethylformamide solutions. *Macromolecular Materials and Engineering*, 301, 401-413.

Asquith, R.S., & Carthew, P. (1972). An investigation of the mechanism of alkaline degradation of cystine in intact protein. *Biochimica et Biophysica Acta*, 278, 8-14.

Astbury, W.T., & Bell, F.O. (1941). Nature of the intramolecular fold in alpha-keratin and alpha-myosin. *Nature*, 147, 696-699.

Astbury, W.T., & Woods H.J. (1934). X ray studies of the structure of hair, wool, and related fibres. II. The molecular structure and elastic properties of hair keratin. *Proceedings of the Royal Society of London. Series B*, 314-316.

Ayutthaya, S.I.N., Tanpichai, S., & Wootthikanokkhan, J. (2015). Keratin extracted from chicken feather waste: Extraction, preparation and structural characterization of the keratin and keratin/biopolymer films and electrospuns. *Journal of Polymers and the Environment*, 23, 506-516.

Baker, B.M., & Chen, C.S. (2012). Deconstructing the third dimension – how 3D culture microenvironments alter cellular cues. *Journal of Cell Science*, 125, 3015-3024.

Balaji, S., Kumar, R., Sripriya, R., Kakkar, P., Ramesh, D.V., Reddy, P.N.K., & Sehgal, P.K. (2012). Preparation and comparative characterization of keratin-chitosan and keratin-gelatin composite scaffolds for tissue engineering applications. *Materials Science and Engineering C*, 32, 975-982.

Barczyk, M., Carracedo, S., & Gullberg, D. (2010). Integrins. *Cell and Tissue Research*, 339, 269-280.

Barone, J.R., Schmidt, W.F., & Gregoire, N.T. (2006). Extrusion of feather keratin. , 100, 1432-1442.

Bartels, T. (2003). Variations in the morphology, distribution, and arrangement of feathers in domesticated birds. *Journal of Experimental Zoology*, 298B, 91-108.

Bhana, B., Iyer, R.K., Chen, W.L.K., Zhao, R., Sider, K.L., Likhitpanichkul, M., Simmons, C.A., Radisic, M. (2010). Influence of substrate stiffness on the phenotype of heart cells. *Biotechnology and Bioengineering*, 105, 1148-1160.

Bhatia, A., Gupta, R.K., Bhattacharya, S.N., & Choi, H.J. (2009). An investigation of melt rheology and thermal stability of poly(lactic acid)/poly(butylene succinate) nanocomposites. *Journal of Applied Polymer Science*, 114, 2837-2847.

Bhattarai, N., Gunn, J., & Zhang, M. (2010). Chitosan-based hydrogels for controlled, localized drug delivery. *Advanced Drug Delivery Reviews*, 62, 83-89.

Birgersdotter, A., Sandberg, R., & Ernberg, I. (2005). Gene expression perturbation in vitro—a growing case for three dimensional (3D) culture systems. *Seminars in Cancer Biology*, 15, 405-412.

Bissell, M.J., Radisky, D.C., Rizki, A., Weaver, V.M., & Petersen, O.W. (2002). The organizing principle: microenvironmental influences in the normal and malignant breast. *Differentiation; Research and Biological Diversity*, 70, 537-546.

Boakye, M.A.D., Rijal, N.P., Adhikari, U., & Bhattarai, N. (2015). Fabrication and characterization of electrospun PCL-MgO-keratin-based composite nanofibers for biomedical applications. *Materials*, 8, 4080-4095.

Bottcher-Haberzeth, S., Biedermann, T., & Reichmann, E. (2010). Tissue engineering of skin. *Burns*, 36, 450-460.

Brauer, S., Meister, F., Gottlober, R-P., & Nechwatal, A. (2007). Preparation and thermoplastic processing of modified plant proteins. *Macromolecular Materials and Engineering*, 292, 176-183.

Bryant, S.J., Anseth, K.S. (2001). The effects of scaffold thickness on tissue engineered cartilage in photocrosslinked poly(ethylene oxide) hydrogels. *Biomaterials*, 22,619-26.

Carlson, D., Nie, L., Narayan, R., Dubois, P. (1999). Maleation of polylactide (PLA) by reactive extrusion. , 72, 477-485.

Carrel, A., & Ebeling, A.H. (1923). Action on fibroblasts of extracts of homologous and heterologous tissues. *The Journal of Experimental Medicine*, 38, 499-511.

Cascone, M.G., Laus, M., Ricci, D., Sbarbati, del Guerra, R. (1995). Evaluation of poly(vinyl alcohol) hydrogels as a component of hybrid artificial tissues. *Journal of Materials Science: Materials in Medicine*, 6,71-75.

Chang, Y., Ko, C-Y., Shih, Y-J., Quemener, D., Deratani, A., Wei, T-C., Wang, D-M., & Lai, J-Y. (2009). Surface grafting control of PEGylated poly(vinylidene fluoride) antifouling membrane via surface-initiated radical graft copolymerization. *Journal of Membrane Science*, 345, 160-169.

Cheung, T.H., & Rando, T.A. (2013). Molecular regulation of stem cell quiescence. *Natural Reviews Molecular Cell Biology*, 14, 329-340.

Coward-Kelly, G., Chang, V.S., Agbogbo, F.K., & Holtzapple, M.T. (2006). Lime treatment of keratinous materials for the generation of highly digestible animal feed: 1. Chicken feathers. *Bioresource Technology*, 97, 1337-1343.

Crewther, W.G., Fraser, R.D.B., Lennox, F.G., & Lindley, H. (1965). The chemistry of keratins. In *Advances in protein chemistry*. Academic Press, Inc. New York, p191-346.

Cukierman, E., Pankov, R., Stevens, D.R., Yamada, K.M. (2001). Taking cell-matrix adhesions to the third dimension. *Science*, 294, 1708-1712.

Daley, W., Peters, S.B., & Larsen, M. (2008). Extracellular matrix dynamics in development and regenerative medicine. *Journal of Cell Science*, 121, 255-264.

Damodaran, S., & Paraf, A. (1997). Food proteins and their applications. Marcel Dekker, Inc. New York.

Darder, M., Lopez-Blanco, M., Aranda, P., Aznar, A.J., Bravo, J., & Ruiz-Hitzky, E. (2006). Microfibrous chitosan-sepiolite nanocomposites. *Chemistry of Materials*, 18, 1602-1610.

de Guzman, R.C., Merrill, M.R., Richter, J.R., Hamzi, R.I., Greengauz-Roberts, O.K., & Van Dyke, M.E. (2011). Mechanical and biological properties of keratose biomaterials. *Biomaterials*, 32, 8205-8217.

Dennis, H.R., Hunter, D.L., Chang, D., Kim, S., White, J.L., Cho, J.W., Paul, D.R. (2001). Effect of melt processing conditions on the extent of exfoliation in organoclay-based nanocomposites. *Polymer*, 42, 9513-9552.

Dong, C., & Lv, Y. (2016). Application of collagen scaffold in tissue engineering: Recent advances and new perspectives. *Polymers*, 8, doi:10.3390/polym8020042.

Drury, J.L., & Mooney, D.J. (2003). Hydrogels for tissue engineering: scaffold design variables and applications. *Biomaterials*, 24, 4337-4351.

Dulbecco, R. (1952). Production of plaques in monolayers of tissue cultures by single particles of an animal virus. *Proceedings of the National Academy of Sciences*, 38, 747-752.

Eagle, H. (1955). The specific amino acid requirements of mammalian cells (stain HeLaT) in tissue culture. *The Journal of Experimental Medicine*, 1, 37-48.

Fan, J., Lei, T-D., Li, J., Zhai, P-Y., Wang, Y-H., Cao, F-Y., & Liu, Y. (2016). High protein content keratin/poly(ethylene oxide) nanofibers crosslinked in oxygen atmosphere and its cell culture. *Materials & Design*, 104, 60-67.

Fang, J., Niu, H.T., Lin, T., & Wang, X.G. (2008). Applications of electrospun nanofibers. *Chinese Science Bulletin*, 53, 2265-2286.

Feughelman, M. (1997). Mechanical properties and structure of alpha-keratin fibres: wool, human hair and related fibres. University of New South Wales Press, Sidney. p120.

Filipello Marchisio, V., 2000. Karatinophilic fungi: their role in nature and degradation of keratinic substrates. In: Kushawaha, R.K.S., & Guarro, J. (Eds.), Biology of dermatophytes and other keratinophilic fungi. Revista Iberoamericana de Micologia, Bilbao, p86–92. Retrieved from https://www.dermatophytes.reviberoammicol.com/ on April 5th, 2017.

Flanagan, L.A., Ju, Y.E., Marg, B., Osterfield, M., & Janmey, P.A. (2002). Neurite branching on deformable substrates. *Neuroreport*, 13, 2411-2415.

Fong, H., Chun, I., & Reneker, D.H. (1999). Beaded nanofibers formed during electrospinning. *Polymer*, 40, 4585-4592.

Frantz, C., Stewart, K.M., & Weaver, V.M. (2010). The extracellular matrix at a glance. *Journal of Cell Science*, 123, 4195-4200.

Fraser, R.D.B., & MacRae, T.P. (1973). Conformation in fibrous proteins. Academic Press, Inc. New York. Chapter 16.

Fraser, R.D.B., & Parry, D.A.D. (2008). Molecular packing in the feather keratin filament. *Journal of Structural Biology*, 162, 1-13.

Freed, L.E., & Guilak, F. Engineering functional tissues. (2007). In Lanza, R., Langer, R., & Vacanti, J., (Eds.). Principles of Tissue Engineering, 3rd Edition, Academic Press, Amsterdam.

Freshney, R.I. (2006). Basic principles of cell culture. In Vunjak-Novakovic, G., and Freshney, R.I. (Eds.). Culture of Cells for Tissue Engineering. John Wiley & Sons, Inc., Hoboken, NJ, USA.

Friedman, M. (1999). Chemistry, biochemistry, nutrition, and microbiology of lysinoalanine, lanthionine, and histidinoalanine in food and other proteins. *Journal of Agricultural and Food* Chemistry, 47, 1295-1319.

Gey, G.O., Coffman, W.D., & Kubicek, M.T. (1952). Tissue culture studies of the proliferative capacity of cervical carcinoma and normal epithelium. *Cancer Research*, 12, 264-265.

Ghani, S.A., Tan, S.J., & Yeng, T.S. (2013). Properties of chicken feather fiber-filled low-density polyethylene composites: The effect of polyethylene grafted maleic anhydride. *Polymer-Plastics Technology and Engineering*, 52, 495-500.

Gironi, F., & Piemonte, V. (2011). Bioplastics and petroleum-based plastics: Strengths and weaknesses. *Energy Sources, Part A*, 33, 1949-1959.

Goddard, D.R., & Michaelis, L. (1934). A study on keratin. *The Journal of Biological Chemistry*, 106, 605-614.

Graiver, D., Waikul, L.H., Berger, C., & Narayan, R. (2004). Biodegradable soy protein-polyester blends by reactive extrusion process. , 92, 3231-3239.

Greaves, N., Iqbal, S., Baguneid, M., & Bayat, A. (2013). The role of skin substitutes in the management of chronic cutaneous wounds. *Wound Repair and Regeneration*, 21, 194-210.

Groeber, F., Holeiter, M., Hampel, M., Hinderer, S., & Schenke-Layland, K. (2011). Skin tissue engineering – in vivo and in vitro applications. *Advanced Drug Delivery Reviews*, 128, 352-366.

Gstraunthaler, G. (2003). Alternatives to the use of fetal bovine serum: serum-free cell culture. *ALTEX*, 20, 275-281.

Guo, J., Pan, S., Yin, X., He, Y-F., Li, T., & Wang, R-M. (2015). pH-sensitive keratin-based polymer hydrogel and its controllable drug-release behavior. , 132, 41572, doi: 10.1002/app.41572.

Guo, S., & DiPietro, L.A. (2010). Factors affecting wound healing. *Journal of Dental Research*, 89, 219-229.

Harrison, R.G., Greenman, M.J., Mall, F.P., & Jackson, C.M. (1907). Observations of the living developing nerve fiber. *The Anatomical Record*, 1, 116-128.

Hill, P., Brantley, H., & Van Dyke, M. (2010). Some properties of keratin biomaterials: Kerateines. *Biomaterials*, 31, 585-593.

Hill, P., Brantley, H., & Van Dyke, M. 2010. Some properties of keratin biomaterials: Kerateines. *Biomaterials*, 31, 585-593.

Hoffman, B. D., Grashoff, C. and Schwartz, M. A. (2011). Dynamic molecular processes mediate cellular mechanotransduction. *Nature*, 475, 316-323.

Hu, C., Reddy, N., Yan, K., & Yang, Y. (2011). Acetylation of chicken feathers for thermoplastic applications. *Journal of Agricultural and Food Chemistry*, 59, 10517-10523.

Huang, J., Zhang, L., Wei, H., Cao, X. (2004). Soy protein isolate/kraft lignin composite compatibilized with methylene diphenyl diisocyanate. *Journal of Applied Polymer Science*, 93, 624-629.

Huda, M.S., Schmidt, W.F., Misra, M., & Drzal, L.T. (2013). Effect of fiber surface treatment of poultry feather fibers on the properties of their polymer matrix composites. *Journal of Applied Polymer Science*, 128, 1117-1124.

Hummers, W.S., & Offeman, R.E. (1958). Preparation of graphitic oxide. *Journal of the American Chemical Society*, 80, 1339-1339.

Janssen, L.P.B.M. (2004). Reactive extrusion systems. Marcel Dekker, Inc., NY, USA. Chapter 2.

Jin, E., Reddy, N., Zhu, Z., Yang, Y. (2011). Graft polymerization of native chicken feathers for thermoplastic applications. *Journal of Agricultural and Food Chemistry*, 59, 1729-1738.

Karp, J.M., Dalton, P.D., & Shoichet, S. (2003). Scaffolds for tissue engineering. *MRS bulletin*, 28, 301-306.

Kornillowicz-Kowalska, T., & Bohacz, J. (2011). Biodegradation of keratin waste: Theory and practical aspects. *Waste Management*, 31, 1689-1701.

Kuilla, T., Bhadra, S., Yao, D., Kim, N.H., Bose, S., Lee, J.H. (2010). Recent advances in graphene based polymer composites. *Progress in Polymer Science*, 35, 1350-1375.

Kumar, P., Sandeep, K.P., Alavi, S., Truong, V.D., Gorga, R.E. (2010). Preparation and characterization of bio-nanocomposite film based on soy protein isolate and montmorillonite using melt extrusion. *Journal of Food Engineering*, 100, 480-489.

Kundu, J., Poole-Warren, L.A., Martens, P., & Kundu, S.C. (2012). Silk fibroin/poly(vinyl alcohol) photocrosslinked hydrogels for delivery of macromolecular drugs. *Acta Biomateralia*, 8, 1720-1729.

Lemons, J.M.S., Feng, X-J., Bennett, B.D., Legesse-Miller, A., Johnson, E.L., Raitman, I., Pollina, E.A., Rabitz, H.A., Rabinowitz, J.D., & Coller, H.A. (2010) Quiescent Fibroblasts Exhibit High Metabolic Activity. *PLoS Biology*, 8(10): e1000514. doi:10.1371/journal.pbio.1000514

Lev, J., Holba, M., Kalhotka, L., Mikula, P., & Kimmer, D. (2012). Improvements in the structure of electrospun polyurethane nanofibrous materials used for bacterial removal from wastewater. *International Journal of Theoretical and Applied Nanotechnology*, 1, 16-20.

Li, J., Li, Y., Mak, A.F.T., Ko, F., & Qin, L. (2009). Preparation and biodegradation of electrospun PLLA/keratin nonwoven fibrous membrane. *Polymer Degradation and Stability*, 94, 1800-1807.

Li, R., Liu, C., & Ma, J. (2011). Studies on the properties of graphene oxide-reinforced starch biocomposites. *Carbohydrate Polymers*, 84, 631-637.

Li, S., & Yang, X-H. (2014). Fabrication and characterization of electrospun wool keratin/poly(vinyl alcohol) blend nanofibers. *Advances in Materials Science and Engineering*, Article ID 163678.

Liu, W., Misra, M., Askeland, P., Drzal, L.T., Mohanty, A.K. (2005). "Green" composites from soy based plastic and pineapple leaf fiber: fabrication and properties evaluation. *Polymer*, 46, 2710-2721.

Lovette, I.J., & Fitzpatrick, J.W. (2016). Handbook of bird biology, 3rd edition. Willey-Blackwell, Oxford, UK.

Luecha, J., Sozer, N., Kokini, J.L. (2010). Synthesis and properties of corn zein/montmorillonite nanocomposite films. *Journal of Material Science*, 45, 3529-3537.

Ma, T., Chang, P.R., Zheng, P., & Ma, X. (2013). The composites based on plasticized starch and graphene oxide/reduced graphene oxide. *Carbohydrate Polymers*, 94, 63-70.

Maclaren, J.A., Kilpatrick, D.J., & Kirkpatrick, A. (1968). Reduced wool fibres, their preparation and alkylation. *Australian Journal of Biological Sciences*, 21, 805-813.

MacNeil, S. (2008). Biomaterials for skin engineering of skin. *Materials Today*, 11, 26-35.

Madaghiele, M., Demitri, C., Sannino, A., & Ambrosio, L. (2014). Polymeric hydrogels for burn wound care: Advanced skin wound dressings and regenerative templates. *Burns & Trauma*, 2, 153-161.

Malafaya, P.B., Silva, G.A., & Reis, R.L. (2007). Natural-origin polymers as carrier and scaffolds for biomolecules and cell delivery in tissue engineering applications. *Advanced Drug Delivery Reviews*, 59, 207-233.

Marquis, D.M., Guillaume, E., Chivas-Joly, C. (2011). Properties of nanofillers in polymer. In Cuppoletti, J. (Ed.). Nanocomposites and polymers with analytical methods. Intech, Rijeka, Croatia.

Marshall, T., & Williams, K.M. (1986). High resolution two-dimensional electrophoresis of hair proteins without prior S-carboxymethylation. *Electrophoresis*, 7, 524-526.

Martínez-Hernández, A.L., Velasco-Santos, C., de Icaza, M., & Castaño, V.M. (2003). Grafting of methyl methacrylate onto natural keratin. *e-Polymers*, 3, 209–219.

Matthews, B. D., Overby, D. R., Mannix, R. & Ingber, D. E. (2006). Cellular adaptation to mechanical stress: role of integrins, Rho, cytoskeletal tension and mechanosensitive ion channels. *Journal of Cell Science*, 119, 508–518.

Mckittrick, J., Chen, P-Y., Bodde, S.G., Yang, W., Novitskaya, E.E., & Meyers, M.A. (2012). The structure, functions, and mechanical properties of keratin. *JOM*, 64, 449-468.

Mittal, V. 2011. Bio-nanocomposites: future high-value materials. In Mittal, V. (Ed). Nanocomposites with biodegradable polymers. Synthesis, properties, and future perspectives. Oxford University Press, UK.

Nagai, Y., & Nishikawa, T. (1970). Alkali solubilization of chicken feather keratin. *Agricultural and Biological Chemistry*, 34, 16-22.

Nakaji-Hirabayashi, T., Kato, K., & Iwata, H. (2008). Self-assembling chimeric protein for the construction of biodegradable hydrogels capable of interaction with integrins expressed on neural stem/progenitor cells. *Biomacromolecules*, 9, 1411-1416.

Nakamura, A., Arimoto, M., Takeuchi, K., & Fujii, T. (2002). A rapid extraction procedure of human hair proteins and identification of phosphorylated species. *Biological and Pharmaceutical Bulletin*, 25, 569-572.

Ng, C.S., Wu, P., Foley, J., Foley, A., McDonald, M-L., Juan, W-T., Huang, C-J., Lai, Y-T., Lo, W-S., Chen, C-F., Leal, S.M., Zhang, H., Widelitz, R.B., Patel, P.I., Li, W-H., Chuong, C-M.

(2012). The chicken frizzle feather is due to an a-keratin (KRT75) mutation that causes a defective rachis. *PLoS Genetics*, 8, e1002748, 1-16.

Novoselov, K.S., Geim, A.K., Morozov, S.V., Jiang, D., Zhang, Y., Dubonos, S.V., Grigorieva, I.V., & Firsov, A.A. (2004). Electric field effect in atomically thin carbon films. *Science*, 306, 666-669.

Nuttelman, C.R., Mortisen, D.J., Henry, S.M., Anseth, K.S. (2001). Attachment of fibronectin to poly(vinyl alcohol) hydrogels promotes NIH3T3 cell adhesion, proliferation, and migration. *Journal of Biomedical Materials Research*, 57, 217-23.

Nyame, T., Chiang, H.A., & Orgill, D. (2014). Clinical applications of skin substitutes. *The Surgical Clinics of North America*, 94, 839-850.

Orienti, I., Trere, R., Zecchi, V. Hydrogels formed by cross-linked polyvinylalcohol as colon-specific drug delivery systems. *Drug Development and Industrial Pharmacy*, 27, 877-84.

Ozaki, Y., Takagi, Y., Mori, H., & Hara, M. (2014). Porous hydrogel of wool keratin prepared by a novel method: An extraction with guanidine/2-mercaptoethanol solution followed by dialysis. *Materials Science and Engineering Part C*, 42, 146-154.

Parenteau-Bareil, R., Gauvin, R., & Berthod, F. (2010). Collagen-based biomaterials for tissue engineering applications. *Materials*, 3, 1863-1887.

Parsons, J.T., Horwit, A.R., & Schwartz, M.A. (2010). Cell adhesion: integrating cytoskeletal dynamics and cellular tension. *Nature Reviews*, 11, 633-643.

Poole, A.J., Lyons, R.E., & Church, J.S. (2011). Dissolving feather keratin using sodium disulfide for bio-polymer applications. *Journal of Polymers and the Environment*, 19, 995-1004.

Potts, J.R., Dreyer, D.R., Bielawski, C.W., Ruoff, R.S. (2011). Graphene-based polymer nanocomposites. *Polymer*, 52, 5-25.

Ramakrishna, S., Fujihara, K., Teo, W-E., Lim, T-C., & Ma, Z. (2005). An introduction to electrospinning of nanofibers. World Scientific Publishing Co. Pte. Ltd., Singapore.

Raquez, J., Nabar, Y., Srinivasan, M., Shin, B., Narayan, R., & Dubois, P. (2008). Maleated thermoplastic starch by reactive extrusion. *Carbohydrate Polymers*, 74, 159-169.

Ratheesh, G., Venugopal, J.R., Chinappan, A., Ezhilarasu, H., Sadiq, A., & Ramakrishna, S. (2016). 3D fabrication of polymeric scaffolds for regenerative therapy. *ACS Biomaterials Science & Engineering*, doi:10.1021/acsbiomaterials.6b00370

Ratner, B., Hoffman, A., Schoen, F., Lemons, J. 2013. Biomaterials science: An evolving, multidisciplinary endeavor. In Ratner, B., Hoffman, A., Schoen, F., Lemons, J. (Eds.). Biomaterials Science (3rd edition). Academic Press, Oxford, U.K.

Reddy, M.M., Vivekanandhan, S., Misra, M., Bhatia, S.J., & Mohanty, A.K. (2013). Biobased plastics and bionanocomposites: Current status and future opportunities. *Progress in Polymer Science*, 38, 1653-1689.

Reddy, N., Hu, C., Yan, K., Yang, Y. (2011). Thermoplastic films from cyanoethylated chicken feathers. *Materials Science and Engineering*, C31, 1706-1710.

Reddy, N., Jiang, Q., Jin, E., Shi, J., Hou, X., & Yang, Y. (2013). Bio-thermoplastics from grafted chicken feathers for potential biomedical applications. *Colloids and Surfaces B: Biointerfaces*, 110, 51-58.

Reichl, S. (2009). Films based on human hair keratin as substrates for cell culture and tissue engineering. *Biomaterials*, 30, 6854-6866.

Reichl, S., Borrelli, M., & Geerling, G. (2011). Keratin films for ocular surface reconstruction. *Biomaterials*, 32, 3375-3386.

Reinke, J.M., & Song, H. (2012). Wound repair and regeneration. *European Surgical Research*, 49, 35-43.

Richter, J.R., de Guzman, R.C., Greengauz-Roberts, O.K., & Van Dyke, M. (2012). Structure-property relationships of meta-kerateine biomaterials derived from human hair. *Acta Biomateralia*, 8, 274-281.

Rous, P., & Jones, F.S. (1916). A method for obtaining suspensions of living cells from the fixed tissues, and for the plating out of individual cells. *The Journal of Experimental Medicine*, 23, 549-555.

Ruoslathi, E. (1996). RGD and other recognition sequences for integrins. *Annual Review of Cell and Developmental Biology*, 12, 697-715.

Ryan, A.J., & O'Brien, F.J. (2015). Insoluble elastin reduces collagen scaffold stiffness, improves viscoelasticity properties, and induces a contractile phenotype in smooth muscle cells. *Biomaterials*, 73, 296-307.

Sasmal, A., Nayak, P.L., & Sasmal, S. (2009). Degradability studies of green nanocomposites derived from soy protein isolate (Spi)-furfural modified with organoclay. *Polymer-Plastics Technology and Engineering*, 48, 905-909.

Schmidt, W.F. (2001). Microcrystalline keratin: From feathers to composite products. *MRS Proceedings*, 702, U1.5.1.-U1.5.8.

Schrooyen, P.M.M., Dijkstra, P.J., Oberthur, R.C., Bantjes, A., & Feijen, J. (2000). Partially carboxymethylated feather keratins. 1. Properties in aqueous systems. *Journal of Agricultural and Food Chemistry*, 48, 4326-4334.

Schrooyen, P.M.M., Dijkstra, P.J., Oberthur, R.C., Bantjes, A., & Feijen, J. (2001). Stabilization of solutions of feather keratin by sodium dodecyl sulfate. *Journal of Colloid and Interface Science*, 240, 30-39.

Shi, J., & Yang, E. (2015). Green electrospinning and crosslinking of polyvinyl alcohol/citric acid. *Journal of Nano Research*, 32, 32-42.

Singh, R., & Whitesides, G.M. (1993). Thiol-disulfide interchange. In Patai, S., & Rappoport, Z. (Eds.). Sulphur-containing functional groups. John Wiley & Sons Ltd, Chichester, England.

Sisson, K., Zhang, C., Farach-Carson, M.C., Chase, D.B., & Rabolt, J.F. (2009). Evaluation of cross-linking methods for electrospun gelatin on cell growth and viability. *Biomacromolecules*, 10, 1675-1680.

Slack, J. 2007. Molecular biology of the cell. In Lanza, R., Langer, R., & Vacanti J (Eds.). Principles of Tissue Engineering 3rd edition, Academic Press, Amsterdam.

Souza, A.C., Benze, R., Ferrao, E.S., Ditchfield, C., Coelho, A.C.V., & Tadini, C.C. (2012). Cassava starch biodegradable films: Influence of glycerol and clay nanoparticles content on tensile and barrier properties and glass transition temperature. *LWT – Food Science and Technology*, 46, 110-117.

Sridharan, R., Cameron, A.R., Kelly, D.J., Kearney, C., & O'Brien, F.J. (2015). Biomaterial based modulation macrophage polarization: a review and suggested design principles. *Materials Today,* 18, 313-325.

Stankovich, S., Dikin, D.A., Dommett, G.H.B., Kohlhaas, K.M., Zimney, E.J., Stach, E.A., Piner, R.D., Nguyen, S.T., Ruoff, R.S. (2006). Graphene-based composite materials. *Nature*, 442, 282-286.

Stratton, S., Shelke, N.B., Hoshino, K., Rudraiah, S., & Kumbar, S.G. (2016). Boactive polymeric scaffolds for tissue engineering. *Bioactive Materials*, 1, 93-108.

Tachibana, A., Furuta, Y., Takeshima, H., Tanabe, T., & Yamauchi, K. (2002). Fabrication of wool keratin sponge scaffolds for long-term cell cultivation. *Journal of Biotechnology*, 93, 165-170.

Tamada, Y., & Ikada, Y. (1993). Effect of preadsorbed proteins on cell adhesion to polymer surfaces. *Journal of Colloid and Interface Science*, 155, 334-339.

Thevenot, P., Hu, W., & Tang, L. (2008). Surface chemistry influence implant biocompatibility. *Current Topics in Medicinal Chemistry*, 8, 270-280.

Thilagar, S., Arul Jothi, N., Sheikh Omar, A.R., Kamaruddin, M.Y., & Ganabadi, S. (2009). Effect of keratin-gelatin and bFGF-gelatin composite film as a sandwich layer for full-thickness skin mesh graft in experimental dogs. *Journal of Biomedical Materials Research Part B: Applied Biomaterials*, 88B, 12-16.

Thompson, C.J., Chase, G.G., Yarin, A.L., & Reneker, D.H. (2007). Effects of parameters on nanofiber diameter determined from electrospinning model. *Polymer*, 48, 6913-6922.

Thomsen, P., & Gretzer, C. (2001). Macrophage interactions with modified materials surfaces. *Current Opinion in Solid State & Materials Science*, 5, 163-176.

Tibbitt, M.W., & Anseth, K.S. (2009). Hydrogels as extracellular matrix mimics for 3D cell culture. *Biotechnology and Bioengineering*, 103, 655-663.

Tirella, A., Liberto, T., & Ahluwalia, A. (2012). Riboflavin and collagen: New crosslinking methods to tailor the stiffness of hydrogels. *Materials Letters*, 74, 58-61.

Tromel, V.M., & Reuss, M. (1987). Dimanganheptoxid zur selektiven oxidation organischer substrate. *Angewandte Chemie*, 99, 1037-1038.

Ullah, A., Vasanthan, T., Bressler, D., Elias, A.L., & Wu, J. (2011). Bioplastics from feather quill. *Biomacromolecules*, 12, 3826-3832.

Uzun, M., Sancak, E., Patel, I., Usta, I., Akalin, M., & Yuksek, M. (2011). Mechanical behavior of chicken quills and chicken feather fibres reinforced polymeric composites. *Archives of Material Science and Engineering*, 52, 82-86.

Van de Sandt, J.J.M., Bos, T.A., & Rutten, A.A.J.J.L. (1995). Epidermal cell proliferation and terminal differentiation in skin organ culture after topical exposure to sodium dodecyl sulfate. *In Vitro Cellular & Developmental Biology – Animal*, 31, 761-766.

Van Vlierberghe, S., Dubruel, P., & Schacht, E. (2011). Biopolymer-based hydrogels as scaffolds for tissue engineering applications: A review. *Biomacromolecules*, 12, 1387-1408.

Verbeek, C.J.R., van den Berg, L.E. (2009). Recent developments in thermo-mechanical processing of proteinous bioplastics. *Recent Patents on Material Science*, 2, 171-189.

Verma, V., Verma, P., Ray, P., & Ray, A. (2008). Preparation of scaffolds from human hair proteins for tissue-engineering applications. *Biomedical Materials*, 3, 1-12.

Wang, S., Taraballi, F., Tan, L.P., Ng, K.W. (2012). Human keratin hydrogels support fibroblast attachment and proliferation in vitro. *Cell and Tissue Research*, 347, 795-802.

Wang, X., Ding, B., & Li, B. (2013). Biomimetic electrospun nanofibrous structures for tissue engineering. *Materials Today*, 16, 229-241.

Wheeler, T.S., Sbravati, N.D., & Janorkar, A.V. (2013). Mechanical & cell culture properties of elastin-like polypeptide, collagen, bioglass, and carbon nanosphere composites. *Annals of Biomedical Engineering*, 41, 2042-5055.

White, J., & Dalton, S. (2005). Cell cycle control of embryonic stem cells. *Stem Cell Reviews*, 1, 131-138.

Wilson, C., Clegg, R., Leavesley, D., & Pearcy, M. (2005). Mediation of biomaterial-cell interactions by adsorbed proteins. A review. *Tissue Engineering*, 11, 1-18.

Wolfram, L.J., & Underwood, D.L. (1966). The equilibrium between the disulfide linkage in hair keratin and sulfite or mercaptan. *Textile Research Journal*, 36, 947-953.

Woodin, A.M. (1954). Molecular size, shape and aggregation of soluble feather keratin. *Biochemical Journal*, 57, 99-109.

Wu, D-D., Irwin, D.M., & Zhang, Y-P. (2008). Molecular evolution of the keratin associated protein gene family in mammals, role in the evolution of mammalian hair. *BMC Evolutionary Biology*, 8, 241.

Wu, J., & Hong, Y. (2016). Enhancing cell infiltration of electrospun fibrous scaffolds in tissue regeneration. *Bioactive Materials*, 1, 56-64.

Xu, H., Cai, S., Xu, L., & Yang, Y. (2014). Water-stable three-dimensional ultrafine fibrous scaffolds from keratin for cartilage tissue engineering. *Langmuir*, 30, 8461-8470.

Xu. S., Sang, L., Zhang, Y., Wang, X., & Li, X. (2013). Biological evaluation of human hair keratin scaffolds for skin wound repair and regeneration. *Materials Science and Engineering*, C33, 648-655.

Yamauchi, K., Maniwa, M., & Mori, T. (1999). Cultivation of fibroblast cells on keratin-coated substrata. *Journal of Biomaterials Science, Polymer Edition*, 9, 259-270.

Yao, J., Bastiaansen, C.W.M., & Peijs, T. (2014). High Strength and high modulus electrospun nanofibers. *Fibers*, 2, 158-187.

Yen, K-C., Chen, C-Y., Huang, J-Y., Kuo, W-T., & Lin, F-H. (2016). Fabrication of keratin/fibroin membranes by electrospinning for vascular tissue engineering. *Journal of Materials Chemistry B,* 4, 237-244.

Yeung, T., Georges, P.C., Flanagan, L.A., Marg, B., Ortiz, M., Funaki, M., Zahir, N., Ming, W., Weaver, V., & Janmey, P.A. (2005). Effects of substrate stiffness on cell morphology, cytoskeletal structure and adhesion. *Cell Motillity and the Cytoskeleton*, 60, 24-34.

Yoon, D.M., & Fisher, J.P. (2009). Natural and synthetic polymeric scaffolds. In Narayan, R. (Ed.). Biomedical Materials. Springer, New York.

Yu, J., Yu, D.W., Checkla, D.M., Freedberg, I.M., & Bertolino, A.P. (1993). Human hair keratins. *The Journal of Investigative Dermatology*, 101, 56S-59S.

Yu, T., Tutwiler, V.J., & Spiller, K. (2015). The role of macrophages in the foreign body response to implanted biomaterials. In Santambrogio, L. (Ed.). Biomaterials in Regenerative Medicine and the Immune System, Springer, Switzerland.

Yuan, X., Zhang, Y., Dong, C., & Sheng, J. (2004). Morphology of ultrafine polysulfone fibers prepared by electrospinning. *Polymer International*, 53, 1704-1710.

Zayas, J.F. (1997). Functionality of proteins in food. Springer, Berlin. p76-133.

Zhang, S. (2004). Beyond the petri dish. *Nature Biotechnology*, 22, 151-152.

Zhang, X., Tang, K., & Zheng, X. (2016). Electrospinning and crosslinking of Col/PVA nanofiber-microsphere containing salicylic acid for drug delivery. *Journal of Bionic Engineering*, 13, 143-149.

Zhu, J., & Marchant, R.E. (2011). Design properties of hydrogel tissue-engineering scaffolds. *Expert Review of Medical Devices*, 8, 607-626.

Zoccola, M., Aluigi, A., & Tonin, C. (2009). Characterisation of keratin biomass from butchery and wool industry wastes. *Journal of Molecular Structure*, 938, 35-40.

Zoccola, M., Montarsolo, A., Aluigi, A., Varesano, A., Vineis, C., & Tonin, C. (2007). Electrospinning of polyamide 6/modified keratin blends. *e-Polymers*, 105, doi: https://doi.org/10.1515/epoly.2007.7.1.1204

CHAPTER 3. Preparation and characterization of graphite oxide nano-reinforced biocomposites from chicken feather keratin

A version of this chapter has been published: Esparza, Y., Ullah, A., & Wu, J. (2017). Preparation and characterization of graphite oxide nano-reinforced biocomposites from chicken feather keratin. *Journal of Chemical Technology and Biotechnology*, doi:10.1002/jctb.5196

3.1. Introduction

The development of plastics from renewable resources, such as by-products or wastes of agricultural and horticultural activities, is an emerging trend as a possible alternative of petroleum-based plastics in terms of cost, availability and sustainability (Verbeek and van den Berg, 2010; Gonzalez et al., 2011). Feathers are an abundant waste from poultry industry; it is estimated that Canadian poultry industry generates yearly roughly 100,000 tons of feather based on a 7% of the live weight of chicken (Agriculture and Agri-Food Canada, 2014). Although a portion of feathers is used to produce feather meal for animal feed, most of them end in landfills.

Feathers, composed of a central rachis or quill and barbs and barbules, contain about 90% keratin. Feather keratin is a semi-crystalline protein of small molecular weight (~10 kDa), possessing a balanced hydrophilic and hydrophobic amino acid composition being serine, proline, glycine, valine and cysteine the major ones (Schmidt, 2002). The natural strength of feathers is mainly due to the high levels of disulfide bonds between cysteine residues of keratin. Due mainly to their high protein content, availability, and low cost feathers are an interesting resource for the development of different bio-based materials. Feathers barbs (or fibers) have been considered to reinforce several polymeric matrices resulting in improved mechanical and thermal properties (Cheng et al., 2009; Martinez-Hernandez et al., 2011; Ghani et al., 2013; Flores-Hernandez et al., 2014). Feathers can be chemically modified by grafting monomers onto different functional groups of keratin, such as carboxymethylation of keratin thiol groups (Schrooyen et al., 2001), grafting of acrylates (Martinez-Hernandez et al., 2003; Martinez Hernandez et al., 2008; Jin et al., 2011; Li et al., 2016), or acetylation of feathers (Hu et al., 2011). Although the physical properties of modified feather films were improved after

modification, these methods involve time consuming chemical reactions performed in dilute feather or keratin suspensions which generate a great deal of waste and use of harmful chemicals. Processing of whole feathers in bulk quantities in commonly-used plastic machineries such as extruders might offer a more environmentally-friendly and cost-effective alternative for the development of feather plastics (Verbeek and van den Berg, 2010). Although the natural strength of feathers is mainly due to the high levels of disulfide bonds between cysteine residues of keratin, disruption of disulfide bonds and addition of hydrophilic plasticizers are required to improve the thermal processability of feather into plastics (Barone et al., 2006; Ullah et al., 2011). However, mechanical properties of feather plastics, the same as bio-based plastics in general, are weaker and more sensitive to moisture conditions than synthetic plastics, which limit their applications.

Reinforcement of materials with high surface area nanoparticles has gained great attention among researchers and industry. The discovery of the unique strong mechanical and electrical properties of single-layer graphene led to a rapid interest for their uses in composites (Novoselov et al., 2004; Gardella et al., 2015). Chemical oxidation of graphite, followed by chemical, thermal or enzymatic reduction is a common approach to produce single graphene sheets; however, scale up production of graphene in a cost/effective manner has not been achieved yet (Kuilla et al., 2010). Graphite oxide (GO) is an inexpensive intermediate in the production of graphene. GO, being dispersible in water, can interact with hydrophilic biopolymers, leading to enhanced physical properties (Wang et al., 2012; Ma et al., 2013). Several reports have investigated the redox-mediated grafting of oxidized graphite and carbon nanotubes to feather keratin in solution systems (Rodriguez-Gonzalez et al., 2012; Rodriguez-Gonzalez et al., 2013; Estevez-Martinez et al., 2013).

In this work GO with different oxygen contents were prepared by varying the oxidant amount and oxidation time. The reinforcement of chicken feathers with GO was performed in a reactive extrusion system with the aim to improve the mechanical properties of thermoplastics. GO samples were characterized by means of Fourier transform infra-red spectroscopy (FTIR), X-ray photoelectron spectroscopy (XPS), X-ray diffraction (XRD) and transmission electron microscopy (TEM) and the effect of concentration of a selected GO on mechanical properties, thermal properties, and molecular structure of chicken feather plastics fabricated through extrusion and thermo-molding are presented. To the best of our knowledge no reports on the reinforcement of feather plastics using GO, neither its effect on physical properties have been reported.

3.2. Materials and methods

3.2.1. Materials

Graphite, sodium nitrate ($NaNO_3$), potassium permanganate ($KMnO_4$), hydrogen peroxide (H_2O_2), sulfuric acid (H_2SO_4), glycerol ($C_3H_8O_3$), propylene glycol ($C_3H_8O_2$) and sodium sulfite (Na_2SO_3), phosphorous pentoxide (P_2O_5), were obtained from Sigma-Aldrich (Sigma-Aldrich Co. MO, USA).

3.2.2. Chicken feather powder

White chicken feathers (CF) were obtained from the Poultry Research Centre (University of Alberta, Edmonton, Alberta, Canada). Whole chicken feathers were thoroughly washed with hot water and domestic kitchen soap (Green Works®) to remove foreign material. Rinsed CF were allowed to dry at room temperature in a fume hood for three days and then dried at 50°C overnight in an oven. Grinding of CF was achieved by using a cutting mill (Fritsch Pulverisette

15, Fritsch, Germany) with an insert sieve of 0.25 mm perforations. The collected CF powder was stored at 4°C until use. Protein content of CF powder was 92.00% ± 0.40%, measured by Dumas method (N x 6.25) in a Leco Truspec C/N analyzer (Leco Corporation, MI, USA).

3.2.3. Oxidation of graphite

Graphite oxide (GO) was prepared according to the Hummers and Offeman method (Hummers and Offeman, 1958) with modifications. Briefly, 5 g of graphite and 2.5 g or 5 g of sodium nitrate were placed in a 1 L beaker, followed by slow addition of 120 mL of sulfuric acid. The mixture was stirred at 200 rpm for 30, 120, and 240 minutes on an ice bath in order to obtain different oxidation degrees of graphite. 15 g of potassium permanganate were slowly added to the mixture. After one hour of stirring at 35°C ± 3, 92 mL of deionized water were slowly added and stirred for 15 minutes. Neutralization of unreacted potassium permanganate was done by adding 80 mL of deionized water containing 3% H_2O_2. Graphite oxide powder was obtained after repeated cycles of washing/centrifugation with deionized water, followed by sonication for 15 minutes and freeze-drying. Carbon/oxygen (C/O) ratio of GO was determined by X-ray photoelectron spectroscopy (XPS) as described in section 3.2.6. Results are presented in Table 3.1.

Table 3.1. Carbon/oxygen (C/O) ratio of graphite and graphite oxide determined by XPS and differences on GO preparation.

Sample	$NaNO_3$ amount	Stirring time	C/O ratio
Graphite	-	-	35.76
GO A	2.5 g	30 min	2.48
GO B	5 g	2 hours	2.07
GO C	5 g	4 hours	1.55

3.2.4. Preparation of chicken feather plastics

GO was evaluated first at a level of 1% (w/w, GO/CF powder) for different GO samples and then at levels of 0.5, 1.0, 1.5, and 2.0% (w/w) for a selected GO. About 70 g of CF powder, 30 g plasticizer mixture (15 g glycerol and 15 g propylene glycol), 3 g sodium sulfite prepared in 15 mL deionized water, and 23 mL GO dispersion (prepared in deionized water and sonicated 15 minutes), were mixed in a heavy duty blender (CB15, Waring Co., CT, USA) for 8 cycles of 1.5 minutes each, with manual removal of material on the walls of the vessel between every cycle. Extrusion of blends was performed in a counter-rotating twin screw extruder L/D (19/25) (Plasti-Corder PL 2200, Brabender Instruments Inc., NJ, USA) equipped with four heating zones set at 110, 130, 140 and 150°C and at a screw speed of 50 rpm. Blends were forced through a circular die of 7 mm diameter. CF and CF-GO plastic extrudates were ground to a fine powder and compression molded at 150°C for 10 minutes under 5000 psi in a hot press (model 3851-0, Carver Inc. IN, USA). Preparation of blends and extrudates was performed in triplicate.

3.2.5. Mechanical properties

Mechanical testing of compression molded CF and CF-GO plastic films was performed in an Instron machine 5565 (Instron, MA, USA equipped with a load cell of 5 kN at a crosshead speed of 10 mm/min. At least 5 rectangular specimens (60 x 8 mm; length x width) of approximately 0.5 mm thickness were used (exact thickness and width was measured for each specimen with a caliper). Specimens were previously equilibrated at 50% relative humidity for 72 h prior to measurement.

3.2.6. Characterization

Fourier transform infrared (FTIR) spectroscopy analysis was performed on a FTIR spectrometer Nicolet 8700 (Thermo Electron Co. WI, USA). All samples were kept in a hermetic desiccator containing P_2O_5 for two weeks before analysis. Powder samples of graphite, graphite oxides, and feather powder, were thoroughly mixed with KBr and analyzed. For CF plastic samples, compression molded films were analyzed by attenuated total reflectance (ATR) using a grazing angle germanium ATR accessory (GATR™). Graphite powder was analyzed by near-normal reflection/absorbance technique on a gold surface. Spectra were collected at 128 scans and resolution of 4 cm^{-1} from 600-4000 cm^{-1}. Spectra were processed and analyzed with Origin 2015 software (OriginLab Corporation, MA, USA). Secondary derivative of FTIR spectra was used to determine changes in secondary structure of proteins using Savitzky-Golay smooth function at 7 points of window. X-ray photoelectron spectra of graphite and GO powders pellets was analyzed on a Kratos Axis 165 X-ray spectrometer (Kratos Analytical Ltd. UK) equipped with a monochromatic Al Kα radiation (1486.6 eV). The binding energy (BE) was calibrated taking C1s at 284.5 eV as a reference. XPS spectra were analyzed with CasaXPS software package V2.3.16 PR 1.6 (Casa Software Ltd.). Curve fitting of high resolution C1s was performed

assuming a Shirley background and four peaks for GO samples considering a Gaussian/Lorentzian (70%/30%) distribution shape. X-ray diffraction (XRD) was performed using a Rigaku Ultima IV powder diffractometer (Rigaku Co. Japan) with Cu-Kα radiation (0.154 nm), from 5 to 50° 2θ degrees. Interlayer space was calculated using Bragg's equation (Bragg and Bragg, 1913). Thermo-gravimetric analysis (TGA) was performed on a Perkin Elmer Pyris 1 (PerkinElmer Inc. MA, USA) equipment from 25 to 700°C, at a heating rate of 10°C/min under nitrogen atmosphere. Differential scanning calorimetry (DSC) was performed on a TA DSC Q2000 instrument (TA instruments, DE, USA) at 10°C/min from 25 to 300°C, using nitrogen as a purge gas. Transmission electron microscopy (TEM) images of 0.1% w/v GO samples in water, were obtained using a Phillips/FEI (Morgagni) transmission electron microscope (FEI Co. OR, USA) equipped with a Gatan digital camera (Gatan Inc. CA, USA).

3.2.7. Statistical analysis

Data was analyzed by variance, and significant differences were determined using Tukey multiple comparison test at a significance level of 1% using Minitab 17 software package (Minitab Inc., PA, U.S.).

3.3. Results and discussion

3.3.1. Characterization of graphite oxides

FTIR spectra of graphite oxides with different carbon/oxygen ratios confirmed the presence of oxygen functional groups (Figure 3.1). Assignment of FTIR peaks to different oxygen functional groups in graphite oxide was carried out using information reported in the literature. The absorption band within the range of 3423-3437 cm^{-1} in graphite oxide samples can be related to the stretching vibration of OH groups (νO-H) from adsorbed water or hydroxyl groups created

during oxidation (Hontoria-Lucas et al., 1995; Stankovich et al., 2006; Lee and Park, 2014). The peak found at 1724-1735 cm^{-1} is associated with stretching vibrations of the C=O bond (νC=O) present in aldehydes, ketones, carboxylic acids or esters. Peaks around 1620 cm^{-1} have been associated to the vibration of water (Stankovich et al., 2006; Wei et al., 2013), which is less likely due to the conditioning of our samples. Peaks at 1618-1626 cm^{-1} can be assigned to stretching vibrations of un-oxidized carbon skeletal domains (νC=C) (Stankovich et al., 2006; Chen et al., 2010). However, some authors have assigned this later to the appearance of a peak at lower wavenumbers between 1580-1588 cm^{-1} (Hontoria-Lucas et al., 1995; Paredes et al., 2008; Posudievsky et al., 2012). On the other hand, stretching vibrations of C-O bonds (νC-O) are found in the range of 1000-1400 cm^{-1}. Some authors have associated graphite oxide peaks in the neighborhood of 1220-1230 cm^{-1} to νC-O present in different functional groups, such as, carboxylic acid groups (Wei et al., 2013), hydroxyl groups (Stankovich et al., 2006; Paredes et al., 2008) or epoxy groups (Zhou et al., 2011; Posudievsky et al., 2012). Peaks found at 1143 and 1031 cm^{-1} have also been assigned to C-O stretching vibrations (Hontoria-Lucas et al., 1995; Stankovich et al., 2006; Paredes et al., 2008). GO A showed only two important peaks in the region of 1000-1400 cm^{-1}. In contrast, longer time of oxidation resulted in new C-O peaks at 1413, 1223 and 1143 cm^{-1}.

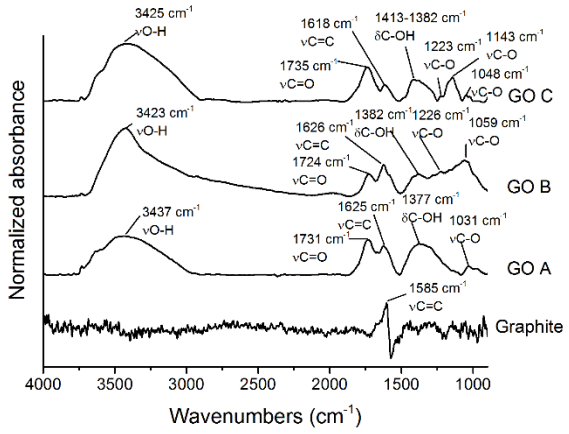

Figure 3.1. FTIR spectra of graphite and graphite oxide samples indicating stretching (ν) and bending (δ) vibration of oxygen functional groups identified.

Complementary XPS analysis was performed to clarify the presence of oxygen functionalities on GO. XPS high resolution C1s spectra of graphite and GO samples are shown in Figure 3.2. Graphite showed a single asymmetric peak centered at 284.5 eV. Peak fitting of C1s peaks was performed to determine chemical changes based on comparison with results found in the literature. The main peak in graphite accounts for sp^2 hybridized carbon (C=C, and C-C with delocalized π electrons). A second peak at 1 eV higher binding energy can be attributed to sp^3 carbon hybridization (Jackson and Nuzzo, 1995), resulting from atmospheric oxidation or contamination (Hontoria-Lucas et al., 1995). A peak found at 291.0 eV accounts for π–π* transitions characteristic of aromatic structures (Wang et al., 2012). This was not seen in GO samples indicating major disruption of the aromatic structure of graphite. In addition to the sp^2 peak at ~284.5, graphite oxides showed other peaks located at higher binding energies (~287 eV) that can be attributed to oxide functional groups (i.e. C-OH, C=O, O-C=O, C-O-C). Oxidation results in a decrease of electrons screening the 1s shell, causing a shift to higher binding energies. Peak fitting of GO high resolution C1s XPS spectra reveals the presence of different

oxygen functional groups (Figure 3.2). Assignation of functional groups was done based on comparison to reported data. Overall our results are in agreement with the reported literature. Shifts of 0.8, 1.7-2, 2.2-2.7 and 3.5-3.8 eV in GO samples are attributed to carbon-sp^3 (Jackson and Nuzzo, 1995; Haubner et al., 2010), C-OH groups, C-O-C groups, and C=O groups (Schniepp et al., 2006; Shin et al., 2009; Tien et al., 2011), respectively. Differences in C1s spectra of graphite oxides were noticed. For GO A (C/O 2.48) peak fitting to four components was not possible. Fit curves revealed the presence of carbon sp^3 in GO A, possibly due to C-C and C-H bonding (Yamada et al., 2013), which was absent in more oxidized graphite samples (GO B, and GO C). A higher content of C-OH groups was determined in GO B. After increasing the oxidation time (GO C), C-OH content decreased while the epoxy group content increased (Table 3.2). Possibly, prolonged oxidation favors the condensation of phenolic groups to ether or epoxy groups (Shao et al., 2012). This is in agreement with the FTIR results, in which an exclusive C-O peak at 1143 cm^{-1} seen in GO C can be attributed to higher epoxy content. On the other hand, carboxyl groups, which are typically assigned to peaks shifted to > 4 eV higher binding energy than sp^2carbon (Yumitori, 2000; Pei and Cheng, 2012) were not seen in GO samples.

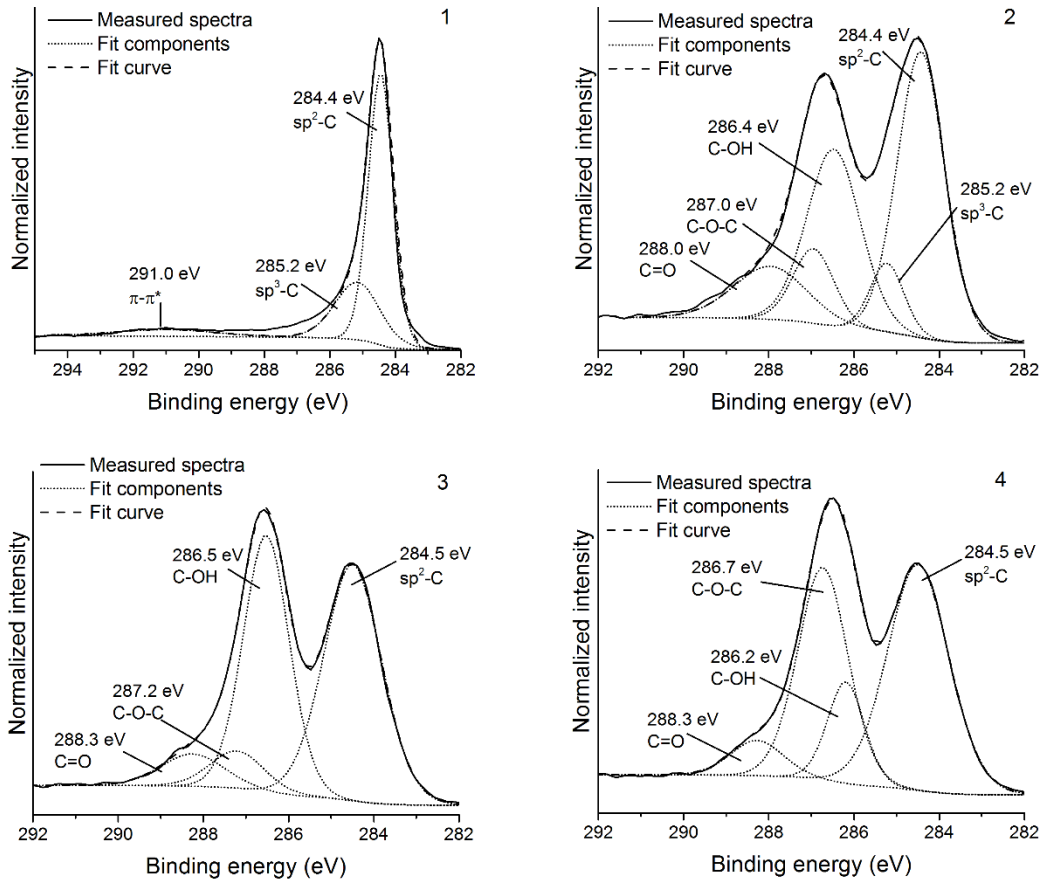

Figure 3.2. High resolution scans of C1s region and peak fitting of graphite (1), GO A (2), GO B (3), and GO C (4).

Table 3.2. Relative amount (%) of functional groups in graphite and graphite oxide samples.

	Area of fit peak, % (FWHM, eV)					
	sp^2	sp^3	π–π*	C-OH	C-O-C	C=O
Graphite	67.03 (0.9)	26.17 (1.6)	6.81 (3.6)	-	-	-
GO A	42.04 (1.3)	7.23 (0.9)	-	29.32 (1.5)	9.47 (1.1)	11.94 (2.0)
GO B	46.35 (1.6)	-	-	39.92 (1.3)	6.86 (1.5)	6.87 (1.7)
GO C	46.1 (1.7)	-	-	12.38 (1.0)	35.37 (1.4)	6.15 (1.5)

Area percentages from XPS high resolution C1s curve fitting. FWHM is the full width at half maximum of fit peaks.

The interlayer distance of graphene sheets in graphite and graphite oxide were measured by X-ray diffraction (XRD) (Figure 3.3). Graphene layers in graphite are closer to each other than in oxidized graphite. A single sharp peak was found in graphite which corresponds to a d-space of 0.34 nm. After oxidation and freeze-drying the major peak in GO samples was found at lower 2θ angles 10.56-11.60°, which corresponds to d-spaces between 0.84-0.76 nm, respectively. These results are in agreement with the reported XRD patterns of graphite and GO (Shin et al., 2009; Tien et al., 2011). Increasing the oxygen content from GO A to GO B did not result in important changes of XRD patterns. However, longer oxidation time resulted in an increase of d-space from 0.76 nm in GO B to 0.84 nm in GO C. In addition, the presence of other peaks at 18.02° (0.49 nm) and 25.85° (0.35 nm) were observed for GO C sample. These peaks might have resulted due to possible condensation of phenolic groups (Shao et al., 2012) (as discussed previously from XPS C1s results) and re-stacking of regions or defects created at longer oxidation times.

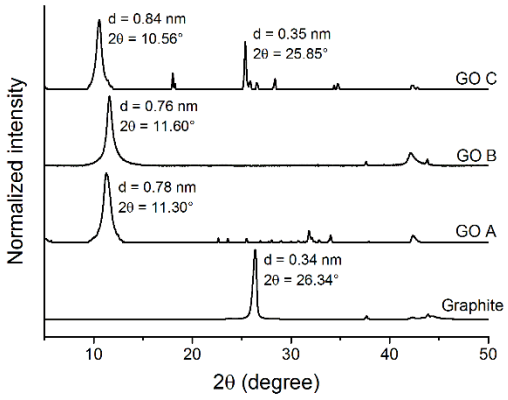

Figure 3.3. XRD diffraction pattern of graphite and graphite oxide samples.

Transmission electron microscopy (TEM) images of graphite showed sharper edges than GO nanosheets (Figure 3.4). TEM images of graphite oxides with different C/O ratios did not show substantial structural differences. Oxidation resulted in fragmentation and wrinkling at the edges of graphite. It is well known that these regions are more susceptible to be oxidized (Dreyer et al., 2010). Addition of graphite and GO samples were evaluated for the reinforcement of CF plastics. GO characterization presented above was used to enrich the analysis of CF-GO plastics.

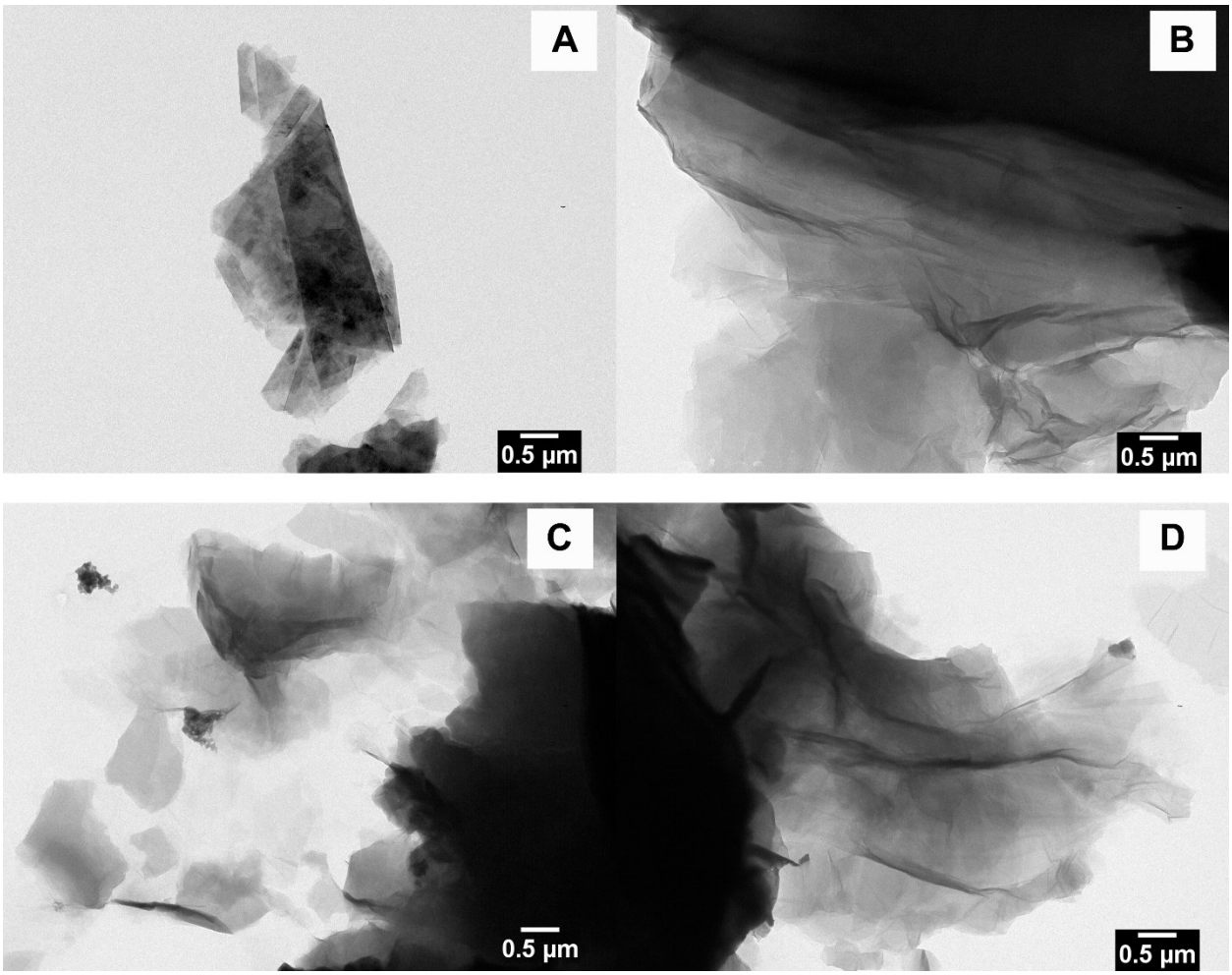

Figure 3.4. Transmission electron microscopy (TEM) micrographs of aqueous suspensions (0.1% wt.) of graphite and graphite oxides used in this study.

3.3.2. Chicken feather plastics

Overall the mechanical properties of CF plastics (and in general any protein based plastic), depend highly on processing consditions, type and amount of plasticizer, relative humidity conditioning, modification of raw material, and presence of reinforcement additives. It has been reported that smaller and more hydrophilic plasticizer molecules result in more ductile CF plastics (Ullah et al., 2011; Ullah et al., 2013). On the other hand lower concentration of plasticizer results in stiffer CF plastics (Barone et al., 2005; Jin et al., 2011). In our case, we have

previously optimized the plasticizer ration, finding that a mixture of propylene glycol/glycerol (50:50) was the most effective in terms of mechanical properties of feather plastics. Glycerol and propylene glycol are small molecules (92 and 76 g/mol, respectively) containing two and three hydroxyl groups, respectively. Their main function is to decrease the glass transition and melting temperatures of keratin in feathers. In terms of mechanical properties, we found that propylene glycol and glycerol contribute to stiffness and ductility, respectively.

3.3.3. Effect of GO with different C/O ratios

Graphite oxide was considered to reinforce CF plastics, since their oxygen functional groups are hypothesized to interact with keratin, thus, resulting in a transfer of load to the graphite oxide. In order to expose keratin functionalities and improve its processability, sodium sulfite was used to reduce the multiple cysteine disulfide bonds found in chicken feather keratin. The effect of 1% addition of graphite and GO samples with different C/O ratio, to feather blends, was evaluated on the tensile mechanical properties of extruded and thermo-molded films (Figure 3.5). Elongation at break of CF-GO and CF plastic film was similar ($p > 0.01$), ranging from 37 to 43% in average. Tensile strength and Young modulus was significantly increased ($p < 0.01$) after addition of 1% wt. of GO B and GO C. Possibly, a higher oxygen content in GO B and GO C is responsible for the higher stiffness of the CF plastic films, by promoting more interactions with feather keratin. GO C did not result in further mechanical improvement compared with GO B, possibly due to decreased proportion of hydroxyl groups at prolonged oxidation (Table 3.2) and re-stacked graphene sheets (Figure 3.3), which might affect GO and CF interactions.

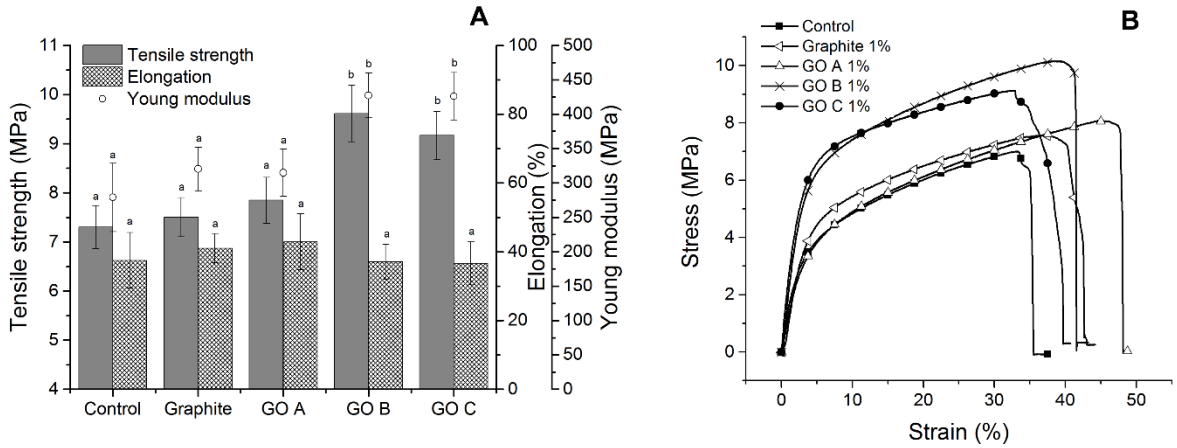

Figure 3.5. Tensile mechanical properties of extruded, thermo-molded CF plastics containing graphite and GO with different C/O ratios (A) and representative stress-strain curves (B). Different letters mean significant differences ($p<0.01$) between different samples for a selected parameter. (3 repetitions x 5 replicate specimens each, data is plot as average ± standard deviation).

3.3.4. Effect of GO concentration

GO B was selected to study the effect of GO concentration on mechanical properties of feather plastics. Mechanical properties of CF plastics containing up to 2% of GO are summarized in Figure 3.6. Incorporation of GO resulted in a significant increase ($p<0.01$) of strength of CF plastics. The highest tensile strength (9.61 MPa) was achieved using 1% GO, which represents a 32% increase compared with the sample at 0% GO addition, and then started to decrease at increasing GO addition. Tensile strength was significant reduced ($p<0.01$) at 2% addition (GO), probably due to partial aggregation of GO at higher concentrations. While the use of graphene is more suitable for aliphatic synthetic resins, the use of oxidized graphene or graphite is more suitable for the reinforcement of hydrophilic polymers including bio-based polymers such as

carbohydrates or proteins (Rodriguez-Gonzalez et al., 2012; Rodriguez-Gonzalez et al., 2013). Tensile strength was reported to increase about two (Wang et al., 2012) or three times (Ma et al., 2013; He et al., 2013) for thermoplastic starch films reinforced with 2.0% wt. of graphene oxide. Although dispersion of GO and protein intercalation would be facilitated in liquid medium than in extrusion, the technique of solution casting to prepare films used in these studies is not a very convenient method for the large production of plastic films as it requires large volumes of solvents/water to be evaporated. Limited number of studies have investigated the reinforcement of polymers with graphene or graphite oxide through melting processing (Potts et al., 2011; Shen et al., 2013).

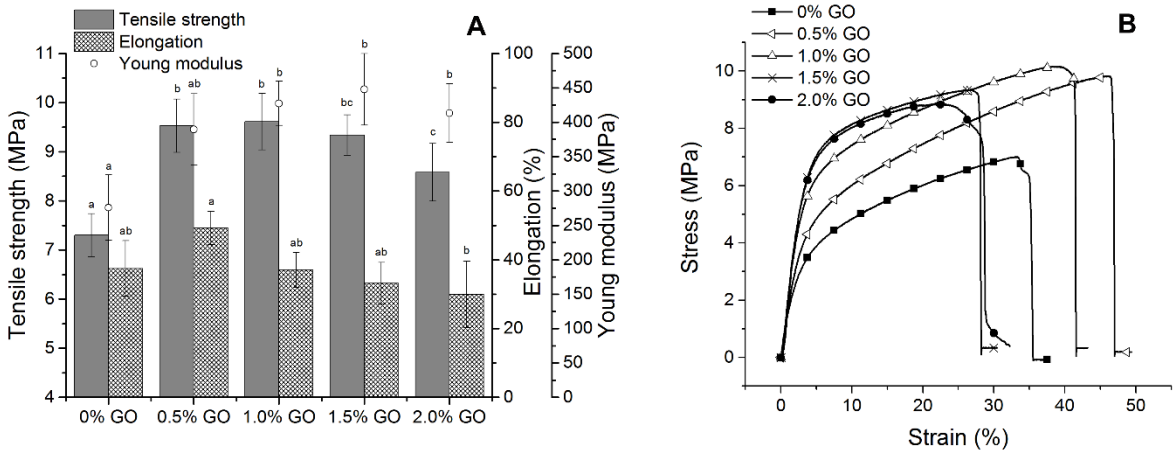

Figure 3.6. Tensile mechanical properties of extruded, thermo-molded CF plastics containing different amounts of GO (GO B) (A) and representative stress-strain curves (B). Different letters mean significant differences ($p<0.01$) between different samples for a selected parameter. (3 repetitions x 5 replicate specimens each, data is plot as average ± standard deviation).

XRD patterns of CF powder is shown in Figure 3.7. CF powder showed two broad peaks (Figure 3.7) located at 9.68° (d = 0.91 nm) and 19.03° (d =0.47 nm) which have been associated

to the α-helix and β-sheet structure of chicken feather keratin, repectively (Rad and Tavanai, 2012; Khosa et al., 2013).

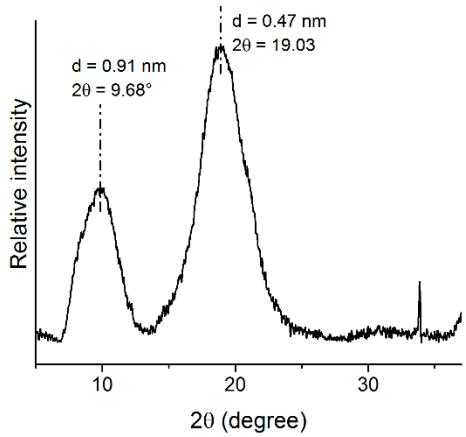

Figure 3.7. X-ray diffraction pattern chicken feather powder.

After extrusion the peak ascribed to α-helix structure remained and a broad peak appeared centered at around 19.5 (Figure 3.8A). The original peak of GO B at 11.60° dissapeared after extrusion of blends, which can be explained by partial re-stacking, as suggested by the small peak seen at 22.70° (Figure 8A), but also by the disruption of the layered structure of GO by the intercalation of plasticizers or keratin chains. In the case of CF plastics containing graphite at 1% wt., the sharp peak at 26.5° remained after extrusion of blends (Figure 3.8B). Due to the closer packing of graphene layers in graphite and its aliphatic nature layer disruption and intercalation did not take place, which can be the reason for the lower tensile strength of graphite-feather plastics.

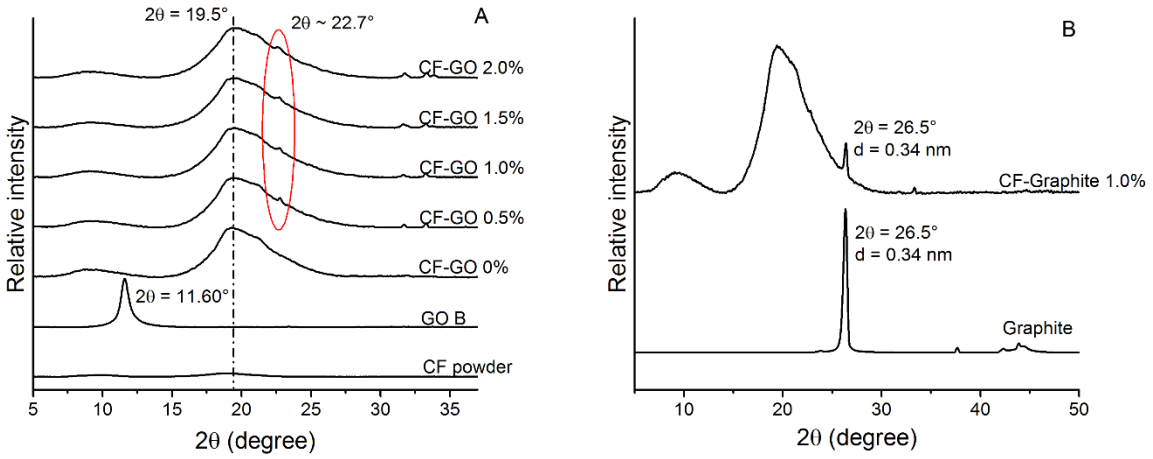

Figure 3.8. X-ray diffraction patterns of GO B and extruded feather plastics (A), and graphite and extruded graphite-feather CF plastics (B).

Changes in functional groups and secondary structure of keratin were evaluated by FTIR (Figure 3.9). Assignment of bands to different functional groups was performed with help of available literature. A broad band seen at around 3300 cm^{-1} (Figure 3.9A) can correspond to OH groups of carboxylic acids, alcohols, or adsorbed moisture, but it can also be attributed of N-H stretching vibration, the so called Amide A region (Kong and Yu, 2007; Ullah et al., 2013). Bands detected at 2800-2962 cm^{-1} can be assigned to C-H stretching vibrations (νC-H). They have been attributed to lipids present in the feathers (Forgacs et al., 2013) but they also can result from amino acids side chain vibrations. Typical Amide I, II and III bands were observed (Figure 9A). Absorption bands observed at 1049 and 1109 cm^{-1} correspond to C-O bonds of glycerol and propylene glycol. While band at 1049 cm^{-1} accounts for C-OH vibrations in carbons C1 and C3 of glycerol, absorption at 1109 cm^{-1} is attributed to C-OH vibration at C2 (Routray et al., 2013). It was noticed that samples containing GO decreased the intensity of the peak at 1109 cm^{-1} when compared to the sample without GO, which was probably due to specific interactions between GO and C2 of glycerol.

Changes in the secondary structure of feather keratin were evaluated by studying the Amide I region of FTIR spectra (1700-1600 cm^{-1}). Second derivative of the single amide I band was used to reveal the overlapped bands in this region (Figure 3.9B). Three bands at 1635, 1666, and 1694 cm^{-1} were found in raw feather which can be assigned to parallel β-sheet, turns, and anti-parallel β-sheet, respectively (Jackson and Mantsch, 1995; Kong and Yu, 2007). This is in accordance to the proposed organization of β-keratins in feathers, in which β-sheets are twisted and held together by turns forming a helical filament (Fraser and Parry, 2008). It has been reported that feather quills and barbs/barbules are predominant in β-sheet, and α-helix structures, respectively (Schmidt, 2002). However, according to other authors (Alibardi and Toni, 2008; Ng et al., 2012), only small amounts of α-keratins are present in barbs, barbules, and down feathers, and especially in early development of feathers. After that, α-keratin filaments are replaced by thinner β-keratin filaments. Second derivative results show changes in the structure of keratin after extrusion (Figure 3.9B). The band at 1694 cm^{-1} in raw feathers disappeared whereas a new band centered at 1684 cm^{-1} revealed a major presence of turns in the keratin structure. Probably, a more disordered conformation was created after extrusion of feathers.

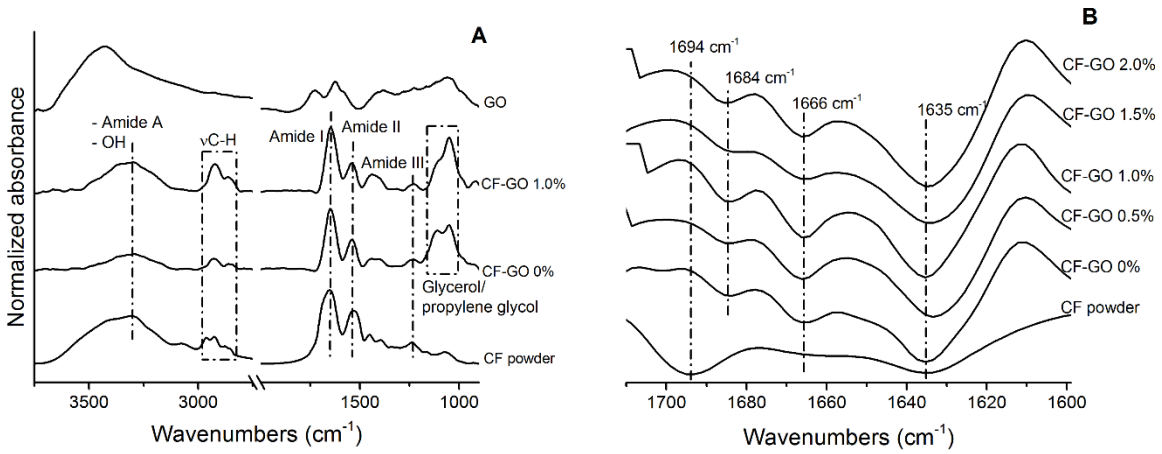

Figure 3.9. FTIR spectra of chicken feather, GO, and selected CF plastics samples (A) and second derivative of amide I FTIR region of feather and CF plastics samples (B).

Chicken feathers are thermally stable materials degrading at temperatures above 250°C (Figures 3.10 and 3.11). TGA thermograms of CF plastics showed more loss of weight at 200°C as the amount of graphite oxide increased (Figure 3.10). Contrarily, it has been suggested that the homogenous dispersion of graphene oxide layers could create a barrier, preventing the emission of decomposition products during the non-oxidative combustion (Valles et al., 2013). From the TGA results, it is not possible to determine the nature of the decomposing products at around 200°C, but it can be hypothesized based on the composition of the materials. The dry percentage of GO is smaller than the weight loss seen in the thermograms at 185°C which increased from 5.9& in CF-GO 0% to 12% in CF-GO 2%. It can be stated that decomposition products other than oxygen functionalities of GO might be released. Propylene glycol has a boiling point of 188.2°C and its amount in the extrudates is 15%; thus, we can hypothesize that the incorporation of GO could result in higher amounts of free propylene glycol. Possibly GO competes with propylene glycol to interact with glycerol and feather keratin. As suggested by FTIR results, GO can preferentially interact with glycerol compared to propylene glycol as propylene glycol has

less hydrophilic nature. At 300°C the weight loss percentage of all samples was similar (around 40%) At this temperature degradation of keratin and GO functionalities, along with glycerol evaporation are responsible for the loss of weight.

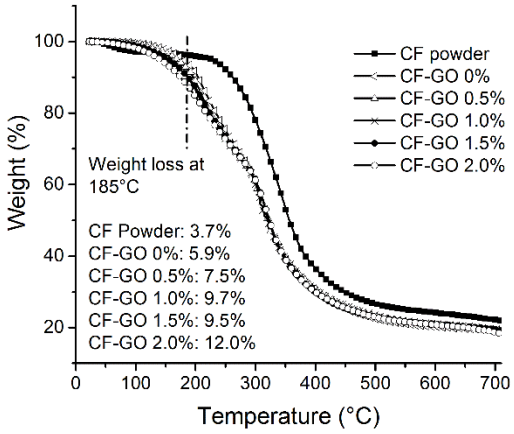

Figure 3.10. *TGA thermographs of CF powder and CF-GO plastics.*

Feather keratin is a semi-crystalline protein (Schmidt, 2002). DSC clearly shows the melting of the crystalline keratin happening from around 210 to 230°C, whereas degradation was noticed after 250°C (Figure 3.11). In CF plastic samples degradation of thermoplastics was observed at around 250°C. The melting of crystalline keratin shifted to a lower temperature (~170°C) than in the raw feathers due to plastization of keratin. Therefore, thermo-molding of CF-GO plastic resin can be performed at temperatures as high as 170°C.

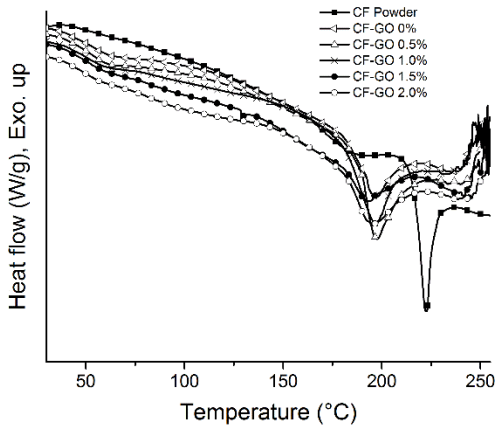

Figure 3.11. DSC thermograms of CF powder and CF-GO plastics.

3.4. Conclusions

Processing of chicken feathers into a plastic material was achieved by extrusion at 150°C with the aid of sodium sulfite, glycerol/propylene glycol mixture, and water. Mechanical properties of thermo-molded plastics were significantly ($p < 0.01$) improved by the addition of graphite oxide at a level of 1% (w/w, GO/feather blend). The tensile strength was increased up to 32% at 1% w/w GO with a C/O ratio of 2.07. Our results suggest that higher proportion of hydroxyl groups and increase of the graphene interlayer space in graphite oxide could result in more protein- and plasticizer-GO interactions. GO is a less expensive and more effective alternative to graphene for the improvement of the physical properties of bio-based protein plastics. In addition, the use of reactive extrusion for its dispersion/reaction represents an environment-friendly alternative for scale up production. Further examination of possible applications of CF-GO plastics as agricultural films, composting bags, and biodegradable containers needs to be considered under different environments.

3.5. References

Agriculture and Agri-Food Canada. Retrieved online from http://www.agr.gc.ca/ on February 11th, 2015.

Alibardi, L., & Toni, M. (2008). Cytochemical and molecular characteristics of the process of cornification during feather morphogenesis. *Progress in Histochemistry and Cytochemistry*, 43, 1-69.

Barone, J.R., Schmidt, W.F., & Gregoire, N.T. (2006) Extrusion of feather keratin. *Journal of Applied Polymer Science*, 100, 1432-1442.

Barone, J.R., Schmidt, W.F., & Liebner, C.F.E. (2005). Thermally processed keratin films. *Journal of Applied Polymer Science*, 97, 1644-1651.

Bragg, W.H., & Bragg, W.L. (1913). The reflection of X-rays by crystals. *Proceedings of the Royal Society of London A*, 428-438.

Chen, W., Yan, L., & Bangal, P.R. (2010). Preparation of graphene by the rapid and mild thermal reduction of graphene oxide induced by microwaves. *Carbon*, 48, 1146-1152.

Cheng, S., Lau, K., Liu, T., Zhao, Y., Lam, P., & Yin, Y. (2009). Mechanical and thermal properties of chicken feather fiber/PLA green composites. *Composites Part B: Engineering*, 40, 650-654.

Dreyer, D.R., Park, S., Bielawski, C.W., & Ruoff, R.S. (2010). The chemistry of graphene oxide. *Chemical Society Reviews*, 39, 228-240.

Estévez-Martínez, Y., Velasco-Santos, C., Martínez-Hernández, A.L., Delgado, G., Cuevas-Yáñez, E., Alaníz-Lumbreras, D., Duron-Torres, S., & Castaño, V.M. (2013). Grafting of multiwalled carbon nanotubes with chicken feather keratin. *Journal of Nanomaterials*, Volume 2013, Article ID 702157.

Flores-Hernández, C.G., Colin-Cruz, A., Velasco-Santos, C., Castaño, V.M., Rivera-Armenta, J.L., Almendarez-Camarillo, A., Garcia-Casillas, P.E., & Martínez-Hernández, A.L. (2014). All green composites from fully renewable biopolymers: Chitosan-starch reinforced with keratin from feathers, *Polymers*, 6, 686-705.

Forgacs, G., Lundin, M., Taherzadeh, M.J., & Horvath, I.D. (2013). Pretreatment of chicken feather waste for improved biogas production. *Applied Biochemistry and Biotechnology*, 169, 2016-2028.

Fraser, R.D.B., & Parry, D.A.D. (2008). Molecular packing in the feather keratin filament. *Journal of Structural Biology*: 162, 1-13.

Gardella, L., Furfaro, D., Galimberti, M., & Monticelli, O. (2015). On the development of a facile approach based on the use of ionic liquids: preparation of PLLA (sc-PLA)/high surface area nano-graphite systems. *Green Chemistry*, 17, 4082-4088.

Ghani, S.A., Tan, S.J., & Yeng, T.S. (2013). Properties of chicken feather fiber-filled low-density polyethylene composites: The effect of polyethylene grafted maleic anhydride. *Polymer-Plastics Technology and Engineering*, 52, 495-500.

Gonzalez, D., Campos, A.R., Cunha, A.M., Santos, V., & Parajo, J.A. (2011). Manufacture of fibrous reinforcements for biodegradable biocomposites from Citysus scoparius. *Journal of Chemical Technology and Biotechnology*, 86, 575-583.

Haubner, K., Murawski, J., Olk, P., Eng, L.M., Ziegler, C., Adolphi, B., & Jaehne, E. (2010). The route to functional graphene oxide. *ChemPhysChem*, 11, 2131-2139.

He, Y., Wang, X., Wu, D., Gong, Q., Qiu, H., Liu, Y., Wu, T., Ma, J., & Gao, J. (2013). Biodegradable amylose films reinforced by graphene oxide and polyvinyl alcohol. *Materials Chemistry and Physics*, 142, 1-11.

Hontoria-Lucas, C., Lopez-Peinado, A.J., Lopez-Gonzalez, J.D., Rojas-Cervantes, M.L., & Martin-Aranda, R.M. (1995). Study of oxygen-containing groups in a series of graphite oxides: Physical and chemical characterization. *Carbon*, 33, 1585-1592.

Hu, H., Reddy, N., Yan, K., & Yang, Y. (2011). Acetylation of chicken feathers for thermoplastic applications. *Journal of Agricultural and Food Chemistry*, 59, 10517-10523.

Hummers, W.S., & Offeman, R.E. (1958). Preparation of graphitic oxide. *Journal of the American Chemical Society*, 80, 1339-1339.

Jackson, M., & Mantsch, H.H. (1995). The use and misuse of FTIR spectroscopy in the determination of protein structure. *Critical Reviews in Biochemistry and Molecular Biology*, 30, 95-120.

Jackson, S.T., & Nuzzo, R.G. (1995). Determining hybridization differences for amorphous carbon from the XPS C1s envelope. *Applied Surface Science*, 90, 195-203.

Jin, E., Reddy, N., Zhu, Z., & Yang, Y. (2011). Graft polymerization of native chicken feathers for thermoplastic applications. *Journal of Agricultural and Food Chemistry*, 59, 1729-1738.

Khosa, M.A., Wu, J., & Ullah, A. (2013). Chemical modification, characterization, and application of chicken feathers as novel biosorbents. *RSC Advances*, 3, 20800-20810 (2013).

Kong, J., & Yu, S. (2007). Fourier transform infrared spectroscopic analysis of protein secondary structures. *Acta Biochimica et Biophysica Sinica*, 39, 549-559.

Kuilla, T., Bhadra, S., Yao, D., Kim, N.H., Bose, S., & Lee, J.H. (2010). Recent advances in graphene based polymer composites. *Progress in Polymer Science*, 35, 1350-1375.

Lee, S-Y., & Park, S-J. (2014). Isothermal exfoliation of graphene oxide by a new carbon dioxide pressure swing method. *Carbon*, 68, 112-117.

Li, M., Jin, E., & Zhang, L. (2016). Effects of graft modification on the water solubility, apparent viscosity, and adhesion of feather keratin for warp sizing. *Journal of the Textile Institute*, 107, 395-404.

Ma, T., Chang, P.R., Zheng, P., & Ma, X. (2013). The composites based on plasticized starch and graphene oxide/reduced graphene oxide. *Carbohydrates Polymers*, 94, 63-70.

Martínez-Hernández, A.L., & Velasco-Santos, C. Keratin Fibers from Chicken Feathers: Structure and Advances. In Dullart, R., & Mousques, J. (Eds.). Polymer Composites. Keratin: Structure, Properties and Applications, Nova Science Publishers Inc., Hauppauge, NY, USA, (2011) p149–211.

Martínez-Hernández, A.L., Santiago-Valtierra, A.L., & Alvarez-Ponce, M.J. (2008). Chemical modification of keratin biofibres by graft polymerisation of methyl methacrylate using redox initiation. *Materials Research Innovations*, 12, 184-191.

Martínez-Hernández, A.L., Velasco-Santos, C., de Icaza, M., & Castaño, V.M. (2003). Grafting of methyl methacrylate onto natural keratin. *e-Polymers*, 3, 209–219.

Ng, C.S., Wu, P., Foley, J., Foley, A., McDonald, M-L., Juan, W-T., Huang, C-J., Lai, Y-T., Lo, W-S., Chen, C-F., Leal, S.M., Zhang, H., Widelitz, R.B., Patel, P.I., Li, W-H., & Chuong, C-M. (2012). The chicken frizzle feather is due to an α-keratin (KRT75) mutation that causes a defective rachis. *PLOS Genetics*, 8:e1002748, 1-16.

Novoselov, K.S., Geim, A.K., Morozov, S.V., Jiang, D., Zhang, Y., Dubonos, S.V., Grigorieva, I.V., & Firsov, A.A. (2004). Electric field effect in atomically thin carbon films. *Science*, 306, 666-669.

Paredes, J.I., Villar-Rodil, S., Martinez-Alonso, A., & Tascon, J.M.D. (2008). Graphene oxide dispersions in organic solvents. *Langmuir*, 24, 10560-10564.

Pei, S., & Cheng, H-M. (2012). The reduction of graphene oxide. *Carbon*, 50, 3210-3228.

Posudievsky, O.Y., Khazieieva, O.A., Koshechko, V.G., & Pokhodenko, V.D. (2012). Preparation of graphite oxide by solvent-free mechanochemical oxidation of graphite. *Journal of Materials Chemistry*, 22, 12465-12467.

Potts, J.R., Murali, S., Zhu, Y., Zhao, X., & Ruoff, R.S. (2011). Microwave-exfoliated graphite oxide/polycarbonate composites. *Macromolecules*, 44, 6488-6495.

Rad, Z.P., & Tavanai, H. (2012). Production of feather keratin nanopowder through electrospraying. *Journal of Aerosol Science*, 51, 49-56.

Rodríguez-González, C., Kharissova, O.V., Martínez-Hernández, A.L., Castaño, V.M., & Velasco-Santos, C. (2013). Graphene oxide sheets covalently grafted with keratin obtained from chicken feathers. *Digest Journal of Nanomaterials and Biostructures*, 8, 127-138.

Rodríguez-González, C., Martínez-Hernández, A.L., Castaño, V.M., Kharissova, O.V., Ruoff, R.S., & Velasco-Santos, C. (2012). Polysaccharide nanocomposites reinforced with graphene oxide and keratin-grafted graphene oxide. *Industrial & Engineering Chemistry Research*, 51, 3619-3629.

Routray, M., Rout, S.N., Mohanty, G.C., & Nayak, P.L. (2013). Preparation and characterization of soy protein isolate films processed by compression and casting. *Journal of Chemical and Pharmaceutical Research*, 5, 752-761.

Schmidt, W. (2002). Microcrystalline keratin: From feathers to composite products. *Materials Research Society Symposium Proceedings*, 702, U1.5.1-U1.5.8.

Schniepp, H.C., Li, J-L., McAllister, M.J., Sai, H., Herrera-Alonso, M., Adamson, D.H., Prud'homme, R.K., Car, R., Saville, D.A., & Aksay, I.A. (2006). Functionalized single graphene sheets derived from splitting graphite oxide. *The Journal of Physical Chemistry B*, 110, 8535-8539.

Schrooyen, P.M.M., Dijkstra, P.J., Oberthür, R.C., Bantjes, A., & Feijen, J. (2001). Partially carboxymethylated feaher keratins. 2. Thermal and mechanical properties of films. *Journal of Agricultural and Food Chemistry*, 49, 221-230.

Shao, G., Lu, Y., Wu. F., Yang, C., Zeng, F., & Wu, Q. (2012). Graphene oxide: The mechanism of oxidation and exfoliation. *Journal of Materials Science*, 47, 4400-4409.

Shen, B., Zhai, W., Tao, M., Lu, D., & Zheng, W. (2013). Enhanced interfacial interaction between polycarbonate and thermally reduced graphene induced by melt blending. *Composites Science and Technology*, 86, 109-116.

Shin, H-J., Kim, K.K., Benayad, A., Yoon, S-M., Park, H.K., Jung, I-S., Jin, M.H., Jeong, H-K., Kim, J.M., Choi, J-Y., & Lee, Y.H. (2009). Efficient reduction of graphite oxide by sodium borohydride and its effect on electrical conductance. *Advanced Functional Materials*, 19, 1987-1992.

Stankovich, S., Piner, R.D., Nguyen, S.T., & Ruoff, R.S. (2006). Synthesis and exfoliation of isocyanate-trated graphene oxide nanoplatelets. *Carbon*, 44, 3342-3347.

Tien, H-W., Huang, Y-L., Yang, S-Y., Wang, J-Y., & Ma, C-C.M. (2011). The production of graphene nanosheets decorated with silver nanoparticles for use in transparent, conductive films. *Carbon*, 49, 1550-1560.

Ullah, A., & Wu, J. (2013). Feather fiber-based thermoplastics: Effects of different plasticizers on material properties. *Macromolecular Materials and Engineering*, 298, 153-162.

Ullah, A., Vasanthan, T., Bressler, D., Elias, A.L., & Wu, J. (2011). Bioplastics from feather quill. *Biomacromolecules*, 12, 3826-3832.

Valles, C., Kinloch, I.A., Young, R.J., Wilson, N.R., & Rourke, J.P. (2013). Graphene oxide and base-washed graphene oxide as reinforcements in PMMA nanocomposites. *Composites Science and Technology*, 88, 158-164.

Verbeek, C.J.R., & van den Berg, L.E. (2010). Extrusion processing and properties of protein-based thermoplastics. *Macromolecular Materials and Engineering*, 295, 10-21.

Wang, Y., Shi, Z., Yu, J., Chen, L., Zhu, J., & Hu, Z. (2012). Tailoring the characteristics of graphite oxide nanosheets for the production of high-performance poly(vinyl alcohol) composites. *Carbon*, 50, 5525-5536.

Wei, L., Wu, F., Shi, D., Hu, C., Li, X., Yuan, W., Wang, J., Zhao, J., Geng, H., Wei, H., Wang, Y., Hu, N., & Zhang, Y. (2013). Spontaneous intercalation of long chain alkyl ammonium into edge-selectively oxidized graphite to efficiently produce high-quality graphene. *Scientific Reports*, 3, 1-9.

Yamada, Y., Yasuda, H., Murota, K., Nakamura, M., Sodesawa, T., & Sato, S. (2013). Analysis of heat-treated graphite oxide by X-ray photoelectron spectroscopy. *Journal of Materials Science*, 48, 8171-8198.

Yumitori, S. (2000). Correlation of C1s chemical state intensities with the O1s intensity in the XPS analysis of anodically oxidized glass-like carbon samples. *Journal of Materials Science*, 35, 139-146.

Zhou, X., Zhang, J., Wu, H., Yang, H., Zhang, J., & Guo, S. (2011). Reducing graphene oxide via hydroxylamine: A simple and efficient route to graphene. *The Journal of Physical Chemistry*, 115, 11957-11961.

CHAPTER 4. Molecular mechanism and characterization of self-assembly of feather keratin gelation

4.1. Introduction

Gel scaffolds prepared from proteins are of particular interest due to their abundance, biodegradability, compatibility with biological systems and the presence of peptide motif important for cell adhesion (Drury and Mooney, 2003; Jonker et al., 2012). Keratins are fibrous proteins widely found in animal tissues including hair, skin epidermis, wool, hooves, scales and feathers. Keratin hydrogel scaffolds from hair and wool have demonstrated good biocompatibility for tissue engineering applications (Tachibana et al., 2002; Aboushwareb et al., 2009; Hill et al., 2010). However, there is scanty information on feather keratin derived hydrogels in literature.

Keratins from chicken feather are an abundant yet underutilized protein source. As a result of poultry processing, over 65 million tons of feathers are generated worldwide (Zhao et al., 2012). Keratin accounts for more than 90% (w/w) of feathers. A remarkable feature of feather keratins is their high content of cysteine residues and disulfide bonds, which confer strength and impermeability to keratinous tissues. Solubilization of keratin is a limiting factor for the development of films, coatings and gels (Schrooyen et al., 2001). Thiols, sulfites, and urea are often used to solubilize keratins (Nakamura et al., 2002). However, aggregates formed after removal of the denaturing chemicals are considered as an undesirable phenomena from the processing point of view (Tonin et al., 2007; Nakaji-Hirabayashi et al., 2008). The aggregation resultant from dialysis or dilution of reduced feather keratin solution was reported early (Woodin, 1953). More recently it was found that the reformation of disulfide bonds during dialysis of feather keratin was the main factor for the formation of aggregates (Schrooyen et al., 2000). Therefore, blocking of cysteine thiols was applied to solublilize keratins, either using chemical grafting (Ikkai and Nato, 2002; Yuan et al., 2008; Zhou and Wang, 2011), oxidation

into sulfonic acids (De Guzman et al., 2011), or by the formation of keratin sodium dodecyl sulfate (SDS) complexes (Schrooyen et al., 2001; Yin et al., 2013; Xu and Yang, 2014). The heat-induced gelation of S-carboxymethyl wool keratin derivative has been studied (Ikkai and Nato, 2002). It was determined that the gelation was triggered by the exposure and assembly of hydrophobic α-helical regions in the central part of keratins chains followed by the formation of disulfide bonds. It is reported that upon substantial denaturation of the α-helix structure gel formation did not take place. In this study the reformation of disulfide bonds might be impaired by the chemical modification of keratin. Suprisingly, the spontaneous aggregation of fully reduced keratin has not been widely explored as an advantage for the fabrication of strong hydrogels.

Hydrogels from fully reduced wool and hair keratin have remarkable mechanical properties (Fujii and Ide, 2004; Hill et a., 2010; Richter et al., 2012; Ozaki et al., 2014). Feather keratins differ from wool and hair since they have lower molecular weight, and are predominant in β-sheet secondary conformation (Bragulla and Homberger, 2009). It has been recognized that disulfide bonds play a major role in the formation of small aggregates in feather keratin solutions (Schrooyen et al., 2000; Han et al., 2015). However, it has not been determined at which extent disulfide reformation or other intermolecular interactions are necessary for the formation and modulation of viscoelastic properties of feather keratin gels. Viscoelastic and physical properties of hydrogel scaffolds can affect different aspects of cellular behavior including, cell adhesion, morphology, survival and tissue regeneration (Lo et al., 2000). Therefore, the determination of conditions and mechanisms that control the gelation of fully reduced feather keratin could help to modulate physical and biological properties of hydrogels.

In this study hydrogels from fully reduced feather keratin were prepared by dialysis. The objectives of this work were to study the molecular mechanism on self-assembly of feather keratin gels formed during dialysis of keratin extracts and to characterize the structural and viscoelastic properties of hydrogels prepared under various pHs and temperatures.

4.2. Materials and methods

4.2.1. Materials and chemicals

White chicken feathers were obtained from the Poultry Research Centre of the University of Alberta (Edmonton, AB, Canada). After exhaustive washing with hot water and domestic soap (Green Works®), feathers were allowed to dry in a fume hood followed by drying at 50°C overnight in an oven. Dried feathers were ground in a cutting mill (Fritsch Pulverisette 15, Fritsch, Germany) with an insert sieve of circular perforations of 1 mm diameter. Ground feathers were defatted with petroleum ether for 5 h in a soxhlet apparatus. The defatted feathers were recovered and the residual solvent was allowed to evaporate overnight at room temperature. Defatted feather powder was stored at 4°C for further uses. Urea, thiourea, sodium metabisulfite, N-ethylmaleimide (NEM), 5,5'-dithiobis(2-nitrobenzoic acid) (DNTB; Ellman's reagent), hydrogen peroxide, 1,4-dithiothreitol (DTT), formaldehyde solution 36.5-38%, and sodium dodecyl sulfate (SDS) were obtained from Sigma-Aldrich (St Louis, MO, U.S.).

4.2.2. Amino acid analysis

Chicken feather powder samples were digested with 6 N HCl for quantification of all amino acids, with exception of cysteine. For cysteine, separate samples were previously hydrolyzed with performic acid. Cysteine was determined as cysteic acid and results expressed as half-cystine content according to the method reported by Moore (1963). Hydrolyzed samples were

derivatized with PITC (phenylisothiocyanate) and analyzed in a HPLC system equipped with a Supelcosil LC-18 reverse phase column and a UV detector (254 nm). Individual amino acids concentration was calculated from the retention times and peak areas of a standard amino acid mixture (Sigma-Aldrich, U.S.). Total nitrogen in keratinous samples was determined in a Leco Truspec C/N analyzer (Leco Corp. MI, U.S.).

4.2.3. Preparation of feather keratin hydrogels

Extraction of keratin was achieved by mixing 13.3 g of defatted feather powder with 200 mL of extracting solution consisting of 5 M urea, 2.6 M thiourea and 5% w/v sodium metabisulfite at pH 7.0, 50°C for 5 h. Non-solubilized feather powder was removed by filtration through a metallic sieve (53 μm) and the filtrate was used for gelation experiments. The protein concentration of the gelling solution was calculated to 4.20% ± 0.20 w/v, measured by Dumas's method of freeze dried gels in a Leco Truspec C/N Analyzer (Leco Corporation, MI, USA). Gelation of keratin samples (50 mL aliquots) was induced by dialysis using a molecular weight cut-off of 3,500 Da for 5 days at 4°C with change of the outer distilled water twice per day. The volume ratio during dialysis was 40 mL of distilled water per 1 mL of keratin solution.

4.2.4. Protein electrophoresis

Extracted keratin from feathers was solubilized in glycine-SDS running buffer containing 5% v/v 2-mercaptoethanol. Samples were diluted 1:1 volume ratio with loading buffer and loaded into 10-20% precast polyacrylamide gels (Bio-Rad Laboratories Inc. U.S). Electrophoresis was run at 200 V. Proteins were stained with Coommassie blue according to regular SDS-PAGE protocols (Laemmli et al., 1970).

4.2.5. Effects of cysteine thiols on gelation

To study the effect of cysteine thiol groups on gelation, keratin solution recovered by filtration after extraction was reacted with various N-ethylmaleimide (NEM)/cysteine molar ratios (1.0, 2.5, 5.0 and 10.0; namely NEM 1, NEM 2.5, NEM 5.0 and NEM 10, respectively) in order to prevent disulfide bond re-formation. The pH was rapidly re-adjusted to 7 and the solution was stirred at room temperature for 1 h. Gelation was induced by dialysis for 5 days at 4°C with change of the outer water twice per day.

4.2.6. Determination of blocked cysteine

A modified Ellman's method was used to determine the total SH groups in the presence of sodium sulfite (Thannhauser et al., 1984). The amount of modified SH groups in NEM modified keratin was calculated according to Schrooyen *et al*., (2000) using the following equation:

$$\text{Degree of modification} = \frac{SH_k - SH_{\text{mod}k}}{SH_k} \times 100$$

Where SH_k and $SS_{mod\ k}$ are the total μmol of SH of unmodified keratin and NEM-modified keratin (after dialysis and freeze drying), respectively. A molar extinction coefficient of 14,150 mM^{-1} cm^{-1} for the Ellman's chromophore molecule (5-thio-2-nitrobenzoic acid) was applied in the calculation (Riddles et al., 1979).

4.2.7. Proton nuclear magnetic resonance (^{1}H-NMR) of NEM-modified keratin

^{1}H-NMR of keratin and NEM modified keratin samples was recorded in an Angilent/Varian MR400 spectrometer (400 Hz). To yield soluble samples, 0.1% w/v keratins were heated for 24 h at 50°C in extracting solution consisting of 5 M urea, 2.6 M thiourea and 5% w/v sodium metabisulfite at pH 7.0. After dialysis (5 days) samples were freeze dried. Keratin samples were dissolved in D_2O for H-NMR.

4.2.8. Time of flight-secondary ion mass spectrometry (TOF-SIMS) of NEM-modified keratin

Ion mass spectra of keratin and N-ethylmaleimide (NEM) modified keratin powder pellets was recorded using a TOF-SIMS imaging spectrometer (ION-TOF GmbH, Münster, Germany), equipped with a dual beam profiling (Ar/O2/Cs for layer removal and Ga for analysis).

4.2.9. Fourier transform infrared spectroscopy (FTIR)

Fourier transform infrared (FTIR) spectroscopy analysis of keratin samples was performed in a Nicolet iS50 FTIR spectrometer (Thermo Scientific Inc., WI, USA) equipped with a single bounce ATR diamond crystal at 64 scans with a resolution of 4 cm^{-1} from 400-4000 cm^{-1}. Secondary structure of keratin was evaluated by Fourier self-deconvolution (FSD) treatment of the amide I region (1600-1700 cm^{-1}) of FTIR spectra using Omnic 8.1 software, considering a bandwidth of 26 cm^{-1} and an enhancement factor of 2.5. Characteristic secondary structure peaks in this region were compared with the reported literature.

4.2.10. Thermal analysis

Differential scanning calorimetry (DSC) of powder keratin samples was performed in a TA DSC Q2000 instrument (TA Instruments, DE, USA) at a heating rate of 10°C/min from 25 to 300°C using nitrogen as purge gas.

4.2.11. Effect of pH and temperature on gelation

Solubilized chicken feather (13.3 g in 200 mL of KES) was filtered through a metallic sieve (53 μm). Aliquots of 50 mL of solubilized chicken feather (keratin) were adjusted to pH 3, 5, 7, and 9 (at room temperature) and stirred for 1 h before inducing gelation by dialysis as described previously. To study the effect of temperature, a new batch of solubilized chicken feather was separated in aliquots of 40 mL and were heated at 50, 60, 70, 80, or 90°C (pH 7) in a water bath

for 1 h. Sol-gel transition was induced by dialysis and soluble protein recovered after gelation was quantified using a Lowry protein assay kit (Thermo Scientific, USA) using bovine serum albumin as the standard. SDS-PAGE of soluble proteins was performed under reducing conditions.

4.2.12. Small amplitude oscillatory shear measurements (SAOS)

Rheological characterization of keratin gels was carried out using frequency sweeps from 1 to 10 Hz at a strain rate of 0.5%, within the linear viscoelastic region, on a Physica MCR 301 rheometer (Anton Paar, Graz, Austria). All measurements were performed at 25°C, with a probe gap of 1 mm. To have an insight of molecular interactions, gels were soaked in different destabilizing solutions (SDS 3% w/v, urea 5 M, fresh DTT 100 mM pH 9, and urea 5 M + 100 mM fresh DTT pH 9) for 24 h at room temperature (22°C) prior to measurement.

4.2.13. Zeta potential measurement

Zeta potential of keratin solutions at different pHs was measured in triplicate in a Malvern Zetasizer Nano ZSP Instrument (Malvern Instruments Ltd. UK) using 3 runs per sample.

4.2.14. Statistics

Experiments were performed in triplicate unless otherwise specified. Significant differences were determined by analysis of variance followed by Tukey multiple comparison test at a level of confidence of 95%.

4.3. Results and Discussion

4.3.1. Characterization of feather keratin

Feather contains 92.0 ± 0.4% protein, which is characterized by a high proportion of non-polar amino acids and cysteine amino acids (Table 4.1). The major amino acids in feather are glycine,

serine, leucine, cysteine and glutamic acid. Feather keratins have a molecular weight of around 10 kDa (Figure 4.1), in comparison to keratin size of 40-65 kDa from hair and wool (Bragulla and Homberger, 2009).

Table 4.1. Amino acid composition of chicken feathers (μmol/g)

Arginine	626 ± 34
Lysine	366 ± 34
Aspartic acid	543 ± 50
Glutamic acid	959 ± 68
Histidine	73 ± 5
Serine	1540 ± 66
Threonine	428 ± 39
Half-cystine	1140 ± 105
Tyrosine	177 ± 9
Glycine	2186 ± 129
Alanine	665 ± 47
Valine	761 ± 59
Leucine	1185 ± 75
Isoleucine	436 ± 33
Proline	343 ± 7
Phenylalanine	374 ± 29
Methionine	43 ± 3
Nitrogen %	16.2 ± 0.1
Polar/charged amino acids	49%
Non-polar amino acids	51%

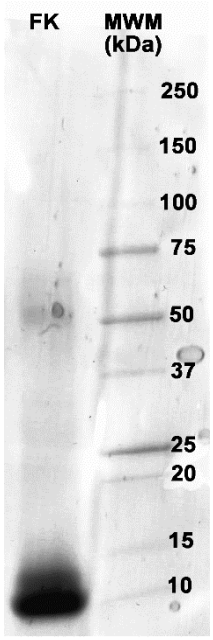

Figure 4.1. *SDS-PAGE of extracted feather keratin (FK)*

4.3.2. Gelation mechanism of feather keratin

Keratin can form small aggregates or gels after removal of urea and reducing agents. Blocking of cysteine thiols can prevent the formation of small keratin aggregates (Schrooyen et al., 2000). However the degree of blocking has not been studied regarding to the formation of gels nor the effects on their viscoelastic properties. N-ethylmaleimide (NEM) at different concentrations was used to block cysteine thiol (-SH) groups of keratin. Cysteine thiols in keratin are highly nucleophilic moeties that react with unsaturated bonds of NEM to produce a stable conjugate through a thioether bond formation (Wong 1991). The reaction of NEM and thiols is highly specific at neutral pH (Figure 4.2). The formation of keratin-NEM conjugate was confirmed by time of flight-secondary ion mass spectrometry (ToF-SIMS, Figure 4.3) and ^{1}H-NMR (Supporting information, Figure S4.1). An increased intensity of NEM ion at 125 amu (atomic mass unit) was observed for NEM 5 and NEM 10 samples (Figure 4.3). The ^{1}H-NMR spectra of

keratin-NEM showed the presence of NEM peaks, which were absent in the spectra non modified keratin (Supporting information, Figure S4.1).

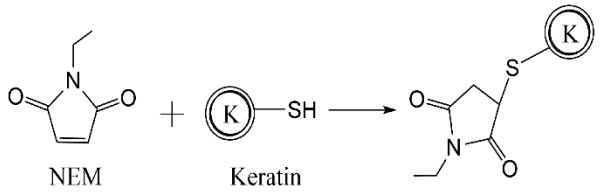

Figure 4.2. *Schematic of reaction between keratin thiols and NEM.*

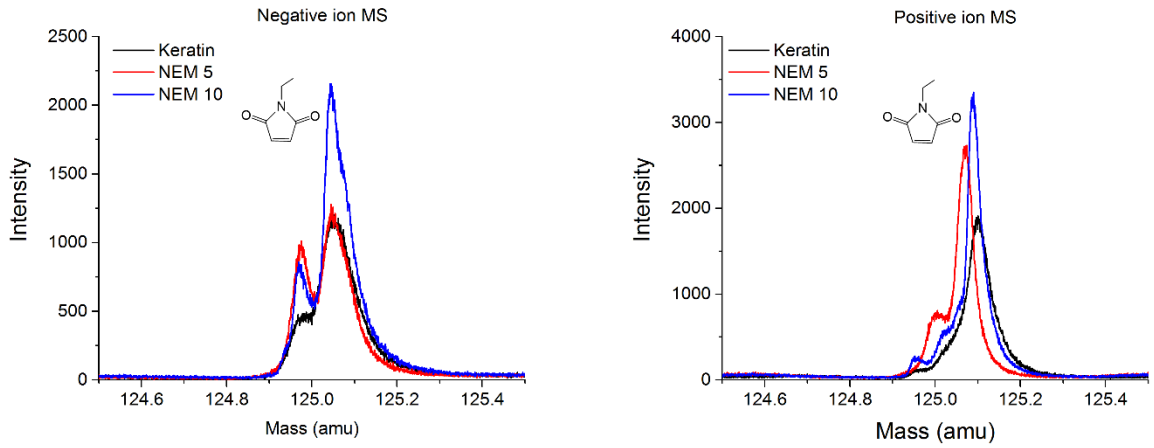

Figure 4.3. Positive and negative ion TOF-SIMS spectra of feather keratin and NEM-modified keratins. Graphs are enlarged to show the mass peak of NEM at 125 amu.

FTIR spectra of feather, keratin and NEM-modified keratin showed typical amide regions (Figure 4.4A). FTIR did not shown any characteristic absorption band associated to urea, thiourea nor sodium sulfite, indicating that dialysis removes any detectable trace of these salts. After extraction, a small band at 1024 cm^{-1} was observed in keratin samples. This can be due to the formation of S-keratin thiosulfates (keratin-SSO_3^-) in presence of sulfite (Nomura et al., 2002). Secondary structure of feather keratin was altered after extraction and NEM modification (Figure 4.4B). The main peak in the Fourier self-deconvoluted amide I region of feather sample

at 1633 cm^{-1} is attributed to β-sheet conformation (Kong and Yu, 2007). This peak remained after keratin extraction and NEM modification. This can be explained by the fact that cysteine residues are predominantly located at the ends of the keratin chain and such terminal regions of keratin are almost devoid of secondary structure (Arai et al., 1983). Therefore, NEM modification should not affect directly the organization of keratin in the central part. Other bands in the FSD amide I region such as 1639-1654 cm^{-1} and 1642-1660 cm^{-1} correspond to unordered and α-helix structures, respectively, whereas bands in between 1660-1694 cm^{-1} can correspond to turns, and β-sheet structures (Barth, 2007).

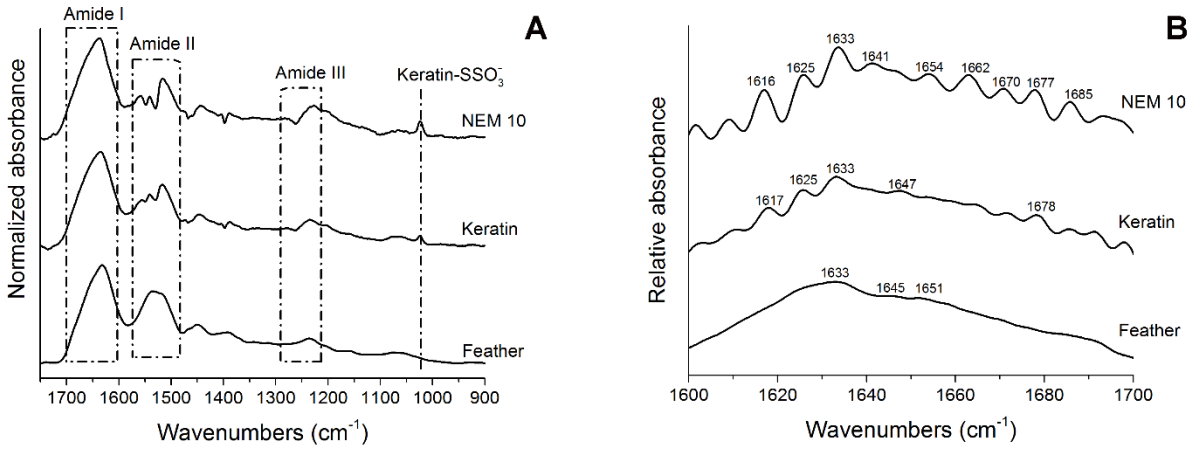

Figure 4.4. FTIR spectra (A) and Fourier self-deconvoluted amide I region (B) of chicken feathers, keratin and NEM modified keratin.

DSC analyses of NEM modified keratin revealed a small shift of the denaturation of crystalline keratin (225.21°C) to lower temperatures, which can be atributed to a reduced capacity of cross-linking due to the incorporation of NEM (Figure 4.5).

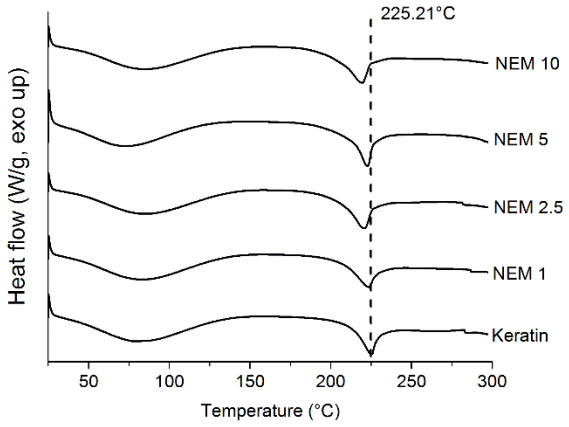

Figure 4.5. DSC thermograms of freeze dried keratin and keratin modified with different molar excess ratios of NEM/Cysteine.

Blocking of keratin thiols was also evaluated by measuring the total –SH groups in freeze dried keratin gels after NEM-modification (Figure 4.6A). A gradual increase in the degree of thiol blocking was observed with increasing molar ratios of NEM to cysteine. Visually weak gels were observed for NEM 1, NEM 2.5 and NEM 5 where 53.5, 58.1 and 71.3% of thiol groups were blocked, respectively. Storage modulus of keratin hydrogels decreased from 10^4-7.5x10^3 Pa to around 1x10^3 Pa as the amount of NEM/cysteine molar ratio increased from 0 to 5 (Figure 4.6B). Gelation did not occur after treating keratin with 10 NEM/cysteine molar ratio where 82.4% of cysteine thiols were blocked (Figure 4.6A and 4.6C). A similar trend of decrease of storage modulus (G') has been observed when hair keratin cysteine thiols were blocked with iodoacetamide (Han et al., 2015). Hydrogels from SDS-extracted keratin were formed only after inducing disulfide crosslinking with hydrogen peroxide. Hydrogels at a concentration of 20% w/v had G' below 10^4 Pa (Wang et al., 2017). SDS can form stable complexes with keratin affecting the ability of disulfide crosslinking.

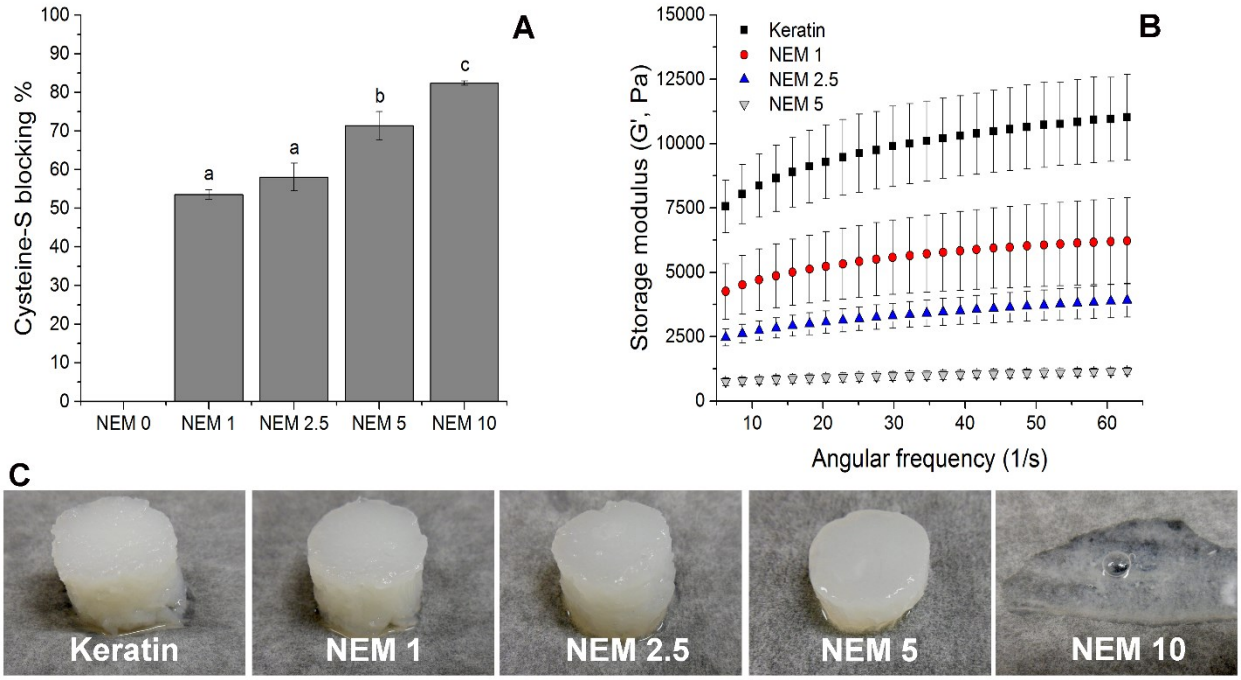

Figure 4.6. Effects of different NEM/cysteine molar ratios on percentage of thiol blocking (A), storage modulus under frequency sweep (B) and visual appearance of gels (C). Different letters mean significant differences between samples ($p<0.05$).

At pH 7, NEM modification is specific for cysteine thiol groups, even in the presence of thiourea (Tyagarajan et al., 2003). Thus, the inhibition of gelation after NEM treatment can be explained by a high degree of blocking of cysteine –SH which are necessary for disulfide crosslinking and the formation of a gel network. In the absence of cysteine thiols keratins assemble into weak gels stabilized mainly by hydrophobic interactions (Ikkai and Nato, 2002; Han et al., 2015).

To elucidate better the intermolecular forces involved in keratin gelation, gels were subjected to small amplitude oscillatory shear (SAOS) measurements after soaking in different destabilizing solutions. Keratin gels were soaked for 24 h in SDS 3%, urea 5 M, or dithiothreitol

(DTT) 100 mM solutions aiming to disrupt mainly hydrophobic interactions, hydrogen/hydrophobic and disulfide bonds, respectively (Bennion and Daggett, 2003; Naidu and Prabhu, 2011). A reduction of storage modulus (Figure 4.7A) after soaking in SDS and urea indicated that gels are partially stabilized by hydrophobic and hydrogen bond interactions. A higher reduction of G' in SDS soaked gels compared to urea suggest a greater importance of hydrophobic interactions over hydrogen bonds on the stability of keratin gel. It is evident that soaking gels in DTT resulted in the most significant decrease of G' suggesting that disulfide bonds play a crucial role in stabilizing the gel. Gels were completely solubilized only when disulfide and hydrogen bonds and hydrophobic interactions were disrupted by soaking in DTT/urea solution (Figure 4.7B).

In solubilization of keratin urea increases the dielectric constant of water. This can facilitate the penetration of urea and other chemicals in the hydrophobic regions of protein, which result in greater solvation of polar and non-polar groups (Klotz, 1996; Rossky 2008). Previously buried disulfide bonds are disrupted by sulfite, resulting in complete solubilization of feather keratin. Removal of reducing and chaotropic agents (such as urea) during dialysis would facilitate protein-protein interactions (e.g. hydrophobic, hydrogen bonds) and cysteine thiol re-oxidation and thus aggregation. At a minimal concentration of ~3%, this leads to the formation of a gel network as represented in Figure 4.7C.

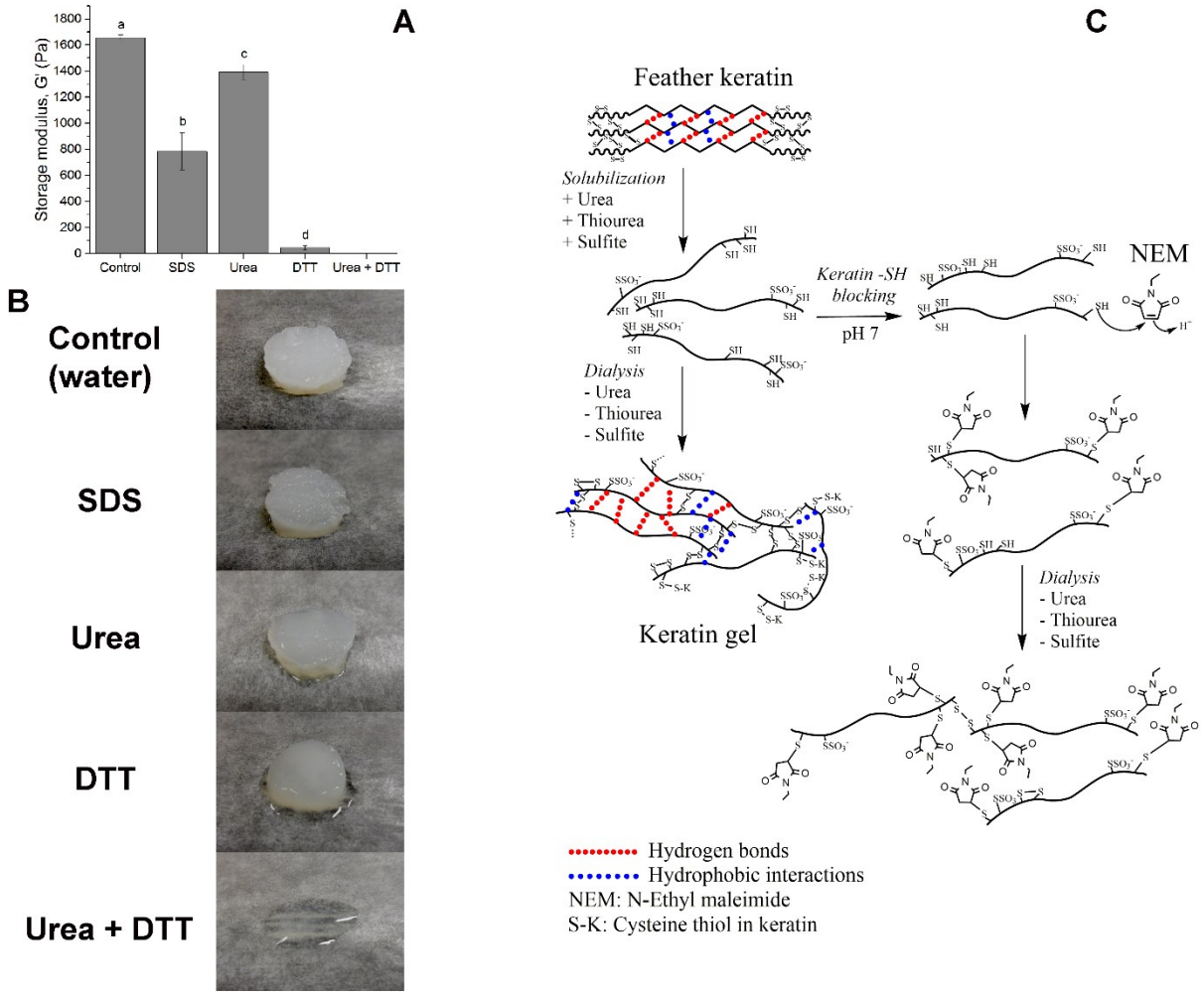

Figure 4.7. Storage modulus of feather keratin gels formed at pH 7 soaked in different solutions reported as the average of three replicates measured at an angular frequency of 5 s^{-1} (A) and their color photographs (B). Proposed mechanism and schematic representation of gelation of feather keratin during dialysis (C).

4.3.3. Effects of pH and temperature on gelation

pH affects the net charge of proteins, and thus the ultrastructure and gelation keratin. After keratin extraction, aliquots were adjusted to different pHs and dialyzed. Rapid gelation occurred at pH 3 and 9, resulting in an opaque coagulum; a more homogenous in appearance and

translucent gel was formed at pH 7, but not at pH 5 (Figure 4.8A). pH had a profound effect on the net charge of keratin molecules in solution (Figure 4.8B). It was observed that between pH 3 and 4, the net surface charge of keratin was close to zero, the isoelectric point of keratin in the salt solution (urea, thiourea and sodium metabisulfite); therefore rapid aggregation of keratin at pH 3 led to the formation of an opaque coagulum with a high storage modulus (G' >> 25,000 Pa, Figure 4.8C). The formation of opaque coagulum from hair keratins at pH of 4-4.5 has also been suggested to happen due to isoelectric precipitation; the gels had a maximum modulus of around 1000 Pa at 5% keratin concentration (Wang et al., 2015). Rapid aggregation of keratin was also observed at pH 9. Although keratins are negatively charged at pH 9, deprotonation of cysteine thiol groups at a pH close to the pKa of cysteine thiols forms highly reactive thiolate anions (−S) that could increase thiol-disulfide exchange reaction rates and thiol oxidation, leading to rapid aggregation (Lo Conte and Carroll, 2013). At pH 7, in absence of isoelectric precipitation or thiol-disulfide exchange reactions, gelation proceeded slowly therefore keratin solution leads to a homogenous gel. The rate of keratin gelation can also be controlled by dialysis conditions. Ozaki et al., (2014) reported fast formation of wool keratin hydrogel during dialysis at 25°C using a volume ratio of 400 mL of water per 1 mL keratin solution. In our case slow gelation was induced by dialysis performed at 4°C with a volume ratio of 40 mL per 1 mL of keratin solution.

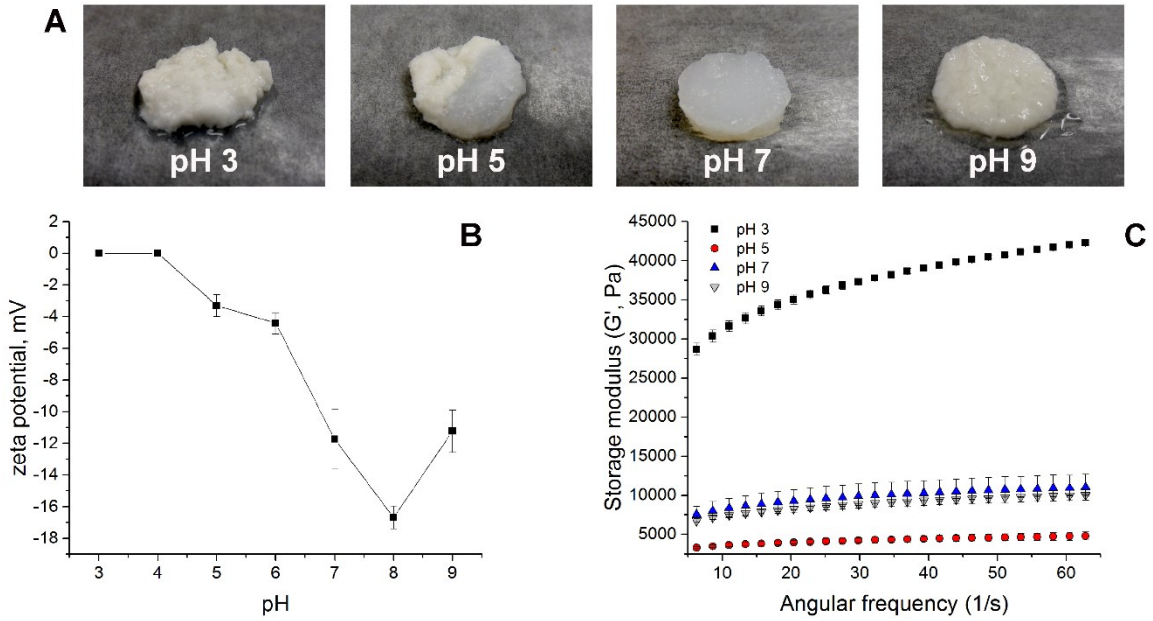

Figure 4.8. Color photographs of keratin gels formed during dialysis of keratin solutions at different pH values (A) and z-potential of keratin solutions at different pH values (B). Frequency sweeps of keratin gels formed after dialysis of keratin solutions at different pH values (C).

The effect of heating keratin solutions on gelation was studied. Keratin gels showed a translucent appearance at 50-70°C while opaque at 80 and 90°C (Figure 4.9A). Storage modulus of gels substantially decreased after pre-heating keratin solutions at 70°C and higher (Figure 4.9B). After gelation, the remaining soluble proteins were analyzed by SDS-PAGE. Keratin heated at 80°C and 90°C showed more intense bands of proteins with molecular weight (MW) of 50, 25, 10-15 kDa, and 5-10 kDa (Figure 4.9C). The presence of small MW proteins (5-10 kDa) could be attributed to the scission of peptide bonds at high temperatures (Tonin et al., 2007; Yin et al., 2013). The partial hydrolysis of keratin at 80-90°C resulted in higher content of soluble protein in the dialysate; therefore, keratin concentration in gels was reduced (Figure 4.9D). Overall these changes could explain the weaker viscoelastic properties of gels from heated

keratin solutions. Heating could also lead to carbamylation of keratin. Urea decomposition at high temperatures forms cyanate, which would facilitate carbamylation (additional NH-C=O group) of protein amino terminus, and lysine and arginine side chains (Stark et al., 1960; Hagel et al., 1971). Carbamylation can affect the net charge, ultrastructure, and therefore gelation of keratin.

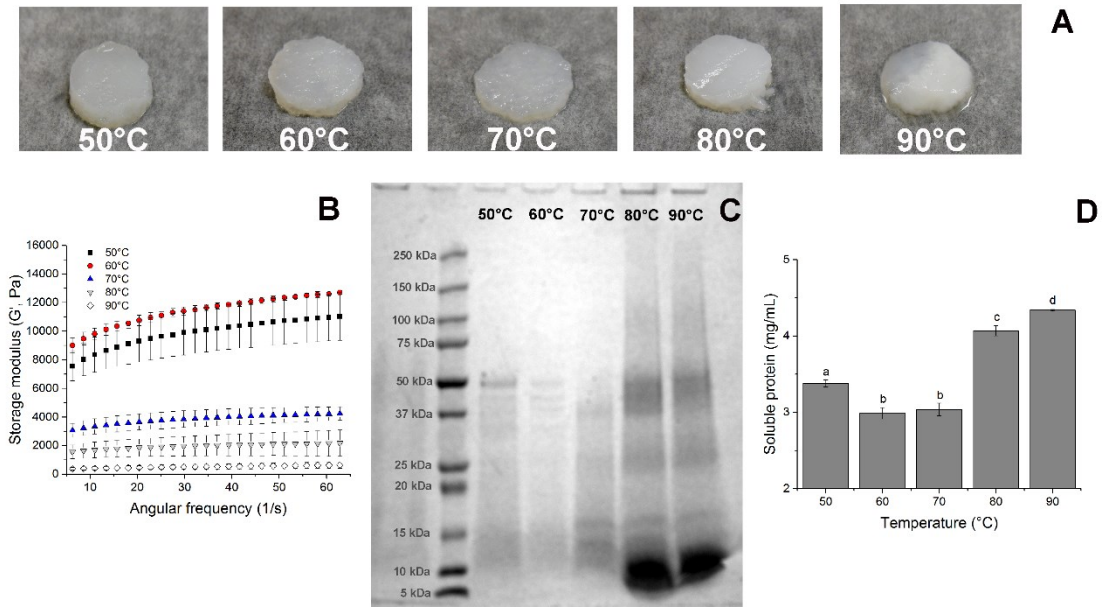

Figure 4.9. Digital photographs (A) and frequency sweeps of keratin gels formed (B) during dialysis of keratin solutions after heating for 1 hour at different temperatures; Soluble protein concentration (C) and SDS-PAGE (D) of keratins recovered after dialysis and heating at different temperatures.

4.4. Conclusions

The gelation of feather keratin upon dialysis is triggered by intermolecular protein-protein interactions and reformation of disulfide bonds. The viscoelastic properties of keratin gels can be controlled by manipulating the re-oxidation and density of disulfide bond cross-links during

dialysis. Therefore, increasing cysteine thiol blocking is inversely related to the storage modulus of gels. In addition, blocking of above 82% cysteine thiols inhibit the gelation of feather keratin, although the protein still forms small aggregates. Keratin gels are mainly stabilized by disulfide bonds, although complete dissolution is only possible after disrupting hydrogen bonds and hydrophobic interactions as well. The appearance and viscoelastic properties of gels are also affected by the pH, and temperature. Homogenous gels can be prepared at pH 6-7 and temperatures below 70°C. Tunable viscoelastic properties of feather keratin could be further explored for preparation of engineered scaffolds for regeneration of specific body tissues. Further studies are needed to understand the suitability of feather keratin hydrogels for biomedical applications.

4.5. References

Aboushwareb, T., Eberli, D., Ward, C., Broda, C., Holcomb, J., Atala, A., & Van Dyke M. (2009). A keratin biomaterial gel hemostat derived from human hair: Evaluation in a rabbit model of lethal liver injury. *Journal of Biomedical Materials Research Part B: Applied Biomaterials*, 90, 45-54.

Arai, K.M., Takahashi, R., Yokote, Y., & Akahane, K. (1983). Amino-acid sequence of feather keratin from fowl. *European Journal of Biochemistry*, 132, 501-507.

Barth, A. 2007. Infrared spectroscopy of proteins. *Biochimica et Biophysica Acta*, 1767, 1073-1101.

Bennion, B. J., & Daggett, V. (2003). The molecular basis for the chemical denaturation of proteins by urea. *Proceedings of the National Academy of Sciences,* 100, 5142-5147.

Bragulla, H.H., & Homberger, D.G. (2009). Structure and functions of keratin proteins in simple, stratified, keratinized and cornified epithelia. *Journal of Anatomy*. 214, 516-559.

de Guzman, R.C., Merrill, M.R., Richter, J.R., Hamzi, R.I., Greengauz-Roberts, O.K., & Van Dyke, M.E. (2011). Mechanical and biological properties of keratose biomaterials. *Biomaterials,* 32, 8205-8217.

Drury, J. L., & Mooney, D. J. (2003). Hydrogels for tissue engineering: scaffold design variables and applications. *Biomaterials*, 24, 4337-4351.

Hagel, P., Gerding, J.J.T., Fieggen, W., & Bloemendal, H. (1971). Cyanate formation in solutions of urea: I. Calculation of cyanate concentrations at different temperatures and pH. *Biochimica et Biophysica Acta,* 243, 366-373.

Han, S., Ham, T. R., Haque, S. Sparks, J. L., & Saul, J. M. (2015). Alkylation of human hair keratin for tunable hydrogel erosion and drug delivery in tissue engineering applications. *Acta Biomaterialia*, 23, 201-213.

Hill, P., Brantley, H., & Van Dyke, M. (2010). Some properties of keratin biomaterials: Kerateines. *Biomaterials*, 31, 585-593.

Ikkai, F., & Naito, S. (2002). Dynamic light scattering and circular dichroism studies on heat-induced gelation of hard-keratin protein aqueous solutions. *Biomacromolecules* 3, 482-487.

Jonker, A. M., Lowik, D. W. P. M., & Hest, J. C. M. (2012). Peptide- and protein-based hydrogels. *Chemistry of Materials*, 24, 759-773.

Klotz, I.M. (1996). Equilibrium constants and free energies in unfolding of proteins in urea solutions. *Proceedings of the National Academy of Sciences*, 93, 14411-14415.

Kong, J., & Yu, S. (2007). Fourier transform infrared spectroscopic analysis of protein secondary structures. *Acta Biochimica et Biophysica*, 39, 549-559.

Lo, C.M., Wang, H.B., Dembo, M., & Wang, Y.L. (2000). Cell movement is guided by the rigidity of the substrate. *Biophysical Journal*, 79, 144-152.

Lo Conte, M., & Carroll, K.S. (2013). The Chemistry of thiol oxidation and detection. In Jakob, U., & Reichmann, D. (Eds.). Oxidative Stress and Redox Regulation. Springer, Dordrecht, NL.

Naidu, K.T., & Prabhu, N.P. (2011). Protein-surfactant interaction: Sodium dodecyl sulfate-induced unfolding of ribonuclease A. *The Journal of Physical Chemistry B,* 115, 14760-14767.

Nakaji-Hirabayashi, T., Kato, K., & Iwata, H. (2008). Self-assembling chimeric protein for the construction of biodegradable hydrogels capable of interaction with integrins expressed on neural stem/progenitor cells. *Biomacromolecules*, 9, 1411-1416.

Nakamura, A., Arimoto, M., Takeuchi, K., & Fujii, T. (2002). A rapid extraction procedure of human hair proteins and identification of phosphorylated species. *Biological and Pharmaceutical Bulletin*, 25, 569-572.

Nomura, Y., Nakato, H., Ishii, Y., & Shirai, K. (2002). Characterization of S-sulfokeratin from pig hair and its use as a modifier of type I collagen gel. *Bioscience, Biotechnology, and Biochemistry*, 66, 1382-1385.

Riddles, P.W., Blakeley, R.L., & Zerner, B. (1979). Ellman's reagent: 5,5'-dithiobis(2-nitrobenzoic acid)-a reexamination. *Analytical Biochemistry,* 94, 75-81.

Rossky P.J. (2008). Protein denaturation by urea: Slash and bond. *Proceedings of the National Academy of Sciences*, 105, 16825-16826.

Schrooyen, P.M.M., Dijkstra, P.J., Oberthur, R.C., Bantjes, A., & Feijen, J. (2001). Stabilization of solutions of feather keratins by sodium dodecyl sulfate. *Journal of Colloid and Interface Science,* 240, 30-39.

Schrooyen, P.M.M., Dijkstra, P.J., Oberthur, R.C., Bantjes, A., & Feijen, J. (2000). Partially carboxymethylated feather keratins. 1. Properties in aqueous systems. *Journal of Agricultural and Food Chemistry,* 48, 4326-4334.

Stark, G.R., Stein, W.H., & Moore, S. (1960). Reactions of the cyanate present in aqueous urea with amino acids and proteins. *The Journal of Biological Chemistry,* 235, 3177-3181.

Tachibana, A., Furuta, Y., Takeshima, H., Tanabe, T., & Yamauchi, K. (2002). Fabrication of wool keratin sponge scaffolds for long-term cell cultivation. *Journal of Biotechnology*, 93, 165-170.

Thannhauser, T.W., Konishi, Y., & Scheraga, H.A. (1984). Sensitive quantitative analysis of disulfide bonds in polypeptides and proteins. *Analytical Biochemistry,* 138, 181-188.

Tonin, C., Aluigi, A., Vineis, C., Varesano, A., Montarsolo, A., & Ferrero, F. (2007). Thermal and structural characterization of poly(ethylene-oxide)/keratin blend films. *Journal of Thermal Analysis and Calorimetry,* 89, 601-608.

Tyagarajan, K., Pretzer, E., & Wiktorowicz, J.E. (2003). Thiol reactive dyes for fluorescence labeling of proteomic samples. *Electrophoresis*, 24, 2348-2358.

Wang, S., Wang, Z., Min Foo, S. E., Tan, N. S., Yuan, Y., Lin, W., Zhang, Z., & Ng, K. W. (2015). Culturing fibroblasts in 3D human hair keratin hydrogels. *ACS Applied Materials & Interfaces,* 7, 5187-5198.

Wong, S.S. (1991). Chemistry of protein conjugation and crosslinking. CRC Press, U.S. p30-32.

Woodin, A.M. (1954). Molecular size, shape and aggregation of soluble feather keratin. *Biochemistry Journal,* 57, 99-109.

Xu, H., Cai, S., Xu, L., & Yang, Y. (2014). Water-stable three-dimensional ultrafine fibrous scaffolds from keratin for cartilage tissue engineering. *Langmuir*, 30, 8461-8470.

Yin, X-C., Li, F-Y., He, Y-F., Wang, Y., & Wang, R-M. (2013). Study of effective extraction of chicken feather keratins and their films for controlling drug release. *Biomaterials Science,* 1, 528-536.

Yuan, J., Shen, J., & Kang, I-K. (2008). Fabrication of protein-doped PLA composite nanofibrous scaffolds for tissue engineering. *Polymer International*, 57, 1188-1193.

Zhao, W., Yang, R., Zhang, Y., & Wu, L. (2012). Sustainable and practical utilization of feather keratin by an innovative physicochemical pretreatment: high density steam flash-explosion. *Green Chemistry,* 14, 3352-3360.

Zhou, B., & Wang, H. (2011). The optimization of regeneration feather protein/PVA composite fiber's production technology using gray clustering analysis. *Advanced Materials Research*, 332-334, 500-504.

4.6. Appendix A: Supplementary Information

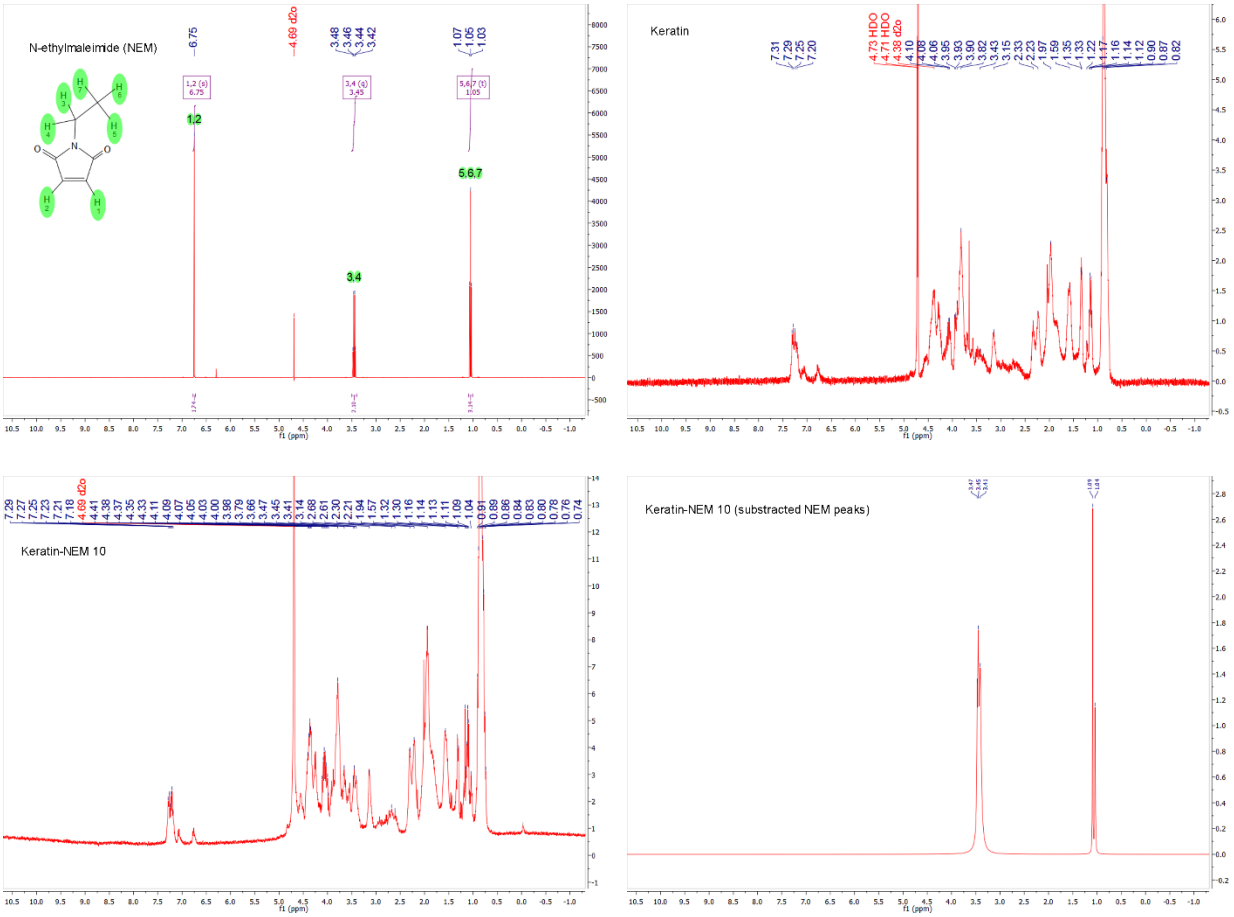

Figure S4.1. H-NMR of N-ethylmaleimide (NEM), keratin, and NEM-modified keratin. The last figure shows the substracted keratin peaks from keratin-NEM 10 sample, which show the presence of characteristic NEM groups (δ +1.04-1.09, -CH3; δ +3.41-3.47 -CH2-), absent in keratin sample.

CHAPTER 5. Characterization of hydrogels scaffolds from chicken feather keratin prepared by dialysis self-assembly

5.1. Introduction

Hydrogels are hydrophilic polymeric networks dispersed in a water phase and stabilized by chemical or physical interactions. They can absorb from 10-20% up to thousand times their dry weight in water maintaining a three dimensional structure that facilitates diffusion of solutes (Hoffman, 2002; Rutz and Shah, 2016). Therefore, they are excellent materials for biomedical applications including drug delivery, scaffolds for cell culture and tissue regeneration (Drury and Mooney, 2003). Hydrogels are fabricated from a variety of synthetic and natural polymers. Among them fibrous proteins have received special attention due to their structural similarity to the extracellular matrix (ECM) and the presence of integrin binding sites for improved cell adhesion (Floren et al., 2016).

Keratins are a family of fibrous proteins giving the structure of different animal tissues including skin, hair, nails, wool, horns, and feathers. Keratin films and hydrogels promote the adhesion of cells (Tachibana et al., 2002; Reichl, 2009), are biocompatible (Hill et al., 2010) and can accelerate the healing process of skin wounds (Xu et al., 2013; Wang et al., 2017). Structural, interfacial, and mechanical properties of hydrogels play important role in cell adhesion, proliferation, morphology and biocompatibility of scaffolds. The preparation of keratin hydrogels with emphasis on the modulation of their physical and mechanical properties for biomedical application is scarce.

Keratins are insoluble proteins stabilized by abundant cysteine residues forming covalent disulfide bonds. Solubilization of keratin is achieved after destabilization of hydrophobic and hydrogen bond interactions and disruption of disulfide bonds with thiol or sulfite chemicals. Disrupted disulfide bonds have the tendency to re-form if thiol or sulfite chemicals are diluted or removed. This has been normally considered a limitation in the processing of keratin

biomaterials. Water stable keratin solutions are obtained after the irreversible blockage of cysteine thiols by alkylation or peracetic acid treatment (Pace et al., 2013; Poranki et al., 2014; Guo et al., 2015), and formation of sodium dodecyl sulfate (SDS) complexes (Schrooyen et al., 2001; Wang et al., 2017); however, keratin hydrogels prepared afterwards show low mechanical properties. Hydrogels in which cysteine thiols are fully available for disulfide crosslinking have not been widely explored to fabricate strong keratin scaffolds. Fast gelation upon dilution of fully reduced hair keratin has been reported but mechanical properties of hydrogels not determined (Fujii and Ide, 2004; Nakaji-Hirabayashi et al., 2008). Hair keratin extracted for 12 h at pH 10.2 using thioglycolic acid as disulfide bond reducing agent resulted in water soluble keratin containing 10% cysteine. Hydrogels obtained were mechanically resistant and maintain 60% of their original diameter after 6 months of subcutaneous implantation in mice (Hill et al., 2010). However, an important aspect is that extraction at pH 10-11 for long time (12-15 h) result in reduced arginine content and partial hydrolysis and fragmentation of keratin (Hill et al., 2010; Richter et al., 2012; Burnett et al., 2013; Sinkiewicz et al., 2016). Although it has not been determined, it is probable that the ends of the keratin chain in which cysteine residues are predominantly located, were more susceptible to hydrolysis. We hypothesize that feather keratin extracted under milder conditions with the presence of cysteine thiols can result in stronger hydrogels.

Fully reduced wool keratin resulted in hydrogels with high mechanical strength, although the gelation concentration and pH of extraction solution was not specified (Ozaki et al., 2014). The self-assembly of fully reduced feather keratin during dialysis has been reported as a method to fabricate hydrogels with superior mechanical properties (Chapter 4). However, scaffolds have not been characterized for their physical and biological properties.

The objectives of this work were to prepare and characterize feather keratin hydrogels produced by self-assembly of fully reduced keratin solutions of different concentrations. Feather keratin hydrogels are characterized by their viscoelastic, physical and structural properties and their relation with cultured human dermal fibroblasts.

5.2. Materials and Methods

5.2.1. Materials and Chemicals

White chicken feathers were obtained from the Poultry Research Centre of the University of Alberta (Edmonton, AB, Canada). After exhaustive washing with hot water and domestic soap (Green Works®), feathers were allowed to dry in a fume hood followed by drying at 50°C overnight in an oven. Dried feathers were ground in a cutting mill (Fritsch Pulverisette 15, Fritsch, Germany) with an insert sieve of circular perforations of 1 mm diameter. Ground feathers were defatted with petroleum ether for 5 h in a soxhlet apparatus. The defatted feathers were recovered and the residual solvent was allowed to evaporate overnight. Defatted feather powder was stored at 4°C until further use. Urea, thiourea, sodium metabisulfite, Formaldehyde solution 36.5-38%, was obtained from Sigma-Aldrich (St Louis, MO, U.S.). Dulbecco's Modified Eagle's Medium (DMEM), fetal bovine serum (FBS), antibiotic-antimycotic mix, 1 M HEPES solution, non-essential amino acid solution (NEAA), phosphate saline buffer (PBS), Alamar blue, and 4',6-diamidino-2-phenylindole, dihydrochloride (DAPI) were obtained from ThermoFischer (Waltham, MA, U.S.). Cytopainter phalloidin-iFluor 488 reagent was obtained from Abcam (Abcam Inc. Canada).

5.2.2. Preparation of feather keratin hydrogels

Keratin was extracted by stirring 13.3 g of defatted feather powder with 200 mL of keratin extracting solution (KES) consisting of 5 M urea, 2.6 M thiourea and 5% w/v sodium metabisulfite at pH 7.0, 50°C for 5 h. Extracted keratin was recovered by filtration through a metallic sieve (53 μm). The keratin sol was dialyzed for 5 days at 4°C and the white gel formed was freeze dried to obtain keratin powder. This powder was solubilized in KES at room temperature for 4 h to final concentrations of 5, 7.5, 10, and 12.5% w/v. The sol-gel process was induced by dialysis at 4°C for 5 days with change of the outer distilled water twice per day.

5.2.3. Small amplitude oscillatory shear measurements (SAOS)

Rheological characterization of keratin hydrogels was carried out using frequency sweeps from 1 to 10 Hz at a strain of 1% within the linear viscoelastic region, on a Physica MCR 301 (Anton Paar, Graz, Austria). All measurements were performed at 25°C, with a probe gap of 1 mm.

5.2.4. Fabrication of hydrogel scaffolds

Keratin hydrogels prepared at concentrations of 5.0, 7.5, 10.0, and 12.5% w/v were cut into 16 mm diameter discs, placed on 24-well culture plates, frozen at -20°C for 24 h and lyophilized for 48 h. The obtained aerogels were cut to a final thickness of 2 mm for their use as cellular scaffolds.

5.2.5. Scaffold characterization

Cross sections of scaffolds were mounted in SEM stubs with double coated adhesive carbon tabs and gold sputtered for scanning electron microscopy imaging (Tescan Vega 3 SEM, Tescan, Czech Republic). Samples were scanned at an accelerating voltage of 5 kV. Water uptake capacity was determined gravimetrically after soaking scaffolds in PBS pH 7.4 at room temperature for 24 h. Porosity was calculated as the void fraction after soaking scaffolds of

known dimensions in absolute ethanol overnight using a reported procedure (Lai et al., 2012). Void volume was calculated from the weight of ethanol absorbed by the scaffold and results are presented as void fraction percentage.

5.2.6. Cell culture

Adult human dermal fibroblasts (HDFa) cell (Cell Applications, Inc. CA, U.S.) were used for *in vitro* culture on keratin scaffolds. Cells of passage 3 were harvested by trypsinization and re-suspended in Dulbecco's Modified Eagle's Medium (DMEM) media containing 10% fetal bovine serum (FBS) and antibiotic-antimycotic mix. Keratin hydrogel scaffolds were placed in 24-well culture plates and sterilized by soaking in ethanol solutions. First, gradually from 10 to 70%, at increasing rate of 20%, for 30 min each, and then washed with ethanol solutions (gradually from 70 to 10%, in reverse order as above) and sterile PBS pH 7.4 three times. Sterile scaffolds were soaked in 600 µl of media and incubated overnight in humidified environment at 37°C and 5% CO_2. Four media-soaked scaffolds were seeded by pouring 50 µL of HDFa suspension with a micropipette on the center of scaffolds (1.6 x 10^6 cells/mL); the other two scaffolds were not seeded and used as control samples. Cells were allowed to adhere to scaffolds by incubation for 4 hours. Then, scaffolds were washed gently with sterile PBS to remove non-attached cells and transferred with forceps to sterile 24-well culture plates containing 600 µL complete media per well. The scaffolds were flipped to maintain the seeded face of scaffolds submerged and the non-seeded face up. Sterile glass cover slips were seeded and placed in 6-wells plates used as control. Media was replaced every other day. Cell growth was quantified after 1, 7, 14 and 21 days of incubation. The scaffolds were transferred to new 24-well culture plates with media containing 10% Alamar blue® probe. After further incubation for 4 h the

fluorescence of reduced Alamar blue was measured at 560/590 ex/em and cell metabolic activity was quantified according to the manufacturer specifications.

5.2.7. Cell imaging

After 21 days of cell culture scaffolds were fixed with 4% formaldehyde in PBS solutions for 24 h at room temperature. Scaffolds were dehydrated gradually in ethanol/water solutions and embedded in paraffin. Cross sections (~10 μm) were mounted on glass slides, stained with Hematoxylin and Eosin (H&E), and images taken in a brightfield microscope (Zeiss Primo Vert, Zeiss, Germany). A separate set of cross sections was permeabilized with a 0.2% Triton-X100 PBS solution and stained with DAPI and phalloidin to visualize nuclei and actin filaments, respectively. Images were taken in a florescence microscope (Zeiss Axio, Zeiss, Germany)

5.2.8. Statistics

Experiments were run in triplicate unless otherwise specified. Differences between measurements were determined by ANOVA of the data using a confidence level of 95%, followed by Tukey's multiple comparison test.

5.3. Results and Discussion

5.3.1. Rheology of keratin hydrogels

Gelation of feather keratin during dialysis is triggered mainly by the re-oxidation of disulfide bonds, hydrogen bonds and hydrophobic interactions upon the removal of sodium sulfite and urea (Chapter 4). The mechanical and viscoelastic properties of hydrogels can affect phenotype, adhesion, proliferation and survival of cells (Engler et al., 2006; Yan and Pochan, 2010). Viscoelastic properties of hydrogels can be modified by changing the polymer concentration (Holt el al., 2008; Levental et al., 2007). Keratin hydrogels were fabricated through dialysis of

keratin solutions of different concentrations (5, 7.5, 10 and 12.5 wt. %). The viscoelastic properties of the resultant keratin hydrogels were measured and are presented in Figures 5.1A and 5.1B. Amplitude sweeps were conducted in order to determine the linear viscoelastic range of hydrogels (Figure 5.1A). The limit of the linear viscoelastic region for all keratin hydrogels was determined to be 2-4% of strain; therefore, 1% strain was used for frequency sweeps. Keratin hydrogels exhibited an elastic solid-like behavior as the storage modulus (G') was greater than the loss modulus (G'') over the frequency range for all the concentrations (Figure 5.1B). Storage modulus of hydrogels increased with the keratin concentrations. This can be explained by a higher density of protein-protein interactions at higher concentrations.

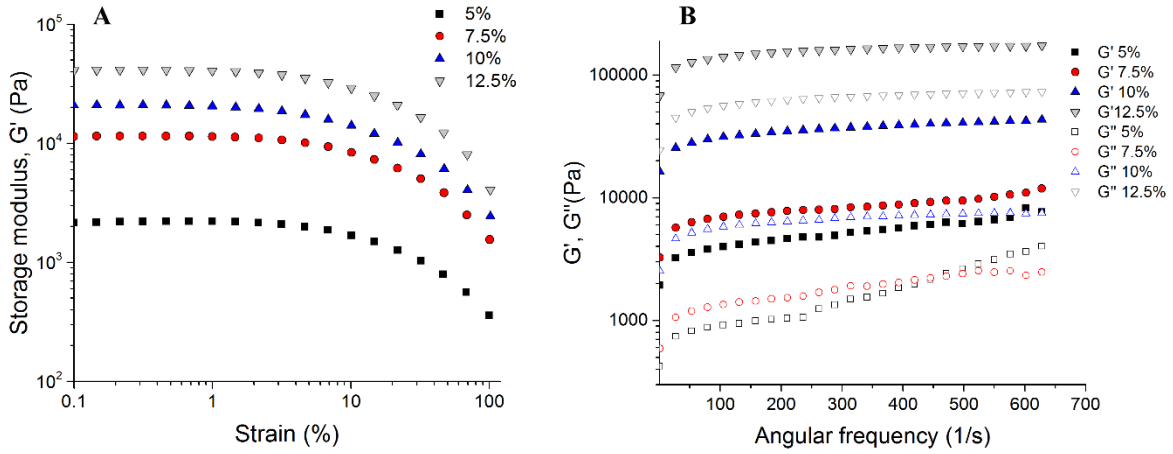

Figure 5.1. Storage modulus over frequency sweeps of feather keratin hydrogels prepared at different concentrations.

Rheological properties of keratin hydrogels prepared under different extraction and gelation methods is reported in the literature. Wang et al., (2015) reported that hair keratin coagulates at 5% w/v prepared by sodium disulfide extraction and isoelectric precipitation had storage modulus close to 10^3 Pa. Hair keratin extracted with thioglycolic acid at pH 11 and lyophilized was reconstituted to 6% and 20% w/v in water and allowed to gel at 37°C. The

resultant hydrogels had storage modulus between $2x10^2$-$2.5x10^2$ Pa (Burnett et al., 2013) and 10^3-10^4 Pa, respectively (Richter et al., 2012). Tomblyn et al., (2016) also extracted hair keratin with thioglycolic acid; gels prepared at 8 and 20% w/v, had G' of 10^2-10^3, and slightly above 10^4 Pa, respectively. Wool keratin extracted with guanidine hydrochloride and 2-mercaptoethanol resulted in hydrogels with G' of 10^3-10^4, although exact gelation concentration (<10% w/v) and pH during extraction were not specified (Ozaki et al., 2014). Feather keratin hydrogels at 20% w/v prepared from SDS-extracted keratin had a maximum storage modulus below $5x10^3$ Pa (Wang et al., 2017). The storage modulus of our feather keratin hydrogel at 5% wt. was in the range of $2x10^3$ to $7x10^3$ Pa. According to Vanderhooft et al., (2008) this is within the range of shear modulus of liver, fat, relaxed muscle and breast gland tissues (10^3-10^4 Pa). Keratin hydrogels prepared at concentrations of 10 and 12.5% had modulus within the range of dermis, connective tissue and contracted muscle (10^5-10^6 Pa). Higher storage modulus of our keratin hydrogels, at comparable concentration, can be explained by the greater formation of disulfide bonds. In hydrogels from SDS-extracted feather keratin reported by Wang et al., (2017), SDS-keratin complexes are hard to dissociate and physically block the reformation of disulfide bonds (Schrooyen et al., 2001).

5.3.2. Characterization of hydrogel scaffolds

The swelling properties of scaffolds are related to their capacity to supply nutrients inside the matrix. It is also a good indicator of the surface area available for cells to adhere (Silva et al., 2014). Water uptake of scaffolds was inversely proportional to keratin concentrations. Stiffer keratin hydrogels formed at 12.5% showed the lowest water uptake capacity; while keratin hydrogels at 5% absorbed more than 15 (1585 ± 65%) times their own weight in water (Figure 5.2A). Porosity of scaffolds was also affected by keratin concentrations. The highest porosity

(92%) was observed for scaffolds prepared at 5% feather keratin (Figure 5.2B); increasing of keratin concentration resulted in a gradual decrease of porosity. The void fraction of 7.5, 10 and 12.5% keratin hydrogels was 69, 59, and 64%, respectively. Porosity of hydrogel scaffolds is mainly affected by the capacity of the polymer to entrap water during the gel formation. Hydrogels from SDS-extracted keratin of 10-20% w/v had porosities of 77-82% (Wang et al., 2017). SDS forms stable complexes with keratin that promote repulsion and formation of keratin-micelles (Schrooyen et al., 2001). This result in limited keratin crosslinking and high water entrapment leading to increased porosity. High density of protein-protein interactions at high protein concentration affects negatively water entrapment, and subsequently porosity (Haugh et al., 2010).

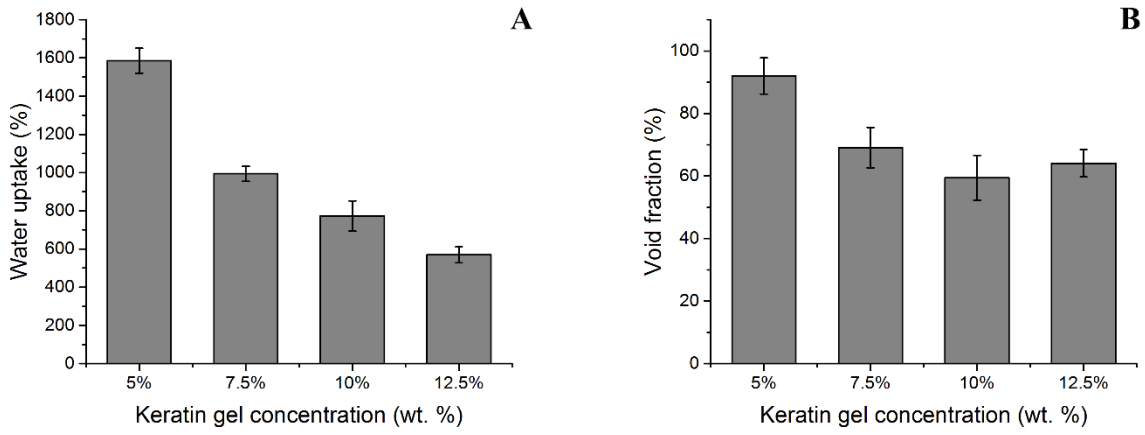

Figure 5.2. Water uptake capacity (A) and porosity (B) of feather keratin hydrogels prepared at different concentrations.

Scanning electron microscopy (SEM) images of cross sections of scaffolds showed some differences on their microstructure (Figure 5.3). Scaffold prepared at 5, 7.5 and 10% w/v showed a structure composed of thin flakes-like keratin forming a highly porous structure (Figure 5.3A, 5.3B and 5.3C). Scaffolds at 12.5% w/v keratin resulted in a very compact structure of keratin

with irregular shaped pores (Figure 5.3D). Pore size did not follow any trend with respect to keratin concentration. Overall the pore size of keratin scaffolds was in the range of 61-314 μm (Table 5.1).

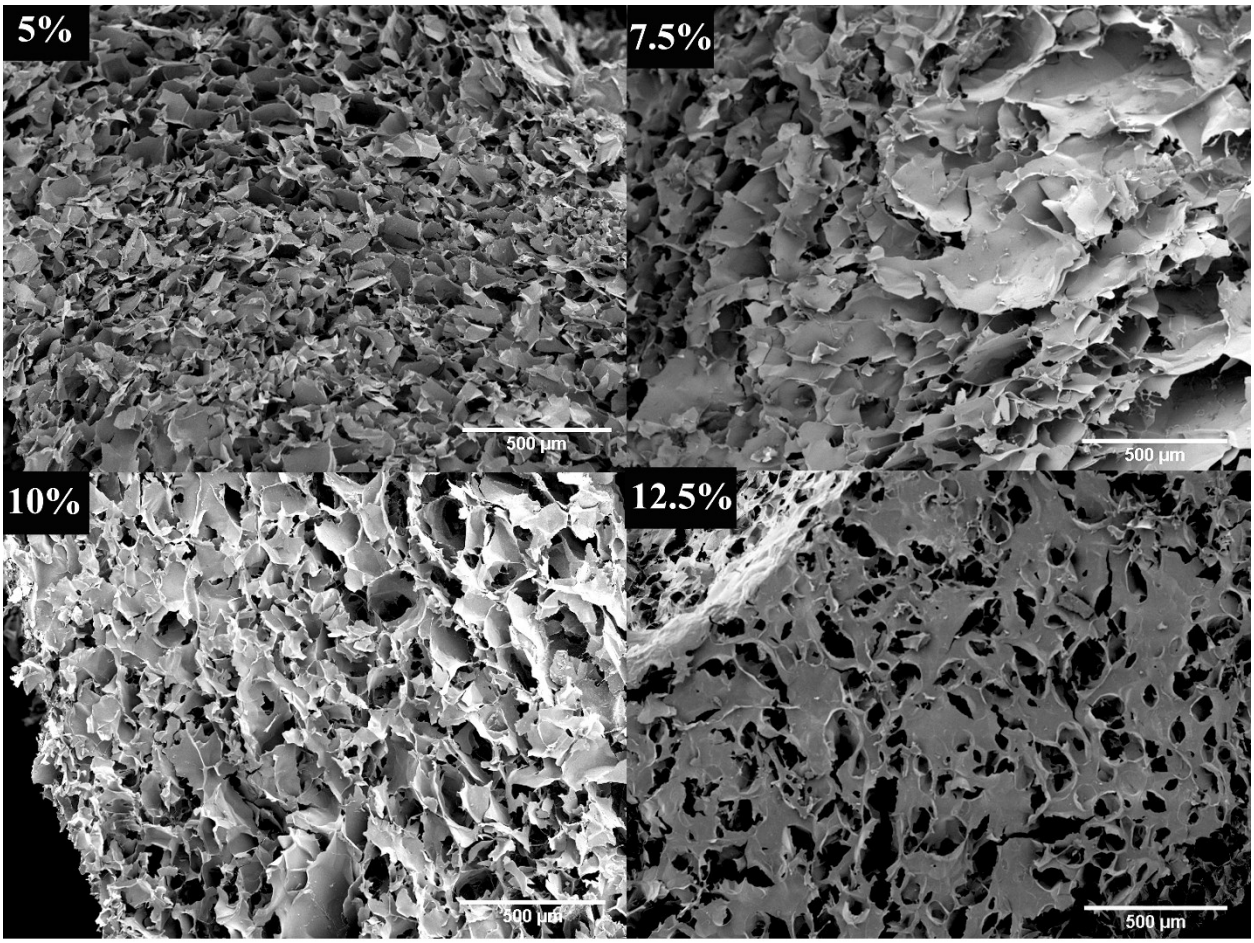

Figure 5.3. Scanning electron micrograph of feather keratin hydrogel scaffolds prepared at different concentrations.

Table 5.1. Pore size characterization of feather keratin scaffolds prepared at different concentrations.

	5%	7.5%	10%	12.5%
Average	136.2	188.8	172.9	130.5
st. dev.	23.1	50.3	44.7	46.7
Range	96.7-173.5	92.9-313.8	75.2-250.7	61.2-214.2

5.3.3. Cell proliferation in keratin scaffolds

Feather keratin scaffolds were evaluated for their potential as cellular scaffolds for skin regeneration. Adult human dermal fibroblasts (HDFa) were seeded on feather keratin scaffolds and cultured for up to 21 days (Figure 5.4). Overall keratin scaffolds were not cytotoxic and supported the growth of HDFa. A higher cell proliferation rate was determined on keratin scaffolds than on 2D culture on glass used as control. This can be explained by the increased available surface in the 3D environment provided by keratin scaffolds. Proliferation rate of HDFa on keratin scaffolds showed to be higher on scaffolds prepared at lower concentrations at 7 days of incubation. However after that cell proliferation did not differ much. At the end of the culture period (21 days), higher proliferation on 5, 7.5 and 12.5% scaffolds was determined. Proliferation on 10% scaffolds was slightly lower ($p<0.05$) compared with 5 and 12.5%.

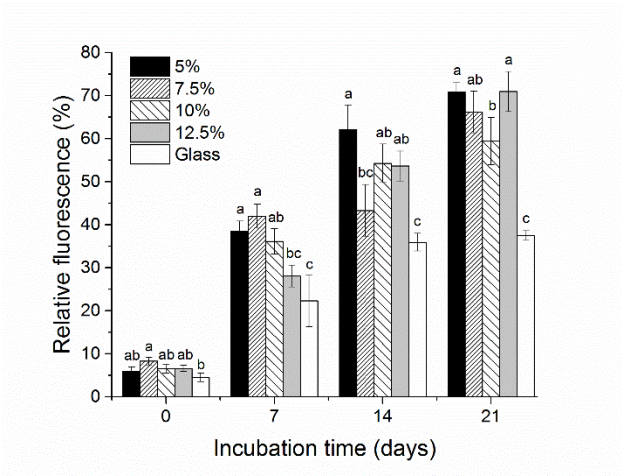

Figure 5.4. Proliferation of HDF on feather keratin hydrogel scaffolds prepared at different concentrations and glass cover slides used as control.

Cell proliferation and eventually tissue regeneration are closely related to the ability of cells to adhere to the surface of biomaterials. Cells adhesion to the ECM is mediated by transmembrane integrins and proteins containing integrin binding sites. Cell adhesion to glass or scaffolds surface is mediated by proteins containing integrin binding sites present in the serum-containing media (fibronectin, vitronectin and laminin), synthetized by the cells during the first hours of culture or naturally present on the scaffold surface. These proteins are rapidly adsorbed at the surface of scaffolds (Hayman and Ruoslahti, 1979). Integrin binding sites have not been reported in feather keratin, therefore it is likely that serum proteins such as fibronectin and vitronectin adsorbed onto feather keratin scaffold surfaces and mediated cell adhesion and subsequent proliferation (Steele et al., 1992; Rosso et al., 2013). The selective affinity of protein to adsorb at the surface of scaffold can also modulate body reactions to foreign implants (Boehler et al., 2011). Feather keratins are composed of around 50/50 ratio of hydrophobic/hydrophilic amino acid residues (Chapter 4), which is generally associated with a

higher adsorption of serum proteins, decreased monocyte/macrophage adhesion and reduced foreign body reactions (Xu and Siedlecki, 2007; Arima and Iwata, 2007; Boehler et al., 2011). Feather keratin scaffolds were stable under physiological conditions and maintained their structure after 21 days of cell culture (Figure 5.5). A high density of disulfide bond during hydrogel formation prevented solvation of keratins scaffolds (Chapter 4). This property could be helpful to accelerate healing of non-healing wounds (Hill et al., 2010)

Differences in cell behavior were observed for gels of different keratin concentration. Figure 5.5 shows histological staining (H&E) of keratin scaffolds after 21 days of culture. Cells were able to penetrate through the pores of scaffolds. However, a greater distribution of cells along the cross section was observed in scaffolds with higher porosity 5 and 7.5% (Figures 5.5A and 5.5B). It is possible that less porous and compact 10 and 12.5% scaffolds impaired cell infiltration and limited the growth to the seeded face of scaffolds. After 21 days, cells were randomly distributed in the hydrogel scaffolds and lacked of abundant cell-cell interaction; a similar distribution that is found in the normal connective tissue (Slack et al., 2005). Cells adhered to keratin and developed different morphologies including elongated cells adhered along or adhered to multiple points of keratin fibers (Figure 5.6).

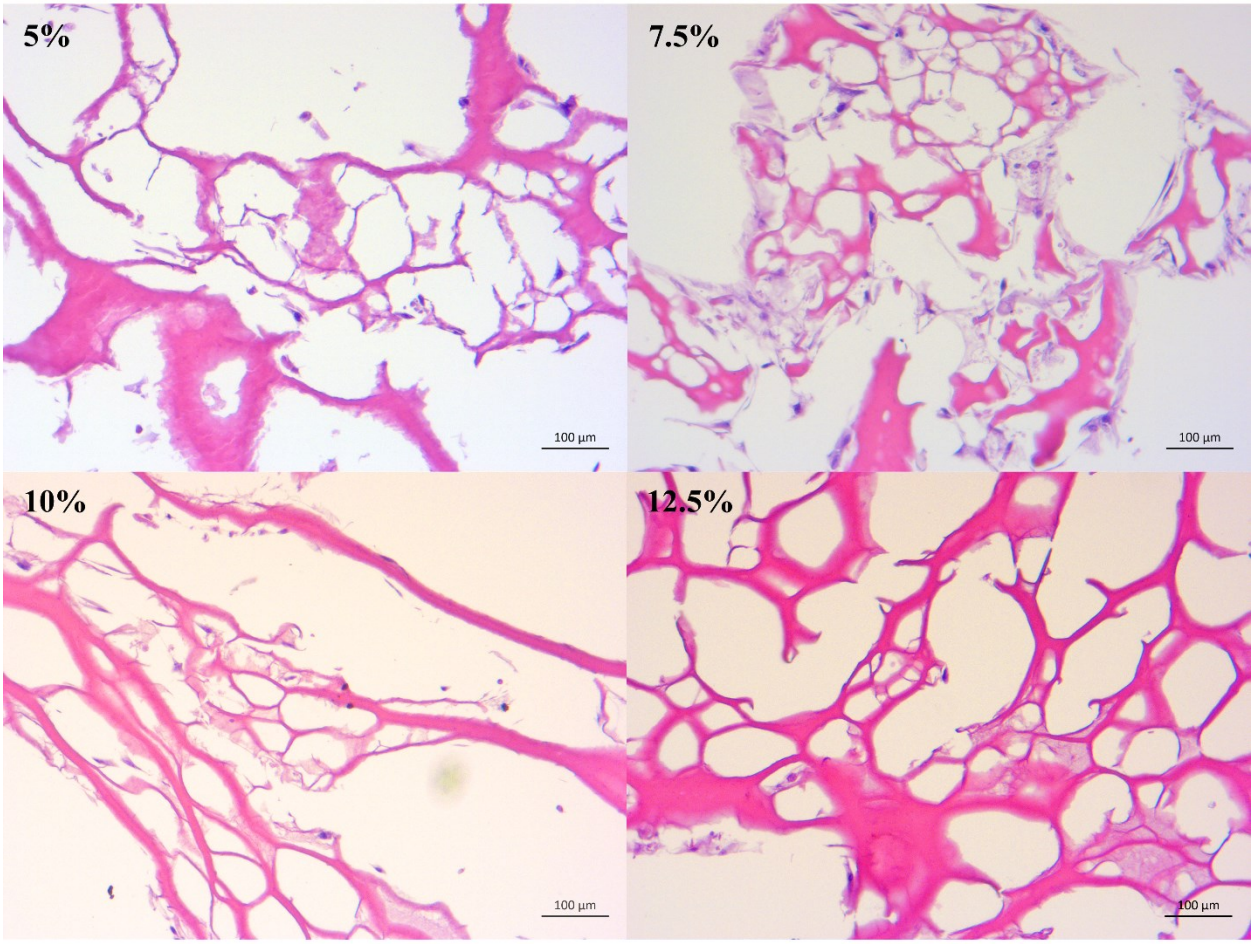

Figure 5.5. Cross-section of H&E stained feather keratin scaffolds of different concentrations after 21 days of culture with HDFa (keratin is stained red and cells dark purple).

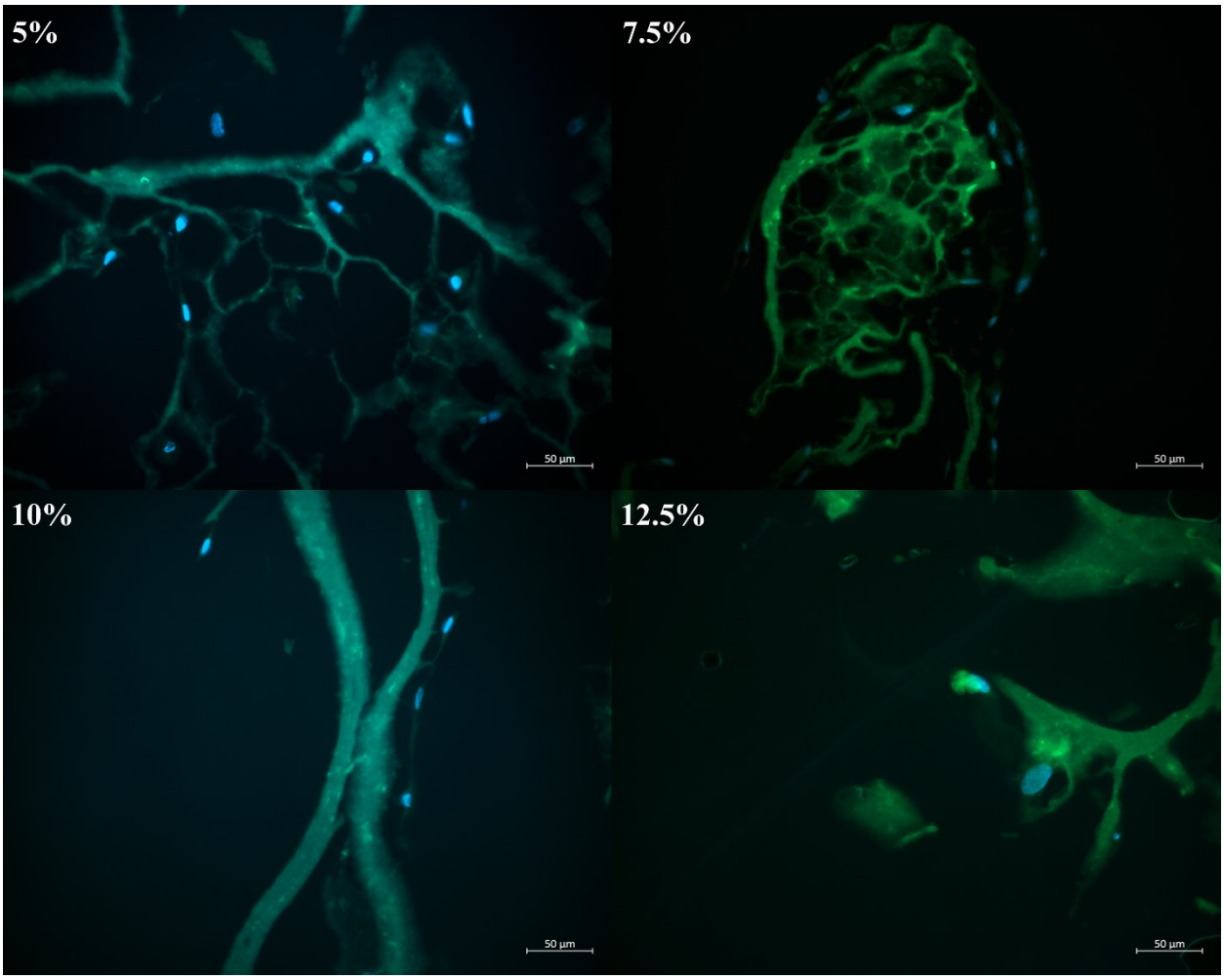

Figure 5.6. Fluorescence micrographs of feather keratin scaffolds prepared at different concentrations cultured with HDFa for 21 days, showing cell structure (nuclei in blue and actin in green) and keratin fibres (auto-fluorescence green).

5.4. Conclusions

Feather keratin was used to prepare hydrogel scaffolds. The viscoelastic properties of hydrogels were affected by keratin concentrations. Storage modulus of hydrogels was increasing at increasing concentrations of keratin; however, high storage modulus resulted in hydrogels with lower swelling capacity and porosity. Scaffolds were able to support the culture of HDFa over a

period of 21 days. Proliferation of HDFa was the highest on scaffolds prepared at 5, 7.5, and 12.5% although significant differences were not determined between 7.5 and 10% scaffolds ($p>0.05$). Penetration of cells into scaffolds was observed to be affected by keratin concentrations; higher concentration resulted in a more dense arrangement of keratin with separate pores structure which could have limited the infiltration of cells to growth on the surface of scaffolds.

5.5. References

Arima, Y., & Iwata, H. (2007). Effect of wettability and surface functional groups on protein adsorption and cell adhesion using well-defined mixed self-assembled monolayers. *Biomaterials*, 28, 3074-3082.

Boehler, R.M., Graham, J.G., & Shea, L.D. (2011). Tissue engineering tools for modulation of the immune response. *Biotechniques*, 51, 239-passim.

Burnett, L.R., Rahmany, M.B., Richter, J.R., Aboushwareb, T.A., Eberli, D., Ward, C.L., Orlando, G., Hantgan, R.R., & Van Dyke, M.E. (2013). Hemostatic properties and the role of cell receptor recognition in human hair keratin protein hydrogels. *Biomaterials*, 34, 2632-2640.

Drury, J.L., & Mooney, D.J. (2003). Hydrogels for tissue engineering: scaffold design variables and applications. *Biomaterials*, 24, 4337-4351.

Engler, A.J., Sen, S., Sweeney, H.L., & Discher, E. (2006). Matrix elasticity directs stem cell lineage specification. *Cell*, 126, 677-689.

Floren, M., Migliaresi, C., & Motta, A. (2016). Processing techniques and applications of silk hydrogels in bioengineering. *Journal of Functional Biomaterials*, 7, doi: 10.3390/jfb7030026.

Fujii, T., & Ide, Y. (2004). Preparation of translucent and flexible human hair protein film and their properties. *Biological and Pharmaceutical Bulletin*, 27, 1433-1436.

Guo, J., Pan, S., Yin, X., He, Y-F., Li, T., & Wang, R-M. (2015). pH-sensitive keratin-based polymer hydrogel and its controllable drug-release behavior. *Journal of Applied Polymer Science*, 132, 41572, doi: 10.1002/app.41572.

Haugh, M.G., Murphy, C.M., & O'Brien, F.J. (2010). Novel freeze-drying methods to produce a range of collagen-glycosaminoglycan scaffolds with tailored mean pore sizes. *Tissue Engineering: Part C*, 16, 887-894.

Hayman, E.G., & Ruoslahti, E. (1979). Distribution of fetal bovine serum fibronectin and endogenous rat cell fibronectin in extracellular matrix. *Journal of Cell Biology*, 89, 255-259.

Hill, P., Brantley, H., & Van Dyke, M. (2010). Some properties of keratin biomaterials: Kerateines. *Biomaterials*, 31, 585-593.

Hoffman, A.S. (2002). Hydrogels for biomedical applications. *Advanced Drug Delivery Reviews*, 54, 3-12.

Holt, B., Tripathi, A., & Morgan, J. (2008). Viscoelastic response of human skin to low magnitude physiologically relevant shear. *Journal of Biomechanics*, 41, 2689-2695.

Lai, J-Y., Li, Y-T., Cho, C-H., & Yu T-C. (2012). Nanoscale modification of porous gelatin scaffolds with chondroitin sulfate for corneal stromal tissue engineering. *International Journal of Nanomedicine*. 1101-1114.

Levental, I., Goerges, P.C., & Janmey, P.A. (2007). Soft biological materials and their impact on cell function. *Soft Matter*, 3, 299-306.

Nakaji-Hirabayashi, T., Kato, K., & Iwata, H. (2008). Self-assembling chimeric protein for the construction of biodegradable hydrogels capable of interaction with integrins expressed on neural stem/progenitor cells. *Biomacromolecules*, 9, 1411-1416.

Ozaki, Y., Takagi, Y., Mori, H., & Hara, M. (2014). Porous hydrogel of wool keratin prepared by a novel method: An extraction with guanidine/2-mercaptoethanol solution followed by dialysis. *Materials Science and Engineering C*, 42, 146-154.

Pace, La., Plate, F.J., Mannava, S., Barnwell, J.C., Koman, L.A., Li, Z., Smith, T.L., Van & Dyke, M. (2014). A human hair keratin hydrogel scaffold enhances median nerve regeneration in nonhuman primates: An electrophysiological and histological study. *Tissue Engineering Part A*, 20, 507-517.

Poranki, D., Whitener, W., Howse, S., Mesen, T., Howse, E., Burnell, J., Greengauz-Roberts, O., Molnar, J., & Van Dyke, M. (2014). Evaluation of skin regeneration after burns in vivo and rescue of cells after thermal stress in vitro following treatment with a keratin biomaterial. *Journal of Biomaterials Applications*, 29, 26-35.

Reichl, S. (2009). Films based on human hair keratin as substrates for cell culture and tissue engineering. *Biomaterials*, 30, 6854-6866.

Richter, J.R., de Guzman, R.C., Greengauz-Roberts, O.K., & Van Dyke, M. (2012). Structure-property relationships of meta-kerateine biomaterials derived from human hair. *Acta Biomaterialia*, 8, 274-281.

Rosso, F., Marino, G., Grimaldi, A., Cafiero, G., Chiellini, E., Chiellini, F., Barbarisi, M., & Barbarisi, A. (2013). Vitronectin absorbed on nanoparticles mediate cell

viability/proliferation and uptake by 3T3 Swiss albino mouse fibroblasts: in vitro study. *BioMed Research International*, Article ID 539348.

Rouse, J.G., & Van Dyke, M.E. (2010). A review of keratin-based biomaterials for biomedical applications. *Materials*, 3, 999-1014.

Rutz, A.L, & Shah, R.N. (2016). Protein-based hydrogels. In Kalia, S. (Ed.). Polymeric Hydrogels as Smart Biomaterials. Springer, Cham, Switzerland.

Schrooyen, P.M.M., Dijkstra, P.J., Oberthur, R.C., Bantjes, A., & Feijen, J. (2001). Stabilization of solutions of feather keratins by sodium dodecyl sulfate. *Journal of Colloid and Interface Science,* 240, 30-39.

Silva, R., Singh, R., Sarker, B., Papageorgiou, D.G., Juhasz, J.A., Roether, J.A., Cicha, I., Kaschta, J., Schubert, D.W., Chrissafis, K., Detsch, R., & Boccaccini, A.R. (2014) Hybrid hydrogels based on keratin and alginate for tissue engineering. *Journal of Materials Chemistry B*, 2, 5441-5451.

Sinkiewicz, I., Sliwinska, A., Staroszczyk, H., & Kolodziejska, I. (2016). Alternative methods of preparation of soluble keratin from chicken feathers. *Waste and Biomass Valorization*, DOI 10.1007/s12649-016-9678-y

Slack, J. (2007). Molecular biology of the Cell. In Lanza, R., Langer, R., & Vacanti, J. (Eds.). Principles of Tissue Engineering. Third Edition. Academic Press, Burlington, Ma, USA.

Steele, J.G., Johnson, G., & Underwood, P.A. (1992). Role of serum vitronectin and fibronectin in adhesion of fibroblasts following seeding onto tissue culture polystyrene. *Journal of Biomedical Materials Research*, 26, 861-884.

Tachibana, A., Furuta, Y., Takeshima, H., Tanabe, T., & Yamauchi, K. (2002). Fabrication of wool keratin sponge scaffolds for long-term cell cultivation. *Journal of Biotechnology*, 93, 165-170.

Tomblyn, S., Pettit Kneller, E.L., Walker, S.J., Ellenburg, M.D., Kowalczewski, C.J., Van Dyke, M., Burnett, L., & Saul, J.M. (2016). Keratin hydrogel carrier system for simultaneous delivery of exogenous growth factors and muscle progenitor cells. *Journal of Biomedical Materials Research B: Applied Biomaterials*, 104B, 864-879.

Vanderhooft, J.L., Alcoutlabi, M., Magda, J.J., & Prestwich, G.D. (2008). Rheological properties of cross-linked hyaluronan-gelatin hydrogels for tissue engineering. *Macromolecular Bioscience*, 9, 20-28.

Vasconcelos, A., & Cavaco-Paulo, A. (2013). The use of keratin in biomedical applications. *Current Drug Targets*, 14, 612-619.

Wang, J., Hao, S., Luo, T., Cheng, Z., Li, W., Gao, F., Guo, T., Gong, Y., & Wang, B. (2017). Feather keratin hydrogel for wound repair: Preparation, healing effect and biocompatibility evaluation. *Colloids and Surfaces B: Biointerfaces*, 149, 341-350.

Wang, S., Wang, Z., Foo, S.E.M., Tan, N.S., Yuan, Y., Lin, W., Zhang, Z., & Ng, K.W. (2015). Culturing fibroblasts in 3D human hair keratin hydrogels. *ACS Applied Materials & Interfaces*, 7, 5187-5198.

Xu, L-C., & Siedlecki, C.A. (2007). Effects of surface wettability and contact time on protein adhesion to biomaterial surfaces. *Biomaterials*, 28, 3273-3283.

Xu, S., Sang, L., Zhang, Y., Wang, X., & Li, X. (2013). Biological evaluation of human hair keratin scaffolds for skin wound repair and regeneration. *Materials Science and Engineering C*, 33, 648-655.

Yan, C., & Pochan, D.J. (2010). Rheological properties of peptide-based hydrogels for biomedical and other applications. *Chemical Society Reviews*, 39, 3528-3540.

CHAPTER 6. Hydrogels from feather keratin show stronger and higher cell proliferation than those from hair and wool keratins

6.1. Introduction

Hydrogels are polymeric materials characterized as an organized crosslinked network that absorb and retain substantial amounts of water. Hydrogels have been explored in several promising application areas such as wound healing, wound dressings and skin substitutes. Hydrogels can maintain a moist wound environment that accelerate healing, reduces pain and infections, contributing to reduced overall health care costs (Winter 1962; Hinnman and Malibach, 1963; Nemeth et al., 1991; Ovington, 2001; Jones and San Miguel, 2006; Abdelrahman and Newton, 2011).

Among other macromolecules investigated for hydrogels fabrication, keratin shows interesting potential due to their abundant availability, promotion of cell adhesion, *in vivo* biocompatibility and accelerated wound healing properties (Verma et al., 2008; Hill et al., 2009; de Guzman et al., 2011). Keratins are a family of intermediate filament proteins found in the structures of different tissues in mammals (hair, nails, skin, fur, sheep wool, horns, and hooves), and birds (e.g. bird feathers and beaks). A common characteristic of keratins, regardless of the animal class, is the high abundance of cysteine residues forming disulfide bonds. However, mammalian and avian keratins show distinct variations among amino acid composition, molecular weight, and protein secondary structures (Bragulla and Homberger, 2009). Mammalian keratins are heterogeneous proteins that consist predominantly of α-helical conformation and have a molecular weight of 10 - 75 kDa; whereas, feather keratins (avian keratins) consist mostly of homogenous β-sheet conformation with a molecular weight of 10 kDa (Fraser, 1972). Mammalian keratins possess integrin binding sites on their amino acid sequence that promote cell adhesion; however, such integrin binding sites have not been identified in feather keratins yet (Tachibana et al., 2002; Vasconcelos and Cavaco-Paulo, 2013). These

variations play an important role in the fabrication and physical and biological properties of hydrogels scaffolds.

Several previous studies have reported keratin hydrogels that are prepared using keratins of different sources, different extraction conditions and gelation methods. Hydrogels from hair and wool keratin have been prepared by aggregation in the presence of divalent cations (Hirabayashi et al., 2008), crosslinking of keratin solutions by air oxidation (Aboushwareb et al., 2008; Hill et al., 2010), freeze-drying (Tachibana et al., 2002; Xu et al., 2013), or induced with hydrogen peroxide (Wang et al., 2017). Partial blocking of cysteine thiol groups followed by freeze-drying was also used in preparing keratin hydrogels (Sierpinski et al., 2008; Saul et al., 2011; Han et al., 2015). It has also been reported that fully reduced feather keratin can self-assemble into strong hydrogels via disulfide bonds and hydrophobic/hydrogen bond interactions (Ozaki et a., 2014; Chapters 4 and 5). Different keratin extraction conditions such as manipulation of pH, temperature, concentration of urea, presence/absence of SDS, and addition of different thiol reducing agents (thioglycolic acid, mercaptoethanol, sulfites) have been employed (Nakamura et al., 2002; Tonin et al., 2007) Therefore, evaluation and comparison of the effect of different keratin sources on hydrogel properties is a difficult task. Current literature lacks comprehensive studies on the fabrication and characterization of keratin hydrogels of different sources prepared under the same conditions. We hypothesize that keratin from different sources have different hydrogel properties.

In this work, keratins from human hair, sheep wool and chicken feathers were used to prepare hydrogel scaffolds by self-assembly of keratin solutions through dialysis. Keratins were extracted by sulfitolysis and characterized for their chemical and conformational properties (amino acid composition, molecular weight, secondary structure, and thermal properties). The

objectives of this study were to characterize and compare the rheological (storage modulus), physical (porosity, pore size, swelling capacity, and water contact angle) and *in vitro* cell compatibility of hydrogel scaffolds prepared from mammalian and avian keratins. The results of this study could help to understand the gelation mechanisms of different keratins and the modulation of viscoelastic and microstructural properties for their application in tissue engineering.

6.2. Materials and Methods

6.2.1. Keratin extraction

Male hair of random age (from a local barber shop, Edmonton, AB, Canada), Merino wool (Paradise Fibers, U.S.) and white chicken feathers (Poultry Research Centre, University of Alberta) were cut with scissors and sieved through a stainless steel sieve of 1 mm aperture. Hair, wool and feather particles were defatted for 5 h with petroleum ether in a soxhlet apparatus. Keratins were extracted with a solution containing 5 M urea, 2.6 M thiourea, and 5% w/v sodium metabisulfite (keratin extraction solution, KES) adjusted at pH 7.00 with 6 M NaOH. Briefly, 13.3 g of each defatted raw material was mixed with 200 mL of KES in 500 mL jacketed beakers and kept at 50°C with help of a water recirculating bath. The extraction was carried out for 5 h with stirring at 350 rpm on a stirring plate. Extracted solution was filtered through a 53 μm metallic mesh and dialyzed against distilled water using cellulose dialysis tubes (Fischer Brand, U.S.) with molecular weight cut-off 3,500 Da for 5 days at 4°C with two changes of the outer water per day.

6.2.2. Preparation of keratin hydrogels and scaffolds

The gel formed during dialysis was washed with running distilled water, frozen at -20°C and lyophilized to yield keratin powders. Keratin gels were prepared by re-solubilizing keratin powders at 7.5% w/v in KES at pH 7 for 4 h. at room temperature. The gel-sol process was induced by dialysis for 5 days. Gels were cut into 16 mm diameter discs, placed in 24-well culture plates, frozen and lyophilized. Aerogels formed were cut into specimens of 2 mm thickness and used as cellular scaffolds.

6.2.3. Amino acid composition

Hair, wool and chicken feathers were digested with 6 N HCl for quantification of amino acids, with exception of cysteine. For cysteine, separate samples were previously hydrolyzed with performic acid. Cysteine was determined as cysteic acid and results expressed as half-cystine content according to the method reported by Moore (1963). Hydrolyzed samples were derivatized with PITC (phenylisothiocyanate) and analyzed in a HPLC system equipped with a Supelcosil LC-18 reverse phase column and a UV detector (254 nm). Individual amino acid concentrations were determined from the retention times and peak areas of a standard amino acid mixture (Sigma-Aldrich, U.S.). Total nitrogen in keratinous samples was determined using a Leco Truspec C/N analyzer (Leco Corp. MI, U.S.).

6.2.4. Keratin thermal and conformational properties

Thermal properties of raw materials and extracted keratins were studied by differential scanning calorimetry (DSC) in a DSC Q2000 instrument (TA Instruments, DE, U.S.). DSC analysis was carried out using dry samples of ~5 mg heated from 25 to 300°C, at a heating rate of 10°C/min. Molecular weight of extracted keratins was determined by SDS-PAGE. Keratins were solubilized in glycine-SDS buffer in the presence of β-mercaptoethanol (Laemmli et al., 1970).

Infrared spectra of keratins were obtained using a FT-IR Nicolet iS50 spectrometer (Thermo Scientific Inc., WI, USA) using a single bounce diamond ATR accessory. Samples were analyzed at 64 scans with a resolution of 4 cm^{-1} from 400-4000 cm^{-1}. Secondary structure of keratins was evaluated by Fourier self-deconvolution (FSD) treatment of the amide I region (1600-1700 cm^{-1}) FTIR spectra using Omnic 8.1 software, after automatic ATR correction and considering a FSD bandwidth of 26 cm^{-1} and an enhancement factor of 2.5. The position of secondary structure-related peaks in this region was compared with the reported literature (Goormaghtigh et al., 1990; Barth, 2007).

6.2.5. Rheology of keratin gels

Viscoelastic properties of keratin hydrogels were analyzed in a Physica MCR 301 rheometer (Anton Paar, Austria). Gels were evaluated by frequency sweeps from 1 to 10 Hz, under a 0.5% strain which was in the linear viscoelastic range as measured by previous amplitude sweeps. All measurements were performed at 25°C, with a probe gap of 1 mm.

6.2.6. Physical properties of scaffolds

Cross sections of scaffolds were gold sputter coated for scanning electron microscopy (SEM) analysis. Samples were scanned at an accelerating voltage of 5 kV (Tescan Vega 3 SEM, Tescan, Czech Republic). Pore size was determined by measuring the longest distance of pores from representative SEM images using ImageJ 1.48 software. Swelling capacity was determined gravimetrically after soaking dry scaffolds of known weight for 24 h at room temperature. Wet scaffolds were gently wiped out with cheese cloth to remove excess of water and the final weight was recorded. Results are presented as weight percentage of water absorbed relative to the dry weight of scaffolds. Porosity was calculated according to Lai et al., (2012), as the void fraction after soaking scaffolds of known dimensions in absolute ethanol overnight. Void volume was

calculated from the weight of ethanol absorbed by the scaffold, and results presented as void fraction percentage.

6.2.7. Preparation of chicken gelatin scaffolds (used as control)

Collagen was extracted from whole spent hen carcass using a pH-shifting process. Whole spent hen carcass was ground using meat grinder (Hollymatic Co., IL, USA), mixed with deionized water in a 1:4 (w/w) ratio and homogenized for 2.5 minutes using Waring heavy duty blender (CB15, Waring Co., CT, USA). For resulting meat slurry, pH was adjusted to 11.0 using 3M NaOH solution and stirred for 30 min at 500 rpm. After centrifugation (10000*g*, 4°C and 20 minutes), the supernatant was discarded (myofibrillar proteins) and the bottom solid precipitate was collected for collagen extraction. The precipitate was first mixed with 0.5M acetic acid in a 1:15 (w/v) ratio, and stirred for 24 hours at 4°C. The recovered precipitate after centrifugation (10000*g*, 4°C, and 20 minutes) was dispersed in deionized water in a 1:20 (w/v) ratio and heated to 90°C for 1 hour with continuous stirring. After stirring, the slurry was homogenized at high speed (15000 rpm, 2 minutes) and centrifuged (10000g, 4°C and 20 min) to collect the supernatant containing collagen. The pH of the supernatant was adjusted to 7.0 using 1M NaOH and dialyzed (5 KDa MW cut off cellulose dialysis tubes) for two days at 4°C. All precipitates were freeze dried and stored at -20°C until further use. The freeze-dried gelatin obtained from the pH-shifting method was ground into a fine powder and used to fabricate sponge scaffolds. Briefly, gelatin was re-suspended and stirred for 3 hours at room temperature in deionized water at a concentration of 7.5% w/v. 1 mL aliquots were poured into 24-wells of tissue culture plate and kept at 4°C for 24 h for gel settlement. Gelatin gels were frozen at -20°C for 24 h and lyophilized for 2 days. Insoluble gelatin scaffolds were achieved after glutaraldehyde crosslinking. Lyophilized gels were treated with 1 mL of a mixture of glutaraldehyde in acetone

(1:19) for 2 h, and washed extensively with ethanol aqueous solutions (80-50%) and deionized water in order to remove glutaraldehyde. Hydrated crosslinked gelatin gels were finally freeze-dried again to obtain gelatin scaffolds. Scaffolds were cut to a final thickness of 2 mm.

6.2.8. Cell culture

Adult human dermal fibroblasts (HDFa, Cell Applications Inc. San Diego, CA, U.S.) of passage 10 were harvested by trypsinization and resuspended in DMEM media containing 10% FBS and antibiotic/antimycotic mix. Chicken feather, hair and wool keratin hydrogel scaffolds were placed in 24-well culture plates and sterilized by soaking in ethanol aqueous solution 70% for 30 min (gradually from 10%, 30%, 50% and 70%). After washing with aqueous ethanol solutions (70 to 10%) and sterile PBS pH 7.4 three times, the scaffolds were soaked in complete media and incubated overnight in humidified environment at 37°C and 5% CO_2. Four media-impregnated scaffolds were seeded with 50 μL of HDF cells suspension (7.5×10^4 cells/mL) and incubated for 2 h to allow attachment of cells. Scaffolds were gently rinsed with PBS to remove non-attached cells and transferred to a new 24-well tissue culture plate. Scaffolds were incubated at 37°C, 5% CO_2 humidified environment for up to 12 days. Media was replaced every other day with 500 μL of fresh complete DMEM. Gelatin scaffolds (from spent hen meat) were used as control material. Two non-seeded scaffolds of each sample were used as control. Cell growth was quantified by Alamar blue® probe according to the manufacturer instructions (Thermo Scientific, U.S.). Cell number was estimated based on a calibration curve constructed from known cell concentrations (measured by counting cells on a hemacytometer using Tryphan blue) versus fluorescence of cells incubated for four hours with media containing 10% Alamar blue.

6.2.9. Cell imaging

After 12 days, scaffolds were fixed with 4% formaldehyde solutions for 24 h at room temperature, and washed with sterile PBS three times. Scaffolds sections (7 μm thick) were stained with hematoxylin & eosin. Representative images were taken in a brigthfield microscope (Primo Vert, Zeiss, Germany).

6.2.10. Statistics

Experiments were performed in triplicate unless otherwise specified. Data was treated by analysis of variance with a confidence level of 95%. Significant differences between samples were determined by Tukey multiple comparison test with a confidence level of 95%. Statistical analyses were carried out using Minitab v17 software (Minitab Inc., PA, U.S.).

6.3. Results

6.3.1. Characterization of keratins

Keratins extracted from feathers, hair and wool were analyzed by SDS-PAGE in presence of β-mercaptoethanol (Figure 6.1). Hair and wool keratins are heterogeneous proteins with molecular weights ranging from around 10 to 75 kDa. Keratin-associated proteins in hair and wool samples (KAPs; < 20 kDa) were detected in SDS-PAGE (Figure 6.1). Feather keratins are smaller proteins of around 10 kDa (Figure 6.1). While hair and wool keratins are composed of around 400-500 amino acid residues, feather keratins are smaller proteins composed of around 100 amino acids residues (Supplementary Information, Figures S6.1-S6.3). Keratinous samples were analyzed by their amino acid composition (Table 6.1). The highest proportion of non-polar/polar amino acids was determined in chicken feathers (51/49%) followed by wool (43/57%) and hair (34/66%). Glycine, serine, leucine, cysteine, and glutamic acid were the most abundant amino

acids found in the three samples. Hair had the highest concentration of cysteine, followed by wool and feather. Cysteine residues are mostly located at the C- and N- terminus of keratins (Supplementary Information, Figures S6.1-S6.3).

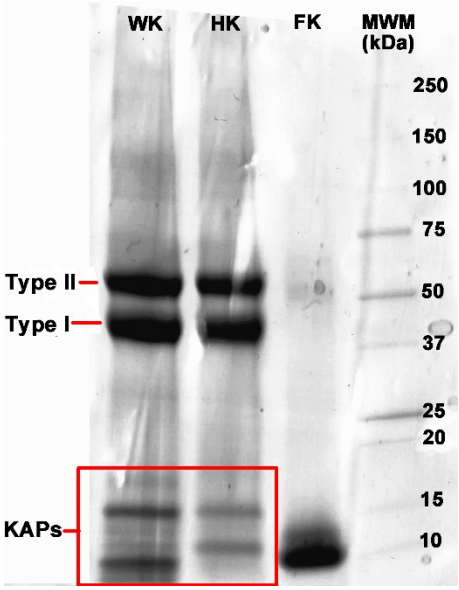

Figure 6.1. SDS-PAGE of keratin extracted from chicken feathers (FK), hair (HK), wool (WK), chicken feather (MWM, molecular weight marker; KAPs, keratin-associated proteins).

Table 6.1. Amino acid composition of chicken feathers, hair and wool (μmol/g)

	Feather	Hair	Wool
Arginine	626 ± 34	672 ± 34	718 ± 45
Lysine	366 ± 34	494 ± 35	518 ± 43
Aspartic acid	543 ± 50	407 ± 20	451 ± 21
Glutamic acid	959 ± 68	1125 ± 58	1058 ± 54
Histidine	73 ± 5	106 ± 10	57 ± 50
Serine	1540 ± 66	1108 ± 60	1034 ± 67
Threonine	428 ± 39	558 ± 28	502 ± 23
Half-cystine	1140 ± 105	2024 ± 98	1197 ± 55
Tyrosine	177 ± 9	147 ± 16	282 ± 15
Glycine	2186 ± 129	905 ± 27	1278 ± 95
Alanine	665 ± 47	448 ± 24	513 ± 29
Valine	761 ± 59	455 ± 23	445 ± 20
Leucine	1185 ± 75	861 ± 44	990 ± 58
Isoleucine	436 ± 33	228 ± 12	257 ± 13
Proline	343 ± 7	326 ± 7	554 ± 150
Phenylalanine	374 ± 29	153 ± 8	232 ± 13
Methionine	43 ± 3	54 ± 51	39 ± 40
Nitrogen %	16.2 ± 0.1	16.0 ± 0.6	16.3 ± 0.4
Polar/charged amino acids	49%	66%	57%
Non-polar amino acids	51%	34%	43%

Differences in keratin thermal properties were studied by DSC. Broad endothermic transitions observed from 50-100°C can be attributed to the evaporation of adsorbed moisture (Figure 6.2A and 6.2B). Endothermic peaks from 227-236°C were observed for all keratin raw materials (Figure 6.2A). It was observed that after the extraction, dialysis and lyophilization, the denaturation peak of keratins shifted to lower temperatures (Figure 6.2B and Table 6.2). This could be explained by altered molecular organization causing earlier mobility onset in all keratins.

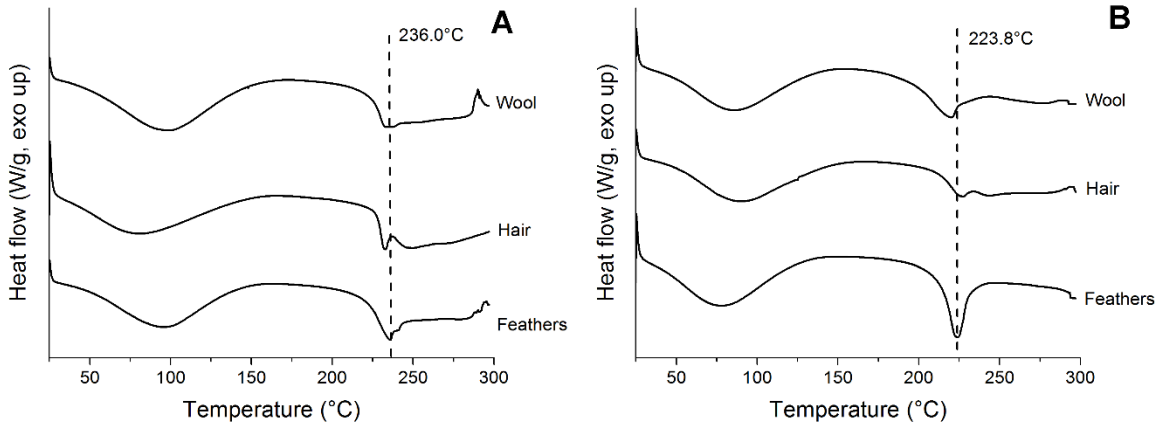

Figure 6.2. DSC thermograms of different keratin raw materials (A) and extracted and lyophilized keratins (B).

Table 6.2. Summary of melting temperatures of keratin from different sources and treatments.

	Melting peak temperature (°C)		
	Full fat	**Defatted**	**Keratin**
Feathers	237.4	236.0	223.8
Hair	232.1	232.6	223.9
Wool	237.7	234.0	222.4

Keratin raw materials and extracted keratins were analyzed by FTIR (Figure 3). FTIR spectra showed characteristic protein absorption bands, amide I (C=O stretching vibrations; νC=O), amide II (C-N stretching and N-H bending; νC-N and δN-H, respectively) and amide III (C-N stretching and N-H bending; νC-N and δN-H, respectively) (Figure 6.3A). After extraction the appearance of a small absorption bands at around 1024 cm^{-1} was observed (Figure 6.3C). This can be attributed to the presence of keratin-SSO_3^- functional groups resultant from the sulfitolysis of keratins in presence of sodium sulfite (Nomura et al., 2002).

Fourier self-deconvolution (FSD) was used to resolve peaks in the amide I region that can be assigned to different secondary structures. Feather, showed a more prominent peak centered at around 1633 cm^{-1}, which is characteristic of β-sheet structures, whereas, hair and wool showed more pronounced peaks at 1650 and 1644 cm^{-1}, which can be ascribed to α-helix and unordered structures, respectively (Figure 6.3B). These results were in accordance with XRD diffraction patterns of keratinous samples (Figure 6.4). Extracted and raw keratins presented different absorption bands in the FSD of amide I region (Figure 6.3D). Specific assignation of these bands can be adventurous since their ranges overlap. However, it can be said that bands in between 1615-1638 cm^{-1} corresponds to β-sheet, while 1639-1654 cm^{-1} and 1642-1660 cm^{-1} can be

attributed to unordered and α-helix structures, respectively. Bands in 1660-1694 cm^{-1} can correspond to turns, and β-sheet structures (Barth, 2007).

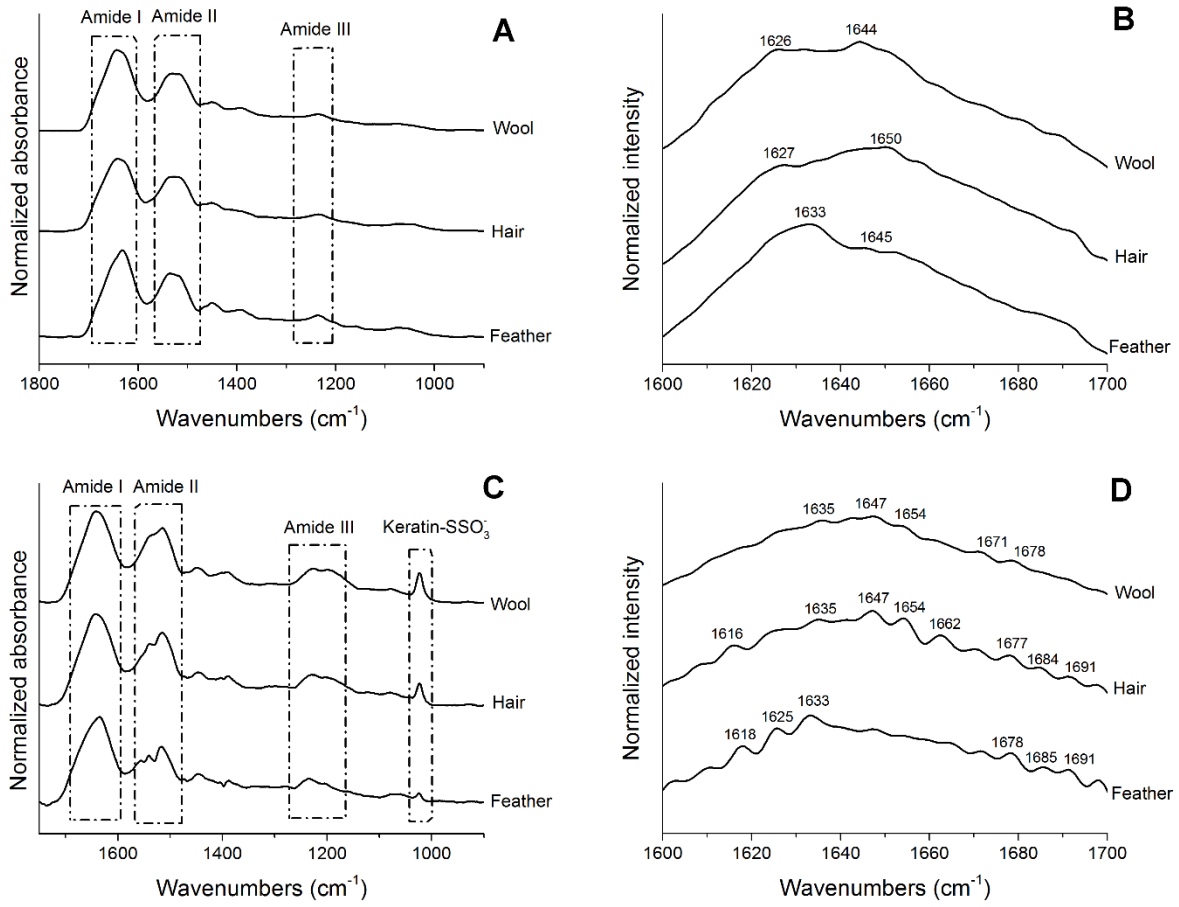

Figure 6.3. FTIR spectra and Fourier self-deconvoluted amide I region of keratin raw materials (A and B) and extracted keratins (C and D). Peaks in the Fourier self-deconvoluted spectra were assigned to secondary structures of protein; numbers above peaks indicate the corresponding wavenumbers.

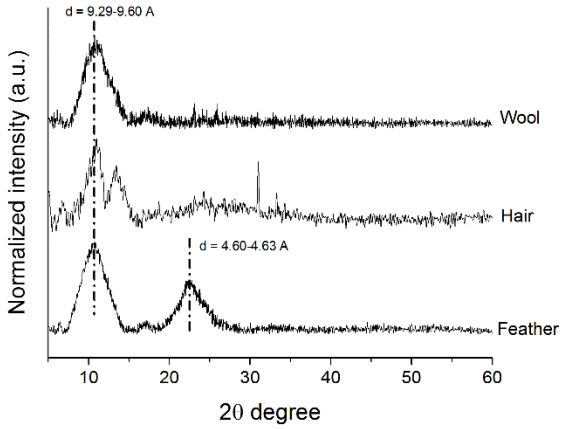

Figure 6.4. X-ray diffraction pattern of keratins. X-ray diffraction patterns of keratins powders were analyzed in a Rigaku Ultima IV powder diffractometer (Rigaku Co. Japan) using Co-Kα radiation (0.179 nm) from 5 to 50 2θ degrees.

6.3.2. Rheology of keratin gels

Extracted keratins formed gels of different appearance during dialysis (Figure 6.5A). Feather keratins at 7.5% w/v formed firm gels that were easy to handle and cut into discs, while gels from hair and wool keratin were weaker and more difficult to handle. Small amplitude oscillatory shear (SAOS) measurements were used to determine the viscoelastic properties of keratin gels over frequency sweeps (Figure 6.5B). Feather keratin showed substantially higher storage modulus (G', 7600-11000 kPa) than hair (G', 655-636 kPa) and wool (G', 62-163 Pa) keratin hydrogels (Figure 6.5B).

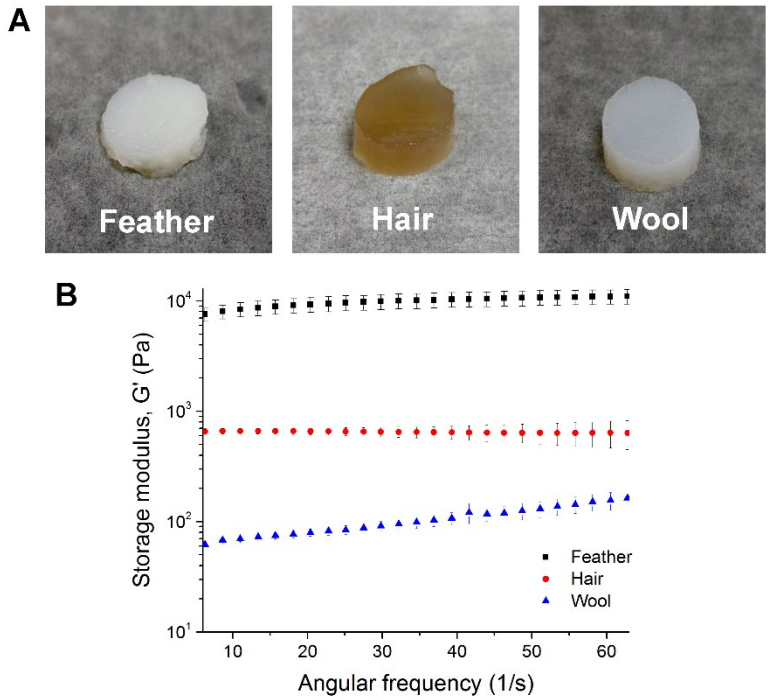

Figure 6.5. Color photograph (A) and storage modulus (B) frequency sweeps of keratin hydrogels (7.5% w/v, pH 7).

6.3.3. Physical and biological properties of keratin scaffolds

Keratin hydrogels were freeze-dried to form porous materials that could be used as dermal scaffolds and ultimately for tissue regeneration of skin injuries (Figure 6.6A and 6.6B). Gelatin scaffolds were prepared and used for comparison purposes. Scaffolds showed similar porosities between 86.9-90.0%, although porosity of wool keratin scaffold (69.5%) was significantly lower ($p<0.05$, Table 2). Feather keratin scaffolds showed the largest mean pore size (209.5 μm); however, all scaffolds showed a broad pore size range (Table 6.3). Swelling capacity of scaffolds was significantly different among the keratinous sources used to fabricate scaffolds. Higher swelling capacity was determined for hair and wool (> 3000%) compared with feather scaffolds (~1500%). Surface hydrophilicity was evaluated by contact angle measurements. Feather and

hair keratin scaffolds showed similar contact angle values, while wool scaffolds showed a significant lower value (Table 6.3), indicating a more hydrophilic surface. Measurement of gelatin scaffold could not be performed due to the rapid absorption of the water drop on the surface.

Figure 6.6. Color photographs (A) and SEM top sections micrographs (B) of keratin and gelatin scaffolds used. (scale bar is 500 μm).

Table 6.3. Physical properties of scaffolds prepared from different keratins at 7.5% w/v.

	Porosity	Pore size (Range; mean)	Water uptake	Contact angle
Feather	89.4 ± 5.7%[a]	149.6-277.3 μm; 209.5 ± 38.5 μm	1575.7 ± 118.5%[a]	88.3 ± 2.2°[a]
Hair	86.9 ± 5.3%[a]	85.5-211.6 μm; 141.0 ± 28.5 μm	3286.7 ± 367.6%[b]	87.3 ± 2.9°[a]
Wool	69.5 ± 7.3%[b]	117.3-277.0 μm; 182.9 ± 44.8 μm	3368.5 ± 390.0%[b]	81.0 ± 2.6°[b]
Gelatin	90.0 ± 3.1%[a]	103.7-244.4 μm; 155.9 ± 38.9 μm	1149.2 ± 154.2%[a]	ND

Different letters superscript within the same column indicate significant differences between samples ($p<0.05$).

Cell proliferation of fibroblasts was significantly higher ($p<0.05$) on feather keratin scaffolds than hair and wool keratin scaffolds after 11 days of culture (Figure 6.7A). Feather keratin scaffolds showed similar cell proliferation to spent hen gelatin scaffolds after 15 days. Histological top sections of feather keratin scaffolds without and with cells cultured for 15 days, are shown in figure 6.7B and 6.7C, respectively. Keratin fibers were stained purple with H&E dye. After soaking in media kertatin fibers maintained their structure (Figure 6.7B). Partial break down of keratin fibers can be observed after culturing fibroblasts on feather scaffolds (Figure 6.7C); however, keratin fibers can also be damaged during sample preparation steps such as, sectioning, mounting, and staining.

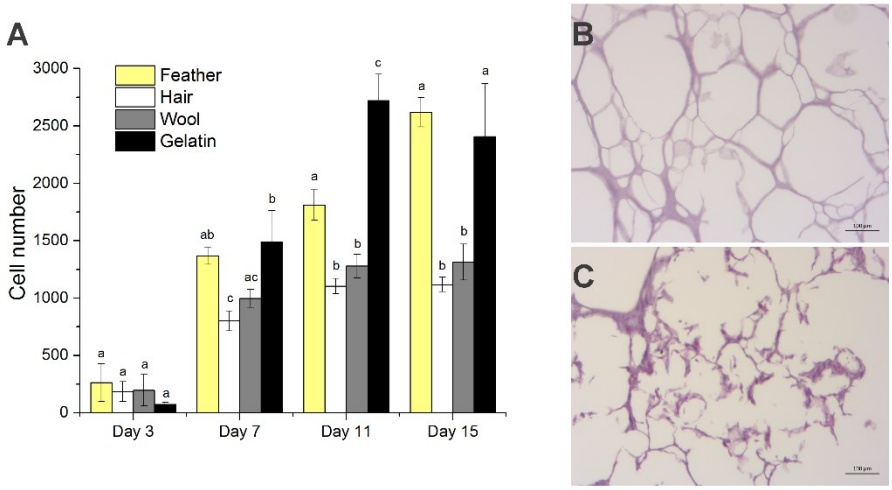

Figure 6.7. Proliferation of human dermal fibroblasts (HDF) on keratin and gelatin scaffolds (A). H&E staining of feather keratin scaffold sections after incubation for 15 days without cells (B, control) and human dermal fibroblasts (C); scale bar is 100 μm, 10x.

6.4. Discussion

It is well known that keratins from mammals differ from those of bird and reptiles, both structurally and chemically (Vincent, 2012). Our SDS-PAGE results were in agreement with the literature. Keratins from hair and wool are heterodimer intermediate filaments (IF) composed of keratin types I (acidic, 40-50k kDa) and II (neutral/basic, 55-65 kDa). KAPs form extensive crosslinking with IF through disulfide bonds, affecting strength and rigidity (Wu et al., 2008; Fujii et al., 2013). Different from hair and wool, feather keratin is composed of around 90% of homogenous 10.4 kDa proteins (Fraser et al., 1972). The amino acid composition of keratinous samples was in accordance with the reported literature (Harrap and Woods, 1964; Robbins and Kelly, 1970; Leon et al., 1972; Gousterova et al., 2005).

Semi-crystalline ultrastructure of keratins was confirmed by DSC (Figure 6.2). The denaturation of crystalline portions of raw keratinous samples (227-236°C) shifted to lower

temperatures after extraction (~223°C). After dialysis and lyophilization keratins re-arrange into a semi-crystalline structure, however, a certain degree of order in the crystalline ultrastructure is lost.

Differences in the secondary structure of mammalian and avian keratins were determined by FTIR analysis (Figure 6.3). Our results were in agreement with early studies that hair and wool keratins are mostly formed by α-helices (Astbury and Woods, 1934). These helical domains are present in the central part of keratin filaments and assemble into heterodimeric coiled coil structures by combination of basics and acidic subunits (Yu et al., 1993). In the case of feather keratins, they are mostly composed of β-sheet structures (Fraser and Parry, 2008). Although, small portions of α-helix keratin can be found in feather barbs/barbules and down feathers, especially in the early development of feathers (Alibardi and Toni, 2008; Ng et al., 2012). During extraction of keratins, urea, thiourea and sodium sulfite act disrupting the secondary structure of keratins. This was confirmed by the appearance of multiple peaks in the FSD FTIR analysis of extracted keratins (Figure 6.3D). Consequently with DSC analysis, FTIR results suggest that a degree of disorder was introduced in the structure of keratin after extraction.

Keratins were dissolved at 7.5% w/v and formed gels during dialysis. Rheological properties of gels were studied by SAOS measurements. A higher storage modulus (G') is related to the ability of the material to store energy to return to its original shape after being subjected to strain. It can be used as a measure of the strength or solid-like behavior of hydrogels. The higher strength of feather compared to hair and wool keratin hydrogels can be explained by differences in their chemical composition and structure. The strength and stability of keratin gels can be explained by the formation of multiple covalent disulfide bonds (Chapter

4). Cysteine groups are located at higher density at the end of keratin chains, (Arai et al., 1983; Supplementary Information Figures S6.1-S6.3); they can act as anchor points in the self-assembly of keratin chains. However, even hair keratins had a higher concentration of cysteine residues than feather, hydrogels were weaker. This can be explained by the fact that re-formation of disulfide bonds depend on the proximity of two cysteine residues and their spatial availability to participate in thiol/disulfide exchange reactions. Long keratin chains in hair and wool can result in more entanglement resulting physical hindering of cysteine residues for re-oxidation (Figure 6.8). In fact, more intense keratin-thiosulfate peaks in FTIR for hair and wool keratins (Figure 6.3C) can account for cysteine groups unable to re-oxidize into disulfides. In such case, wool and hair keratins might have formed weaker gels stabilized by a lesser amount of disulfide bonds. It has been suggested that when cysteine thiols are not available for crosslinking, keratins form weak gels stabilized merely by hydrophobic and electrostatic interactions (Ikkai and Nato, 2002; Han et al., 2015). Differences in keratin secondary structures can also account for differences in gel physical properties. α-helix keratins in hair and wool are elastic fibers that can be irreversible stretched into β-sheets conformation (Bendit, 1957; Kreplak et al., 2004). Instead feather keratin is composed mainly of ordered and rigid β-sheet structures that cannot be further stretched, resulting in more mechanically resistant hydrogels. A combined effect of the higher molecular weight and the high proportion of α-keratins in hair and wool can explain the weaker mechanical stability and high water uptake capacity of hair and wool keratin hydrogels (Figure 6.8).

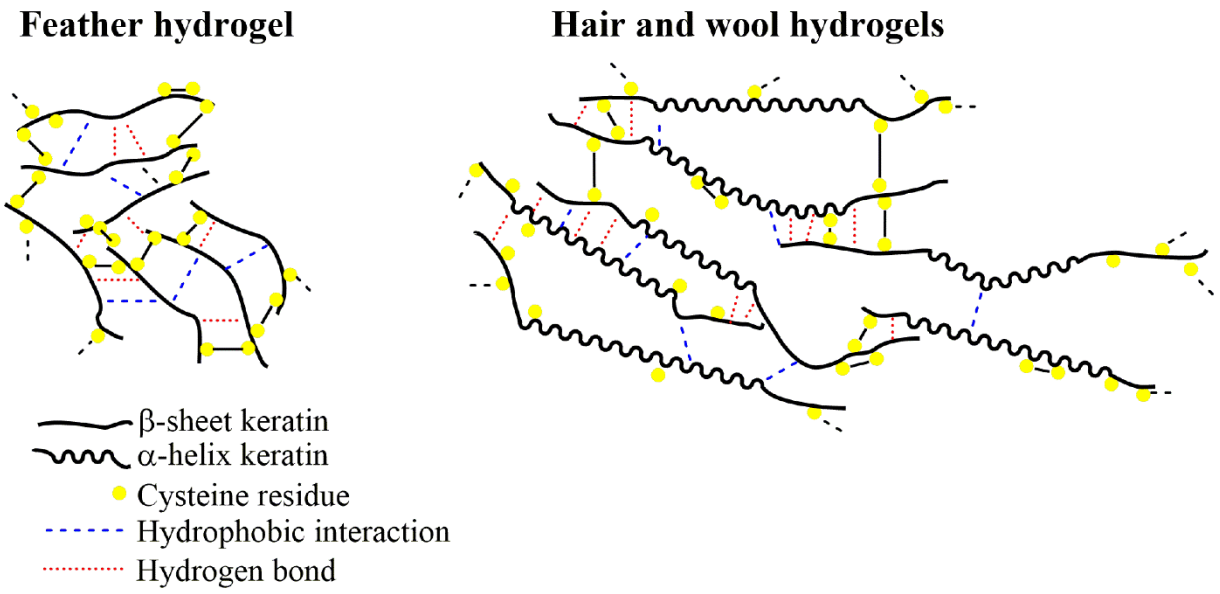

Figure 6.8. Scheme of proposed self-assembly of keratin hydrogels indicating major intermolecular forces (disulfide bonds, hydrophobic interactions and hydrogen bonds). Low molecular weight feather keratin allow more chances of disulfide formation. Higher molecular weight hair and wool keratins can result in more physical entanglement of keratin chains leading to physical hindering of cysteine residues unable for crosslinking. Rigid β-sheets in feather keratin result in stiffer hydrogels than those from elastic α-helix keratins in hair and wool.

Keratin hydrogels were lyophilized to form porous hydrogel scaffolds. Properties of scaffold materials such as porosity, appropriate pore size for cell infiltration, pore interconnectivity, swelling capacity, and appropriate mechanical strength, have been reported to have a positive effect on cellular adhesion and growth (Chang and Wang, 2011). Hair and wool keratin hydrogels were able to swell and entrap more water than feather keratin hydrogels. This can be explained by the stretch ability of α-helix keratins in hair and wool. In the case of feather hydrogels a rigid structure by dense disulfide crosslinking β-sheet keratins limits the swelling capacity (Balakrishnan et al., 2005).

Integrin binding sequences that mediate cell attachment have been reported on gelatin, and hair and wool keratins; however, they have not been recognized in chicken feather keratin (Dedhar et al., 1987; Ruoslahti, 1996; Tachibana et al., 2002; Supplementary Information Figure S6.1-S6.3). It is possible that the higher cell growth rate obserbed on feather keratin scaffolds may be related to its superior viscoelastic properties. It has been demonstrated that fibroblasts attach and spread preferentially to stiffer substrates (Yeung et al., 2005), and that they preferentially migrate from softer to stiffer substrate gradients, developing a broader and flattened morphology in the latter (Lo et al., 2000). The adsorption of proteins present in FBS such as fibronectin and vitronectin can mediate cell attachment, and subsequently proliferation on scaffolds (Rosso et al., 2013; Deng et al., 2014). This adsorption might be favored by the presence of numerous hydrophobic amino acid residues in feather keratin (Tamada and Ikada, 1993; Xu and Siedlecki, 2007).

Partial breakdown of keratin fibers of scaffolds was observed after 15 days of culture (Figure 6.7B and 6.7C). Although further studies would be required to confirm this, as this can also result from sectioning and mounting of scaffold during the preparation of histological samples.

6.5. Conclusions

Keratins from hair, wool and chicken feather were extracted and characterized. Differences in molecular weight, cysteine content, and conformational properties of keratins resulted in self-assembly of hydrogels with significant differences in mechanical properties. Smaller molecular weight and β-sheet conformation of feather keratins resulted in more mechanically robust hydrogels. Higher molecular weight and α-helix conformation of hair and wool keratins resulted into weaker, but flexible hydrogels able to absorb high amounts of water (3000%). Fibroblasts

proliferated at higher rates in stiffer feather keratin hydrogel scaffolds. Partial degradation of feather keratin fibers was observed after 15 days of cell culture. Stronger hydrogels from avian keratins could serve in the fabrication of advanced wound healing biomaterials. Further in vitro and in vivo evaluation of hydrogel scaffolds would support the potential of feather keratins for would healing applications.

6.6. References

Abdelrahman, T., & Newton, H. (2011). Wound dressings: Principles and practice. *Surgery (Oxford)*, 29, 491-495.

Aboushwareb, T., Eberli, D., Ward, C., Broda, C., Holcomb, J., Atala, A., & Van Dyle, M. (2009). A keratin biomaterial gel hemostat derived from human hair: Evaluation in a rabbit model of lethal liver injury. *Journal of Biomedical Materials Research Part B: Applied Biomaterials*, 90, 45-54.

Abrigo, M., McArthur, S.L., & Kingshott, P. (2014). Electrospun nanofibers as dressing for chronic wound care: Advances, challenges, and future prospects. *Macromolecular Bioscience*, 14, 772-792.

Alibardi, L., & Toni, M. (2008). Cytochemical and molecular characteristics of the process of cornification during feather morphogenesis. *Progress in Histochemistry and Cytochemistry*, 43, 1-69.

Aluigi, A., Vineis, C., Varesano, A., Mazzuchetti, G., Ferrero, F., & Tonin, C. (2008). Structure and properties of keratin/PEO blend nanofibres. *European Polymer Journal*, 44, 2465-2475.

Arai, K.M., Takahashi, R., Yokote, Y., & Akahane, K. (1983). Amino-acid sequence of feather keratin from fowl. *European Journal of Biochemistry*, 132, 501-507.

Astbury, W.T., & Woods, H,J. (1934). X-ray studies of the structure of hair, wool, and related fibres. II. The molecular structure and elastic properties of hair keratin. *Philosophical Transactions of the Royal Society of London. Series A*, 232, 333-394.

Balaji, S., Kumar, R., Sripriya, R., Kakkar, P., Ramesh, D.V., Reddy, P.N.K., & Sehgal, P.K. (2012). Preparation and comparative characterization of keratin-chitosan and keratin-gelatin composite scaffolds for tissue engineering applications. *Materials Science and Engineering C*, 32, 975-982.

Balakrishnan, B., Mohanty, M., Umashankar, P.R., & Jayakrishnan, A. (2005). Evaluation of an in situ forming hydrogel wound dressing based on oxidized alginate and gelatin. *Biomaterials*, 26, 6335-6342.

Barth, A. (2007). Infrared spectroscopy of proteins. *Biochimica et Biophysica Acta*, 1767, 1073-1101.

Bendit, E.G. (1957). The α□β transformation in keratin. *Nature*, 179, 535.

Boateng, J.S., Matthews, K.H., Stevens, H.N.E., & Eccleston, G.M. (2008). Wound healing dressings and drug delivery systems: A review. *Journal of Pharmaceutical Sciences*, 97, 2892-2923.

Bonvallet, P.P., Schultz, M.J., Mitchell, E.H., Bain, J.L., Culpepper, K., Thomas, S.J., & Bellis, S.L. (2015). Microporous dermal-mimetic electrospun scaffolds pre-seeded with fibroblasts promote tissue regeneration in full-thickness skin wounds. *Plos ONE*, 10, e0122359. doi: 10.1371/journal. Pone.0122359.

Bragulla, H.H., & Homberger, D.G. (2009). Structure and functions of keratin proteins in simple, stratified, keratinized and cornified epithelia. *Journal of Anatomy*, 214, 516-559.

Chang, H-I., & Wang, Y. (2011). Cell responses to surface and architecture of tissue engineering scaffolds. In D, Eberli. (Ed.). Regenerative Medicine and Tissue Engineering – Cell and Biomaterials. InTech, DOI: 10.5772/21983.

De Guzman, R.C., Merrill, M.R., Richter, J.R., Hamzi, R.I., Greengauz-Roberts, O.K., & Van Dyke, M.E. (2011). Mechanical and biological properties of keratose biomaterials. *Biomaterials*, 32, 8205-8217.

Dedhar, S., Ruoslahti, E., & Pierschbacher, M. (1987). A cell surface receptor complex for collagen type I recognizes the Arg-Gly-Asp sequence. *The Journal of Cell Biology*, 104, 585-593.

Delgado, L.M., Bayon, Y., Pandit, A., & Zeugolis, I. (2015). To cross-link or not to cross-link? Cross-linking associated foreign body response of collagen-based devices. *Tissue Engineering Part B*, 21, 298-313.

Deng, J., Ren, T., Zhu, J., Mao, Z., & Gao, C. (2014). Adsorption of plasma proteins and fibronectin on poly(hydroxylethyl methacrylate) brushes of different thickness and their relationship with adhesion and migration of vascular smooth muscle cells. *Regenerative Biomaterials*, 1, 17-25.

Fonder, M.A., Lazarus, G.S., Cowan, D.A., Aronson-Cook, B., Kohli, A.R., & Mamelak, A.J. (2008). Treating the chronic wound: A practical approach to the care of nonhealing wounds and wound care dressings. *Journal of the American Academy of Dermatology*, 58 185–206.

Fraser, R.B.D., Mac Rae, T.P., & Rogers, G.E. (1972). Keratins- their Composition, Structure and Biosynthesis. CC Thomas Publishing, Springfield, IL, USA.

Fraser, R.D., & Parry, D.A. (2008). Molecular packing in the feather keratin filament. *Journal of Structural Biology*, 162, 1-13.

Fujii, T., & Li, D. (2008). Preparation and properties of protein films and particles from chicken feathers. *Journal of Biological Macromolecules*, 8, 48-55.

Fujii, T., Takayama, S., & Ito, Y. (2013). A novel purification procedure for keratin-associated proteins and keratin from human hair. *Journal of Biological Macromolecules,* 13, 92-106.

Goormaghtigh, E., Cabiaux, V., & Ruysschaert, J-M. (1990). Secondary structure and dosage of soluble and membrane proteins by attenuated total reflection Fourier-transform infrared spectroscopy on hydrated films. *European Journal of Biochemistry*, 193, 409-420.

Gousterova, A., Braikova, D., Goshev, I., Christov, P., Tishinov, K., Vasileva-Tonkova, E., Haertle, T., & Nedkov, P. (2005). Degradation of keratin and collagen containing wastes by newly isolated thermoactinomycetes or by alkaline hydrolysis. *Letters in Applied Microbiology*, 40, 335-340.

Guo, J., Pan, S., Yin, X., He, Y-F., Li, T., & Wang, R-M. (2014). pH-sensitive keratin-based polymer hydrogel and its controllable drug-release behavior. *Journal of Applied Polymer Science*, 132, 41572. doi: 10.1002/app.41572.

Han, S., Ham, T.R., Haque, S., Sparks, J.L., & Saul, J.M. (2015). Alkylation of human hair keratin for tunable hydrogel erosion and drug delivery in tissue engineering applications. *Acta Biomaterialia*, 23, 201-213.

Harrap, B.S., & Woods, E.F. (1964). Soluble derivatives of feather keratin. 1. Isolation, fractionation and amino acid composition. *Biochemical Journal*, 92, 8-18.

Hill, P., Brantley, H., & Van Dyke, M. (2010). Some properties of keratin biomaterials: Kerateines. *Biomaterials*, 31, 585-593.

Hinnman, C.D., & Maibach, H.I. (1963). Effect of air exposure and occlusion on experimental human skin wounds. *Nature*, 200, 377-378.

Ikkai, F., & Naito, S. (2002). Heat-induced gelation of hard-keratin protein aqueous solutions. *Biomacromolecules*, 3, 482-487.

Katoh, K., Shibayama, M., Tanabe, T., & Yamauchi, K. (2004). Preparation and physicochemical properties of compression-molded keratin films. *Biomaterials*, 25, 2265-2272.

Jones, A.M., & San Miguel, L. (2006). Are modern wound dressings a clinical and cost-effective alternative to the use of gauze? *Journal of Wound Care*, 15, 65-69.

Kreplak, L., Doucet, J., Dumas, P., & Briki, F. (2004). New aspects of the α-helix to β-sheet transition in stretched hard α-kertain fibers. *Biophysical Journal*, 87, 640-647.

Laemmli, U.K. (1970). Cleavage of structural proteins during the assembly of the head of bacteriophage T4. *Nature*, 227, 680-685.

Lai, J-Y., Li, Y-T., Cho, C-H., & Yu, T-C. (2012). Nanoscale modification of porous gelatin scaffolds with chondroitin sulfate for corneal stromal tissue engineering. *International Journal of Nanomedicine*, 7, 1101-1114.

Leon, N.H. (1972). Structural aspects of keratin fibres. *Journal of the Society of Cosmetic Chemists*, 23, 427-445.

Li, J., Li, Y., Li, L., Mak, A.F.T., Ko, F., & Qin, L. (2009). Preparation and biodegradation of electrospun PLLA/keratin nonwoven fibrous membrane. *Polymer Degradation and Stability*, 94, 1800-1807.

Lo, C.M., Wang, H.B., Dembo, M., & Wang, Y.L. (2000). Cell movement is guided by the rigidity of the substrate. *Biophysical Journal*, 79, 144-152.

Ma, B., Wang, X., Wu, C., & Chang, J. (2014). Crosslinking strategies for preparation of extracellular matrix-derived cardiovascular scaffolds. *Regenerative Biomaterials*, 81-89.

Mason, B.N., Califano, J.P., & Reinhart-King, C.A. (2012). Matrix stiffness: A regulator of cellular behavior and tissue formation. In Bhatia, S.K. (Ed.). Engineering Biomaterials for Regenerative Medicine. Springer, New York, USA.

Moore, S. (1963). On the determination of cystine as cysteic acid. *The Journal of Biological Chemistry*, 238, 235-237.

Nemeth, A.J., Eaglstein, W.H., Taylor, J.R., Peerson, L.J., & Falanga, V. (1991). Faster healing and less pain in skin biopsy sites treated with an occlusive dressing. *Archives of Dermatology*, 127, 1679-1683.

Ng, C.S., Wu, P., Foley, J., Foley, A., McDonald, M-L., Juan, W-T., Huang, C-J., Lai, Y-T., Lo, W-S., Chen, C-F., Leal, S.M., Zhang, H., Widelitz, R.B., Patel, P.I., Li, W-H., & Chuong, C-M. (2012). The chicken frizzle feather is due to an α-keratin (KRT75) mutation that causes a defective rachis. *PLoS Genetics,* 8:e1002748, 1-16.

Nomura, Y., Nakato, H., Ishii, Y., & Shirai, K. (2002). Characterization of S-sulfokeratein from pig hair and its use as a modifier of type I collagen gel. *Bioscience, Biotechnology, and Biochemistry,* 66, 1382-1385.

Ovington, L.G. (2001). Hanging wet-to-dry dressings out to dry. *Home Healthcare Nurse*, 19, 477-483.

Ovington, L.G. (2007). Advances in wound dressings. *Clinics in Dermatology*, 25, 33-38.

Petersen, A., Joly, P., Bergmann, C., Korus, G., & Duda GN. (2012). The impact of substrate stiffness and mechanical loading on fibroblast-induced scaffold remodeling. *Tissue Engineering: Part A*, 18, 1804-1817.

Reichl, S., Borrelli, M., & Geerling, G. (2011). Keratin films for ocular surface reconstruction. *Biomaterials*, 32, 3375-3386.

Robbins, C.R., & Kelly, C.H. (1970). Amino acid composition of human hair. *Textile Research Jorunal*, 40, 891-896.

Rosso, F., Marino, G., Grimaldi, A., Cafiero, G., Chiellini, E., Chiellini, F., Barbarisi, M., & Barbarisi, A. (2013). Vitronectin absorbed on nanoparticles mediate cell viability/proliferation and uptake by 3T3 swiss albino mice fibroblasts: In vitro study. *BioMed Research International*, doi: 10. 1155/2013/539348.

Ruoslahti, E. (1996). RGD and other recognition sequences for integrins. *Annual Review of Cell and Developmental Biology*, 12, 697-715.

Sierpinski, P., Garrett, J., Ma, J., Apel, P., Klorig, D., Smith, T., Koman, L.A., Atala, A., Van Dyke, M. (2008). The use of keratin biomaterials derived from human hair for the promotion of rapid regeneration of peripheral nerves. *Biomaterials*, 29, 118-128.

Silva, R., Singh, R., Sarker, B., Papageorgiou, D.G., Juhasz, J.A., Roether, J.A., Cicha, I., Kaschta, J., Schubert, D.W., Chrissafis, K., Detsch, R., & Boccaccini. (2014). Hybrid hydrogels based on keratin and alginate for tissue engineering. *Journal of Materials Chemistry B*, 2, 5441-5451.

Sridhar, R., Prabhakaran, M.P., & Ramakrishna, S. (2013). Synthetic enroutes to engineer electrospun scaffolds for stem cells and tissue regeneration. In Ramalingam, M., Jabbari, E., Ramakrishna, S., & Khademhosseini, A. (Eds.). Micro and nanotechnologies in engineering stem cells and tissues. John Wiley & Sons, Inc, New Jersey, USA.

Tachibana, A., Furuta, Y., Takeshima, H., Tanabe, T., & Yamauchi, K. (2002). Fabrication of wool keratin sponge scaffolds for long-term cell cultivation. *Journal of Biotechnology*, 93, 165-170.

Tamada, Y., & Ikada, Y. (1993). Effect of preadsorbed proteins on cell adhesion to polymer surfaces. *Journal of Colloid and Interface Science*, 155, 334-339.

Verma, V., Verma, P., Ray, P., & Ray, A.R. (2008). Preparation of scaffolds from human hair proteins for tissue-engineering applications. *Biomedical Materials*, 3, 025007.

Vincent, J. (2012). Structural Biomaterials. Princeton University Press, New Jersey, USA, Chapter 2.

Winter, G.D. (1962). Formation of scab and the rate of epithelialization of superficial wounds in the skin of the young domestic pig. *Nature*, 193, 293-294.

Wu, D-D., Irwin, D.M., & Zhang, Y-P. (2008). Molecular evolution of the keratin associated protein gene family in mammals, role in the evolution of mammalian hair. *BMC Evolutionary Biology*, 8, 241-256.

Xu, H., Cai, S., Xu, L., & Yang, Y. (2014). Water-stable three-dimensional ultrafine fibrous scaffolds from keratin for cartilage tissue engineering. *Langmuir*, 30, 8461-8470.

Xu, L-C., & Siedlecki, C.A. (2007). Effects of surface wettability and contact time on protein adhesion to biomaterial surfaces. *Biomaterials*, 28, 3273-3283.

Yeung, T., Georges, P.C., Flanagan, L.A., Marg, B., Ortiz, M., Funaki, M., Zahir, N., Ming, W., Weaver, V., & Janmey, P.A. (2005). Effects of substrate stiffness on cell morphology, cytoskeletal structure and adhesion. *Cell Motillity and the Cytoskeleton*, 60, 24-34.

Yin, X-C., Li, F-Y., He, Y-F., Wang, Y., & Wang, R-M. (2013). Study of effective extraction of chicken feather keratins and their films for controlling drug release. *Biomaterials Science*, 1, 528-536.

Yu, J., Yu, D.W., Checkla, D.M., Freedberg, I.M., & Bertolino, A.P. (1993). Human hair keratins. *Journal of Investigative Dermatology*, 10, 56S-59S.

Zhu, J, % Marchant RE. (2011). Design properties of hydrogel tissue-engineering scaffolds. *Expert Review of Medical Devices*, 8, 607-626.

6.7. Appendix B: Supplementary Information

Figure S6.1. Amino acid sequence of chicken feather keratins (A: UniProt P02450; B: Arai et al., 1983) and cysteine residues (orange).

**Recognized integrin binding sequences recopilated from Ruoslahti 1996.*

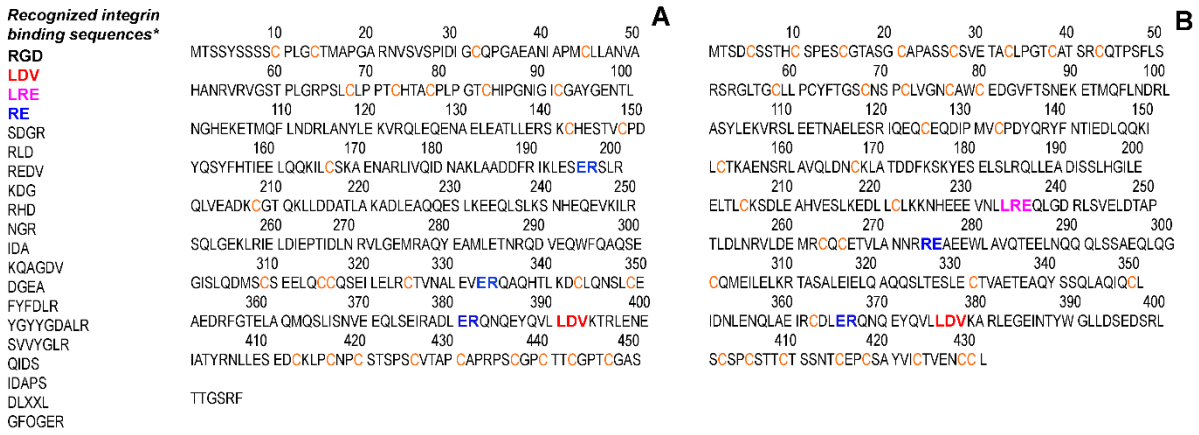

Figure S6.2. Amino acid sequence of human hair keratins (A: UniProt O76015; B: UniProt Q6A162) highlighting the presence of recognized integrin binding sequences and cysteine residues (orange).

** Recognized integrin binding sequences recopilated from Ruoslahti 1996.*

Figure S6.3. Amino acid sequence of sheep wool keratins (A: UniProt P02534; B: UniProt P15241) highlighting the presence of recognized integrin binding sequences and cysteine residues (orange).

** Recognized integrin binding sequences recopilated from Ruoslahti 1996.*

CHAPTER 7. Preparation and characterization of thermally crosslinked poly(vinyl alcohol)/feather keratin nanofiber scaffolds

7.1. Introduction

Mats of non-woven nanofibers have been widely explored for tissue engineering applications. They have large surface area to volume ratio and microporous network. The small diameter of nanofibers (50-500 nm) mimic the ultrastructure of the natural extracellular matrix (ECM) of tissues, which is related to enhanced adhesion, proliferation, migration and differentiation of cells (Barnes et al., 2007; Abrigo et al., 2014).

Electrospinning is a versatile and straightforward technology for the fabrication of nanofibers. In electrospinning process a viscoelastic polymer solution is fed to a capillary tip that is connected to a high voltage source. The high voltage causes a high electrostatic charge at the droplet surface. Once the intensity of the electrical field overcomes the surface tension of the solution, a liquid jet is released from the tip towards a collector with opposite charge or grounded target (Thompson et al., 2007). During the travel of the jet, the solvent evaporates and the polymer stretches and becomes thin due to the charge repulsion at the surface which tends to increase the surface area of the jet. The surface tension of the solution tends to reduce the surface area by breaking up the jet into spherical droplets; however, this phenomena is prevented by viscoelastic forces of the polymeric solution (Ramakrishna et al., 2005; Aslanzadeh et al., 2015). Proteins have shown to ptomote cell attachment and therefore there is increasing interest to develop nanofiber scaffolds from them (Yoon and Fisher, 2009; Zhu and Marchant, 2011).

Keratins are naturally abundant proteins found in animal tissues including hair, wool, horns, hooves, nails, reptile scales and bird beaks and feathers. Due to their remarkable mechanical properties they have been widely explored for the fabrication of scaffolds showing excellent biocompatibility, enhanced cell adhesion and proliferation and accelerated wound healing (Reichl, 2009; Hill et al., 2010; Xu et al., 2013; Wang et al., 2017). However,

electrospinning of keratins is challenging due to their poor viscoelastic properties, low molecular weight, and insolubility in water and organic solvents. The addition of sodium dodecyl sulfate (SDS) in the extraction of keratin is often used to improve its solubility (Park et al., 2015; Fan et al., 2016; Aluigi et al., 2007; Aluigi et al., 2008; Ayutthaya et al., 2015; Xu et al., 2014). SDS forms stable complexes with keratin but are difficult to remove during dialysis (Schrooyen et al., 2001). Due to its toxicity the release of SDS might have negative effect in implanted scaffolds. The treatment of feather keratin in aqueous alkaline solutions has been reported to improve their solubility. It is also reported that released peptides can promote wound healing (Thilagar et al., 2009; McPherson and Hardy, 2011).

In order to improve the viscoelasticity of keratin solutions, polymer aids are generally used. However, in most cases polymer/keratin blends are dissolved in harmful solvents to facilitate electrospinning such as 2,2,2-trifluoroethanol (Boakye et al., 2015), formic acid (Yen et al., 2016; Li and Yang, 2014; Aluigi et al., 2013; Ayutthaya et al., 2015), chloroform/N-dimethylformamide (Li et al., 2009), and 1,1,1,3,3,3-hexafluoro-2-isopropanol (Yuan et al., 2009). In addition, harmful crosslinking chemicals including glutaraldehyde vapor (Yuan et al., 2009) and glioxal (Park et al., 2015) are needed to impart water stability to keratin/polymer fibers. It is highly desirable to develop keratin nanofiber scaffolds from electrospinning of aqueous solutions by using environmentally friendly solvents and crosslinking reagents. This would minimize the risk of toxicity for biomedical applications.

Polyvinyl alcohol is a water soluble polymer, biocompatible with human tissues (Schmedlen et al., 2002). Due to its excellent viscoelastic properties, PVA has been investigated for the fabrication of electrospun mats (Zhang et al., 2005). Wool keratin extracted with SDS was mixed with PVA in formic acid solution and electrospun nanofibers were characterized;

however, crosslinking was not performed and water stability of nanofiber was not evaluated (Li and Yang, 2014). Preparation of hair keratin/PVA blend electrospun fibers were reported by Park et al., (2015). Crosslinking of fibers with glioxal resulted in loss of the porous structure and fusion of fibers. In both studies cell culture properties of PVA/keratin scaffolds were not investigated.

The main objective of this study was to fabricate and characterize electrospun feather keratin based nanofiber scaffolds using environmentally friendly solvents and crosslinking methods. PVA was used as polymer aid for electrospinning of keratin in aqueous solution. The rheology of feather keratin/PVA solutions was studied with relation to fiber morphology. Citric acid was used for thermal crosslinking of nanofiber. Chemical and ultrastructural properties of nanofiber were evaluated by FTIR, DSC, and XPS. The biological performance of keratin/PVA electrospun mats was investigated in vitro by culture of human dermal fibroblasts.

7.2. Methodology

7.2.1. Feather keratin

White chicken feathers were obtained from the Poultry Research Centre of the University of Alberta (Edmonton, AB, Canada), washed exhaustively with hot water and domestic soap, and oven dried at 50°C. Dried feathers were ground in a cutting mill (Fritsch Pulverisette 15, Fritsch, Germany) with an insert sieve of circular perforations of 1 mm diameter. Ground feathers were defatted with petroleum ether for 5 h in a soxhlet apparatus. Defatted feather powder (10.0 g) was stirred for 24 h in 250 mL 1 M NaOH. Soluble feather keratin (FK) was recovered by filtration (53 μm metallic mesh). The filtrate was neutralized with HCl and centrifuged (10,000g x 15 minutes). The clear supernatant was desalted using a solid phase extraction cartridge (Sep-

pak tC18 Vac 35cc 10 g, Waters, U.S.). Salt was eluted with a 0.1% trifluoroacetic acid (TFA) solution in double distilled water (dd-H2O). Keratin was recovered after elution with 50 and 100% acetonitrile aqueous 0.1% TFA solutions. Recovered keratin was freeze dried and stored at -20°C until its use.

7.2.2. Cytotoxicity of feather keratin

Feather keratin (FK) powder was dissolved at different concentrations (from 0.4 to 1.6 mg/mL) in Dulbecco's Modified Eagle's Medium (DMEM) containing 10% fetal bovine serum (FBS) and antibiotic-antimycotic mix (ThermoFischer, MA, U.S.). Solutions were sterilized by filtration through 0.2 μm low protein binding syringe membranes (Pall Co. U.S.). Adult human dermal fibroblasts (HDFa, Cell Applications, Inc. CA, U.S.) of passage 2 were subcultured by trypsinization and grown in 24-well plates for 48 hours (in a humidified environment at 37°C and 5% CO_2). Then, cells were treated with feather keratin/media solutions and incubated for 48 hours. Cell viability was calculated from the relative fluorescence of Alamar Blue (ThermoFischer, MA, U.S.) according to the manufacturer's specifications (excitation 560 nm/emission 590 nm). A control solution of media without feather keratin was considered as 100% viability.

7.2.3. Preparation of electrospinning solutions

Polyvinyl alcohol (PVA, 87-89% hydrolyzed with a molecular weight of 85,000-124,000 g/mol; Sigma-Aldrich, MO, U.S.) solution was prepared by slowly adding 5 g of PVA into 50 mL of deionized water (10% w/v). PVA was dissolved by stirring overnight at 80°C in a stirring plate. After cooling down at room temperature, 1.2 g of citric acid were added and the final pH was adjusted to 6.0 with 6 M NaOH. Citric acid was added as a post-processing PVA crosslinking agent (See section 2.5). A 10% w/v solution of feather keratin (FK) was prepared by dissolving

1.0 g of freeze dried FK powder in 10 mL of deionized water at room temperature. Electrospinning solutions were prepared as described in Table 1. The total solid content was maintained at 10% w/v. The mass ratio of FK to PVA was varied from 0 (PVA) to 30% (FK30) as summarized in Table 7.1. Solutions were stirred overnight to ensure homogeneity before electrospinning. Conductivity of solutions was measured with a handheld conductivity meter (EC-3, HM Digital, Inc., CA, U.S.).

Table 7.1. Composition of electrospinning solutions and mean fiber diameter of electrospun fibers.

Solution	PVA 10%	FK 10%	Conductivity	Mean fiber diameter
FK 10%	-	10 mL	3265 μS/cm	Spraying
PVA	10 mL	-	14160 μS/cm	565 ± 154 nm
FK10	9 mL	1 mL	13190 μS/cm	469 ± 144 nm
FK20	8 mL	2 mL	9615 μS/cm	274 ± 42 nm
FK30	7 mL	3 mL	8855 μS/cm	353 ± 102 nm (beads 1.4 ± 0.5 μm)

7.2.4. Rheological properties of FK/PVA solutions

Steady shear measurements of solutions (0.1-100 s^{-1}) were performed on a Physica MCR 301 (Anton Paar, Graz, Austria) equipped with a 50 mm diameter plate/plate measuring tool, using a sample gap of 1 mm. Small amplitude oscillatory shear measurements were performed at 5% which was in the linear viscoelastic region of solutions. Angular frequency was varied from 0.628 to 628 s^{-1}. All rheological measurements were performed after equilibrating solutions at 25°C. Measurements were performed in duplicate.

7.2.5. Electrospinning

A horizontal electrospinning apparatus setup was used (Figure 7.1). Solution was loaded into a 10 mL syringe with an attached 20 G flat-tip needle that served as spinneret. A syringe pump (Geneq, Inc., Canada) was used to deliver a constant solution flow of 5 μL/min. The spinneret was connected to a high voltage source (Gamma High Voltage Research, Inc., FL, U.S.) providing a positive voltage of 20 kV. A stationary flat collector plate covered in aluminum foil was positioned 15 cm from the spinneret. Electrospinning was run for 3 hours. Electrospun fibers were oven dried at 60°C overnight to remove any residual moisture. In order to render fibers insoluble, non-woven mats were crosslinked by heating at 140°C for two hours in a convection oven. Mats were carefully peeled off from the aliminium foil, cut into circles of 16 mm diameter with help of a metal cap, and stored at 4°C for further utilization.

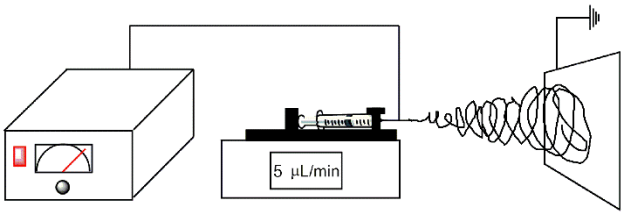

Figure 7.1. Schematic of the electrospinning setup.

7.2.6. Scanning electron microscopy (SEM)

Crosslinked electrospun fiber mats were soaked for 1 h in double distilled-H_2O, dehydrated with 70 and 100% ethanol solutions and mounted in SEM stubs with help of double coated carbon adhesive tabs. Mats were analyzed using a Zeiss Evo LS15 EP-SEM (Zeiss, Germany) equipped with a Bruker energy dispersive X-ray spectroscopy (EDXS) system. Samples were coated with carbon and analyzed under an accelerating voltage of 20 kV. The diameter of fibers, and average

pore size was determined on at least 50 fibers and pores, respectively, using ImageJ 1.51h image analysis software.

7.2.7. Characterization of keratin/PVA nanofibers

Infrared spectra of nanofiber mats, PVA, citric acid and feather keratin were obtained using a FT-IR Nicolet iS50 spectrometer (Thermo Scientific Inc., WI, U.S.) using a single bounce diamond ATR accessory. Samples were analyzed at 128 scans with a resolution of 4 cm^{-1} from 400-4000 cm^{-1}, spectra were corrected for ATR using Omnic 8.1 software. Thermal properties were studied by differential scanning calorimetry (DSC) in a DSC Q2000 instrument (TA Instruments, DE, U.S.). DSC analysis was carried out using dry samples of ~2-3 mg heated from 25 to 300°C at a heating rate of 10°C/min. A first run from 25 to 210°C was performed in order to remove the thermal history of samples containing PVA.

X-ray photoelectron spectroscopy (XPS) of samples was carried out on a Kratos Axis 165 X-ray spectrometer (Kratos Analytical Ltd., UK) equipped with a monochromatic Al Kα radiation (1486.6 eV). The binding energy (BE) was calibrated taking C1s main peak at 284.5 eV as a reference. XPS spectra were analyzed with CasaXPS software package V2.3.16 PR 1.6 (Casa Software Ltd.). Curve fitting of high resolution C1s was performed assuming a Shirley background and considering a Gaussian/Lorentzian (70%/30%) distribution shape.

7.2.8. Cell culture

Adult human dermal fibroblasts (HDFa) cell (Cell Applications, Inc. CA, U.S.) were used for *in vitro* culture on electrospun keratin/PVA mats. Cells of passage 3 were harvested by trypsinization and re-suspended in DMEM containing 10% FBS and antibiotic-antimycotic mix (ThermoFischer, MA, U.S.). Electrospun mats were secured with CellCrown™ inserts (Sigma-Aldrich, MO, U.S.), placed in 24-well culture plates and sterilized by soaking in ethanol

solutions. First, gradually from 10 to 70%, at increasing rate of 20%, for 30 min each, and then washed with ethanol solutions (gradually from 70 to 10%, in reverse order as above) and sterile PBS pH 7.4 three times. Sterile scaffolds were soaked in 1 mL of media and incubated overnight in humidified environment at 37°C and 5% CO_2. Four media-soaked scaffolds were seeded with 10 μL of HDFa suspension (2 x 10^6 cells/mL); the other two scaffolds were not seeded and used control samples. Cells were allowed to adhere to scaffolds by incubation for 4 hours. Then, scaffolds were washed gently with sterile PBS to remove non-attached cells and transferred with forceps to sterile 24-well culture plates containing 1 mL media per well. Media was replaced every other day. Cell growth was quantified after 1, 7, and 14 days of incubation. The scaffolds were transferred to new 24-well culture plates with media containing 10% Alamar blue® probe. After further incubation for 4 h the fluorescence of reduced Alamar blue was measured at 560/590 ex/em and cell growth was quantified according to the manufacturer specifications. Results are reported as mean of two independent experiments. Differences were determined from analysis of variance and Tukey test at 95% confidence using Minitab 17 software.

7.2.9. Cell imaging

After 14 days of cell culture cells on electrospun mats were treated with 4% formaldehyde solution for 20 minutes at room temperature. A set of samples was stained for nuclei imaging with 4',6-diamidino-2-phenylindole, dihydrochloride (DAPI) following manufacturer's protocol (ThermoFischer, MA, U.S.). Images were taken in a florescence microscope (Zeiss Axio, Zeiss, Germany). A second set of fixed samples was dehydrated gradually with ethanol solutions (10, 30, 50, 70 and 100%) and mounted in SEM stubs with double coated carbon adhesive tabs. SEM analysis was performed as described in section 7.2.6.

7.3. Results and discussion

7.3.1. Feather keratin (FK)

Chicken feathers were treated with 1 M NaOH to obtain soluble keratin. The final recovery of keratin was 54.5% based on the dry weight feathers. The nitrogen content of FK was 14.9%. Cell cytotoxicity assay showed that FK at different concentrations did not affect the normal growth of fibroblasts (Figure 7.2).

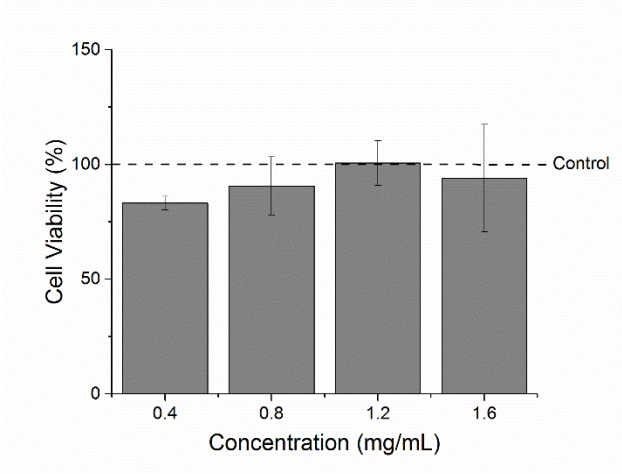

Figure 7.2. Cell cytotoxicity of alkaline treated feather keratin (FK).

7.3.2. Electrospinning of FK/PVA

Electrospinning of FK resulted in spraying of the solution. This is mostly due to the poor viscoelasticity of low molecular polymer solutions, unable to hold the electrostatic repulsion caused by the high voltage (Ramakrishna et al., 2005). Polyvinyl alcohol (PVA) was used as polymer aid for the electrospinning. Citric acid was added to PVA solution as a post-electrospinning crosslinker. The PVA/citric acid solution had high conductivity (14160 μS/cm), which is mainly due to the addition of citric acid (Table 7.1). The conductivity of FK/PVA

solutions decreased at increasing FK/PVA ratio from 10 to 30. This is due to lower conductivity of the FK solution (3265 μS/cm).

The steady state shear viscosity of PVA and FK/PVA solutions is shown in Figure 7.3A. The viscosity of PVA solution without citric acid showed little dependence on the shear rate. This is typical of PVA solutions with low degree of hydrolysis (72-90%), where hydrogen bond interactions are partially prevented by the presence of hydrophobic acetate groups (Briscoe et al., 2000; Liu et al., 2012). Addition of citric acid resulted in slight increased viscosity of PVA solution. This has also been determined by Shi and Yang, (2015); however, the effect of citric acid on viscosity of PVA solutions has not been explained. The viscosity of FK/PVA solutions decreased as the concentration of FK increased. This is mainly due the dilution of the PVA solution with low molecular weight FK (Gao et al., 2010). FK10 (FK/PVA mass ratio 10/90) showed little dependence on shear rate, whereas, FK20 and FK30 showed shear thinning behavior at low shear stress (Figure 7.3A).

Linear viscoelastic properties with frequency sweeps of PVA and FK/PVA solutions are shown in Figures 7.3B and 7.3C. All solutions had G'' > G' (loss modulus > storage modulus) at all frequencies and showed increasing values of G' and G'' at increasing frequencies. At low frequency (long time scale) polymer chains have sufficient time to disentangle, whereas at high frequency (short time scale) polymer entanglements (physical crosslinking points) cannot dissociate (Riedo et al., 2015). G' and G'' decreased at decreased PVA concentrations (addition of FK), which is explained by a decreased amount of entanglements as well as inter- and intra-hydrogen bond interactions of PVA (Gao et al., 2010). Possibly, small keratin peptides interfere with intermolecular PVA interactions.

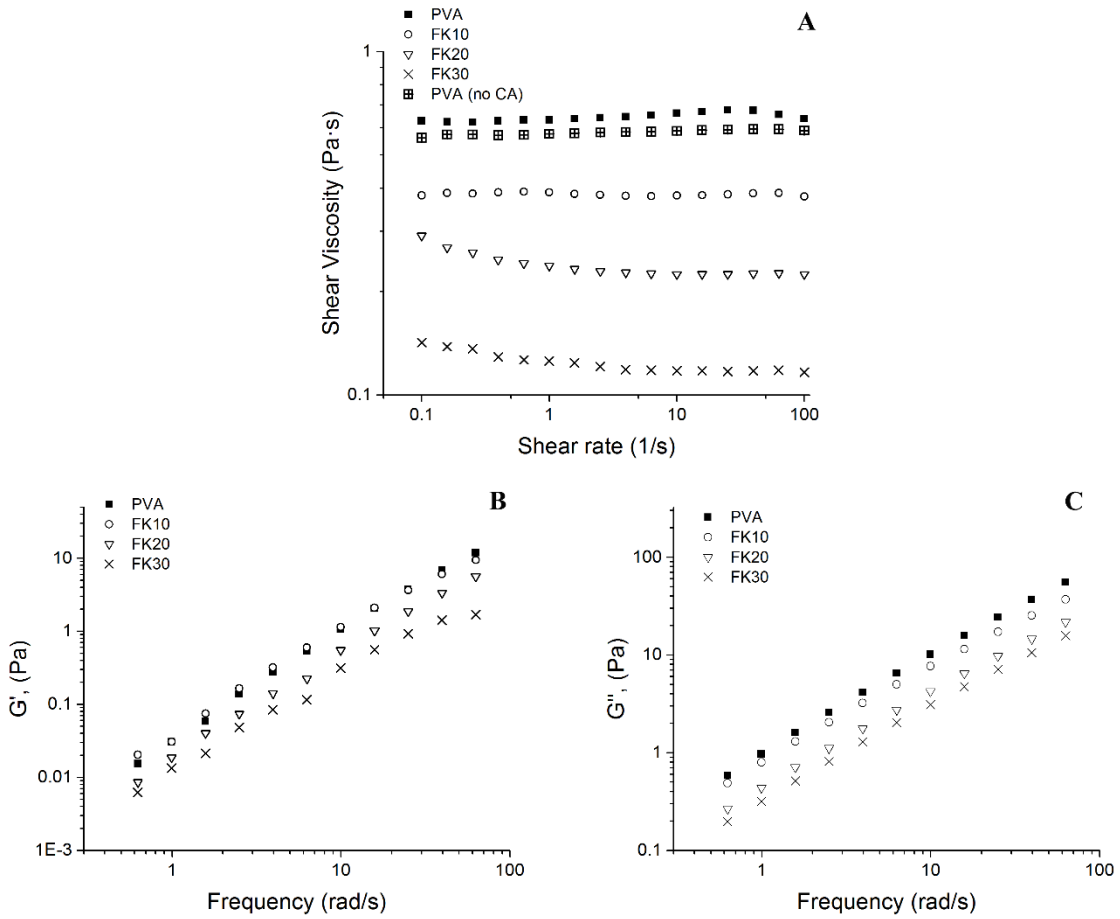

Figure 7.3. Logarithmic plot of shear viscosity versus shear rate (A) and frequency sweeps of FK/PVA solutions showing storage (B) and loss modulus (C).

Electrospinning of 10% PVA solution (0% FK) resulted in nanofibers with an average diameter of 565 nm. Increasing the concentrations of FK to 10 and 20% resulted in the reduction of the fiber diameter to 469 and 274 nm respectively. FK at 30% resulted in beads on fiber structures with an average fiber diameter of 353 nm and containing beads of 1.4 μm (Table 7.1 and Figure 7.4A). The reduction of fiber diameter could be attributed to the reduction in the viscosity of the FK10 and FK20 solutions (Figure 7.3A). Reduced viscoelastic forces result in less resistance to axial stretching during whipping of the electrospinning jet, leading to smaller

diameter fibers (Nezarati et al., 2013). However, if the viscoelastic forces are further reduced and surpassed by the capillary action of surface tension, the jet tends to break into droplets (Thompson et al., 2007; Aslanzadeh et al., 2016). This result in formation of beads and junctions of fibers as seen in FK30 (Figure 7.4A).

Higher conductivity facilitates the formation of thinner fibers (Ramakrishna et al., 2005). However, electrospun FK/PVA fibers showed an opposite trend, being smaller diameter at lower conductivities (Table 7.1). This could be explained by a stronger effect of viscoelastic properties on fiber diameter as discussed above.

After collecting fibers for 3 hours on a grounded plate, the resultant mats had a thickness of 400-500 μm. Cross section SEM images revealed that fibers were packed and randomly oriented in the thickness directions (Figure 7.4B).

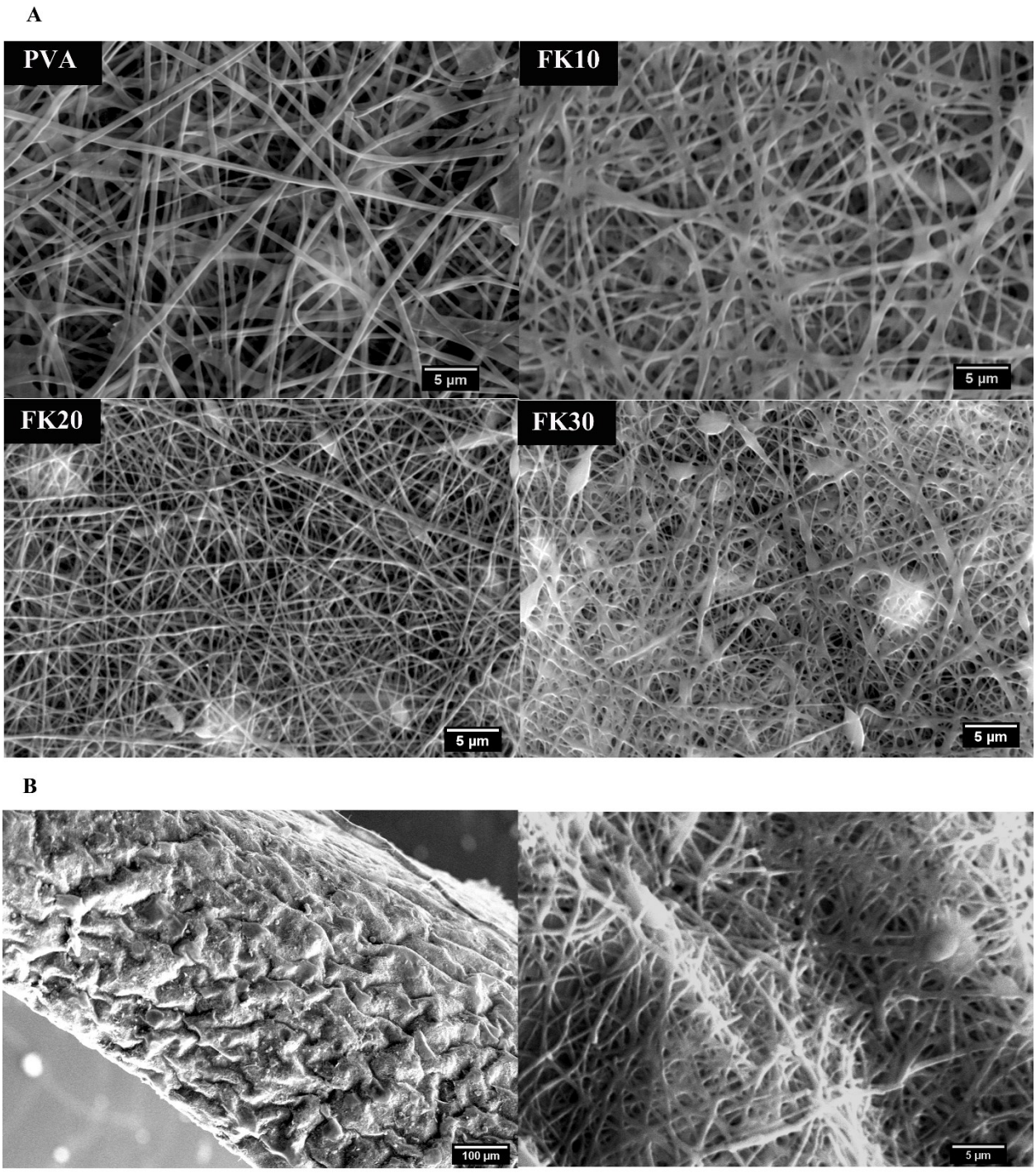

Figure 7.4. SEM images of FK/PVA electrospun fibers (A, magnification is 6 kX), and cross section of FK10 electrospun fibers (B, at 300X [left] and 6 kX [right] magnification).

7.3.3. Characterization of FK/PVA nanofiber mats

Crosslinking of PVA nanofibers increase the stability of mats in aqueous systems; however, it is generally achieved through exposure to glutaraldehyde and glyoxal solutions and vapors. Nevertheless, besides toxicity, these crosslinking agents cause fibers fuse each other, collapsing the porous structure (Taepaiboon et al., 2007; Wang and Hsieh, 2010). Citric acid has been considered a safer and environmentally friendly crosslinker for PVA. Citric acid has three carboxyl groups that can react with hydroxyl groups of PVA, forming ester bonds (Shi and Yang, 2015; Zhao et al., 2015). Thermal crosslinking of PVA/citric acid yielded water insoluble nanofiber mats. The structure and morphology of electrospun fiber mats was not altered due to crosslinking (Figure 7.4A and 7.4B). Chemical and ultrastructural changes of PVA and FK/PVA fibers after crosslinking were studied by FTIR, DSC, and XPS. FTIR of neat PVA, citric acid and crosslinked PVA mat is shown in Figure 7.5A. The broad band observed between 3000-3500 cm^{-1} is in response of stretching vibration of O-H bonds participating in H-bonding. The sharp absorption band at 3494 cm^{-1} in neat PVA corresponds to the stretching vibration of free OH groups (not forming hydrogen bond) (Ali et al., 2009). Free OH absorption band was absent in the PVA mats. Possibly after electrospinning free OH groups previously hindered in the crystalline structure of PVA, were more exposed and able to participate in hydrogen bonds. Absorption bands related to ester groups (COO-R) were located at 1736 and 1710 cm^{-1} in neat PVA. These bands arise from acetate groups remaining from polyvinyl acetate in the manufacture of 87-89% hydrolyzed PVA. The asymmetric and symmetric stretching vibrations of carboxyl groups (COOH) of citric acid were observed at 1742 and 1697 cm^{-1}, respectively (Figure 7.5A). After electrospinning and thermal crosslinking of PVA and citric acid, the stretching vibration of new ester bonds was located at 1735 and 1716 cm^{-1}. However, these also

can arise from ester bonds of the neat PVA acetate groups (1736 and 1710 cm^{-1}). A new intense band centered at 1585 cm^{-1} was observed in PVA mats. This corresponds to the presence of carboxylate (COO^-) groups from citric acid and the release acetate groups (CH_3COO^-) of PVA after the thermal treatment (Awada et al., 2014). Stretching vibration of C-O arising from alcohol and ester functional groups were attributed to multiple bands between 1300-1000 cm^{-1} (1241, 1140, 1082, 1047, 1021 cm^{-1}). The crystalline structure of PVA was maintained after electrospinning and crosslinking (Figure 7.5B). The glass transition temperature of amorphous PVA was determined at 71°C, whereas the melting temperature peak of crystalline regions of PVA was 186°C (Figure 7.5B). Thermal crosslinking of PVA and citric acid resulted in a slight shift of glass transition and melting temperatures to 75 and 189°C, respectively. This can be attributed to a reduced mobility of crosslinked PVA chains.

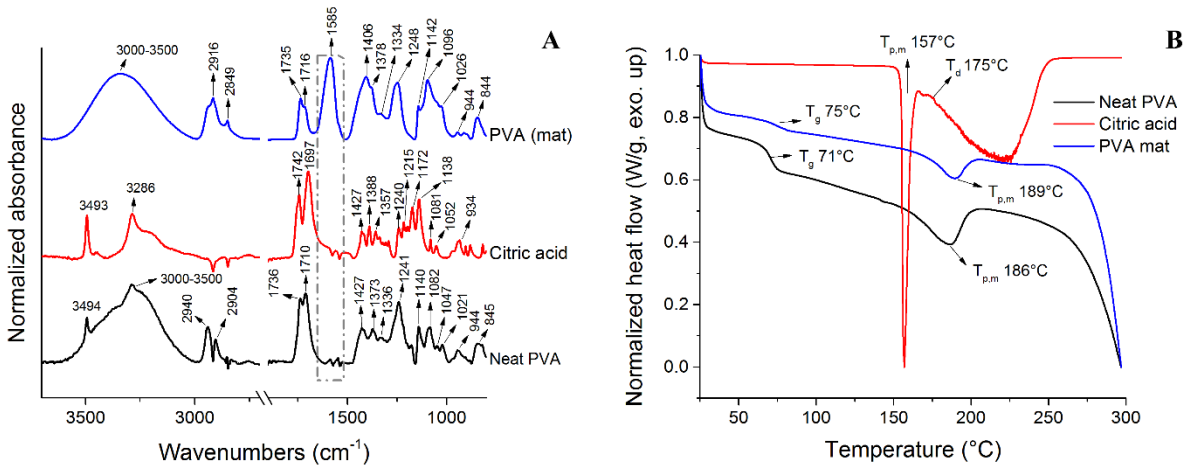

Figure 7.5. FTIR spectra (A) and DSC thermograms (B, Tg: glass transition, Tp,m: melting peak temperature; Td: decomposition temperature) of neat PVA, citric acid, and crosslinked PVA electrospun fiber mats.

Changes in the infra-red (IR) spectra of electrospun mats after the incorporation of feather keratin (FK) are shown in Figures 7.6A and 7.6B. The carbonyl band at 1735 cm^{-1} shifted slightly to 1732 cm^{-1} in FK30. A more prominent peak at 1714 cm^{-1} was observed in FK20 and FK30 samples. Carboxyl groups of proteins can react with hydroxyls of PVA. In addition amine groups can react with carboxyl groups of citric acid (Xu et al., 2015). Characteristic amide I and amide II protein absorption bands were observed for FK powder (Figure 7.6A and 7.6B). Amide I band results in response to stretching vibrations of C=O (νC=O) and C-N (νC-N) bonds. Increasing the concentration of FK in PVA mats resulted in a gradual increase of intensity at around 1650 cm^{-1}. Amide II band arises from in plane bending vibration of N-H (δN-H) and stretching vibration (ν) of C-N and C-C bonds. The appearance of a sharp shoulder in the amide II region at around 1540 cm^{-1} is also ascribed to the presence of FK in PVA mats. The incorporation of keratin in PVA fibers was also confirmed by XPS (Figure 7.7). A peak attributed to amide groups was detected from the C1s spectra of FK/PVA mats. The intensity of the peak increased with the concentration of keratin in the mats. DSC thermograms showed a small shift to lower temperatures in the melting temperature of PVA with the addition of FK (Figure 7.8). This can be explained by a plasticizing effect of small keratin peptides.

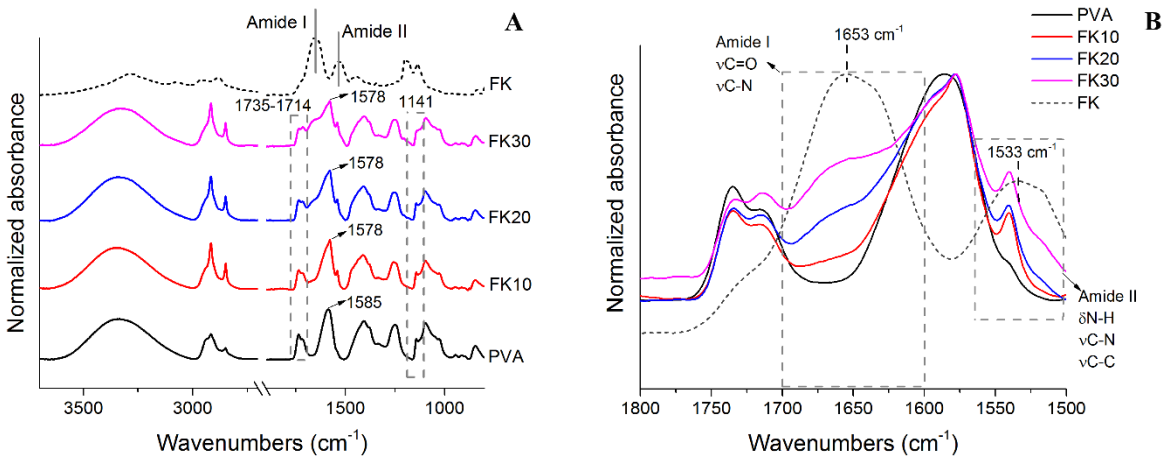

Figure 7.6. FTIR spectra (A), and amide I and amide II regions (B) of FK/PVA nanofiber mats.

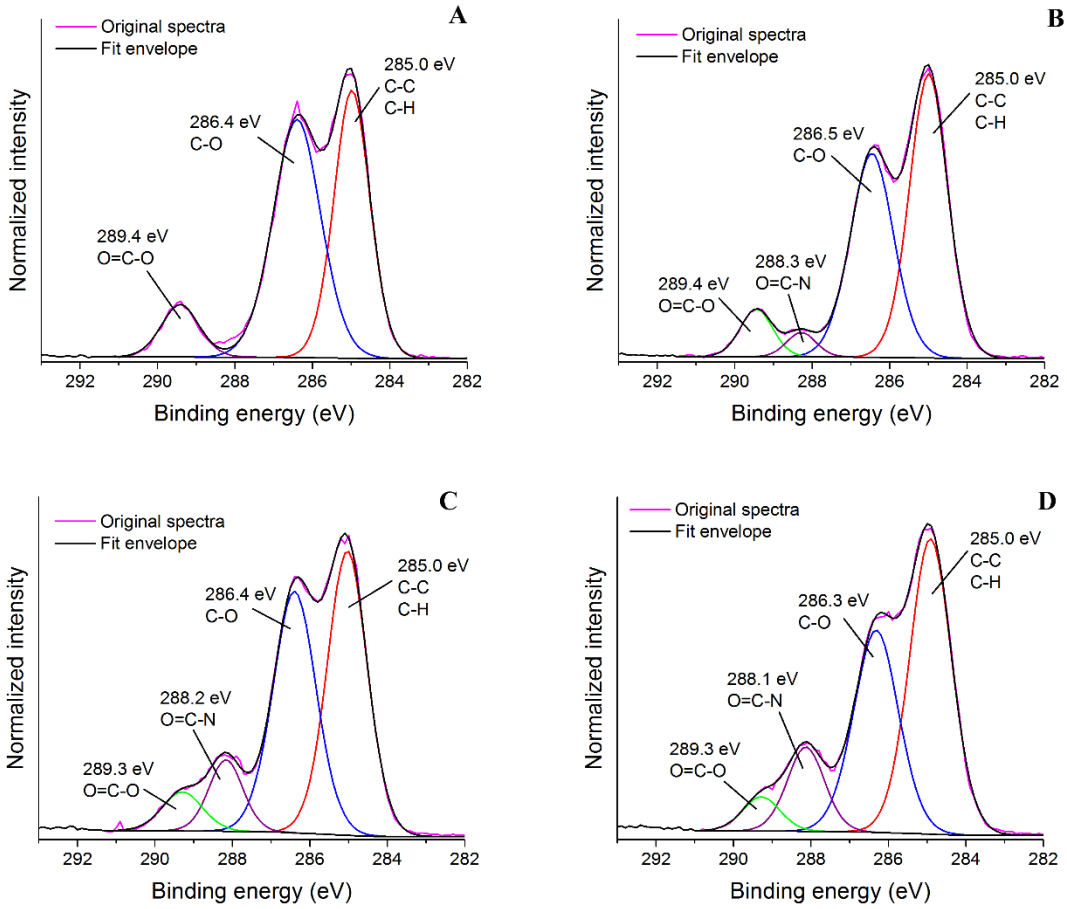

Figure 7.7. Curve fitting of C1s XPS spectra of PVA (A), FK10 (B), FK20 (C), and FK30 (D) nanofiber mats.

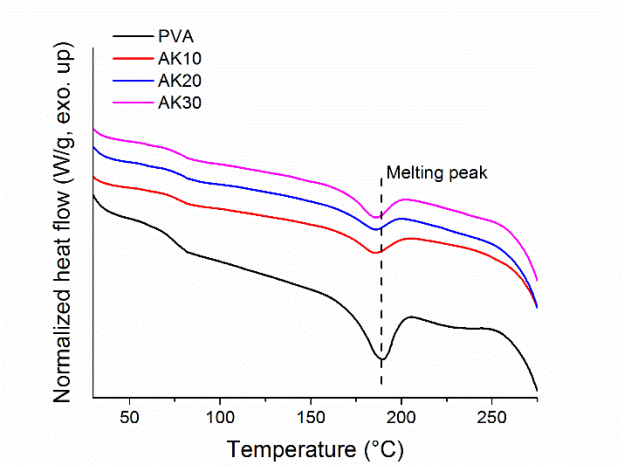

Figure 7.8. DSC thermograms of FK/PVA nanofiber mats.

7.3.4. Cell proliferation on FK/PVA nanofiber mats

The proliferation of human dermal fibroblasts (HDFa) on electrospun FK/PVA fibers was evaluated. Scaffolds were attached to plastic rings in order to prevent wrapping and floatation in the media. It is well known that the effective transfer of mechanical load to the substrate have important effects on proliferation and morphology of fibroblasts. For instance, fibroblasts cultured on collagen substrates unable to develop tension enter into a quiescent state and a significant proportion of cells undergo apoptosis (Grinnell, 2003; Hadjipanayi et al., 2009). Figure 7.9 shows the proliferation of HDFa on electrospun mats, quantified by the relative fluorescence of Alamar blue after 0, 7, and 14 days of incubation. Cells showed similar initial adhesion (time 0) on mats containing feather keratin (FK10 and FK20) and PVA alone. Cell proliferation increased after 14 days of incubation, being the highest in FK20 mats. This can be explained by the incorporation of keratin in PVA nanofibers. Proteins increase the adhesion and proliferation of cells by presenting integrin binding motifs and also by modifying the surface properties of scaffolds (Arima and Iwata, 2007; Thevenot et al., 2008). Although FK30 had higher content of keratin, the average fiber diameter was higher and contained beads, which

reduced the surface area to volume ratio for cell proliferation. Fibroblasts grew scattered and forming discrete groups in electrospun mats (Figure .10, left). After 14 days of incubation cells were fixed with glutaraldehyde and analyzed by SEM (Figure 7.10, right). Cells adhered to the surface of mats; however the small pore size and packed structure affected cell infiltration. This is a well-known limitation of electrospun scaffolds. Different techniques such as air deposition, special collectors, and manipulation of the charge of the polymer solution could be used to obtain less packed electrospun scaffolds (Blakeney et al., 2011; Wu and Hong, 2016; Cai et al., 2013).

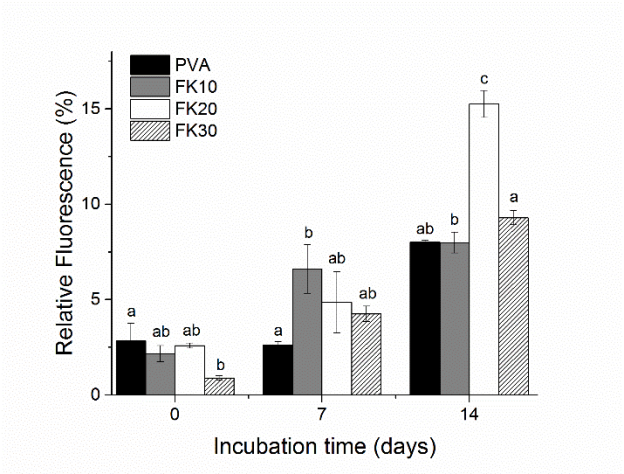

Figure 7.9. HDFa proliferation on FK/PVA electrospun mats quantified by Alamar blue relative fluorescence.

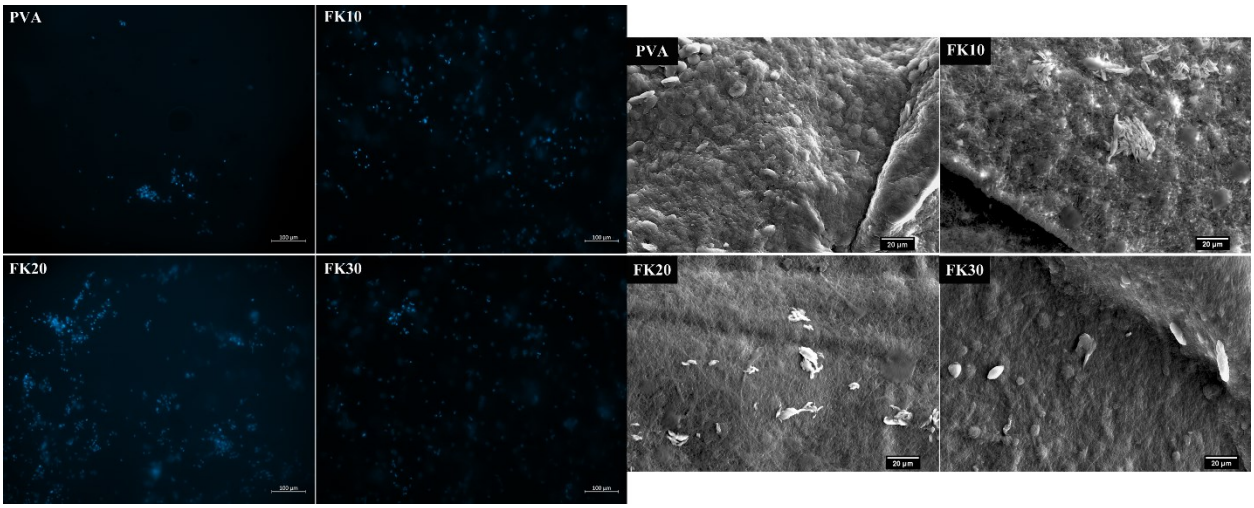

Figure 7.10. Fluorescence micrographs of cell nuclei (left) and SEM images (right) of HDFa after 14 days of incubation on FK/PVA electrospun mats.

7.4. Conclusions

Keratin from chicken feathers was solubilized in alkaline conditions. Hydrolysis of keratin into soluble peptides did not result in cytotoxic effect on fibroblasts. Aqueous solutions of keratin/PVA/citric acid containing up to 30% keratin were successfully electrospun into nanofiber mats. FTIR and XPS results confirmed that feather keratin was successfully incorporated in PVA nanofibers obtained by electrospinning. Thermal crosslinking between hydroxyl groups of PVA and carbonyl groups of citric acid improved the stability of nanofibers in aqueous solution. The fiber diameter and morphology of electrospun mats was affected by the viscoelastic properties of FK/PVA solutions. Reduction of viscosity of FK10 and FK20 solutions resulted in smaller diameter nanofibers. Incorporation of 30% FK (FK30) resulted in beads on fibers type of morphology, which was attributed to poor viscoelasticity of the solution.. Electrospun mats supported the growth of fibroblasts. After 14 days cell proliferation was higher in mats containing 20% feather keratin, which can be attributed to the enhanced biocompatibility

of proteins. Cells grew predominantly on the surface of electrospun mats, with limited infiltration. Further directions to enhance cell infiltration are required towards the preparation of less packed nanofibers scaffolds.

7.5. References

Abrigo, M., McArthur, S.L., & Kingshott, P. (2014). Electrospun nanofibers as dressings for chronic wound care: Advances, challenges and future prospects. *Macromolecular Bioscience*, 14, 772-792.

Ali, Z.I., Ali, F.A., & Hosam, A.M. (2009). Effect of electron beam irradiation on the structural properties of PVA/V2O2 xerogel. Spectrochimica Acta Part A: *Molecular and Biomolecular Spectroscopy*, 72, 868-875.

Aluigi, A., Corbellini, A., Rombaldoni, F., & Mazzuchetti, G. (2013). Wool-derived keratin nanofiber membranes for dynamic adsorption of heavy-metal ions from aqueous solutions. *Textile Research Journal*, 83, 1574-1586.

Aluigi, A., Varesano, A., Montarsolo, A., Vineis, C., Ferrero, F., Mazzuchetti, G., & Tonin, C. (2007). Electrospinning of keratin/poly(ethylene oxide) blend nanofibers. *Journal of Applied Polymer Science*, 104, 863-870.

Aluigi, A., Vineis, C., Varesano, A., Mazzuchetti, G., Ferrero, F., & Tonin, C. (2008). Structure and properties of keratin/PEO blend nanofibers. *European Polymer Journal*, 44, 2465-2475.

Arima, Y., & Iwata, H. (2007). Effect of wettability and surface functional groups on protein adsorption and cell adhesion using well-defined mixed self-assembled monolayers. *Biomaterials*, 28, 3074-3082.

Aslanzadeh, A., Zhu, Z., Luo, Q., Ahvazi, B., Boluk, Y., & Ayranci, C. (2016). Electrospinning of colloidal lignin in poly(ethylene oxide) N,N-dimethylformamide solutions. *Macromolecular Materials and Engineering*, 301, 401-413.

Awada, H., Montplaisir, D., & Daneault, C. (2014). Cross-linking of papers based on thermomechanical pulp fibers by polycarboxylic acids: Influence on the wet breaking length. *Industrial & Engineering Chemistry Research*, 53, 4312-4317.

Ayutthaya, S.I.N., Tanpichai, S., & Wootthikanokkhan, J. (2015). Keratin extracted from chicken feather waste: Extraction, preparation and structural characterization of the keratin and keratin/biopolymer films and electrospuns. *Journal of Polymers and the Environment*, 23, 506-516.

Barnes, C.P., Sell, S.A., Boland, E.D., Simpson, D.G., & Bowlin, G.L. (2007). Nanofiber technology: Designing the next generation of tissue engineering scaffolds. *Advanced Drug Delivery Reviews*, 59, 1413-1433.

Blakeney, B.A., Tambralli, A., Anderson, J.M., Andukuri, A., Lim, D-J., Dean, D.R., & Jun, H-W. (2011). Cell infiltration and growth in a low density, uncompressed three-dimensional electrospun nanofibrous scaffold. *Biomaterials*, 32, 1583-1590.

Boakye, M.A.D., Rijal, N.P., Adhikari, U., & Bhattarai, N. (2015). Fabrication and characterization of electrospun PCL-MgO-keratin-based composite nanofibers for biomedical applications. *Materials*, 8, 4080-4095.

Briscoe, B., Luckham, P., & Zhu, S. (2000). The effects of hydrogen bonding upon the viscosity of aqueous poly(vinyl alcohol) solutions. *Polymer*, 41, 3851-3860.

Cai, S., Xu, H., Jiang, Q., Yang, Y. (2013). Novel 3D electrospun scaffolds with fibers oriented randomly and evenly in three dimensions to closely mimic the unique architectures of

extracellular matrices in soft tissues: Fabrication and mechanism study. *Langmuir*, 29, 2311-2318.

Fan, J., Lei, T-D., Li, J., Zhai, P-Y., Wang, Y-H., Cao, F-Y., & Liu, Y. (2016). High protein content keratin/poly(ethylene oxide) nanofibers crosslinked in oxygen atmosphere and its cell culture. *Materials & Design*, 104, 60-67.

Gao, H-W., Yang, R-J., He, J-Y., & Yang, L. (2010). Rheological behaviors of PVA/H2O solutions of high-polymer concentration. Journal od Applied Polymer Science, 116, 1459-1466.

Grinnell, F. (2003). Fibroblast biology in three-dimensional collagen matrices. *Trends in Cell Biology*, 13, 264-269.

Hadjipanayi, E., Mudera, V., & Brown, R.A. (2009). Close dependence of fibroblasts proliferation on collagen scaffold matrix stiffness. *Journal of Tissue Engineering and Regenerative Medicine*, 3, 77-84.

Hill, P., Brantley, H., & Van Dyke, M. (2010). Some properties of keratin biomaterials: Kerateines. *Biomaterials*, 31, 585-593.

Li, J., Li, Y., Mak, A.F.T., Ko, F., & Qin, L. (2009). Preparation and biodegradation of electrospun PLLA/keratin nonwoven fibrous membrane. *Polymer Degradation and Stability*, 94, 1800-1807.

Li, S., & Yang, X-H. (2014). Fabrication and characterization of electrospun wool keratin/poly(vinyl alcohol) blend nanofibers. *Advances in Materials Science and Engineering*, Article ID 163678.

Liu, F., Nishikawa, T., Shimizu, W., Sato, T., Usami, H., Amiya, S., Ni, Q-Q., & Murakami, Y. (2012). Preparation of fully hydrolyzed polyvinyl alcohol electrospun nanofibers with diameters of sub-200 nm by viscosity control. *Textile Research Journal*, 82, 1635-1644.

McPherson, R.A., & Hardy, G. (2011). Clinical and nutritional benefits of cysteine-enriched protein supplements. *Current Opinion in Clinical Nutrition and Metabolic Care*, 14, 562-568.

Nezarati, RM., Eifert, M.B., & Cosgriff-Hernandez, E. (2013). Effects of humidity and solution viscosity on electrospun fiber morphology. *Tissue Engineering: Part C*, 19, 810-819.

Park, M., Shin, H.K., Panthi, G., Rabbani, M.M., Alam, A-M., Choi, J., Chung, H-J., Hong, S-T., & Kim, H-Y. (2015). Novel preparation and characterization of human hair-based nanofibers using electrospinning process. *International Journal of Biological Macromolecules*, 76, 45-48.

Ramakrishna, S., Fujihara, K., Teo, W-E., Lim, T-C., & Ma, Z. (2005). An introduction to electrospinning of nanofibers. World Scientific Publishing Co. Pte. Ltd., Singapore.

Reichl, S. (2009). Films based on human hair keratin as substrates for cell culture and tissue engineering. *Biomaterials*, 30, 6854-6866.

Riedo, C., Caldera, F., Poli, T., & Chiantore, O. (2015). Poly(vinylalcohol)-borate hydrogels with improved features for the cleaning of cultural heritage surfaces. *Heritage Science*, 3, 23-34.

Schmedlen, R.H., Masters, K.S., & West, J.L. (2002). Photocrosslinkable polyvinyl alcohol hydrogels that can be modified with cell adhesion peptides for use in tissue engineering. *Biomaterials*, 23, 4325-4332.

Schrooyen, P.M.M., Dijkstra, P.J., Oberthur, R.C., Bantjes, A., & Feijen, J. (2001). Stabilization of solutions of feather keratins by sodium dodecyl sulfate. *Journal of Colloid and Interface Science*, 240, 30-39.

Shi, J., & Yang, E. (2015). Green electrospinning and crosslinking of polyvinyl alcohol/citric acid. *Journal of Nano Research*, 32, 32-42.

Taepaiboon, P., Rungsardthong, U., & Supaphol, P. (2007). Effect of cross-linking on properties and release characteristics of sodium salicylate-loaded electrospun poly(vinyl alcohol) fibre mats. *Nanotechnology*, 18, doi:10.1088/0957-4484/18/17/175102

Thevenot, P., Hu, W., & Tang, L. (2008). Surface chemistry influence implant biocompatibility. *Current Topics in Medicinal Chemistry*, 8, 270-280.

Thilagar, S., Jothi, N.A., Omar, A.R.S., Kamaruddin, M.Y., & Ganabadi, S. (2009). Effect of keratin-gelatin and bFGF-gelatin composite film as a sandwich layer for full-thickness skin mesh graft in experimental dogs. *Journal of Biomedical Materials Research Part B: Applied Biomaterials*, 88, 12-16.

Thompson, C.J., Chase, G.G., Yarin, A.L., & Reneker, D.H. (2007). Effects of parameters on nanofiber diameter determined from electrospinning model. *Polymer*, 48, 6913-6922.

Wang, J., Hao, S., Chenz, Z., Li, W., Gao, F., Guo, T., Gong, Y., & Wang, B. (2017). Feather keratin hydrogel for wound repair: Preparation, healing effect and biocompatibility evaluation. *Colloids and Surfaces B: Biointerfaces*, 149, 341-350.

Wang, Y., & Hsieh, Y-L. (2010). Crosslinking of polyvinyl alcohol (PVA) fibrous membranes with glutaraldehyde and PEG diacylchloride. *Journal of Applied Polymer Science*, 116, 3249-3255.

Wu, J., & Hong, Y. (2016). Enhancing cell infiltration of electrospun fibrous scaffolds in tissue regeneration. *Bioactive Materials*, 1, 56-64.

Xu, H., Cai, S., Xu, L., & Yang, Y. (2014). Water-stable three-dimensional ultrafine fibrous scaffolds from keratin for cartilage tissue engineering. *Langmuir*, 30, 8461-8470.

Xu, H., Shen, L., Xu, L., Yang, Y. (2015). Low-temperature crosslinking of proteins using non-toxic citric acid in neutral aqueous medium: Mechanism and kinetic study. *Industrial Crops and Products*, 74, 234-240.

Xu, S., Sang, L., Zhang, Y., Wang, X., & Li, X. (2013). Biological evaluation of human hair keratin scaffolds for skin wound repair and regeneration. *Materials Science and Engineering C*, 33, 648-655.

Yen, K-C., Chen, C-Y., Huang, J-Y., Kuo, W-T., & Lin, F-H. (2016). Fabrication of keratin/fibroin membranes by electrospinning for vascular tissue engineering. *Journal of Materials Chemistry B*, 4, 237-244.

Yoon, D.M., & Fisher, J.P. 2009. Natural and synthetic polymeric scaffolds. In Narayan, R. (Ed.). Biomedical Materials. Springer, New York.

Yuan, J., Xing, Z-C., Park, S-W., Geng, J., & Kang, I-K. (2009). Fabrication of PHBV/keratin composite nanofibrous mats for biomedical applications. *Macromolecular Research*, 17, 850-855.

Zhang, C., Yuan, X., Wu, L., Han, Y., & Sheng, J. (2005). Study on morphology of electrospun poly(vinyl alcohol) mats. *European Polymer Journal*, 41, 423-432.

Zhao, R., Wang, Y., Li, X., Sun, B., Jiang, Z., & Wang, C. (2015). Water-insoluble sericin/b-cyclodextrin/PVA composite electrospun nanofibers as effective adsorbents towards methylene blue. *Colloids and Surfaces B: Biointerfaces*, 136, 375-382.

Zhu, J., & Marchant, R.E. (2011). Design properties of hydrogel tissue-engineering scaffolds. *Expert Review of Medical Devices*, 8, 607-626.

CHAPTER 8. Conclusions and Recommendations

8.1. Conclusions

Chicken feathers are considered a low-value by-product or waste from the poultry industry. It is estimated that 8-9 million tons are generated annually worldwide. Keratin is a fibrous protein that makes up to 90% of the composition of chicken feathers. Keratin is characterized by unusual amounts of cysteine residues (7-10%) forming disulfide bonds, which confers strength and impermeability to chicken feathers. It was hypothesized that feather keratin can be transformed into different materials including plastics, hydrogels and nanofibers. The study of keratin chemistry and technology resulted in the novel materials with adequate mechanical stability.

Keratin-based plastics are a renewable alternative to petroleum-based plastics. They can compete in term of cost and performance with bio-based plastics made from food sources such as starch- and soy protein-plastics. Several efforts have been made to turn feathers into a thermoplastic material (Barone et al., 2006; Barone and Arikan, 2007; Ullah et al., 2011); however the mechanical strength and sensitivity to moisture are still aspects that have not been improved. In the first part of this research, chicken feather, with the aid of glycerol and propylene glycol plasticizers, was processed into plastic films through extrusion at high temperature (150°C) and compression molding (120°C). Feather films were improved by the incorporation of graphite oxide (GO) during extrusion processing. Three batches of graphite oxide were synthesized containing different carbon to oxygen ratios (C/O 2.48, 2.07, and 1.55). C/O ratio 2.07 at 1% incorporation resulted in the highest tensile strength, which was explained by its higher content of hydroxyl groups than GO with 2.48 and 1.55 C/O. The effect of GO concentration was determined to affect the tensile properties of feather plastic films. The maximum tensile strength (9.61 MPa) was obtained after incorporation of 1% GO, which was

attributed to intercalation of keratin into graphene sheets as determined by XPS analyses, and molecular interactions between oxygen functionalities of GO with keratin and plasticizers. GO is an inexpensive reinforcement nanoparticle for hydrophilic polymers such as keratin. Possible applications of feather plastics as agricultural films and biodegradable containers needs to be evaluated, considering the performance of the material under different environmental conditions.

Keratin is also a valuable protein for the fabrication of biomaterials. Materials in which cells can adhere, proliferate and ultimate regenerate tissue structure and function are a great medical advance in healing of skin and other tissues and organs. Keratin has demonstrated to be biocompatible with human tissues and to accelerate wound healing (Rouse and Van Dyke, 2010; Cavaco-Paulo et al., 2013). Hydrogels from hair and wool keratin have been investigated (Ozaki et al., 2014; Aboushwareb et al., 2008; Hill et al., 2010). The modulation and understanding of hydrogel viscoelastic properties and its effect on cell growth performance have not been widely explored. In this research hydrogels from feather keratin were fabricated through self-assembly during controlled dialysis. The re-formation of disulfide bonds during dialysis was determined as the main stabilizing force in hydrogels, although hydrophobic and hydrogen bond interactions were important as well. Viscoelastic properties of hydrogels were controlled by quantitative blocking of cysteine thiols. Storage modulus G', decreased as the content of blocked cysteine thiols increased. Gelation of feather keratin was prevented by blocking 82% of keratin thiols. pH of the keratin solution previous dialysis affected the gelation process and appearance of gels. pH 3 and 9 resulted in fast gelation that led to opaque gels, which was explained by increased protein aggregation due to isoelectric precipitation and increase of disulfide exchange reactions, respectively. Homogenous gels were obtained from keratin solutions adjusted to pH 7 and pre-heated at 50°C. These conditions were used to prepare hydrogels at different keratin

concentrations (5, 7.5, 10 and 12.5% w/v). Increasing keratin concentrations resulted in hydrogels with higher storage modulus. The storage modulus of our feather keratin hydrogel at 5% wt. was in the range of $2x10^3$ to $7x10^3$ Pa. Keratin hydrogels prepared at concentrations of 10 and 12.5% had modulus in the range of 10^5-10^6 Pa, which is within the range of viscoelasticity of dermis, connective tissue and contracted muscle (Vanderhooft et al., 2008). The viscoelastic properties of feather keratin hydrogels were superior to those reported in the literature (Wang et al., 2017). This is mainly due to the use of keratin with fully reduced disulfide bonds in this research. That is without use of thiol blocking agents. Hydrogels scaffolds supported the growth of dermal fibroblasts for 21 days; although there were not important differences in cell proliferation, it was observed that cells were more able to penetrate in hydrogels prepared at 5 and 7.5%, which is mainly explained by their higher porosity.

Other sources of keratin such as hair and wool have been more often investigated than feather for the fabrication of hydrogels. However, the literature lacks of studies of hydrogels fabricated under same keratin extraction and gelation conditions, which makes comparisons difficult. Since feather keratin differ in chemical and conformational properties to mammalian keratin different hydrogel properties were expected. Keratins from feathers, human hair, and sheep wool were used to fabricate hydrogels by self-assembly dialysis at a concentration of 7.5% under conditions established in Chapter 4 and Chapter 5. The viscoelastic properties of hydrogels differed greatly. Feather keratin hydrogels had storage modulus of 7600-11000 Pa, while hair and wool keratin hydrogels had modulus below 1000 Pa. This difference was explained by differences in molecular weight and conformation of avian feather and mammalian keratins. Mammalian keratins are mostly α-helical proteins that can be stretched when swelled; therefore, their gels had superior swelling capacity but weaker viscoelastic properties. Feather keratin are

smaller β-sheet proteins that cannot be stretched, therefore, that assembled into a rigid gel structure. Dermal fibroblasts proliferate at higher rates on feather keratin hydrogels, which was explained by their superior mechanical properties, which are more representative of viscoelastic properties of normal human dermis.

The fabrication of keratin nanofiber scaffolds was also investigated. Nanofiber scaffolds can mimic the microstructure of the extracellular matrix of tissues; therefore, they can modulate cell behavior for effective tissue regeneration (Barnes et al., 2007; Abrigo et al., 2014). Keratin was hydrolyzed with 1 M NaOH and the resultant peptides (< 2000 g/mol) were electrospun using poly(vinyl alcohol) (PVA) and citric acid as polymer aid and crosslinking agent, respectively. Nanofibers containing up to 30% keratin were fabricated and crosslinked without the use of harmful solvents and crosslinking chemicals. The diameter of fibers decreased from 565 nm in PVA to 274 nm in PVA fibers containing 20% keratin. Dermal fibroblasts showed the highest proliferation on electrospun mats containing 20% keratin which was explained by the superior biological properties of keratin, but also due to a higher surface area to volume ratio than mats containing 30% keratin. Infiltration of cells was impaired by the dense packed structure of nanofibers.

8.2. Recommendations for future studies

The nanostructure and chemistry of graphene oxide layers in the CF-GO composites needs further characterization. It is possible that partial or complete delamination of graphene oxide layers occurred during processing. In addition, graphene oxide nanosheets could be transformed into graphene due to thermal processing.

Feather plastics could be studied for their application as agricultural films and biodegradable pots. However, their mechanical strength could be affected by the relative humidity of the environment. Their performance needs to be evaluated in terms of mechanical stability and biodegradability under conditions of use. In addition, strategies to reduce the moisture sensitivity should be investigated. In this regard, replacement of hydrophilic plasticizers, such as glycerol, for more hydrophobic plasticizers is suggested. Feather keratin could be modified to increase the compatibility with hydrophobic plasticizers and prevent phase separation. For instance partial grafting of vinyl monomers or PEGylation onto hydroxyl or thiol groups could increase the hydrophobicity of keratin.

Hydrogels from feather keratin showed remarkable viscoelastic properties. Evaluation of other mechanical properties would support their application in skin dermis or other tissues. For instance, compression, bending, torsion and tearing properties of keratin hydrogels need to be evaluated. One of the limitations of hydrogels was their compacted microstructure when prepared at higher concentrations (10 and 12.5%), which limited cell infiltration. It would be desired that cells are seeded and embedded during the gelation of keratin. This would ensure homogenous dispersion of cells in the scaffold. One of the challenges in trapping the cells during gelation, is their survival due to the presence of high concentration of urea, thiourea and sodium metabisulfite. A possible approach would be incorporating an aliquot of cell suspension at an

intermediate stage of keratin dialysis, when lower concentration of salts are present. In addition, gelation could be performed at 37°C instead of 4°C. Cell viability after gelation can be quantified to optimize cell seeding during gelation.

Hydrogels can be evaluated in *in vivo* experiments. Procedures in animal models include the implantation of hydrogel scaffold in induced full-thickness wounds. In order to evaluate the properties of hydrogels it would be necessary to characterize the formation of granulation tissue surrounding the implant, cytotoxicity, infiltration of cells, wound closure, formation of scar, and tissue regeneration over time.

Electrospinning of keratin at higher concentrations or even keratin alone is highly desirable. Xu et al., (2014) achieved electrospinning of feather keratin mixed with SDS. Unfortunately, SDS is a harmful detergent that is hard to remove due to the formation of keratin complexes. In addition fibers were thick with diameter of few micrometers. Feather keratin dissolved in urea, thiourea and sodium metabisulfite has low viscoelastic properties and protein-protein interactions; however increasing the concentration to above 40% keratin can result in high viscoelasticity. The concentration of salts (urea, thiourea, and sodium metabisulfite) would spike the conductivity of the solution which could result in reduction of fiber diameter. However, if the viscoelastic properties are surpassed by electrostatic repulsion the jet can break into droplets. The study of electrospinning conditions of keratin in this solution has not been investigated. Salts in electrospun fibers can be washed out later by exhaustive soaking in water. Keratin can be crosslinked during aqueous removal of salts or accelerated by exposure to hydrogen peroxide.

REFERENCES

Abdelrahman, T., & Newton, H. (2011). Wound dressings: Principles and practice. *Surgery (Oxford)*, 29, 491-495.

Aboushwareb, T., Eberli, D., Ward, C., Broda, C., Holcomb, J., Atala, A., & Van Dyle, M. (2009). A keratin biomaterial gel hemostat derived from human hair: Evaluation in a rabbit model of lethal liver injury. *Journal of Biomedical Materials Research Part B: Applied Biomaterials*, 90, 45-54.

Abrigo, M., McArthur, S.L., & Kingshott, P. (2014). Electrospun nanofibers as dressing for chronic wound care: Advances, challenges, and future prospects. *Macromolecular Bioscience*, 14, 772-792.

Agriculture and Agri-Food Canada. Retrieved online from http://www.agr.gc.ca/ on February 11th, 2015.

Ahn, H.K., Huda, M.S., Smith, M.C., Mulbry, W., Schmidt, W.F., & Ill, J.B.R. (2011). Biodegradability of injection molded bioplastics pots containing polylactic acid and poultry feather fiber. *Bioresource Technology*, 102, 4930-4933.

Ali, Z.I., Ali, F.A., & Hosam, A.M. (2009). Effect of electron beam irradiation on the structural properties of PVA/V2O2 xerogel. Spectrochimica Acta Part A: *Molecular and Biomolecular Spectroscopy*, 72, 868-875.

Alibardi, L., & Toni, M. (2008). Cytochemical and molecular characteristics of the process of cornification during feather morphogenesis. *Progress in Histochemistry and Cytochemistry*, 43, 1-69.

Aluigi, A., Corbellini, A., Rombaldoni, F., & Mazzuchetti, G. (2013). Wool-derived keratin nanofiber membranes for dynamic adsorption of heavy-metal ions from aqueous solutions. *Textile Research Journal*, 83, 1574-1586.

Aluigi, A., Sotgiu, G., Ferroni, C., Duchi, S., Lucarelli, E., Martini, C., Posati, T., Guerrini, S., Ballestri, M., Corticelli, F., & Varchi, G. (2016). Chlorin e6 keratin nanoparticles for photodynamic anticancer therapy. *RSC Advances*, 6, 33910-33918.

Aluigi, A., Tonetti, C., Vineis, C., Tonin, C., & Mazzuchetti, G. (2011). Adsorption of copper(II) ions by keratin/PA6 blend nanofibers. *European Polymer Journal*, 47, 1756-1764.

Aluigi, A., Varesano, A., Montarsolo, A., Vineis, C., Ferrero, F., Mazzuchetti, G., & Tonin, C. (2007). Electrospinning of keratin/poly(ethylene oxide) blend nanofibers. *Journal of Applied Polymer Science*, 104, 863-870.

Aluigi, A., Vineis, C., Varesano, A., Mazzuchetti, G., Ferrero, F., & Tonin, C. (2008). Structure and properties of keratin/PEO blend nanofibers. *European Polymer Journal*, 44, 2465-2475.

Annabi, N., Mithieux, S.M., Boughton, E.A., Ruys, A.J., Weiss, A.S., & Dehghani, F. (2009). Synthesis of highly porous crosslinked elastin hydrogels and their interaction with fibroblasts in vitro. *Biomaterials*, 30, 4550-4557.

Arai, K.M., Takahashi, R., Yokote, Y., & Akahane, K. (1983). Amino-acid sequence of feather keratin from fowl. *European Journal of Biochemistry*, 132, 501-507.

Arima, Y., & Iwata, H. (2007). Effect of wettability and surface functional groups on protein adsorption and cell adhesion using well-defined mixed self-assembled monolayers. *Biomaterials*, 28, 3074-3082.

Aslanzadeh, A., Zhu, Z., Luo, Q., Ahvazi, B., Boluk, Y., & Ayranci, C. (2016). Electrospinning of colloidal lignin in poly(ethylene oxide) N,N-dimethylformamide solutions. *Macromolecular Materials and Engineering*, 301, 401-413.

Asquith, R.S., & Carthew, P. (1972). An investigation of the mechanism of alkaline degradation of cystine in intact protein. *Biochimica et Biophysica Acta*, 278, 8-14.

Astbury, W.T., & Bell, F.O. (1941). Nature of the intramolecular fold in alpha-keratin and alpha-myosin. *Nature*, 147, 696-699.

Astbury, W.T., & Woods, H.J. (1934). X ray studies of the structure of hair, wool, and related fibres. II. The molecular structure and elastic properties of hair keratin. *Proceedings of the Royal Society of London. Series B*, 314-316.

Awada, H., Montplaisir, D., & Daneault, C. (2014). Cross-linking of papers based on thermomechanical pulp fibers by polycarboxylic acids: Influence on the wet breaking length. *Industrial & Engineering Chemistry Research*, 53, 4312-4317.

Ayutthaya, S.I.N., Tanpichai, S., & Wootthikanokkhan, J. (2015). Keratin extracted from chicken feather waste: Extraction, preparation and structural characterization of the keratin and keratin/biopolymer films and electrospuns. *Journal of Polymers and the Environment*, 23, 506-516.

Baker, B.M., & Chen, C.S. (2012). Deconstructing the third dimension – how 3D culture microenvironments alter cellular cues. *Journal of Cell Science*, 125, 3015-3024.

Balaji, S., Kumar, R., Sripriya, R., Kakkar, P., Ramesh, D.V., Reddy, P.N.K., & Sehgal, P.K. (2012). Preparation and comparative characterization of keratin-chitosan and keratin-gelatin composite scaffolds for tissue engineering applications. *Materials Science and Engineering C,* 32, 975-982.

Balakrishnan, B., Mohanty, M., Umashankar, P.R., & Jayakrishnan, A. (2005). Evaluation of an in situ forming hydrogel wound dressing based on oxidized alginate and gelatin. *Biomaterials*, 26, 6335-6342.

Barczyk, M., Carracedo, S., & Gullberg, D. (2010). Integrins. *Cell and Tissue Research*, 339, 269-280.

Barnes, C.P., Sell, S.A., Boland, E.D., Simpson, D.G., & Bowlin, G.L. (2007). Nanofiber technology: Designing the next generation of tissue engineering scaffolds. *Advanced Drug Delivery Reviews*, 59, 1413-1433.

Barone, J. R., & Arikan, O. (2007). Composting and biodegradation of thermally processed feather keratin polymer. *Polymer Degradation and Stability*, 92, 859-867.

Barone, J.R. & Schmidt, W. (2006). Compositions and films comprised of avian feather keratin. US Patent US7066995 B1.

Barone, J.R., Schmidt, W.F., & Gregoire, N.T. (2006). Extrusion of feather keratin. *Journal of Applied Polymer Science*, 100, 1432-1442.

Barone, J.R., Schmidt, W.F., & Liebner, C.F.E. (2005). Thermally processed keratin films. *Journal of Applied Polymer Science*, 97, 1644-1651.

Bartels, T. (2003). Variations in the morphology, distribution, and arrangement of feathers in domesticated birds. *Journal of Experimental Zoology*, 298B, 91-108.

Barth, A. (2007). Infrared spectroscopy of proteins. *Biochimica et Biophysica Acta*, 1767, 1073-1101.

Bendit, E.G. (1957). The α□β transformation in keratin. *Nature*, 179, 535.

Bennion, B. J., & Daggett, V. (2003). The molecular basis for the chemical denaturation of proteins by urea. *Proceedings of the National Academy of Sciences,* 100, 5142-5147.

Bhana, B., Iyer, R.K., Chen, W.L.K., Zhao, R., Sider, K.L., Likhitpanichkul, M., Simmons, C.A., Radisic, M. (2010). Influence of substrate stiffness on the phenotype of heart cells. *Biotechnology and Bioengineering*, 105, 1148-1160.

Bhatia, A., Gupta, R.K., Bhattacharya, S.N., & Choi, H.J. (2009). An investigation of melt rheology and thermal stability of poly(lactic acid)/poly(butylene succinate) nanocomposites. *Journal of Applied Polymer Science*, 114, 2837-2847.

Bhattarai, N., Gunn, J., & Zhang, M. (2010). Chitosan-based hydrogels for controlled, localized drug delivery. *Advanced Drug Delivery Reviews*, 62, 83-89.

Birgersdotter, A., Sandberg, R., & Ernberg, I. (2005). Gene expression perturbation in vitro—a growing case for three dimensional (3D) culture systems. *Seminars in Cancer Biology*, 15, 405-412.

Bissell, M.J., Radisky, D.C., Rizki, A., Weaver, V.M., & Petersen, O.W. (2002). The organizing principle: microenvironmental influences in the normal and malignant breast. *Differentiation; Research and Biological Diversity*, 70, 537-546.

Blakeney, B.A., Tambralli, A., Anderson, J.M., Andukuri, A., Lim, D-J., Dean, D.R., & Jun, H-W. (2011). Cell infiltration and growth in a low density, uncompressed three-dimensional electrospun nanofibrous scaffold. *Biomaterials*, 32, 1583-1590.

Boakye, M.A.D., Rijal, N.P., Adhikari, U., & Bhattarai, N. (2015). Fabrication and characterization of electrospun PCL-MgO-keratin-based composite nanofibers for biomedical applications. *Materials*, 8, 4080-4095.

Boateng, J.S., Matthews, K.H., Stevens, H.N.E., & Eccleston, G.M. (2008). Wound healing dressings and drug delivery systems: A review. *Journal of Pharmaceutical Sciences*, 97, 2892-2923.

Boehler, R.M., Graham, J.G., & Shea, L.D. (2011). Tissue engineering tools for modulation of the immune response. *Biotechniques*, 51, 239-passim.

Bonvallet, P.P., Schultz, M.J., Mitchell, E.H., Bain, J.L., Culpepper, K., Thomas, S.J., & Bellis, S.L. (2015). Microporous dermal-mimetic electrospun scaffolds pre-seeded with fibroblasts promote tissue regeneration in full-thickness skin wounds. *Plos ONE*, 10, e0122359. doi: 10.1371/journal. Pone.0122359.

Bottcher-Haberzeth, S., Biedermann, T., & Reichmann, E. (2010). Tissue engineering of skin. *Burns*, 36, 450-460.

Bragg, W.H., & Bragg, W.L. (1913). The reflection of X-rays by crystals. *Proceedings of the Royal Society of London A*, 428-438.

Bragulla, H.H., & Homberger, D.G. (2009). Structure and functions of keratin proteins in simple, stratified, keratinized and cornified epithelia. *Journal of Anatomy*. 214, 516-559.

Brauer, S., Meister, F., Gottlober, R-P., & Nechwatal, A. (2007). Preparation and thermoplastic processing of modified plant proteins. *Macromolecular Materials and Engineering*, 292, 176-183.

Brebu, M., & Spiridon, I. (2011). Thermal degradation of keratin waste. Journal of Analytical and *Applied Pyrolysis*, 91, 288-295.

Briscoe, B., Luckham, P., & Zhu, S. (2000). The effects of hydrogen bonding upon the viscosity of aqueous poly(vinyl alcohol) solutions. *Polymer*, 41, 3851-3860.

Bryant, S.J., Anseth, K.S. (2001). The effects of scaffold thickness on tissue engineered cartilage in photocrosslinked poly(ethylene oxide) hydrogels. *Biomaterials*, 22,619-26.

Burnett, L.R., Rahmany, M.B., Richter, J.R., Aboushwareb, T.A., Eberli, D., Ward, C.L., Orlando, G., Hantgan, R.R., & Van Dyke, M.E. (2013). Hemostatic properties and the role of cell receptor recognition in human hair keratin protein hydrogels. *Biomaterials*, 34, 2632-2640.

Cai, S., Xu, H., Jiang, Q., Yang, Y. (2013). Novel 3D electrospun scaffolds with fibers oriented randomly and evenly in three dimensions to closely mimic the unique architectures of extracellular matrices in soft tissues: Fabrication and mechanism study. *Langmuir*, 29, 2311-2318.

Carlson, D., Nie, L., Narayan, R., Dubois, P. (1999). Maleation of polylactide (PLA) by reactive extrusion. *Journal of Applied Polymer Science*, 72, 477-485.

Carrel, A., & Ebeling, A.H. (1923). Action on fibroblasts of extracts of homologous and heterologous tissues. *The Journal of Experimental Medicine*, 38, 499-511.

Cascone, M.G., Laus, M., Ricci, D., Sbarbati del Guerra, R. (1995). Evaluation of poly(vinyl alcohol) hydrogels as a component of hybrid artificial tissues. *Journal of Materials Science: Materials in Medicine*, 6, 71-75.

Chang, H-I., & Wang, Y. (2011). Cell responses to surface and architecture of tissue engineering scaffolds. In D Eberli (Ed.), Regenerative Medicine and Tissue Engineering – Cell and Biomaterials. InTech, DOI: 10.5772/21983.

Chang, Y., Ko, C-Y., Shih, Y-J., Quemener, D., Deratani, A., Wei, T-C., Wang, D-M., & Lai, J-Y. (2009). Surface grafting control of PEGylated poly(vinylidene fluoride) antifouling membrane via surface-initiated radical graft copolymerization. *Journal of Membrane Science*, 345, 160-169.

Chen, W., Yan, L., & Bangal, P.R. (2010). Preparation of graphene by the rapid and mild thermal reduction of graphene oxide induced by microwaves. *Carbon*, 48, 1146-1152.

Cheng, S., Lau, K., Liu, T., Zhao, Y., Lam, P., & Yin, Y. (2009). Mechanical and thermal properties of chicken feather fiber/PLA green composites. *Composites Part B: Engineering*, 40, 650-654.

Cheung, T.H., & Rando, T.A. (2013). Molecular regulation of stem cell quiescence. *Natural Reviews Molecular Cell Biology*, 14, 329-340.

Coward-Kelly, G., Chang, V.S., Agbogbo, F.K., & Holtzapple, M.T. (2006). Lime treatment of keratinous materials for the generation of highly digestible animal feed: 1. Chicken feathers. *Bioresource Technology*, 97, 1337-1343.

Crewther, W.G., Fraser, R.D.B., Lennox, F.G., & Lindley, H. (1965). The chemistry of keratins. In Advances in protein chemistry. Academic Press, Inc. New York, p191-346.

Cukierman, E., Pankov, R., Stevens, D.R., Yamada, K.M. (2001). Taking cell-matrix adhesions to the third dimension. *Science*, 294, 1708-1712.

Daley, W., Peters, S.B., & Larsen, M. (2008). Extracellular matrix dynamics in development and regenerative medicine. *Journal of Cell Science*, 121, 255-264.

Damodaran, S., & Paraf, A. (1997). Food proteins and their applications. Marcel Dekker, Inc. New York.

Darder, M., Lopez-Blanco, M., Aranda, P., Aznar, A.J., Bravo, J., Ruiz-Hitzky, E. (2006). Microfibrous chitosan-sepiolite nanocomposites. *Chemistry of Materials*, 18, 1602-1610.

de Guzman, R.C., Merrill, M.R., Richter, J.R., Hamzi, R.I., Greengauz-Roberts, O.K., & Van Dyke, M.E. (2011). Mechanical and biological properties of keratose biomaterials. *Biomaterials*, 32, 8205-8217.

Dedhar, S., Ruoslahti, E., & Pierschbacher, M. (1987). A cell surface receptor complex for collagen type I recognizes the Arg-Gly-Asp sequence. *The Journal of Cell Biology*, 104, 585-593.

Delgado, L.M., Bayon, Y., Pandit, A., & Zeugolis, I. (2015). To cross-link or not to cross-link? Cross-linking associated foreign body response of collagen-based devices. *Tissue Engineering Part B*, 21, 298-313.

Deng, J., Ren, T., Zhu, J., Mao, Z., & Gao, C. (2014). Adsorption of plasma proteins and fibronectin on poly(hydroxylethyl methacrylate) brushes of different thickness and their relationship with adhesion and migration of vascular smooth muscle cells. *Regenerative Biomaterials*, 1, 17-25.

Dennis, H.R., Hunter, D.L., Chang, D., Kim, S., White, J.L., Cho, J.W., Paul, D.R. (2001). Effect of melt processing conditions on the extent of exfoliation in organoclay-based nanocomposites. *Polymer*, 42, 9513-9552.

Dong, C., & Lv, Y. (2016). Application of collagen scaffold in tissue engineering: Recent advances and new perspectives. *Polymers*, 8, doi:10.3390/polym8020042.

Dreyer, D.R., Park, S., Bielawski, C.W., & Ruoff, R.S. (2010). The chemistry of graphene oxide. *Chemical Society Reviews*, 39, 228-240.

Drury, J. L., & Mooney, D. J. (2003). Hydrogels for tissue engineering: scaffold design variables and applications. *Biomaterials*, 24, 4337-4351.

Dulbecco, R. (1952). Production of plaques in monolayers of tissue cultures by single particles of an animal virus. *Proceedings of the National Academy of Sciences*, 38, 747-752.

Eagle, H. (1955). The specific amino acid requirements of mammalian cells (stain HeLaT) in tissue culture. *The Journal of Experimental Medicine*, 1, 37-48.

Engler, A.J., Sen, S., Sweeney, H.L., & Discher, E. (2006). Matrix elasticity directs stem cell lineage specification. *Cell*, 126, 677-689.

Estévez-Martínez, Y., Velasco-Santos, C., Martínez-Hernández, A.L., Delgado, G., Cuevas-Yáñez, E., Alaníz-Lumbreras, D., Duron-Torres, S., & Castaño, V.M. (2013). Grafting of multiwalled carbon nanotubes with chicken feather keratin. *Journal of Nanomaterials*, Volume 2013, Article ID 702157.

Fan, J., Lei, T-D., Li, J., Zhai, P-Y., Wang, Y-H., Cao, F-Y., & Liu, Y. (2016). High protein content keratin/poly(ethylene oxide) nanofibers crosslinked in oxygen atmosphere and its cell culture. *Materials & Design*, 104, 60-67.

Fang, J., Niu, H.T., Lin, T., & Wang, X.G. (2008). Applications of electrospun nanofibers. *Chinese Science Bulletin*, 53, 2265-2286.

Feughelman, M. (1997). Mechanical properties and structure of alpha-keratin fibres: wool, human hair and related fibres. University of New South Wales Press, Sidney. p120.

Filipello Marchisio, V., 2000. Karatinophilic fungi: their role in nature and degradation of keratinic substrates. In: Kushawaha, R.K.S., Guarro, J. (Eds.), Biology of dermatophytes and other keratinophilic fungi. Revista Iberoamericana de Micologia, p86–92.

Flanagan, L.A., Ju, Y.E., Marg, B., Osterfield, M., & Janmey, P.A. (2002). Neurite branching on deformable substrates. *Neuroreport*, 13, 2411-2415.

Floren, M., Migliaresi, C., & Motta, A. (2016). Processing techniques and applications of silk hydrogels in bioengineering. *Journal of Functional Biomaterials*, 7, doi: 10.3390/jfb7030026.

Flores-Hernández, C.G., Colin-Cruz, A., Velasco-Santos, C., Castaño, V.M., Rivera-Armenta, J.L., Almendarez-Camarillo, A., Garcia-Casillas, P.E., & Martínez-Hernández, A.L. (2014). All green composites from fully renewable biopolymers: Chitosan-starch reinforced with keratin from feathers, *Polymers*, 6, 686-705.

Fonder, M.A., Lazarus, G.S., Cowan, D.A., Aronson-Cook, B., Kohli, A.R., & Mamelak, A.J. (2008). Treating the chronic wound: A practical approach to the care of nonhealing wounds and wound care dressings. *Journal of the American Academy of Dermatology*, 58 185–206.

Fong, H., Chun, I., & Reneker, D.H. (1999). Beaded nanofibers formed during electrospinning. *Polymer*, 40, 4585-4592.

Forgacs, G., Lundin, M., Taherzadeh, M.J., & Horvath, I.D. (2013). Pretreatment of chicken feather waste for improved biogas production. *Applied Biochemistry and Biotechnology*, 169, 2016-2028.

Frantz, C., Stewart, K.M., & Weaver, V.M. (2010). The extracellular matrix at a glance. *Journal of Cell Science*, 123, 4195-4200.

Fraser, R.B.D., Mac Rae, T.P., & Rogers, G.E. (1972). Keratins- their Composition, Structure and Biosynthesis. CC Thomas Publishing, Springfield, IL, USA.

Fraser, R.D., & Parry, D.A. (2008). Molecular packing in the feather keratin filament. *Journal of Structural Biology*, 162, 1-13.

Fraser, R.D.B., & MacRae, T.P. (1973). Conformation in fibrous proteins. Academic Press, Inc. New York. Chapter 16.

Freed, L.E., & Guilak, F. Engineering functional tissues. (2007). In Lanza, R., Langer, R., & Vacanti, J., (Eds.) Principles of Tissue Engineering, 3rd Edition, (Eds.), Academic Press, Amsterdam.

Freshney, R.I. (2006). Basic principles of cell culture. In Vunjak-Novakovic, G., & Freshney, R.I. (Eds.) Culture of Cells for Tissue Engineering. John Wiley & Sons, Inc., Hoboken, NJ, USA.

Friedman, M. (1999). Chemistry, biochemistry, nutrition, and microbiology of lysinoalanine, lanthionine, and histidinoalanine in food and other proteins. *Journal of Agricultural and Food Chemistry*, 47, 1295-1319.

Fujii, T., & Ide, Y. (2004). Preparation of translucent and flexible human hair protein film and their properties. *Biological and Pharmaceutical Bulletin*, 27, 1433-1436.

Fujii, T., & Li, D. (2008). Preparation and properties of protein films and particles from chicken feathers. *Journal of Biological Macromolecules*, 8, 48-55.

Fujii, T., Takayama, S., & Ito, Y. (2013). A novel purification procedure for keratin-associated proteins and keratin from human hair. *Journal of Biological Macromolecules,* 13, 92-106.

Gao, H-W., Yang, R-J., He, J-Y., & Yang, L. (2010). Rheological behaviors of PVA/H2O solutions of high-polymer concentration. *Journal of Applied Polymer Science*, 116, 1459-1466.

Gardella, L., Furfaro, D., Galimberti, M., & Monticelli, O. (2015). On the development of a facile approach based on the use of ionic liquids: preparation of PLLA (sc-PLA)/high surface area nano-graphite systems. *Green Chemistry*, 17, 4082-4088.

Gey, G.O., Coffman, W.D., & Kubicek, M.T. (1952). Tissue culture studies of the proliferative capacity of cervical carcinoma and normal epithelium. *Cancer Research*, 12, 264-265.

Ghani, S.A., Tan, S.J., & Yeng, T.S. (2013). Properties of chicken feather fiber-filled low-density polyethylene composites: The effect of polyethylene grafted maleic anhydride. *Polymer-Plastics Technology and Engineering*, 52, 495-500.

Gironi, F., & Piemonte, V. (2011). Bioplastics and petroleum-based plastics: Strengths and weaknesses. *Energy Sources, Part A,* 33, 1949-1959.

Goddard, D.R., & Michaelis, L. (1934). A study on keratin. *The Journal of Biological Chemistry*, 106, 605-614.

Gong, L., Kinloch, I.A., Young, R.J., Riaz, I., Jalil, R., & Novoselov, K.S. (2010). Interfacial stress transfer in graphene monolayer nanocomposite. *Advanced Materials*, 22, 2694-2697.

Gonzalez, D., Campos, A.R., Cunha, A.M., Santos, V., & Parajo, J.A. (2011). Manufacture of fibrous reinforcements for biodegradable biocomposites from Citysus scoparius. *Journal of Chemical Technology and Biotechnology*, 86, 575-583.

Goormaghtigh, E., Cabiaux, V., & Ruysschaert, J-M. (1990). Secondary structure and dosage of soluble and membrane proteins by attenuated total reflection Fourier-transform infrared spectroscopy on hydrated films. *European Journal of Biochemistry*, 193, 409-420.

Gousterova, A., Braikova, D., Goshev, I., Christov, P., Tishinov, K., Vasileva-Tonkova, E., Haertle, T., & Nedkov, P. (2005). Degradation of keratin and collagen containing wastes by newly isolated thermoactinomycetes or by alkaline hydrolysis. *Letters in Applied Microbiology*, 40, 335-340.

Graiver, D., Waikul, L.H., Berger, C., & Narayan, R. (2004). Biodegradable soy protein-polyester blends by reactive extrusion process. *Journal of Applied Polymer Science*, 92, 3231-3239.

Grazziotin, A., Pimentel, F.A., Sangali, S., de Jong E.V., & Brandelli, A. (2007). Production of feather protein hydrolyzate by keratinolytic bacterium Vibrio sp. Kr2. *Bioresource Technology*, 98, 3172-3175.

Greaves, N., Iqbal, S., Baguneid, M., & Bayat, A. (2013). The role of skin substitutes in the management of chronic cutaneous wounds. Wound Repair and Regeneration, 21, 194-210.
Grinnell, F. (2003). Fibroblast biology in three-dimensional collagen matrices. *Trends in Cell Biology*, 13, 264-269.

Grkovic, M., Stojanovic, D.B., Kojovic, A., Strnad, S., Kreze, T., Aleksic, R., & Uskokovic, P.S. (2015). Keratin-polyethylene oxide bio-nanocomposites reinforced with ultrasonically functionalized graphene. *RSC Advances*, 5, 91280-91287.

Groeber, F., Holeiter, M., Hampel, M., Hinderer, S., & Schenke-Layland, K. (2011). Skin tissue engineering – in vivo and in vitro applications. *Advanced Drug Delivery Reviews*, 128, 352-366.

Gstraunthaler, G. (2003). Alternatives to the use of fetal bovine serum: serum-free cell culture. *ALTEX*, 20, 275-281.

Guo, J., Pan, S., Yin, X., He, Y-F., Li, T., & Wang, R-M. (2015). pH-sensitive keratin-based polymer hydrogel and its controllable drug-release behavior. *Journal of Applied Polymer Science*, 132, 41572, doi: 10.1002/app.41572.

Guo, S., & DiPietro, L.A. (2010). Factors affecting wound healing. *Journal of Dental Research*, 89, 219-229.

Hadjipanayi, E., Mudera, V., & Brown, R.A. (2009). Close dependence of fibroblasts proliferation on collagen scaffold matrix stiffness. *Journal of Tissue Engineering and Regenerative Medicine*, 3, 77-84.

Hagel, P., Gerding, J.J.T., Fieggen, W., & Bloemendal, H. (1971). Cyanate formation in solutions of urea: I. Calculation of cyanate concentrations at different temperatures and pH. *Biochimica et Biophysica Acta,* 243, 366-373.

Han, S., Ham, T. R., Haque, S. Sparks, J. L., & Saul, J. M. (2015). Alkylation of human hair keratin for tunable hydrogel erosion and drug delivery in tissue engineering applications. *Acta Biomaterialia*, 23, 201-213.

Harrap, B.S., & Woods, E.F. (1964). Soluble derivatives of feather keratin. 1. Isolation, fractionation and amino acid composition. *Biochemical Journal*, 92, 8-18.

Harrison, R.G., Greenman, M.J., Mall, F.P., & Jackson, C.M. (1907). Observations of the living developing nerve fiber. *The Anatomical Record*, 1, 116-128.

Haubner, K., Murawski, J., Olk, P., Eng, L.M., Ziegler, C., Adolphi, B., & Jaehne, E. (2010). The route to functional graphene oxide. *ChemPhysChem*, 11, 2131-2139.

Haugh, M.G., Murphy, C.M., & O'Brien, F.J. (2010). Novel freeze-drying methods to produce a range of collagen-glycosaminoglycan scaffolds with tailored mean pore sizes. *Tissue Engineering: Part C*, 16, 887-894.

Hayman, E.G., & Ruoslahti, E. (1979). Distribution of fetal bovine serum fibronectin and endogenous rat cell fibronectin in extracellular matrix. *Journal of Cell Biology*, 89, 255-259.

He, Y., Wang, X., Wu, D., Gong, Q., Qiu, H., Liu, Y., Wu, T., Ma, J., & Gao, J. (2013). Biodegradable amylose films reinforced by graphene oxide and polyvinyl alcohol. *Materials Chemistry and Physics*, 142, 1-11.

Hill, P., Brantley, H., & Van Dyke, M. (2010). Some properties of keratin biomaterials: Kerateines. *Biomaterials*, 31, 585-593.

Hinnman, C.D., & Maibach, H.I. (1963). Effect of air exposure and occlusion on experimental human skin wounds. *Nature*, 200, 377-378.

Hoffman, A.S. (2002). Hydrogels for biomedical applications. *Advanced Drug Delivery Reviews*, 54, 3-12.

Hoffman, B. D., Grashoff, C. and Schwartz, M. A. (2011). Dynamic molecular processes mediate cellular mechanotransduction. *Nature* 475, 316-323.

Holt, B., Tripathi, A., & Morgan, J. (2008). Viscoelastic response of human skin to low magnitude physiologically relevant shear. *Journal of Biomechanics*, 41, 2689-2695.

Hontoria-Lucas, C., Lopez-Peinado, A.J., Lopez-Gonzalez, J.D., Rojas-Cervantes, M.L., & Martin-Aranda, R.M. (1995). Study of oxygen-containing groups in a series of graphite oxides: Physical and chemical characterization. *Carbon*, 33, 1585-1592.

Hu, H., Reddy, N., Yan, K., & Yang, Y. (2011). Acetylation of chicken feathers for thermoplastic applications. *Journal of Agricultural and Food Chemistry*, 59, 10517-10523.

Huang, J., Zhang, L., Wei, H., Cao, X. (2004). Soy protein isolate/kraft lignin composite compatibilized with methylene diphenyl diisocyanate. *Journal of Applied Polymer Science*, 93, 624-629.

Huda, M.S., Schmidt, W.F., Misra, M., & Drzal, L.T. (2013). Effect of fiber surface treatment of poultry feather fibers on the properties of their polymer matrix composites. *Journal of Applied Polymer Science*, 128, 1117-1124.

Hummers, W.S., & Offeman, R.E. (1958). Preparation of graphitic oxide. *Journal of the American Chemical Society*, 80, 1339-1339.

Ikkai, F., & Naito, S. (2002). Heat-induced gelation of hard-keratin protein aqueous solutions. *Biomacromolecules*, 3, 482-487.

Jackson, M., & Mantsch, H.H. (1995). The use and misuse of FTIR spectroscopy in the determination of protein structure. *Critical Reviews in Biochemistry and Molecular Biology*, 30, 95-120.

Jackson, S.T., & Nuzzo, R.G. (1995). Determining hybridization differences for amorphous carbon from the XPS C1s envelope. *Applied Surface Science*, 90, 195-203.

Janssen, L.P.B.M. (2004). Reactive extrusion systems. Marcel Dekker, Inc., NY, USA. Ch. 2.
Jin, E., Reddy, N., Zhu, Z., & Yang, Y. (2011). Graft polymerization of native chicken feathers for thermoplastic applications. *Journal of Agricultural and Food Chemistry*, 59, 1729-1738.

Jones, A.M., & San Miguel, L. (2006). Are modern wound dressings a clinical and cost-effective alternative to the use of gauze? *Journal of Wound Care*, 15, 65-69.

Jonker, A. M., Lowik, D. W. P. M., & Hest, J. C. M. (2012). Peptide- and protein-based hydrogels. *Chemistry of Materials*, 24, 759-773.

Karp, J.M., Dalton, P.D., & Shoichet, S. (2003). Scaffolds for tissue engineering. *MRS Bulletin*, 28, 301-306.

Katoh, K., Shibayama, M., Tanabe, T., & Yamauchi, K. (2004). Preparation and physicochemical properties of compression-molded keratin films. *Biomaterials*, 25, 2265-2272.

Khosa, M.A., Wu, J., & Ullah, A. (2013). Chemical modification, characterization, and application of chicken feathers as novel biosorbents. *RSC Advances*, 3, 20800-20810 (2013).

Klotz, I.M. (1996). Equilibrium constants and free energies in unfolding of proteins in urea solutions. *Proceedings of the National Academy of Sciences*, 93, 14411-14415.

Kong, J., & Yu, S. (2007). Fourier transform infrared spectroscopic analysis of protein secondary structures. *Acta Biochimica et Biophysica*, 39, 549-559.
Kornillowicz-Kowalska, T., & Bohacz, J. (2011). Biodegradation of keratin waste: Theory and practical aspects. *Waste Management*, 31, 1689-1701.

Kreplak, L., Doucet, J., Dumas, P., & Briki, F. (2004). New aspects of the α-helix to β-sheet transition in stretched hard α-kertain fibers. *Biophysical Journal*, 87, 640-647.

Kuilla, T., Bhadra, S., Yao, D., Kim, N.H., Bose, S., & Lee, J.H. (2010). Recent advances in graphene based polymer composites. *Progress in Polymer Science*, 35, 1350-1375.

Kumar, P., Sandeep, K.P., Alavi, S., Truong, V.D., Gorga, R.E. (2010). Preparation and characterization of bio-nanocomposite film based on soy protein isolate and montmorillonite using melt extrusion. *Journal of Food Engineering*, 100, 480-489.

Kundu, J., Poole-Warren, L.A., Martens, P., & Kundu, S.C. (2012). Silk fibroin/poly(vinyl alcohol) photocrosslinked hydrogels for delivery of macromolecular drugs. *Acta Biomateralia*, 8, 1720-1729.

Laemmli, U.K. (1970). Cleavage of structural proteins during the assembly of the head of bacteriophage T4. *Nature*, 227, 680-685.

Lai, J-Y., Li, Y-T., Cho, C-H., & Yu, T-C. (2012). Nanoscale modification of porous gelatin scaffolds with chondroitin sulfate for corneal stromal tissue engineering. *International Journal of Nanomedicine*, 7, 1101-1114.

Lakesan, A., Bakar, F.A., & Hashim, D. (2013). Potential of chicken by-products as sources of useful biological resources. *Waste Management*, 33, 552-565.

Lee, J., Cuddihy, M.J., & Kotov, N.A. (2008). Three dimensional cell culture matrices: State of the art. *Tissue Engineering: Part B*, 14, 61-86.

Lee, S-Y., & Park, S-J. (2014). Isothermal exfoliation of graphene oxide by a new carbon dioxide pressure swing method. *Carbon*, 68, 112-117.

Lemons, J.M.S., Feng, X-J., Bennett, B.D., Legesse-Miller, A., Johnson, E.L., Raitman, I., Pollina, E.A., Rabitz, H.A., Rabinowitz, J.D., & Coller, H.A. (2010) Quiescent Fibroblasts Exhibit High Metabolic Activity. *PLoS Biol*ogy, 8(10): e1000514. doi:10.1371/journal.pbio.1000514.

Leon, N.H. (1972). Structural aspects of keratin fibres. *Journal of the Society of Cosmetic Chemists*, 23, 427-445.

Lev, J., Holba, M., Kalhotka, L., Mikula, P., & Kimmer, D. (2012). Improvements in the structure of electrospun polyurethane nanofibrous materials used for bacterial removal from wastewater. *International Journal of Theoretical and Applied Nanotechnology*, 1, 16-20.

Levental, I., Goerges, P.C., & Janmey, P.A. (2007). Soft biological materials and their impact on cell function. *Soft Matter*, 3, 299-306.

Li, J., Li, Y., Li, L., Mak, A.F.T., Ko, F., & Qin, L. (2009). Preparation and biodegradation of electrospun PLLA/keratin nonwoven fibrous membrane. *Polymer Degradation and Stability*, 94, 1800-1807.

Li, J., Li, Y., Mak, A.F.T., Ko, F., & Qin, L. (2009). Preparation and biodegradation of electrospun PLLA/keratin nonwoven fibrous membrane. *Polymer Degradation and Stability*, 94, 1800-1807.

Li, M., Jin, E., & Zhang, L. (2016). Effects of graft modification on the water solubility, apparent viscosity, and adhesion of feather keratin for warp sizing. *Journal of the Textile Institute*, 107, 395-404.

Li, R., Liu, C., & Ma, J. (2011). Studies on the properties of graphene oxide-reinforced starch biocomposites. *Carbohydrate Polymers*, 84, 631-637.

Li, S., & Yang, X-H. (2014). Fabrication and characterization of electrospun wool keratin/poly(vinyl alcohol) blend nanofibers. *Advances in Materials Science and Engineering*, Article ID 163678.

Liu, F., Nishikawa, T., Shimizu, W., Sato, T., Usami, H., Amiya, S., Ni, Q-Q., & Murakami, Y. (2012). Preparation of fully hydrolyzed polyvinyl alcohol electrospun nanofibers with diameters of sub-200 nm by viscosity control. *Textile Research Journal*, 82, 1635-1644.

Liu, W., Misra, M., Askeland, P., Drzal, L.T., Mohanty, A.K. (2005). "Green" composites from soy based plastic and pineapple leaf fiber: fabrication and properties evaluation. *Polymer*, 46, 2710-2721.

Lo Conte, M., & Carroll, K.S. (2013). The Chemistry of thiol oxidation and detection. In Jakob, U., & Reichmann, D. (Eds.) Oxidative Stress and Redox Regulation. Springer, Dordrecht, NL.

Lo, C.M., Wang, H.B., Dembo, M., & Wang, Y.L. (2000). Cell movement is guided by the rigidity of the substrate. *Biophysical Journal*, 79, 144-152.

Lovette, I.J., & Fitzpatrick, J.W. (2016). Handbook of bird biology, 3rd edition. Willey-Blackwell, Oxford, UK.

Luecha, J., Sozer, N., Kokini, J.L. (2010). Synthesis and properties of corn zein/montmorillonite nanocomposite films. *Journal of Material Science*, 45, 3529-3537.

Ma, B., Wang, X., Wu, C., & Chang, J. (2014). Crosslinking strategies for preparation of extracellular matrix-derived cardiovascular scaffolds. *Regenerative Biomaterials*, 81-89.

Ma, T., Chang, P.R., Zheng, P., & Ma, X. (2013). The composites based on plasticized starch and graphene oxide/reduced graphene oxide. *Carbohydrate Polymers*, 94, 63-70.

Maclaren, J.A., Kilpatrick, D.J., & Kirkpatrick, A. (1968). Reduced wool fibres, their preparation and alkylation. *Australian Journal of Biological Sciences*, 21, 805-813.

MacNeil, S. (2008). Biomaterials for skin engineering of skin. *Materials Today*, 11, 26-35.

Madaghiele, M., Demitri, C., Sannino, A., & Ambrosio, L. (2014). Polymeric hydrogels for burn wound care: Advanced skin wound dressings and regenerative templates. *Burns & Trauma*, 2, 153-161.

Mahmoud, W.E. (2011). Morphology and physical properties of poly(ethylene oxide) loaded graphene nanocomposites prepared by two different techniques. *European Polymer Journal*, 47, 1534-1540.

Malafaya, P.B., Silva, G.A., & Reis, R.L. (2007). Natural-origin polymers as carrier and scaffolds for biomolecules and cell delivery in tissue engineering applications. *Advanced Drug Delivery Reviews*, 59, 207-233.

Marquis, D.M., Guillaume, E., Chivas-Joly, C. (2011). Properties of nanofillers in polymer. In J. Cuppoletti (Ed.). Nanocomposites and polymers with analytical methods. Intech, Rijeka, Croatia.

Marshall, T., & Williams, K.M. (1986). High resolution two-dimensional electrophoresis of hair proteins without prior S-carboxymethylation. *Electrophoresis*, 7, 524-526.

Martínez-Hernández, A.L., & Velasco-Santos, C. Keratin Fibers from Chicken Feathers: Structure and Advances in Polymer Composites. In Dullart, R., & Mousques, J. (Eds.). Keratin: Structure, Properties and Applications. Nova Science Publishers Inc., Hauppauge, NY, USA, (2011) p149–211.

Martínez-Hernández, A.L., Santiago-Valtierra, A.L., & Alvarez-Ponce, M.J. (2008). Chemical modification of keratin biofibres by graft polymerisation of methyl methacrylate using redox initiation. *Materials Research Innovations*, 12, 184-191.

Martínez-Hernández, A.L., Velasco-Santos, C., de Icaza, M., & Castaño, V.M. (2003). Grafting of methyl methacrylate onto natural keratin. *e-Polymers*, 3, 209-219.

Mason, B.N., Califano, J.P., & Reinhart-King, C.A. (2012). Matrix stiffness: A regulator of cellular behavior and tissue formation. In Bhatia, S.K. (Ed.). Engineering Biomaterials for Regenerative Medicine. Springer, New York, USA.

Matthews, B. D., Overby, D. R., Mannix, R. & Ingber, D. E. (2006). Cellular adaptation to mechanical stress: role of integrins, Rho, cytoskeletal tension and mechanosensitive ion channels. *Journal of Cell Science*, 119, 508–518.

Mckittrick, J., Chen, P-Y., Bodde, S.G., Yang, W., Novitskaya, E.E., & Meyers, M.A. (2012). The structure, functions, and mechanical properties of keratin. *JOM*, 64, 449-468.

McPherson, R.A., & Hardy, G. (2011). Clinical and nutritional benefits of cysteine-enriched protein supplements. *Current Opinion in Clinical Nutrition and Metabolic Care*, 14, 562-568.

Mittal, V. 2011. Bio-nanocomposites: future high-value materials. In V. Mittal (Ed). Nanocomposites with biodegradable polymers. Synthesis, properties, and future perspectives. Oxford University Press, UK.

Moore, S. (1963). On the determination of cystine as cysteic acid. *The Journal of Biological Chemistry*, 238, 235-237.

Nagai, Y., & Nishikawa, T. (1970). Alkali solubilization of chicken feather keratin. *Agricultural and Biological Chemistry*, 34, 16-22.

Naidu, K.T., & Prabhu, N.P. (2011). Protein-surfactant interaction: Sodium dodecyl sulfate-induced unfolding of ribonuclease A. *The Journal of Physical Chemistry B,* 115, 14760-14767.

Nakaji-Hirabayashi, T., Kato, K., & Iwata, H. (2008). Self-assembling chimeric protein for the construction of biodegradable hydrogels capable of interaction with integrins expressed on neural stem/progenitor cells. *Biomacromolecules*, 9, 1411-1416.

Nakamura, A., Arimoto, M., Takeuchi, K., & Fujii, T. (2002). A rapid extraction procedure of human hair proteins and identification of phosphorylated species. *Biological and Pharmaceutical Bulletin*, 25, 569-572.

Nakata, R., Tachibana, A., & Tanabe, T. (2014). Preparation of keratin hydrogel/hydroxyapatite composite and its evaluation as controlled drug release carrier. *Materials Science and Engineering C*, 41, 59-64.

Nemeth, A.J., Eaglstein, W.H., Taylor, J.R., Peerson, L.J., & Falanga, V. (1991). Faster healing and less pain in skin biopsy sites treated with an occlusive dressing. *Archives of Dermatology*, 127, 1679-1683.

Nezarati, RM., Eifert, M.B., & Cosgriff-Hernandez, E. (2013). Effects of humidity and solution viscosity on electrospun fiber morphology. *Tissue Engineering: Part C*, 19, 810-819.

Ng, C.S., Wu, P., Foley, J., Foley, A., McDonald, M-L., Juan, W-T., Huang, C-J., Lai, Y-T., Lo, W-S., Chen, C-F., Leal, S.M., Zhang, H., Widelitz, R.B., Patel, P.I., Li, W-H., Chuong, C-M. (2012). The chicken frizzle feather is due to an α-keratin (KRT75) mutation that causes a defective rachis. *PLoS Genet*ics, 8, e1002748, 1-16.

Nomura, Y., Nakato, H., Ishii, Y., & Shirai, K. (2002). Characterization of S-sulfokeratin from pig hair and its use as a modifier of type I collagen gel. *Bioscience, Biotechnology, and Biochemistry*, 66, 1382-1385.

Novoselov, K.S., Geim, A.K., Morozov, S.V., Jiang, D., Zhang, Y., Dubonos, S.V., Grigorieva, I.V., & Firsov, A.A. (2004). Electric field effect in atomically thin carbon films. *Science*, 306, 666-669.

Nuttelman, C.R., Mortisen, D.J., Henry, S.M., Anseth, K.S. (2001). Attachment of fibronectin to poly(vinyl alcohol) hydrogels promotes NIH3T3 cell adhesion, proliferation, and migration. *Journal of Biomedical Materials Research*, 57, 217-23.

Nyame, T., Chiang, H.A., & Orgill, D. (2014). Clinical applications of skin substitutes. *The Surgical Clinics of North America*, 94, 839-850.

Orienti, I., Trere, R., Zecchi, V. Hydrogels formed by cross-linked polyvinylalcohol as colon-specific drug delivery systems. *Drug Development and Industrial Pharmacy*, 27, 877-84.

Ovington, L.G. (2001). Hanging wet-to-dry dressings out to dry. *Home Healthcare Nurse*, 19, 477-483.

Ovington, L.G. (2007). Advances in wound dressings. *Clinics in Dermatology*, 25, 33-38.

Ozaki, Y., Takagi, Y., Mori, H., & Hara, M. (2014). Porous hydrogel of wool keratin prepared by a novel method: An extraction with guanidine/2-mercaptoethanol solution followed by dialysis. *Materials Science and Engineering Part C*, 42, 146-154.

Pace, L.A., Plate, J.F., Mannava, S., Barnwell, J.C., Koman, L.A., Li, Z., Smith, T.L., & Van Dyke, M. (2014). A human hair keratin hydrogel scaffold enhances median nerve regeneration in nonhuman primates: An electrophysiological and histological study. *Tissue Engineering: Part A*, 20, 507-517.

Papadppoulos, M.C., El Boushy, A.R., Roodbeen, A.E., & Ketelaars, E.H. (1986). Effects of processing time and moisture content on amino acid composition and nitrogen characteristics of feather meal. *Animal Feed Science and Technology*, 14, 279-290.

Paredes, J.I., Villar-Rodil, S., Martinez-Alonso, A., & Tascon, J.M.D. (2008). Graphene oxide dispersions in organic solvents. *Langmuir*, 24, 10560-10564.

Parenteau-Bareil, R., Gauvin, R., & Berthod, F. (2010). Collagen-based biomaterials for tissue engineering applications. *Materials*, 3, 1863-1887.

Park, M., Shin, H.K., Panthi, G., Rabbani, M.M., Alam, A-M., Choi, J., Chung, H-J., Hong, S-T., & Kim, H-Y. (2015). Novel preparation and characterization of human hair-based nanofibers using electrospinning process. *International Journal of Biological Macromolecules*, 76, 45-48.

Parsons, J.T., Horwit, A.R., & Schwartz, M.A. (2010). Cell adhesion: integrating cytoskeletal dynamics and cellular tension. *Nature Reviews*, 11, 633-643.

Pei, S., & Cheng, H-M. (2012). The reduction of graphene oxide. Carbon, 50, 3210-3228.

Petersen, A., Joly, P., Bergmann, C., Korus, G., & Duda GN. (2012). The impact of substrate stiffness and mechanical loading on fibroblast-induced scaffold remodeling. *Tissue Engineering: Part A*, 18, 1804-1817.

Poole, A.J., & Church, J.S. (2015). The effects of physical and chemical treatments on Na_2S produced feather keratin films. *International Journal of Biological Macromolecules*, 73, 99-108.

Poole, A.J., Lyons, R.E., & Church, J.S. (2011). Dissolving feather keratin using sodium disulfide for bio-polymer applications. *Journal of Polymers and the Environment*, 19, 995-1004.

Poranki, D., Whitener, W., Howse, S., Mesen, T., Howse, E., Burnell, J., Greengauz-Roberts, O., Molnar, J., & Van Dyke, M. (2014). Evaluation of skin regeneration after burns in vivo and rescue of cells after thermal stress in vitro following treatment with a keratin biomaterial. *Journal of Biomaterials Applications*, 29, 26-35.

Posudievsky, O.Y., Khazieieva, O.A., Koshechko, V.G., & Pokhodenko, V.D. (2012). Preparation of graphite oxide by solvent-free mechanochemical oxidation of graphite. *Journal of Materials Chemistry,* 22, 12465-12467.

Potts, J.R., Dreyer, D.R., Bielawski, C.W., Ruoff, R.S. (2011). Graphene-based polymer nanocomposites. *Polymer*, 52, 5-25.

Potts, J.R., Murali, S., Zhu, Y., Zhao, X., & Ruoff, R.S. (2011). Microwave-exfoliated graphite oxide/polycarbonate composites. *Macromolecules*, 44, 6488-6495.

Rad, Z.P., & Tavanai, H. (2012). Production of feather keratin nanopowder through electrospraying. *Journal of Aerosol Science*, 51, 49-56.

Ramakrishna, S., Fujihara, K., Teo, W-E., Lim, T-C., & Ma, Z. (2005). An introduction to electrospinning of nanofibers. World Scientific Publishing Co. Pte. Ltd., Singapore.

Raquez, J., Nabar, Y., Srinivasan, M., Shin, B., Narayan, R., & Dubois, P. (2008). Maleated thermoplastic starch by reactive extrusion. *Carbohydrate Polymers*, 74, 159-169.

Ratheesh, G., Venugopal, J.R., Chinappan, A., Ezhilarasu, H., Sadiq, A., & Ramakrishna, S. (2016). 3D fabrication of polymeric scaffolds for regenerative therapy. *ACS Biomaterials Science & Engineering*, DOI: 10.1021/acsbiomaterials.6b00370

Ratner, B., Hoffman, A., Schoen, F., Lemons, J. 2013. Biomaterials science: An evolving, multidisciplinary endeavor. In Ratner, B., Hoffman, A., Schoen, F., Lemons, J. (Eds.). Biomaterials Science (3rd edition). Academic Press, Oxford, U.K.

Reddy, M.M., Vivekanandhan, S., Misra, M., Bhatia, S.J., & Mohanty, A.K. (2013). Biobased plastics and bionanocomposites: Current status and future opportunities. *Progress in Polymer Science*, 38, 1653-1689.

Reddy, N. (2015). Non-food industrial applications of poultry feathers. *Waste Management*, 45, 91-107.

Reddy, N., Hu, C., Yan, K., Yang, Y. (2011). Thermoplastic films from cyanoethylated chicken feathers. *Materials Science and Engineering*, C31, 1706-1710.

Reddy, N., Jiang, Q., Jin, E., Shi, J., Hou, X., & Yang, Y. (2013). Bio-thermoplastics from grafted chicken feathers for potential biomedical applications. *Colloids and Surfaces B: Biointerfaces*, 110, 51-58.

Reichl, S. (2009). Films based on human hair keratin as substrates for cell culture and tissue engineering. *Biomaterials*, 30, 6854-6866.

Reichl, S., Borrelli, M., & Geerling, G. (2011). Keratin films for ocular surface reconstruction. *Biomaterials*, 32, 3375-3386.

Reinke, J.M., & Song, H. (2012). Wound repair and regeneration. *European Surgical Research*, 49, 35-43.

Richter, J.R., de Guzman, R.C., Greengauz-Roberts, O.K., & Van Dyke, M. (2012). Structure-property relationships of meta-kerateine biomaterials derived from human hair. *Acta Biomateralia*, 8, 274-281.

Riddles, P.W., Blakeley, R.L., & Zerner, B. (1979). Ellman's reagent: 5,5'-dithiobis(2-nitrobenzoic acid)-a reexamination. *Analytical Biochemistry,* 94, 75-81.

Riedo, C., Caldera, F., Poli, T., & Chiantore, O. (2015). Poly(vinylalcohol)-borate hydrogels with improved features for the cleaning of cultural heritage surfaces. *Heritage Science*, 3, 23-34.
Robbins, C.R., & Kelly, C.H. (1970). Amino acid composition of human hair. *Textile Research Jorunal*, 40, 891-896.

Rodriguez-Gonzalez, C., Kharissova, O.V., Martinez-Hernandez, A.L., Castano, V.M., & Velasco-Santos, C. (2013). Graphene oxide sheets covalently grafted with keratin obtained from chicken feathers. *Digest Journal of Nanomaterials and Biostructures*, 8, 127-138.

Rodríguez-González, C., Martínez-Hernández, A.L., Castaño, V.M., Kharissova, O.V., Ruoff, R.S., & Velasco-Santos, C. (2012). Polysaccharide nanocomposites reinforced with graphene

oxide and keratin-grafted graphene oxide. *Industrial & Engineering Chemistry Research*, 51, 3619-3629.

Rossky P.J. (2008). Protein denaturation by urea: Slash and bond. *Proceedings of the National Academy of Sciences*, 105, 16825-16826.

Rosso, F., Marino, G., Grimaldi, A., Cafiero, G., Chiellini, E., Chiellini, F., Barbarisi, M., & Barbarisi, A. (2013). Vitronectin absorbed on nanoparticles mediate cell viability/proliferation and uptake by 3T3 Swiss albino mouse fibroblasts: in vitro study. *BioMed Research International*, Article ID 539348.

Rous, P., & Jones, F.S. (1916). A method for obtaining suspensions of living cells from the fixed tissues, and for the plating out of individual cells. *The Journal of Experimental Medicine*, 23, 549-555.

Rouse, J.G., & Van Dyke, M.E. (2010). A review of keratin-based biomaterials for biomedical applications. *Materials*, 3, 999-1014.

Routray, M., Rout, S.N., Mohanty, G.C., & Nayak, P.L. (2013). Preparation and characterization of soy protein isolate films processed by compression and casting. *Journal of Chemical and Pharmaceutical Research*, 5, 752-761.

Ruoslahti, E. (1996). RGD and other recognition sequences for integrins. *Annual Review of Cell and Developmental Biology*, 12, 697-715.

Rutz, A.L, & Shah, R.N. (2016). Protein-based hydrogels. In Polymeric Hydrogels as Smart Biomaterials. Kalia, S. (Ed.), Springer, Cham, Switzerland.

Ryan, A.J., & O'Brien, F.J. (2015). Insoluble elastin reduces collagen scaffold stiffness, improves viscoelasticity properties, and induces a contractile phenotype in smooth muscle cells. *Biomaterials*, 73, 296-307.

Sasmal, A., Nayak, P.L., & Sasmal, S. (2009). Degradability studies of green nanocomposites derived from soy protein isolate (Spi)-furfural modified with organoclay. *Polymer-Plastics Technology and Engineering*, 48, 905-909.

Schmedlen, R.H., Masters, K.S., & West, J.L. (2002). Photocrosslinkable polyvinyl alcohol hydrogels that can be modified with cell adhesion peptides for use in tissue engineering. *Biomaterials*, 23, 4325-4332.

Schmidt, W. (2002). Microcrystalline keratin: From feathers to composite products. *Materials Research Society Symposium Proceedings,* 702, U1.5.1-U1.5.8.

Schmidt, W.F. (2001). Microcrystalline keratin: From feathers to composite products. *MRS Proceedings,* 702, U1.5.1.-U1.5.8.

Schniepp, H.C., Li, J-L., McAllister, M.J., Sai, H., Herrera-Alonso, M., Adamson, D.H., Prud'homme, R.K., Car, R., Saville, D.A., & Aksay, I.A. (2006). Functionalized single graphene sheets derived from splitting graphite oxide. *The Journal of Physical Chemistry B*, 110, 8535-8539.

Schrooyen, P.M.M., Dijkstra, P.J., Oberthur, R.C., Bantjes, A., & Feijen, J. (2000). Partially carboxymethylated feather keratins. 1. Properties in aqueous systems. *Journal of Agricultural and Food Chemistry*, 48, 4326-4334.

Schrooyen, P.M.M., Dijkstra, P.J., Oberthur, R.C., Bantjes, A., & Feijen, J. (2001). Stabilization of solutions of feather keratin by sodium dodecyl sulfate. *Journal of Colloid and Interface Science*, 240, 30-39.

Schrooyen, P.M.M., Dijkstra, P.J., Oberthür, R.C., Bantjes, A., & Feijen, J. (2001). Partially carboxymethylated feaher keratins. 2. Thermal and mechanical properties of films. *Journal of Agricultural and Food Chemistry*, 49, 221-230.

Shao, G., Lu, Y., Wu. F., Yang, C., Zeng, F., & Wu, Q. (2012). Graphene oxide: The mechanism of oxidation and exfoliation. *Journal of Materials Science*, 47, 4400-4409.

Shen, B., Zhai, W., Tao, M., Lu, D., & Zheng, W. (2013). Enhanced interfacial interaction between polycarbonate and thermally reduced graphene induced by melt blending. *Composites Science and Technology*, 86, 109-116.

Shi, J., & Yang, E. (2015). Green electrospinning and crosslinking of polyvinyl alcohol/citric acid. *Journal of Nano Research*, 32, 32-42.

Shin, H-J., Kim, K.K., Benayad, A., Yoon, S-M., Park, H.K., Jung, I-S., Jin, M.H., Jeong, H-K., Kim, J.M., Choi, J-Y., & Lee, Y.H. (2009). Efficient reduction of graphite oxide by sodium borohydride and its effect on electrical conductance. *Advanced Functional Materials*, 19, 1987-1992.

Sierpinski, P., Garrett, J., Ma, J., Apel, P., Klorig, D., Smith, T., Koman, L.A., Atala, A., Van Dyke, M. (2008). The use of keratin biomaterials derived from human hair for the promotion of rapid regeneration of peripheral nerves. *Biomaterials*, 29, 118-128.

Silva, R., Singh, R., Sarker, B., Papageorgiou, D.G., Juhasz, J.A., Roether, J.A., Cicha, I., Kaschta, J., Schubert, D.W., Chrissafis, K., Detsch, R., & Boccaccini, A.R. (2014) Hybrid hydrogels based on keratin and alginate for tissue engineering. *Journal of Materials Chemistry B*, 2, 5441-5451.

Singh, R., & Whitesides, G.M. (1993). Thiol-disulfide interchange. In Patai, S., & Rappoport, Z. (Eds.). Sulphur-containing functional groups. John Wiley & Sons Ltd, Chichester, England.

Sinkiewicz, I., Sliwinska, A., Staroszczyk, H., & Kolodziejska, I. (2016). Alternative methods of preparation of soluble keratin from chicken feathers. *Waste and Biomass Valorization*, DOI 10.1007/s12649-016-9678-y

Sisson, K., Zhang, C., Farach-Carson, M.C., Chase, D.B., & Rabolt, J.F. (2009). Evaluation of cross-linking methods for electrospun gelatin on cell growth and viability. *Biomacromolecules*, 10, 1675-1680.

Slack, J. 2007. Molecular biology of the cell. In Lanza, R., Langer, R., & Vacanti, J. (Eds.). Principles of Tissue Engineering 3rd edition, Academic Press, Amsterdam.

Souza, A.C., Benze, R., Ferrao, E.S., Ditchfield, C., Coelho, A.C.V., & Tadini, C.C. (2012). Cassava starch biodegradable films: Influence of glycerol and clay nanoparticles content on tensile and barrier properties and glass transition temperature. *LWT – Food Science and Technology*, 46, 110-117.

Sridhar, R., Prabhakaran, M.P., & Ramakrishna, S. (2013). Synthetic enroutes to engineer electrospun scaffolds for stem cells and tissue regeneration. In Ramalingam, M., Jabbari, E., Ramakrishna, S., & Khademhosseini, A. (Eds.). Micro and nanotechnologies in engineering stem cells and tissues. John Wiley & Sons, Inc, New Jersey, USA.

Sridharan, R., Cameron, A.R., Kelly, D.J., Kearney, C., & O'Brien, F.J. (2015). Biomaterial based modulation macrophage polarization: a review and suggested design principles. *Materials Today*, 18, 313-325.

Stankovich, S., Dikin, D.A., Dommett, G.H.B., Kohlhaas, K.M., Zimney, E.J., Stach, E.A., Piner, R.D., Nguyen, S.T., Ruoff, R.S. (2006). Graphene-based composite materials. *Nature*, 442, 282-286.

Stankovich, S., Piner, R.D., Nguyen, S.T., & Ruoff, R.S. (2006). Synthesis and exfoliation of isocyanate-trated graphene oxide nanoplatelets. *Carbon*, 44, 3342-3347.

Stark, G.R., Stein, W.H., & Moore, S. (1960). Reactions of the cyanate present in aqueous urea with amino acids and proteins. *The Journal of Biological Chemistry,* 235, 3177-3181.

Steele, J.G., Johnson, G., & Underwood, P.A. (1992). Role of serum vitronectin and fibronectin in adhesion of fibroblasts following seeding onto tissue culture polystyrene. *Journal of Biomedical Materials Research*, 26, 861-884.

Stratton, S., Shelke, N.B., Hoshino, K., Rudraiah, S., & Kumbar, S.G. (2016). Boactive polymeric scaffolds for tissue engineering. *Bioactive Materials*, 1, 93-108.

Sundaramurthi, D., Krishnan, U.M., & Sethuraman, S. (2014). Electrospun nanofibers as scaffolds for skin tissue engineering. *Polymer Reviews*, 54, 348-376.

Tachibana, A., Furuta, Y., Takeshima, H., Tanabe, T., & Yamauchi, K. (2002). Fabrication of wool keratin sponge scaffolds for long-term cell cultivation. *Journal of Biotechnology*, 93, 165-170.

Taepaiboon, P., Rungsardthong, U., & Supaphol, P. (2007). Effect of cross-linking on properties and release characteristics of sodium salicylate-loaded electrospun poly(vinyl alcohol) fibre mats. *Nanotechnology*, 18, doi:10.1088/0957-4484/18/17/175102

Tamada, Y., & Ikada, Y. (1993). Effect of preadsorbed proteins on cell adhesion to polymer surfaces. *Journal of Colloid and Interface Science*, 155, 334-339.

Thannhauser, T.W., Konishi, Y., & Scheraga, H.A. (1984). Sensitive quantitative analysis of disulfide bonds in polypeptides and proteins. *Analytical Biochemistry,* 138, 181-188.

Thevenot, P., Hu, W., & Tang, L. (2008). Surface chemistry influence implant biocompatibility. *Current Topics in Medicinal Chemistry*, 8, 270-280.

Thilagar, S., Arul Jothi, N., Sheikh Omar, A.R., Kamaruddin, M.Y., & Ganabadi, S. (2009). Effect of keratin-gelatin and bFGF-gelatin composite film as a sandwich layer for full-thickness

skin mesh graft in experimental dogs. *Journal of Biomedical Materials Research Part B: Applied Biomaterials*, 88B, 12-16.

Thompson, C.J., Chase, G.G., Yarin, A.L., & Reneker, D.H. (2007). Effects of parameters on nanofiber diameter determined from electrospinning model. *Polymer*, 48, 6913-6922.

Thomsen, P., & Gretzer, C. (2001). Macrophage interactions with modified materials surfaces. *Current Opinion in Solid State & Materials Science*, 5, 163-176.

Tibbitt, M.W., & Anseth, K.S. (2009). Hydrogels as extracellular matrix mimics for 3D cell culture. *Biotechnology and Bioengineering*, 103, 655-663.

Tien, H-W., Huang, Y-L., Yang, S-Y., Wang, J-Y., & Ma, C-C.M. (2011). The production of graphene nanosheets decorated with silver nanoparticles for use in transparent, conductive films. *Carbon*, 49, 1550-1560.

Tirella, A., Liberto, T., & Ahluwalia, A. (2012). Riboflavin and collagen: New crosslinking methods to tailor the stiffness of hydrogels. *Materials Letters*, 74, 58-61.

Tomblyn, S., Pettit Kneller, E.L., Walker, S.J., Ellenburg, M.D., Kowalczewski, C.J., Van Dyke, M., Burnett, L., & Saul, J.M. (2016). Keratin hydrogel carrier system for simultaneous delivery of exogenous growth factors and muscle progenitor cells. *Journal of Biomedical Materials Research B: Applied Biomaterials*, 104B, 864-879.

Tonin, C., Aluigi, A., Vineis, C., Varesano, A., Montarsolo, A., & Ferrero, F. (2007). Thermal and structural characterization of poly(ethylene-oxide)/keratin blend films. Journal of Thermal *Analysis and Calorimetry*, 89, 601-608.

Tromel, V.M., & Reuss, M. (1987). Dimanganheptoxid zur selektiven oxidation organischer substrate. *Angewandte Chemie*, 99, 1037-1038.

Tyagarajan, K., Pretzer, E., & Wiktorowicz, J.E. (2003). Thiol reactive dyes for fluorescence labeling of proteomic samples. *Electrophoresis*, 24, 2348-2358.

Ullah, A., & Wu, J. (2013). Feather fiber-based thermoplastics: Effects of different plasticizers on material properties. *Macromolecular Materials and Engineering*, 298, 153-162.

Ullah, A., Vasanthan, T., Bressler, D., Elias, A.L., & Wu, J. (2011). Bioplastics from feather quill. *Biomacromolecules*, 12, 3826-3832.

Uzun, M., Sancak, E., Patel, I., Usta, I., Akalin, M., & Yuksek, M. (2011). Mechanical behavior of chicken quills and chicken feather fibres reinforced polymeric composites. *Archives of Material Science and Engineering*, 52, 82-86.

Valles, C., Kinloch, I.A., Young, R.J., Wilson, N.R., & Rourke, J.P. (2013). Graphene oxide and base-washed graphene oxide as reinforcements in PMMA nanocomposites. *Composites Science and Technology*, 88, 158-164.

Van de Sandt, J.J.M., Bos, T.A., & Rutten, A.A.J.J.L. (1995). Epidermal cell proliferation and terminal differentiation in skin organ culture after topical exposure to sodium dodecyl sulfate. *In Vitro Cellular & Developmental Biology – Animal*, 31, 761-766.

Van Vlierberghe, S., Dubruel, P., & Schacht, E. (2011). Biopolymer-based hydrogels as scaffolds for tissue engineering applications: A review. *Biomacromolecules*, 12, 1387-1408.

Vanderhooft, J.L., Alcoutlabi, M., Magda, J.J., & Prestwich, G.D. (2008). Rheological properties of cross-linked hyaluronan-gelatin hydrogels for tissue engineering. *Macromolecular Bioscience*, 9, 20-28.

Vasconcelos, A., & Cavaco-Paulo, A. (2013). The use of keratin in biomedical applications. *Current Drug Targets*, 14, 612-619.

Verbeek, C.J.R., & van den Berg, L.E. (2010). Extrusion processing and properties of protein-based thermoplastics. *Macromolecular Materials and Engineering*, 295, 10-21.

Verma, V., Verma, P., Ray, P., & Ray, A. (2008). Preparation of scaffolds from human hair proteins for tissue-engineering applications. *Biomedical Materials*, 3, 1-12.

Vincent, J. (2012). Structural Biomaterials. Princeton University Press, New Jersey, USA, Chapter 2.

Wang, J., Hao, S., Chenz, Z., Li, W., Gao, F., Guo, T., Gong, Y., & Wang, B. (2017). Feather keratin hydrogel for wound repair: Preparation, healing effect and biocompatibility evaluation. *Colloids and Surfaces B: Biointerfaces*, 149, 341-350.

Wang, S., Taraballi, F., Tan, L.P., Ng, K.W. (2012). Human keratin hydrogels support fibroblast attachment and proliferation in vitro. *Cell and Tissue Research*, 347, 795-802.

Wang, S., Wang, Z., Foo, S.E., Tan, N.S., Yuan, Y., Lin, W., & Ng, K.W. (2015). Culturing fibroblasts in 3D human hair keratin hydrogels. *ACS Applied Materials & Interfaces*, 7, 5187-5198.

Wang, X., Ding, B., & Li, B. (2013). Biomimetic electrospun nanofibrous structures for tissue engineering. *Materials Today*, 16, 229-241.

Wang, Y., & Hsieh, Y-L. (2010). Crosslinking of polyvinyl alcohol (PVA) fibrous membranes with glutaraldehyde and PEG diacylchloride. *Journal of Applied Polymer Science*, 116, 3249-3255.

Wang, Y., Shi, Z., Yu, J., Chen, L., Zhu, J., & Hu, Z. (2012). Tailoring the characteristics of graphite oxide nanosheets for the production of high-performance poly(vinyl alcohol) composites. *Carbon*, 50, 5525-5536.

Wei, L., Wu, F., Shi, D., Hu, C., Li, X., Yuan, W., Wang, J., Zhao, J., Geng, H., Wei, H., Wang, Y., Hu, N., & Zhang, Y. (2013). Spontaneous intercalation of long chain alkyl ammonium into edge-selectively oxidized graphite to efficiently produce high-quality graphene. *Scientific Reports*, 3, 1-9.

Wheeler, T.S., Sbravati, N.D., & Janorkar, A.V. (2013). Mechanical & cell culture properties of elastin-like polypeptide, collagen, bioglass, and carbon nanosphere composites. *Annals of Biomedical Engineering*, 41, 2042-5055.

White, J., & Dalton, S. (2005). Cell cycle control of embryonic stem cells. *Stem Cell Reviews*, 1, 131-138.

Wilson, C., Clegg, R., Leavesley, D., & Pearcy, M. (2005). Mediation of biomaterial-cell interactions by adsorbed proteins. A review. *Tissue Engineering*, 11, 1-18.

Winter, G.D. (1962). Formation of scab and the rate of epithelialization of superficial wounds in the skin of the young domestic pig. *Nature*, 193, 293-294.

Wolfram, L.J., & Underwood, D.L. (1966). The equilibrium between the disulfide linkage in hair keratin and sulfite or mercaptan. *Textile Research Journal*, 36, 947-953.

Wong, S.S. (1991). Chemistry of protein conjugation and crosslinking. CRC Press, U.S. p30-32.

Woodin, A.M. (1954). Molecular size, shape and aggregation of soluble feather keratin. *Biochemical Journal*, 57, 99-109.

Wu, D-D., Irwin, D.M., & Zhang, Y-P. (2008). Molecular evolution of the keratin associated protein gene family in mammals, role in the evolution of mammalian hair. *BMC Evolutionary Biology*, 8, 241.

Wu, J., & Hong, Y. (2016). Enhancing cell infiltration of electrospun fibrous scaffolds in tissue regeneration. *Bioactive Materials*, 1, 56-64.

Xu, H., Cai, S., Xu, L., & Yang, Y. (2014). Water-stable three-dimensional ultrafine fibrous scaffolds from keratin for cartilage tissue engineering. *Langmuir*, 30, 8461-8470.

Xu, H., Shen, L., Xu, L., Yang, Y. (2015). Low-temperature crosslinking of proteins using non-toxic citric acid in neutral aqueous medium: Mechanism and kinetic study. *Industrial Crops and Products*, 74, 234-240.

Xu, L-C., & Siedlecki, C.A. (2007). Effects of surface wettability and contact time on protein adhesion to biomaterial surfaces. *Biomaterials*, 28, 3273-3283.

Xu, S., Sang, L., Zhang, Y., Wang, X., & Li, X. (2013). Biological evaluation of human hair keratin scaffolds for skin wound repair and regeneration. *Materials Science and Engineering C*, 33, 648-655.

Yamada, Y., Yasuda, H., Murota, K., Nakamura, M., Sodesawa, T., & Sato, S. (2013). Analysis of heat-treated graphite oxide by X-ray photoelectron spectroscopy. *Journal of Materials Science*, 48, 8171-8198.

Yamauchi, K., Maniwa, M., & Mori, T. (1999). Cultivation of fibroblast cells on keratin-coated substrata. *Journal of Biomaterials Science, Polymer Edition*, 9, 259-270.

Yan, C., & Pochan, D.J. (2010). Rheological properties of peptide-based hydrogels for biomedical and other applications. *Chemical Society Reviews*, 39, 3528-3540.

Yao, J., Bastiaansen, C.W.M., & Peijs, T. (2014). High Strength and high modulus electrospun nanofibers. *Fibers*, 2, 158-187.

Yen, K-C., Chen, C-Y., Huang, J-Y., Kuo, W-T., & Lin, F-H. (2016). Fabrication of keratin/fibroin membranes by electrospinning for vascular tissue engineering. *Journal of Materials Chemistry B*, 4, 237-244.

Yeung, T., Georges, P.C., Flanagan, L.A., Marg, B., Ortiz, M., Funaki, M., Zahir, N., Ming, W., Weaver, V., & Janmey, P.A. (2005). Effects of substrate stiffness on cell morphology, cytoskeletal structure and adhesion. *Cell Motillity and the Cytoskeleton*, 60, 24-34.

Yin, X-C., Li, F-Y., He, Y-F., Wang, Y., & Wang, R-M. (2013). Study of effective extraction of chicken feather keratins and their films for controlling drug release. *Biomaterials Science,* 1, 528-536.

Yoon, D.M., & Fisher, J.P. (2009). Natural and synthetic polymeric scaffolds. In Narayan, R. (Ed.). Biomedical Materials. Springer, New York.

Yu, J., Yu, D.W., Checkla, D.M., Freedberg, I.M., & Bertolino, A.P. (1993). Human hair keratins. *The Journal of Investigative Dermatology*, 101, 56S-59S.

Yu, T., Tutwiler, V.J., & Spiller, K. (2015). The role of macrophages in the foreign body response to implanted biomaterials. In Santambrogio, L. (Ed.). Biomaterials in Regenerative Medicine and the Immune System, Springer, Switzerland.

Yuan, J., Shen, J., & Kang, I-K. (2008). Fabrication of protein-doped PLA composite nanofibrous scaffolds for tissue engineering. *Polymer International*, 57, 1188-1193.

Yuan, J., Xing, Z-C., Park, S-W., Geng, J., & Kang, I-K. (2009). Fabrication of PHBV/keratin composite nanofibrous mats for biomedical applications. *Macromolecular Research*, 17, 850-855.

Yuan, X., Zhang, Y., Dong, C., & Sheng, J. (2004). Morphology of ultrafine polysulfone fibers prepared by electrospinning. *Polymer International*, 53, 1704-1710.

Yumitori, S. (2000). Correlation of C1s chemical state intensities with the O1s intensity in the XPS analysis of anodically oxidized glass-like carbon samples. *Journal of Materials Science*, 35, 139-146.

Zayas, J.F. (1997). Functionality of proteins in food. Springer, Berlin. p76-133.

Zhang, C., Yuan, X., Wu, L., Han, Y., & Sheng, J. (2005). Study on morphology of electrospun poly(vinyl alcohol) mats. *European Polymer Journal*, 41, 423-432.

Zhang, S. (2004). Beyond the petri dish. *Nature Biotechnology*, 22, 151-152.

Zhang, X., Tang, K., & Zheng, X. (2016). Electrospinning and crosslinking of Col/PVA nanofiber-microsphere containing salicylic acid for drug delivery. *Journal of Bionic Engineering*, 13, 143-149.

Zhao, R., Wang, Y., Li, X., Sun, B., Jiang, Z., & Wang, C. (2015). Water-insoluble sericin/b-cyclodextrin/PVA composite electrospun nanofibers as effective adsorbents towards methylene blue. *Colloids and Surfaces B: Biointerfaces*, 136, 375-382.

Zhao, W., Yang, R., Zhang, Y., & Wu, L. (2012). Sustainable and practical utilization of feather keratin by an innovative physicochemical pretreatment: high density steam flash-explosion. *Green Chemistry,* 14, 3352-3360.

Zhou, B., & Wang, H. (2011). The optimization of regeneration feather protein/PVA composite fiber's production technology using gray clustering analysis. *Advanced Materials Research*, 332-334, 500-504.

Zhou, X., Zhang, J., Wu, H., Yang, H., Zhang, J., & Guo, S. (2011). Reducing graphene oxide via hydroxylamine: A simple and efficient route to graphene. *The Journal of Physical Chemistry*, 115, 11957-11961.

Zhu, J., & Marchant, R.E. (2011). Design properties of hydrogel tissue-engineering scaffolds. *Expert Review of Medical Devices*, 8, 607-626.

Zoccola, M., Aluigi, A., & Tonin, C. (2009). Characterisation of keratin biomass from butchery and wool industry wastes. *Journal of Molecular Structure*, 938, 35-40.

Zoccola, M., Montarsolo, A., Aluigi, A., Varesano, A., Vineis, C., & Tonin, C. (2007). Electrospinning of polyamide 6/modified keratin blends. *e-Polymers*, 105, doi: https://doi.org/10.1515/epoly.2007.7.1.1204